Functional Polymers Containing Semi-Rigid Alternating Sequences

Jing Huang

Dissertation submitted to the faculty of the Virginia Polytechnic Institute and State University in partial fulfillment of the requirements for the degree of

Doctor of Philosophy
In
Chemistry

S. Richard Turner, Committee Chair
Alan R. Esker, Committee Member
Richard D. Gandour, Committee Member
John B. Matson, Committee Member

October 25th, 2017
Blacksburg, VA

Keywords: alternating copolymers, hypercrosslinked polymers, microgels, CO_2 adsorption, fluorescence, heavy metal ion adsorption

Functional Polymers Containing Semi-Rigid Alternating Sequences

Jing Huang

ABSTRACT

(Academic)

Alternating copolymers represent a special class of copolymers in which the two comonomers copolymerize in a regular alternating sequence along the polymer chain. Of particular interest in our group are the stilbene-maleic anhydride/maleimide alternating copolymers. These copolymers possess sterically congested backbones and precisely placed functional groups arising from the strictly alternating copolymerization. The research in this dissertation is focused on the synthesis, characterization, and potential application of functionalized copolymers that contain semi-rigid alternating copolymer sequences.

The fluorescence properties of a series of non-conjugated, *tert*-butyl carboxylate functionalized alternating copolymers were investigated. Extraordinarily high fluorescent intensity with excellent linearity was observed for the di-*tert*-butyl group-containing stilbene and maleic anhydride alternating copolymer in THF. We attributed the origin of the strong fluorescence to the "through space" $\pi - \pi$ interactions between the phenyl rings from the stilbene and C=O groups from the anhydride. The fluorescence was maintained when the copolymer was deprotected and hydrolyzed and the resulting carboxylic acid-functionalized copolymer was dissolved in water at neutral pH.

The *tert*-butyl carboxylate functionalized alternating copolymer sequences were incorporated into highly crosslinked polymer networks using suspension polymerization. After removing the *tert*-butyl groups by acidic hydrolysis, the surface area of the networks increased significantly. Using this facile two-step strategy, we were able to achieve nanoporous polymers

with BET surface area up to 817 m^2/g and carboxylic acid-functionalized surfaces. The BET surface area of deprotected polymers increased with increasing crosslinking density, and the stilbene-containing polymers showed systematically higher BET surface area than the styrene-containing polymers due to the stiffness of the alternating sequences. The resulting nanoporous polymers have potential to be employed as solid sorbents for CO_2.

The same *tert*-butyl carboxylate functionalized alternating copolymer sequences were also incorporated into microgels via miniemulsion polymerization. The miniemulsion technique ensured the successful synthesis of microgels with ~100 nm diameter using solid stilbene and maleimide monomers. The resulting *tert*-butyl carboxylate-containing microgels were converted into carboxylic acid-containing aqueous microgels by acid hydrolysis. These aqueous microgels showed good and reversible lead and copper ion adsorption capacities.

Amine-functionalized nanoporous polymers were synthesized by the post-modification of highly-crosslinked divinylbenzene-maleic anhydride polymers. High amine-contents were achieved by covalently attaching multiamines to the acid-chloride functionalized polymer surface. The resulting polymers showed medium to high BET surface areas (up to 500 m^2/g) and high CO_2 capture capacities.

Functional Polymers Containing Semi-Rigid Alternating Sequences

Jing Huang

ABSTRACT

(General Audience)

Copolymers are polymers that consist of two or more different monomers in the polymer chain. Research on copolymers can be traced back to the 1930s. Since the early discoveries, the research on copolymers has received considerable attention because of the ease of synthesis and the versatile properties and applications of these materials. Alternating copolymers are one of the most studied types of copolymers. In an alternating copolymer, the two different monomers arrange in a regular alternating sequence along the polymer backbone. Of special interest in our group are the alternating copolymers that contain stilbene (1,2-diphenylethylene). The stilbene-containing alternating copolymers have relatively rigid (semi-rigid) structures, which lead to unusual and interesting properties. The research described in this dissertation is focused on incorporating these semi-rigid alternating copolymers into different types of systems and studying their structure/property relationships. Three different polymeric materials and their properties were explored.

Fluorescent materials can glow when irradiated by a certain wavelength of light. This property is very useful in biomedical sensing, imaging and labeling. The semi-rigid stilbene-containing alternating copolymer exhibited fluorescence with extraordinarily high intensity, solely due to the conjugation from the exact juxtaposition of molecular orbitals. This high intensity fluorescence suggests potential application as novel light-emitting materials.

The increasing atmospheric CO_2 concentrations due to human activities like transportation and manufacturing have caused public concerns. Currently, liquid amine scrubbing

is one of the most well established methods for CO_2 capture in industry. However, due to the solvent evaporation, degradation, and the high energy demand during the solvent regeneration, solid polymeric materials are considered as attractive alternative CO_2 capture materials. We designed two kinds of polymers based on our semi-rigid alternating copolymer sequences, and they both exhibited pores smaller than 2 nm. With the help of different functional groups designed to interact with CO_2, these polymers showed enhancement in CO_2 capture properties, and show the viability as solid sorbents for atmospheric CO_2.

Heavy metal contamination in water is a severe environmental and public health problem. The recent Flint water crisis raised the public awareness of this problem. We synthesized a series of hydrogel beads with diameters in the range of 100-200 nm. The incorporation of these functional alternating copolymer sequence into the microgels led to fast and reversible adsorption of the lead and copper ions in water.

Acknowledgements

I would like to thank my advisor Dr. S. Richard Turner for his mentoring, guidance, and encouragement. I feel extremely fortunate to have an advisor who is so supportive and caring. Through the past five and a half years, I have been deeply influenced by his dedication and passion for polymer science, and it is my lifelong pursuit to be an excellent scientist like he is. I would also like to thank my committee members, Dr. Alan Esker, Dr. Richard Gandour, and Dr. John Matson for their help and guidance in classes, research, and presentation skills.

I would like to acknowledge our collaborators through the years: Dr. Frantisek Svec and his postdocs at Molecular Foundry, Lawrence Berkeley National Laboratory; Dr. Tijana Grove and Dr. Amanda Morris at Virginia Tech for their help with the instrumentation and discussions. I would also like to acknowledge the National Science Foundation (NSF) for funding the research on alternating copolymers.

I would like to thank the Turner group, Dr. Xu Zhou, Dr. Zhengmian Chang, Dr. Alice Savage, Ms. Sarah Blosch, and Mr. Eliot Edling. I truly appreciate their help and friendship.

Finally, I would like to thank my family for supporting me through my PhD journey. I followed my dad's steps in becoming a chemist and I am sure he is proud that I will be the second Dr. Huang in the family. I hope my mom can forgive me for all the late-night calls and tears (and for not getting her good gene for math). Apologies go to my grandparents for not being able to visit them often, and thank you for constantly telling me that I am the best. Special thanks to Andrew Katz, for all your love, support, awesome jokes, and proof reading the dissertation for me.

Attributions

Chapter 1 and **Chapter 2** of this Dissertation were co-authored with Dr. S. Richard Turner, who is a research professor in the Department of Chemistry, Virginia Tech. Dr. Turner is the PI for the NSF project on alternating copolymers; he provided guidance and edited the two review papers.

Chapter 3 was co-authored with Dr. Xi Geng, Mr. Chong Peng, Dr. Tijana Grove and Dr. S. Richard Turner. Dr. Grove is an assistant professor in the Department of Chemistry, Virginia Tech. Dr. Geng was a graduate student in Dr. Grove's research group before he received his PhD degree from the Department of Chemistry, Virginia Tech. He helped with the fluorescence measurements and editing of the manuscript. Dr. Turner was the PI and oversaw the project.

Chapter 4 was co-authored with Dr. Xu Zhou, Dr. Alexandros Lamprou, Dr. Fernando Maya, Dr. Frantisek Svec, and Dr. S. Richard Turner. Dr. Svec was the facility director at The Molecular Foundry, Lawrence Berkeley National Laboratory. Dr. Lamprou and Dr. Maya were postdoctoral researchers at Lawrence Berkeley National Laboratory. They provided BET surface area and CO_2 adsorption measurements. Dr. Turner supervised the project.

Chapter 5 was co-authored with Dr. Xi Geng, Dr. Brian Tissue and Dr. S. Richard Turner. Dr. Geng provided the TEM micrographs and performed the DLS measurements. Dr. Tissue helped with the lead and copper ion measurements using flame atomic adsorption spectrum. Dr. Turner provided oversight for this project.

Chapter 6 was co-authored with Mr. Jie Zhu, Dr. Xi Geng, Mr. Samuel Snyder, Dr. Amanda

Morris and Dr. S. Richard Turner. Dr. Amanda Morris is an associate professor in the Department of Chemistry, Virginia Tech. Mr. Zhu is a graduate student in Dr. Morris's research group. They assisted with the BET surface area CO_2 adsorption measurements and provided helpful discussions. Dr. Geng provided the SEM micrographs of the samples and helpful discussion. Mr. Samuel Snyder was an undergraduate student in the Department of Material Science and Engineering, Virginia Tech. He helped with the precursor synthesis as a summer undergraduate researcher. Dr. Turner was the PI of the NSF project and provided guidance for the project.

Table of Contents

List of Figures

List of Tables

List of Schemes

Chapter 1. Recent Advances in Alternating Copolymers: The Synthesis, Modification, and Applications of Precision Polymers

(Adapted with permission from Huang, J.; Turner, S. R. *Polymer* **2017**, *116*, 572. Copyright 2017 Elsevier.)

1.1 Authors

Jing Huang,[†,‡] and S. Richard Turner*[,†,‡]

[†]Department of Chemistry, Virginia Tech, Blacksburg, VA 24061, United States

[‡]Macromolecules Innovation Institute, Virginia Tech, Blacksburg, VA 24061, United States

1.2 Abstract

Alternating copolymers represent a special class of copolymers, in which the two comonomers copolymerize in a regular alternating sequence along the chain. Their interesting physical and chemical properties, as well as the underlying mechanism, have attracted significant attention in both academia and industry. The electron-donor benzylidene monomers – styrene and stilbene, readily form alternating copolymers with the electron-acceptor monomers – maleic anhydride and *N*-substituted maleimides. The rich chemistry of the substitution groups on these monomers offers enormous combinations for the synthesis of alternating copolymers for different applications. In this paper, we aim to provide a general overview of recent publications on the specific field of these benzylidene-containing alternating copolymers, and the emphasis is placed on the synthetic progress, structure-property relationships, and the applications of these copolymers.

1.3 Introduction

Copolymers are polymers synthesized from two or more species of monomers.[1] The study of copolymers could be traced back to the 1930s since synthetic rubber was invented and

developed.[2] Ever since then, the research on copolymers has received considerable attention because an infinite variety of different copolymer composition could be synthesized and specific desired properties could be tailored by varying the species and composition of the comonomers. Based on different arrangements of the comonomers, the copolymers can be typically categorized as random or statistical copolymers, block or segmented copolymers, graft copolymers, alternating copolymers, periodic copolymers,[3] while some new types of copolymers, such as gradient copolymers[4] and aperiodic copolymers[5] emerged in recent years (Figure 1-1).[6-8]

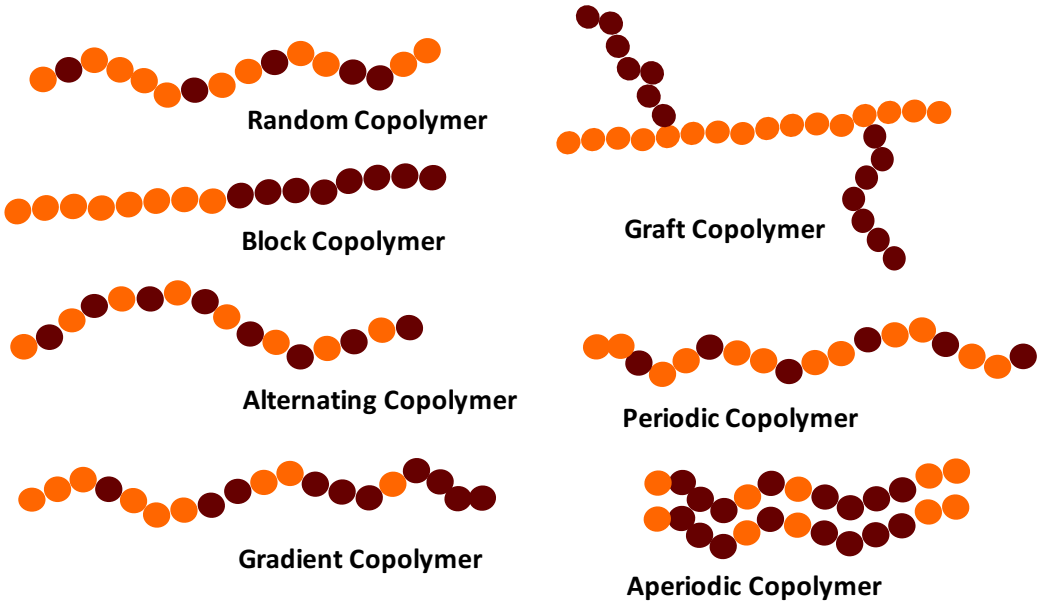

Figure 1-1. Types of copolymers

In an alternating copolymer, the two comonomers arrange in a regular alternating sequence,[1] and the alternating copolymerization is characterized by the product of the two monomer reactivity ratios as $r_1r_2=0$, in which r_1 and r_2 represent the ratio of the rate constant of homopropagation to the rate constant of crosspropagation of each reactive propagating species.[9] In other words, each of the propagating species prefers to add the other monomer rather than react with its own type of monomer. Perfect alternation happens when r_1 and r_2 are both equal to zero, where no dyads or homo-addition will be found in the copolymer, while such dyads can be found when both r_1 and r_2

are very small or one r is small and the other r is zero, where the copolymer shows alternating behavior but does not strictly alternate. The comonomer systems that can form alternating copolymers include electron donor-acceptor pairs, complexes formed with Lewis acids, Ziegler-Natta or metallocene catalyzed ethylene and cis-olefins, zwitterion intermediates, etc. Although two difunctional monomers also polymerize alternatively in step growth, the polymers from step growth are not usually considered as alternating copolymers,[10] and the two units are often seen as one repeat unit. Among all these systems, of special interests are in the radical polymerizable electron donor-acceptor pairs. The electron donor monomers, such as styrene, stilbene, vinyl ethers, dienes and *N*-vinylcarbazole, and electron acceptor monomers, such as maleic anhydride, *N*-substituted maleimides, dialkyl fumarates and fumaronitriles, provide numerous combinations and possibilities in achieving alternating copolymers of different properties and applications.

Several models have been proposed to explain the alternating behavior from a mechanistic point of view (Figure 1-2). The earliest Mayo-Lewis model suggested that the rate constant of the propagation of the polymer chain relates to the terminal radical and the incoming monomer (thus it's also referred as the terminal model).[11] The terminal model could be used to describe the copolymer composition as a function of monomer feed composition, but fails to explain the relationship of rate constant versus monomer feed composition.[12] However, this relationship could be explained well using the penultimate unit model, which suggests that the rate of propagation of the polymer chain does not only rely on the terminal radical, but also on the penultimate monomer unit.[12-15] One plausible interpretation from the theoretical calculations was that the transition state of the propagation can be represented by three hindered rotors, and one of the rotors is greatly affected by the penultimate unit.[16] Another well-known model, the complex participation model suggests that the charge-transfer complex, which is formed *via* the interaction between the electron

donor monomer and the electron acceptor monomer pairs, participates in the copolymerization.[17-18] The existence of the charge-transfer complexes have been confirmed by spectroscopic evidence,[18-21] but it is still questionable whether the complexes are actually added to the propagating radicals, or the complexes dissociate upon the polymerization and only one monomer is added to the propagating chain each time.[22-24] Generally speaking, there still remains a debate over the exact mechanism of the alternating behavior, and efforts are continuously made to study the mechanistic steps behind alternating copolymerization.

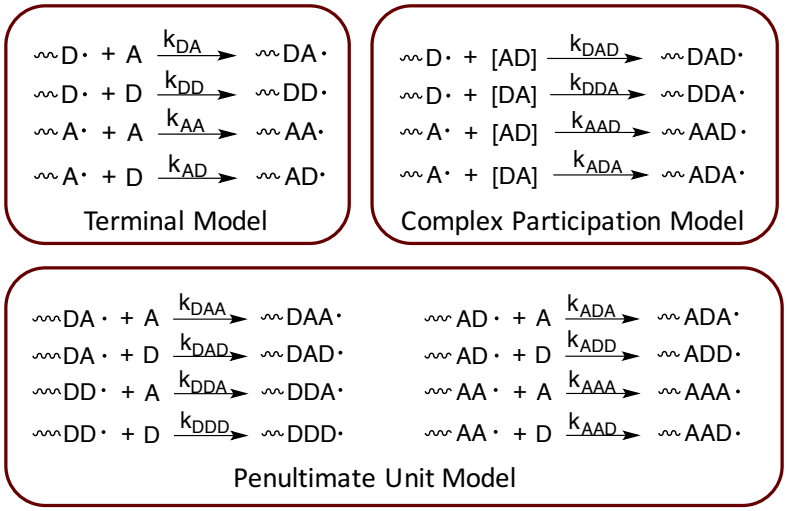

Figure 1-2. Demonstration of three models of the mechanism of alternating copolymerization, D and A represent donor and acceptor monomers, respectively.

Examination of the literature shows that there is a lack of review articles on alternating copolymers since 2000. Cowie's book on alternating copolymers was published in 1985,[10] and a few reviews focusing on the mechanisms of alternating copolymerization[15, 25-26] or specific applications of some alternating copolymers[27] were reported. However, much progress has been made on the synthetic techniques, mechanistic studies, property evaluation and applications. In this review, we specifically focus on the alternating copolymers that were formed by benzylidene monomers styrene or stilbene with maleic anhydride or *N*-substituted maleimides. The detailed synthetic pathways, the miscellaneous modifications, fundamental structure property

measurements, and various applications of the alternating copolymers of styrene or stilbene with maleic anhydride or maleimides monomers will be discussed in this paper.

1.4 Recent development of benzylidene-containing alternating copolymers

1.4.1 Traditional and controlled radical copolymerization for alternating copolymers

The alternating copolymerization of maleic anhydride with styrene was among the earliest academic studied copolymer systems, and one of the earliest studies by Alfrey and Lavin in the early 1940s[28] showed that this copolymer could be prepared using common free radical initiators at 70–80 ˚C.[29] Ever since then, the styrene-maleic anhydride (SMAh) copolymer has been one of the most extensively investigated alternating copolymers. The incorporation of maleic anhydride unit increases the heat resistance of polystyrene proportional to the maleic anhydride content.[30] The thermoplastic SMA has high glass transition temperature, high deflection temperature under load, high heat and chemical resistance, low melt flow rate, good impact, rigidity and dimensional stability.[31] It was fist commercialized by Sinclair Petrochemicals in the 1960s, and in 1972, the injection molding SMAh resin was first used for automotive dashboards by Nova (Arco) Chemicals using the trade name Dylark®, which is no longer produced. Currently, the commercial SMAh products are by Cray Valley (Beaufort, TX, USA) as SMA®, Polyscope (Geleen, NL) as Xiran® and Solenis (Wilmington, DE, USA) as Scripset®.[32] SMAh copolymer finds wide ranging applications as a molding resin in the automotive, packaging and construction industries, as well as a compatibilizer in plastic blends and alloys to improve their mechanical and thermal performance and other properties.[33-34] SMAh was studied as an additive to acrylonitrile butadiene styrene (ABS) copolymer and poly(methyl methacrylate) (PMMA). SMAh could broaden the processing window and increase the surface polarity of the base resin, which is desired for molding and surface painting purposes, respectively. SMAh also increases the miscibility of ABS and

PMMA with other additives and polymers, and reduces phase separation.[33-34] In addition, SMAh and PMMA are fully miscible, and the clear SMAh has minimal influence on the refractive index and transparency of PMMA polymer, which helps to maintain the attractive optical features of PMMA while improving its other properties. However, SMAh polymers are not resistant to UV degradation, therefore they require a UV-resistant protective coating when used for outdoor applications.[31] Moreover, SMAh polymer, along with its hydrolyzed from, styrene-maleic acid (SMA) alternating copolymer were also applied in diverse applications such as surface sizing, pigment dispersion, ink modification, powder coating, leather retanning, floor care products etc.

The early studies mostly focused on the kinetics and mechanism of the alternating copolymerizations.[13, 19, 35-41] The SMAh copolymers are mostly synthesized using free radical polymerization (Scheme 1-1a). The most commonly used initiators are benzoyl peroxide (BPO) and azo-bis-(isobutyronitrile) (AIBN), while spontaneous initiation,[40, 42] UV initiation,[43] and some other initiators[44] were also reported. The copolymerization could be conducted in bulk and common organic solvents such as THF, DMF, acetone, methyl ethyl ketone, benzene, carbon tetrachloride, and saturated hydrocarbons. Supercritical CO_2 was also reported as a suitable synthesis media, especially for high molecular weight SMAh ($Mw>10^6$).[45] Due to the non-homopolymerizable nature of maleic anhydride, no more than 50 mol% of it could be incorporated into the copolymer,[28] and ^{13}C NMR[46] and pyrolysis-gas chromatography[31] showed a strong tendency of 1:1 equimolar alternation at 1:1 infeed of styrene and maleic anhydride unless using a starved feeding technique, in which the infeed maleic anhydride is added in a very low level.[31] However, when the infeed maleic anhydride content is lower than 50 mol%, conventional free radical copolymerization may result in copolymers with compositional drifts,[47] evidenced by ^{13}C NMR that segments with more maleic anhydride and segments with less maleic anhydride are

statistically distributed along the chain.[48] Controlled radical polymerization techniques provide better control over the alternating monomer sequence at imbalanced infeed ratio. (The details and mechanism of controlled radical polymerizations which were elaborated in books and review articles.[49-51]) Both nitroxide mediated polymerization (NMP) (Scheme 1-1b) and reversible addition-fragmentation chain transfer (RAFT) (Scheme 1-1c) are applicable to the synthesis of the SMAh copolymer, while atom transfer radical polymerization (ATRP) seems incompatible for SMAh synthesis, which may due to the interaction of maleic anhydride with the copper complex that is required for ATRP. However, ATRP could be used to copolymerize styrene and *N*-substituted maleimides.[52-55]

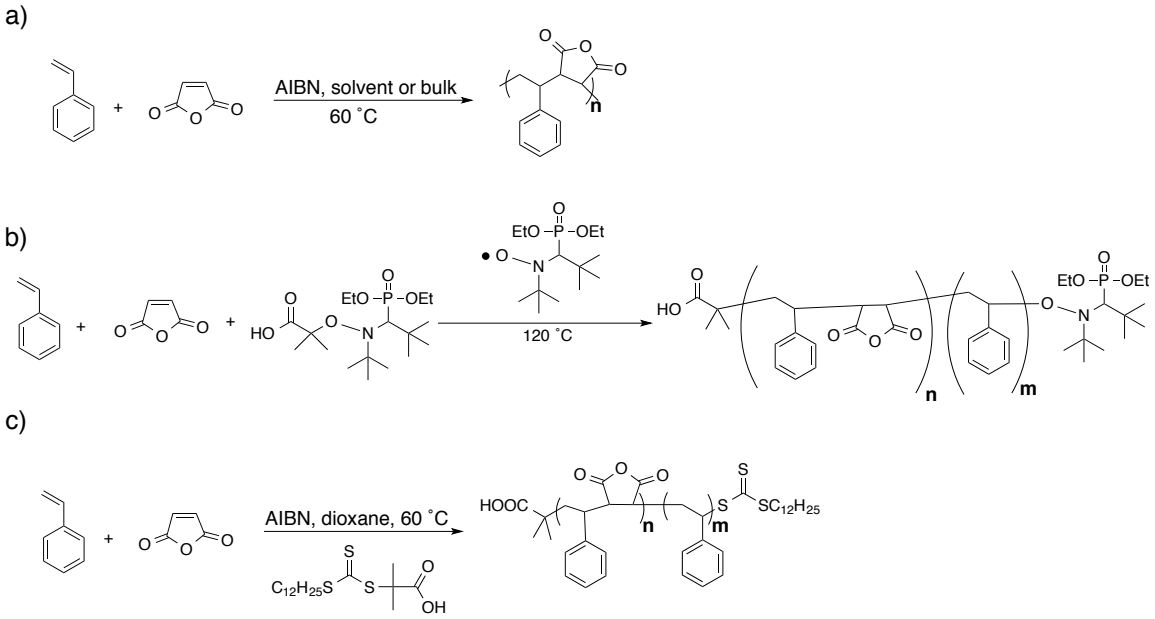

Scheme 1-1. a) Conventional free radical alternating copolymerization of styrene and maleic anhydride;[27] and the one step synthesis of poly((styrene-alt-maleic anhydride)-*b*-styrene) using b) nitroxide mediated polymerization (NMP),[56] or c) reversible addition-fragmentation chain transfer (RAFT) polymerization.[57]

In controlled radical polymerization (CRP), the copolymerization of styrene and maleic anhydride showed a very strong alternating tendency even at imbalanced monomer ratio. That is to say, if the polymerization starts with a very low level of maleic anhydride, the copolymerization

will still start as an alternating copolymerization until all maleic anhydride is consumed, and then the homopolymerization of styrene starts.[58] Eventually, it can yield a block copolymer with an SMAh block and a styrene block in one step (Scheme 1-1b and 1c).[56, 59-61] In contrast, the same situation would result in a heterogeneous mixture of copolymer and homopolymer in conventional radical polymerization.[15] This strong alternating feature has been utilized in sequence control polymerization (see 1.4.4). The choice of RAFT agent in alternating copolymerization is crucial, because it affects the reaction rate and the terminus group of the chain. An initialization period was found at the initial stage of the RAFT polymerization of styrene and maleic anhydride, during which the RAFT agent combines with either styrene or maleic anhydride to form the monomer adduct.[62-63] The preference on monomer selectivity during this step depends on the electronic structure of the RAFT agent, i.e. the electron rich RAFT agent will preferably add to maleic anhydride. Electron spin resonance (ESR) spectroscopy showed that the intermediate propagating radical is predominate with maleic anhydride at the chain ends. This is probably due to the fast addition of the maleic anhydride chain end to the C=S of the RAFT agent.[64] The composition of monomer feed also plays an important role, when the proportion of maleic anhydride was large, the copolymerization rate was faster while the control over the molecular weight and molecular weight distribution was poor.[65] In addition to enhancing the alternating behavior of the copolymerization, CRP also provides pathways to synthesize hybrid composite,[66] nanostructures,[57, 67-68] and different architectures, such as polymer brushes,[69-70] di-blocks,[71] stars and Miktoarm stars,[72] and hyperbranch structures.[73]

1.4.2 Modification and functionalization of alternating copolymers

Maleic anhydride, or succinic anhydride when enchained, can be easily functionalized when the carbonyl carbons are attacked by nucleophiles.[29] Although the stability of the reactive

anhydride groups can be troublesome when the SMAh copolymers are exposed to moisture or other chemical environments, they provide a reactive site for modification of the SMAh copolymers, and several important functionalized polymers were prepared using this chemistry.[27]

One example is the styrene-maleic acid (SMA) alternating copolymer, which is hydrolyzed from the styrene-maleic anhydride copolymer under basic conditions (Scheme 1-2). The hydrophilic carboxylic acid (and/or salt) and the hydrophobic styrene impart to SMA amphiphilic properties, and the amphiphilicity is dependent on the pH of the local environment. The dissociation behavior of SMA copolymers was studied by Colby and coworkers.[74-75] The two carboxyl groups have different pK_as of 6 and 10, which means SMA bears two charges on both carboxyl groups at high pH, one charge at neutral pH, and is not charged at low pH.[76] The conformation and aqueous solubility of SMA are also affected by the local pH: at high or neutral pH, the electrostatic repulsions of the carboxylates prevail and overcome the hydrophobic effect, therefore the polymer adopts a random coil conformation and shows good solubility in aqueous solution; at low pH (lower than pH 6), the carboxylates are protonated and the hydrophobicity of the styrene dominates, which results in a compact globular conformation with poor aqueous solubility.[77] As one of the most significant interfacially active polymers, SMA has been used as a polymeric emulsifier or dispersing agent for various applications, such as for dispersing dyes for ink formulations,[78] but the most common applications of SMA are in life science.[27, 79] SMA forms stable polymeric micelles in aqueous solutions with a low critical micelle concentration.[80] SMA micelles were found to be an excellent tumor-targeting drug delivery system for hydrophobic drug molecules, such as doxorubicin,[81] pirarubicin,[82] and zinc protoporphyrin IX (ZnPP) (Figure 1-3).[83] Because of the unique characteristics of the tumor vasculature, drug molecules of certain sizes tend to accumulate in tumor tissue, which is called the enhanced permeability and retention (EPR)

effect.[84] The size of a single SMA micelle ranges from 100 to 200 nm, depends on the structure of the encapsulated drug and the loading. The large molecular size of SMA micelle-drug complexes showed great therapeutic properties due to the EPR effect.[85] In addition, SMA could noncovalently bind to albumin, which is one of the most biocompatible macromolecules, thus the bound albumin could serve as the second drug carrier and further enhance the EPR effect.[86]

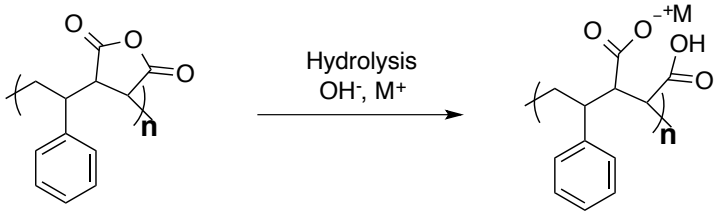

Scheme 1-2. The preparation of SMA copolymer from SMAh through basic hydrolysis.[27]

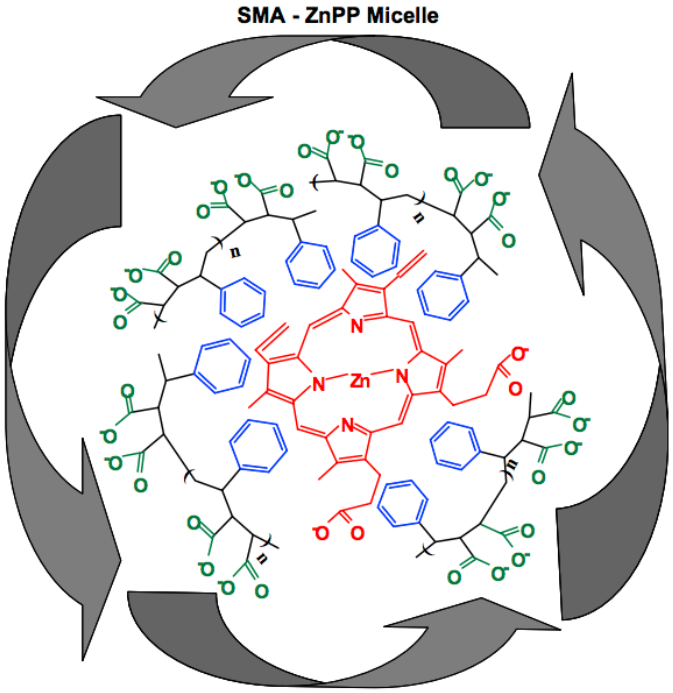

Figure 1-3. The micelle formation of SMA and ZnPP for drug delivery. Each ZnPP (red) is surrounded by four SMA chains, the benzene rings (blue) interact with ZnPP through hydrophobic interaction, and the carboxylic acids (green) provide aqueous solubility. Reprinted from Iyer et al.[83] with permission. Copyright 2007 Elsevier.

Another important application of SMA is on the research of membrane proteins,[27] which usually requires the separation and stabilization of these hydrophobic proteins from cells. In

traditional methods, the membrane proteins are solubilized using small molecule detergent micelles, but often the lipid bilayers are disturbed because of the different physical-chemical properties of the detergents. SMA is now considered as one of the most promising alternatives for membrane solubilization, because it shows a distinctive behavior than other amphiphilic materials: when adding to lipid membranes, it can form discoidal particles spontaneously (Figure 1-4).[87-88] Moreover, these nanodiscs could preserve the bilayer integrity of the lipid as well as the protein functions.[89-90] Therefore, SMA showed the fascinating potential of directly extraction and stabilization of membrane protein from cells in one step.[91] The resulting membrane nanodiscs are termed SMALP (SMA-lipid particles). It is noteworthy that the reported SMA polymers in membrane research were not strictly alternating, and had a ratio of styrene to maleic acid of 2:1 or 3:1, therefore styrene dyads or small blocks may be presented.

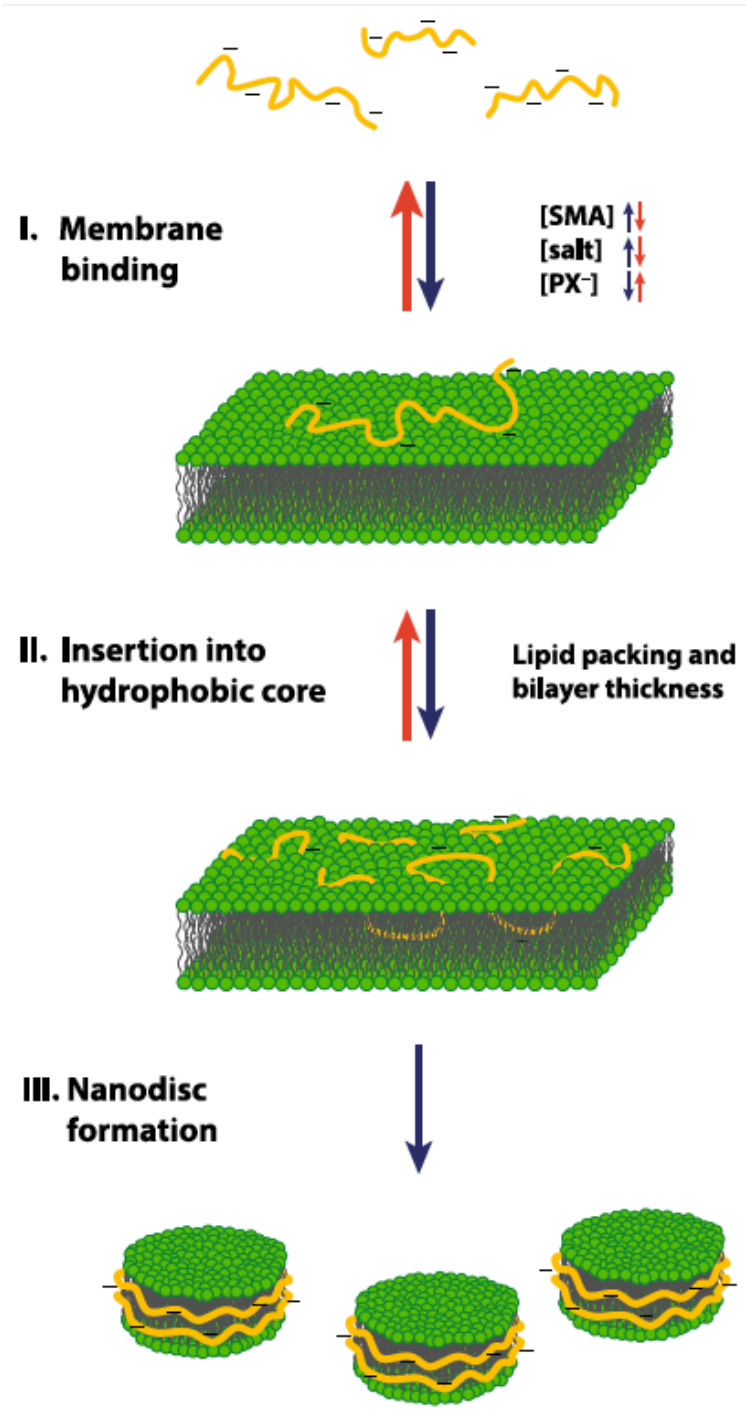

Figure 1-4. The solubilization of lipid membranes by SMA copolymers. SMA first binds with the surface of the membrane with the modulation of the concentration of SMA, salt and negatively charged lipids (PX^-)(I); then SMA inserts into the hydrophobic core of the membrane through the hydrophobic effect (II); finally the membrane is solubilized in the form of nanodiscs (III). Reprinted from Scheidelaar et al.[88] and Dörr et al.[27] with permission. Copyright 2015 Elsevier and 2015 Springer.

SMA copolymer has also been utilized in nanotechnology. SMA could disperse single-walled carbon nanotubes as a surfactant, and in the meanwhile work as templates for binding metal ions and metal nanoparticles.[92] At 50% protonation, SMA could self-assembly into nanotubes[93] due to the stiffening effect of the multiple intrapolymer hydrogen bonding among the acid groups.[94] SMA can also disperse TiO_2 nanocolloidal and patterned on substrates by micro-fluid-contact printing, and well-defined nanostructured TiO_2 layer was achieved by removing the SMA polymers by calcination.[95]

The maleic anhydride groups in SMAh polymers can be easily modified by reacting with amines or hydroxyl groups and forming corresponding amic acid or acid ester, and the amic acid can be further converted to maleimide group with loss of water. Various functional molecules can be introduced to SMAh polymers utilizing this method, which is particularly useful in attaching drug molecules bearing amine groups. SMAh could improve the pharmacological properties of the drugs by increasing their circulatory half-life and increasing their lipid solubility.[96] Moreover, SMAh showed neither teratogenic nor acute or chronic toxic effects.[97] When binding tumor-targeting drugs, they also work to enhance the EPR effect. An important example is using SMAh to deliver the anti-tumor protein neocarzinostatin (NCS).[98-99] In the polymer-drug conjugate, 70% of maleic anhydride groups were reacted with butanol, and the rest were used to bind with NCS (Figure 1-5). The resulting SMANCS conjugate has been clinically used for liver cancer treatment, and commercialized in Japan.[100] Other drugs and biomolecules, such as pirarubicin,[101] fenoprofen, [97] gemfibrozil,[97] and laminin peptide YIGSR,[102] etc.[103] were also conjugated with SMAh by the reaction of amine group with maleic anhydride for delivery. A pH-responsive fluorescent specie, rhodamine-deoxylactam, was attached to SMAh, the fluorescence could be activated by lysosomal pH.[104] The copolymer is likely to accumulate in tumor cells due to the EPR effect, and it could

work as a nanoprobe for detecting tumors. When binding with antimicrobial compounds, the modified copolymer showed high bactericidal effect,[105-106] which enabled the preparation of antibacterial fibers by electronspinning.[105, 107] In addition to bioactive groups, some functional groups could bring interesting properties and applications to SMAh polymer. For example, the insertion of the *N*-sulfonic acid group made SMAh polymer an efficient solid catalyst for a variety of organic reactions;[108] and the modification with diamines,[109] 3-aminobenzoic acid,[110] and aminothiophene derivatives[111] turned SMAh into polymeric sorbents for toxic heavy metal ions like Fe(II), Zn(II), Pb(II), Cu(II), and Cd (II).

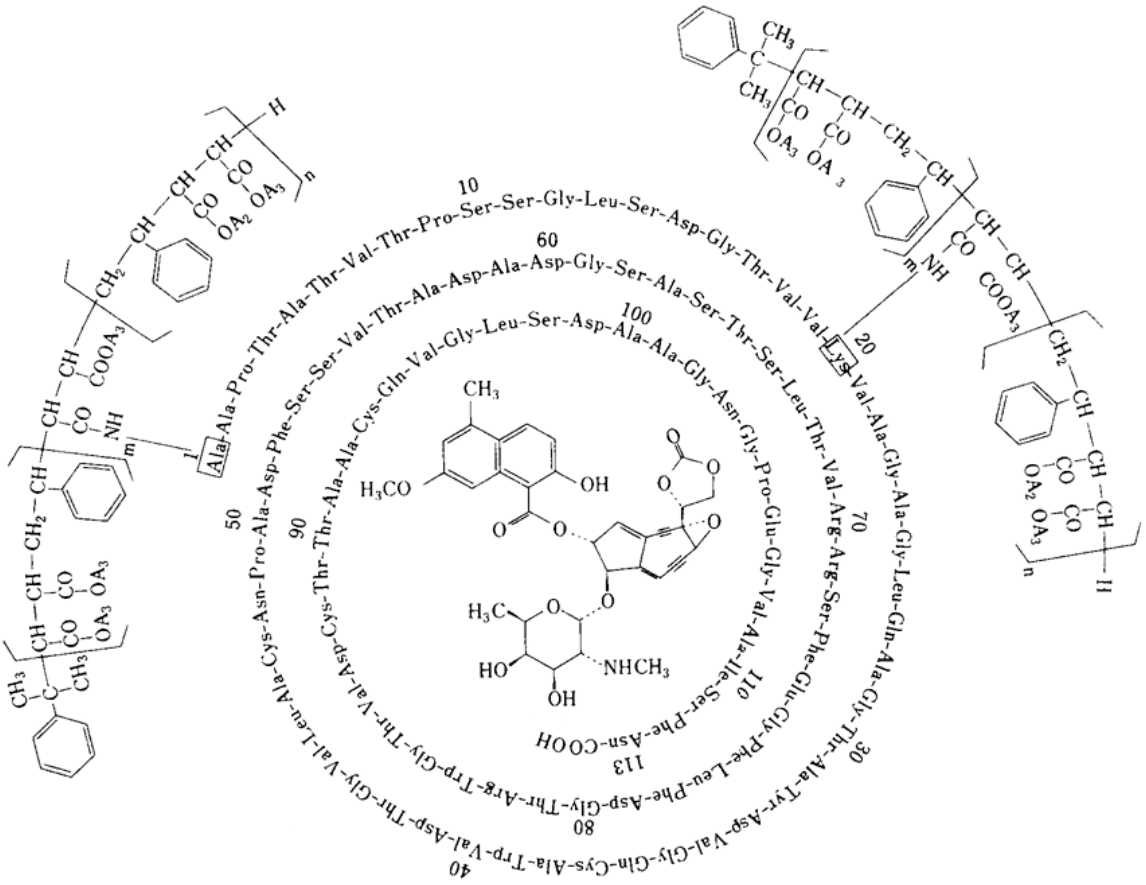

Figure 1-5. The chemical structure of SMANCS. Reprinted from Maeda et al.[99] with permission. Copyright 2013 WILEY-VCH.

Other than binding with functional molecules, the anhydride groups could also be used for purposeful modification of certain surface properties, such as hydrophilicity and complex forming

ability. The ring-opening of the maleic anhydride would result in anionic carboxylate group, which show a pH-dependent amphiphilicity, and the amphiphilicity and their surface activity could be further tuned by binding the anhydride group with different amines or alcohols. For examples, the partially imidized alkyl amines-modified SMAh polymers formed stable latex in water,[112] and the dopamine-modified SMAh polymer self-assembled into stable micelles.[113] The short-chain alkyl amines-modified SMAh polymers showed pH-dependent membrane destabilizing activity, since they are hydrophilic and membrane-inactive at physiological pH, while they become hydrophobic and membrane-disruptive at endosomal pH.[96] The cysteamine-grafted SMAh shows similar behavior as SMA polymer to form nanodiscs with membrane protein, in addition, the pendant SH groups provide sites for functionalization using thiol-reactive chemistry.[114] Cationic quaternary nitrogen units were also inserted to SMAh polymers using the same chemistry.[115] They formed core-shell nanoparticles and showed potential for gene delivery. When binding with aminopyrene, the modified SMAh worked as a "polysoap" surfactant that mimics the structure of DNA to disperse single-walled carbon nanotubes (SWNTs), in which the aromatic base interacts with the SWNT wall, while the charged backbone is at the exterior side of the micelles. Compared to DNA, SMAh is easily modified, more available, and the more flexible structure further improves the SWNT dispersion property.[116]

Some modified SMAh polymers exhibited distinguishable thermal and mechanical properties compared to the unmodified SMAh, and attempts to use these modified SMAh polymers as additives to change the properties of other materials were made. A series of plant oil derivatives were attached to the SMAh polymer, and the epoxidized soybean oil modified SMAh showed a dramatic increase of storage modulus around 190 °C.[117] A novel organic/inorganic polymer hybrid was obtained by the imidization of the SMAh polymer using an amine-containing polyhedral

oligomeric silsesquioxane (POSS).[118] Phase separation was observed in the resulting material, and the films showed excellent transparency and increased hydrophobicity. The methoxyl poly(ethylene glycol) (MPEG) grafted SMAh polymer was added to polyethersulfone (PES) membranes at the phase inversion process.[119] This amphiphilic additive increased the hydrophilicity and protein adsorption resistance of the PES membranes. Aminolyized SMAh polymer as an additive in the wood adhesive urea-formaldehyde (UF) resins during the synthesis could decrease the formaldehyde emission and improve the bonding strength.[120] A smart, electro-active material was achieved by adding the sulfonated aromatic diamine-crosslinked, imidized polymer to poly(vinylidene fluoride) (PVDF) as a potential material for artificial muscles.[121] The obtained ionic membrane exhibited improvement in both electrical and mechanical performance compared to the Nafion-based actuator. SMAh was also used as a compatibilizer in making flame retardant polystyrene material by reacting with the amine groups of the flame retardant poly(diaminodiphenyl methane spirocyclic pentaerythritol bisphosphonate) (PDSPB).[121] The addition of SMAh improved the limiting oxygen index and deduced the peak heat release rate.

The modification of SMAh could also be utilized to achieve polymers of special architectures. Dimethyl-*N, N*-propylamide imidized SMAh was found to self-assemble to nanotubes, which were said to arise from the π-stacking of the styrenes and the van der Waals interactions between the maleimide units.[122] Theoretical studies showed that only racemo-diisotactic configuration of imidized SMAh polymer could form complexes by π-stacking, when the phenyl groups and maleimides are symetrically distributed.[123] Layer-by-layer stacking of SMAh and polyethylenimine (PEI) were reported to fabricate into nanotube structure using an alumina template.[124] Dendronized copolymers were synthesized by attaching poly(amidoamine) dendrons to SMAh. The butylamide terminated poly(amidoamine) dendrons brought thermo-

responsiveness to the copolymer, the copolymers showed lower critical solution temperatures (LCSTs) of 33.1 °C – 49.0 °C, depends on both the generation of the dendrons and the local pH (Figure 1-6).[125] When the dendrons were terminated with the UV-responsive molecule *o*-nitrobenzyl alcohol, the structure of the copolymer aggregates dramatically loosened under UV irradiation, which made this dendronized copolymer a candidate for drug encapsulation and release.[126]

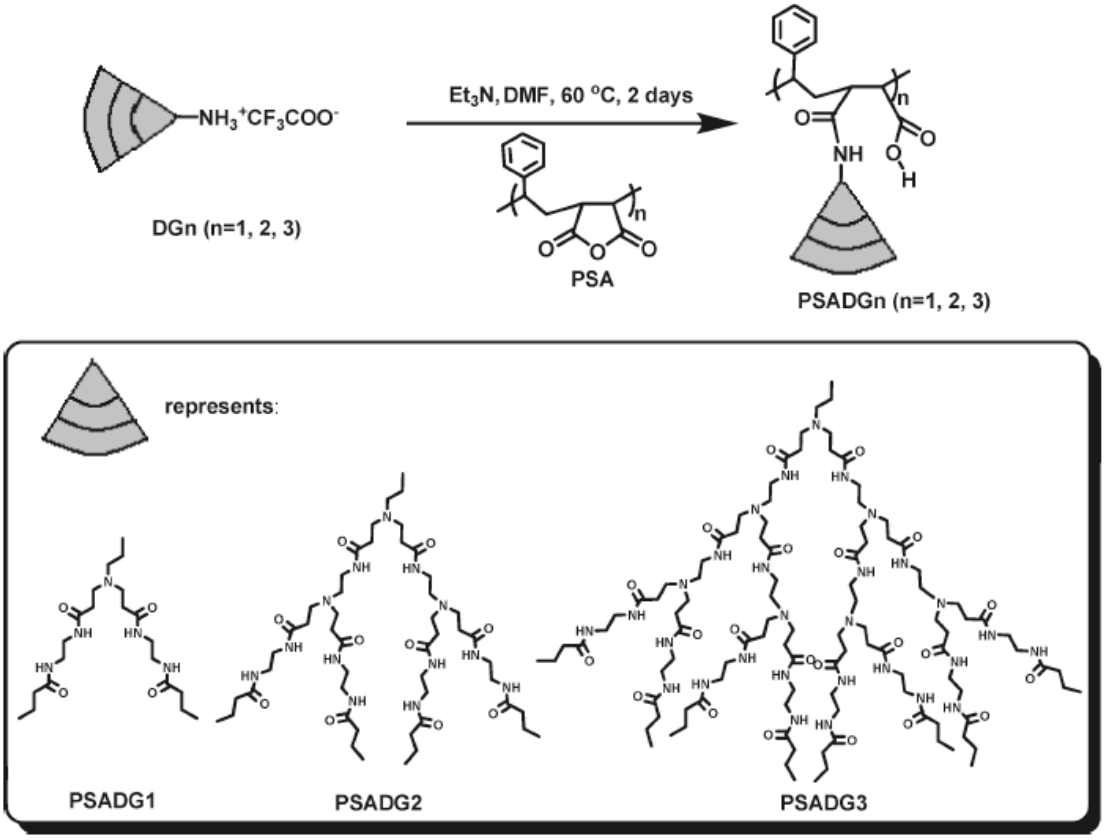

Figure 1-6. Synthesis and structures of thermo-responsive dendrimers. Reprinted with permission from Gao et al.[125] Copyright 2009 American Chemical Society.

Graft copolymers could be prepared by reacting SMAh with amine- or alcohol-terminated polymer chains, the resulting graft polymers bear negative charges on the carboxylate group next to the side chain, and the side chains are designed to impart to the SMAh copolymers a variety of useful properties. One of the commonly used side chain polymer is poly(ethylene glycol)

(PEG).[127-128] The resulting amphiphilic graft copolymer exhibited LCST in the range of 33.7 °C – 74.7 °C, and the LCST is highly dependent on both pH and molecular weight of the side chain PEG.[129] Hydrogel microspheres were also prepared by crosslinking this PEG-grafted SMAh polymer with polyamines, the microsphere swelled in response to increased salt concentration due to the shielding effect of the electrostatic association.[130] When the PEG side chain was attached to SMAh by using lithium alcoholates, the film fabricated using this graft copolymer showed conductivity in the range of 10^{-7} to 10^{-5} $S \cdot cm^{-1}$ due to the anion mobility with segmental motions, and the conductivity further increased to $5x10^{-4}$ $S \cdot cm^{-1}$ after adding BF_3, which suggests this polymer to be considered for potential lithium battery applications.[131] Polyethylenimine was grafted on to SMAh for gene delivery. The copolymer established effective DNA condensation and protect DNA from degradation by DNase.[132] Another strategy to synthesize graft copolymers is to polymerize macromonomers with maleimide or vinylbenzyl endgroups, and which resulted in a highly densely grafted copolymer (graft on each monomer) with alternating side chains.[133] A series of LCST copolymers were synthesized from the polymerization of 4-vinylbenzyl methoxytetra(oxyethylene) ether and *N*-substituted maleimides, and the transition temperature could be tuned by the side chain length.[134] Recently, this method was employed to synthesize graft copolymers with sequence regulated side chains (Figure 1-7). The side chains were first synthesized via atom transfer radical addition to yield halide-ended sequence-controlled oligomers, followed by reacting the halide end with a furan-protected maleimide.[135-136] After deprotection of the furan group, the resulting maleimide-ended macromonomer readily form an alternating copolymer with styrene. Some properties of the copolymers, such as solubility and T_g could be tuned by both the sequence of the side chain and the ratio of the two monomers in the main chain.

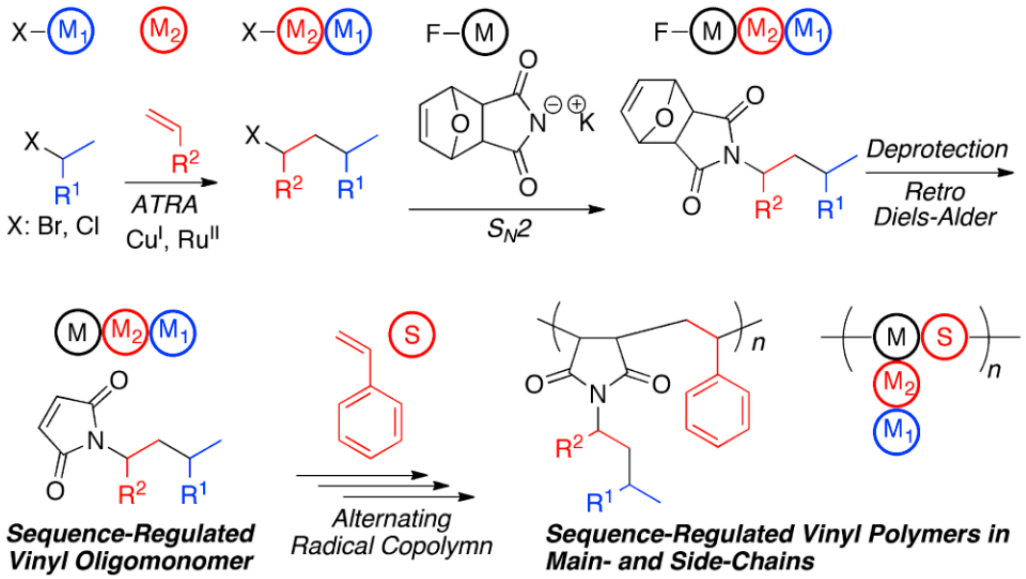

Figure 1-7. Graft copolymer with sequence-regulated side chains by atom transfer radical addition and alternating radical copolymerization. Reprinted from Soejima et al.[136] with permission. Copyright 2015 American Chemical Society.

Functional groups can also be incorporated by using functionalized styrene or *N*-substituted maleimide. A wide variety of functional groups could be attached onto styrene or maleimide monomers using easy chemistry, and the functional groups could impart a variety of physical and chemical properties. For example, a water soluble alternating copolymer was synthesized the free radical polymerization of sulfonated styrene and sodium-*N*-(4-sulfophenyl)-maleimide monomers.[137] Polymers with active pendant double bonds are difficult to be prepared by direct radical polymerization of monomers with two different double bonds, which would result in crosslinked or cyclized structures in most cases. However, an active pendant double bond could be achieved by the direct radical polymerization of *N*-allylmaleimide with substituted styrene due to the strong alternating behavior and predominant fast cross-propagation of styreneic and maleimide double bonds.[138] The pendant double bonds are available for future modification. The RAFT cyclocopolymerization of maleic anhydride and difunctional styrenic monomers that contain tri- or tetra(ethylene glycol) moieties led to a series of copolymers with crown ether

cavities.[139] The crown ether cavities exhibited selectivity for dialkylammonium ions and the copolymers may have potential in size-selective complexations.

1.4.3 Semi-rigid stilbene-containing alternating copolymers

The chain-growth homopolymerization of *trans*-stilbene ((*E)*-1,2-diphenylethylene) is very difficult to achieve because of its steric constraints.[9] However, electron-rich *trans*-stilbene monomer readily radically copolymerize with electron-poor monomers like maleic anhydride or *N*-substituted maleimides in an alternating fashion due to both the electronic effects and reduced steric stress.[140] The first preparation of the stilbene and maleic anhydride alternating copolymer was reported in 1930 by Wagner-Jauregg,[141] and it was also said to be the earliest report of a free radical-copolymerization in literature.[142] The copolymer was insoluble in common solvents and the insolubility was assumed to be from crosslinking.[140-141] Vogl, however, discovered that these copolymers were not crosslinked by finding that the stilbene-maleic anhydride copolymer was soluble in basic solution, when anhydride rings were opened and converted into salts.[143]

Another possible reason of the poor solubility of unsubstituted stilbene and maleic anhydride is the strong aggregation of the copolymers, therefore the solubility of the substituted copolymers greatly increased due to the disruption of copolymer aggregation.[144] Moreover, functional substituents work as a powerful tool in the construction of highly functional polymeric materials. Our group has been working on the design and synthesis of functionalized stilbene and maleic anhydride/*N*-substituted maleimide comonomers and the corresponding alternating copolymers.[140, 144-157] These novel copolymers possess sterically congested backbones and precisely placed functional groups arising from the strictly alternating copolymerization. We have incorporated these alternating sequences into block copolymers and crosslinked copolymers and studied their interesting properties and potential applications.

Most of the substituted stilbenes in our studies were synthesized by the Wittig–Horner reaction (Scheme 1-3).[158] The substituents include methyl,[144, 149] dialkyl amino,[145, 148, 154-155] and *tert*-butyl carboxylate.[146-147, 149-150, 152-153] Both the type and the position of the substituents on the stilbene monomer affect the rate of the copolymerization and the properties of the copolymers. Stilbene with electron-donating groups, like methyl and dialkyl amino groups undergo faster copolymerization while the stilbene bearing electron-withdrawing carboxylate needs a higher temperature to efficiently copolymerize.[147] The *N*-substituted maleimides were usually synthesized from a two-step route, in which maleic anhydride was mixed with a primary amine to produce a maleamic acid, which was then dehydrated to form a maleimide. The substituents have minimal effect on the electron-deficient nature of maleimides, but different from maleic anhydride, maleimides can radically homopolymerize.[159] Therefore, although alternating copolymerization predominates when stilbene or styrene monomers are present, there will be maleimide-maleimide dyads in the copolymers.[140]

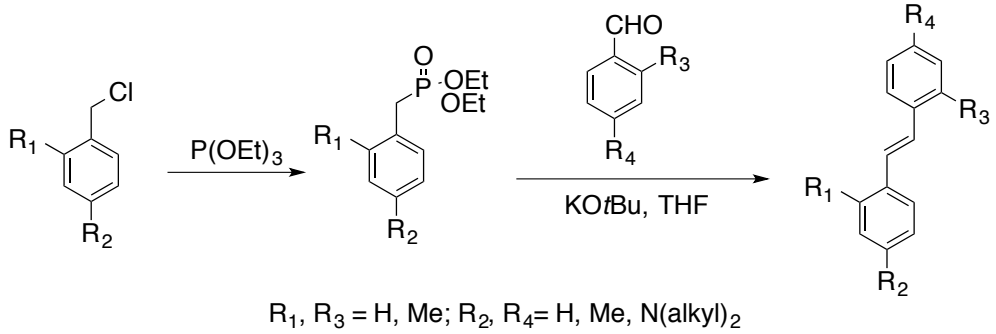

Scheme 1-3. Synthesis of substituted trans stilbenes using Wittig-Horner reaction. Reproduced from Li et al.[144] with permission. Copyright 2010 Elsevier.

Our initial studies of substituted stilbene-maleic anhydride alternating copolymers indicated significant chain stiffening in solution, as evidenced by a constant hydrodynamic radius (10 nm) in the temperature range of 10 ˚C and 40 ˚C, and no observable glass transition below 250 ˚C.[155] Furthermore, the ^{1}H NMR of these polymers showed broad backbone and aromatic peaks,[144] which

is related to strong homonuclear dipolar coupling and slow proton relaxation rates.[160] Double-quantum heteronuclear local field solid state NMR showed that the maleic anhydride was enchained in all *cis* configuration when *N,N,N',N'*-tetraethyl-4, 4'-diaminostilbene was the comonomer.[148] Moreover, the cast film of the stilbene and *N*-(2-methylphenyl)maleimide copolymer exhibited large negative birefringence induced from the conformational constraints.[157] All this evidence revealed the hindered rotation and the limited movement of these alternating copolymers due to their sterically crowded backbones. A detailed study on the chain stiffness of a series of *tert*-butyl group-containing stilbene and styrene alternating copolymers was conducted using SEC and SAXS, and the persistence lengths (l_p) of these copolymers fell into the range of 2 and 6 nm.[147] Compared to the flexible polystyrene (l_p=0.9 nm)[161] and the rigid polyphenylene (l_p=13 nm)[162], these alternating copolymers are classified as semi-rigid polymers (Figure 1-8). The same series of copolymers also showed nanoporosity, which is due to the internal free volume resulted from the inefficient chain packing, and the BET surface area of these polymers increased as the increasing of the l_p.[151] When the semi-rigid stilbene-maleimide alternating sequence was incorporated into divinyl benzene hypercrosslinked polymers, the precursors showed increased T_g, which reduces some pore collapsing during the post-crosslinking step.[149]

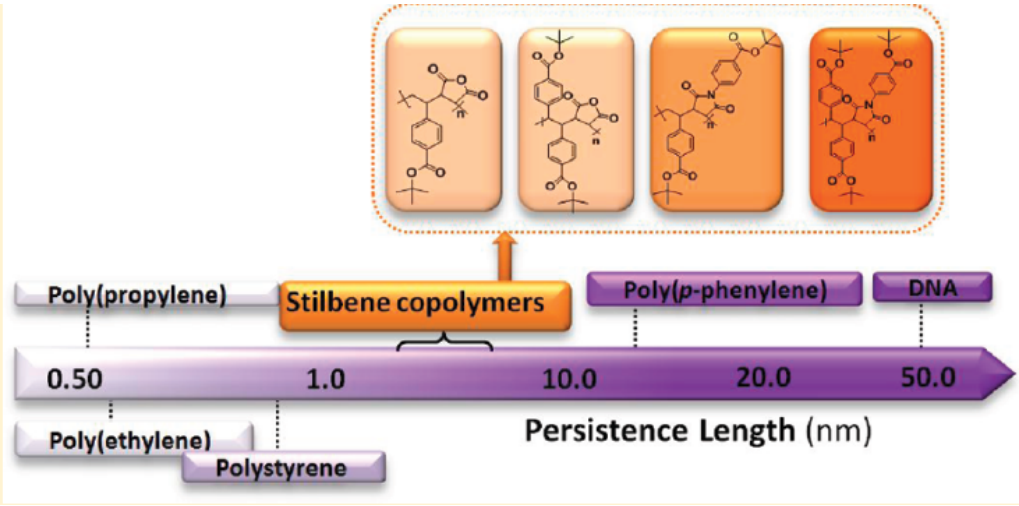

Figure 1-8. The comparison of the persistence length of a series of semi-rigid alternating copolymers with other polymers. Reprinted from Li et al.[147] with permission. Copyright 2012 American Chemical Society.

Among the various functional groups we incorporated into the alternating copolymers, the dialkylamino[145, 148, 154-155, 157] and the *tert*-butyl carboxylate[146-147, 150-153] groups are of special interests, since they can be converted to ammonium and carboxylic acid, respectively. In addition, the enchained maleic anhydride groups can be hydrolyzed and form two carboxylic acid groups. Using the chemistry described above, we synthesized a series of semi-rigid polyelectrolytes and polyampholytes.[145, 152-154, 156] The polyampholyte diblock copolymers formed polyion complexes, and exhibited an unusual "like-charge" attraction in response to pH and salt changes (Figure 1-9).[145, 156] This antipolyelectrolyte effect is manifested by the semi-rigid polymer backbone induced dipole-dipole interactions of the condensed counter ions. The polyanions were prepared from the *tert*-butyl group protected precursors, and the organic soluble precursors facilitated accurate molecular weight determination by SEC.[153] The resulting polyanions showed excellent anti-HIV activity. It is hypothesized that the increased rigidity of the polyanions enhanced the electrostatic interaction with the V3 loop of the HIV-1 glycoprotein 120 or glycoprotein 41.[146] This deprotection strategy was also utilized in a novel two-step synthesis of nanoporous polymers. The semi-rigid

polymer backbone along with the high crosslinking density resulted in a highly functionalized network with high BET surface areas (up to 817 m^2/g) and good potential in CO_2 capture applications (Figure 1-10).[150]

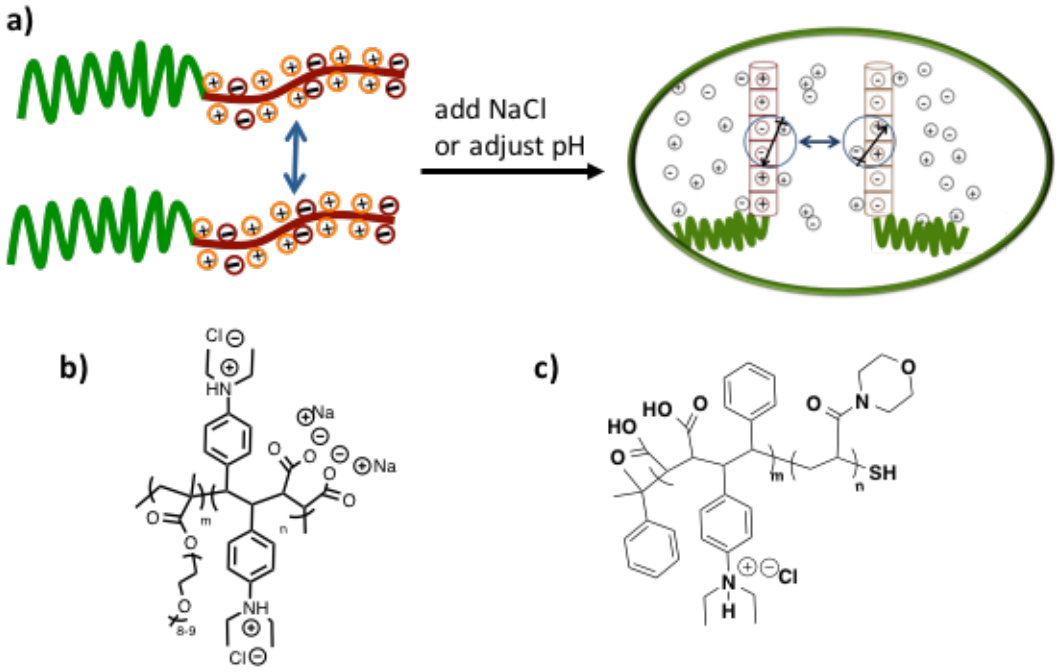

Figure 1-9. a) The graphic demonstration of "like-charge" attraction, and the structures of two block copolymers b) OEGMA-b-(TEDASti-alt-MA) and c) (DEASti-alt-MA)-b-ACMO that shows "like-charge" attraction. Reproduced with permission from Savage et al.,[156] Mao et al.,[145] and Savage et al.,[154] respectively. Copyright 2016 WILEY-VCH, 2007 American Chemical Society, and 2014 WILEY-VCH.

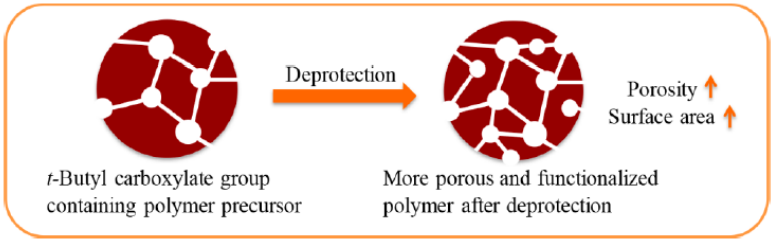

Figure 1-10. Nanoporous polymers from cross-linked polymer precursors via *tert*-butyl group deprotection. Reprinted from Huang et al.[150] with permission. Copyright 2015 American Chemical Society.

The alternating copolymerization behavior of stilbene and maleic anhydride or maleimide was also used to synthesize specially structured polymers. For example, a processable polymer

resin was resulted from the self-polymerization of a stilbene-maleimide A-B monomer,[163] and the single-chain polymer nanoparticles were synthesized from the alternating copolymerization of maleic anhydride or *N*-ethyl maleimide with stilbene functionalized polystyrene chains.[164]

1.4.4 Sequence-controlled alternating copolymers

Biomacromolecules, such as DNA and protein, store enormous genetic or functional information by arranging the sequence of nucleic acids or amino acids in their primary structures. However, synthetic polymerization techniques usually lack control over the monomer sequential arrangement. Although the library of synthetic polymers contains hundreds of thousands of different monomers, the potential of information storage in synthetic polymers is still limited.[165] Much effort has been invested to tap this potential in synthetic copolymer, however, the resulting step-by-step solid synthesis or other semibiological approaches are restricted by the speed and scale of synthesis.[166]

Over the last decade, the unique kinetic feature of donor-acceptor alternating copolymerization has inspired polymer chemists to design a new strategy in the sequence-controlled polymerization. In 2007, Lutz and coworkers first introduced a sequence-control strategy, which is based on the ATRP copolymerization of donor and acceptor monomer pairs (Figure 1-11).[167] The basic principle of this method was utilized time-controlled addition of a small amount (usually 1 mole equiv. as compared to initiator) of the acceptor monomers (i.e. *N*-substituted maleimides) during the controlled polymerization of a large excess donor monomer (i.e. styrene).[167] The strong alternating copolymerization tendency of the newly added acceptor with the donor monomers leads to an immediate consumption of the acceptor monomer. Ideally, one acceptor monomer is inserted into each polymer chain at the same chain-location after each addition. However, although the alternating copolymerization is kinetically favored, the

distribution of the acceptor in each chain is not strictly uniform and remains statistical in a rather narrow range.[166] Still, this method revealed new opportunities for precisely encoding information into polymer chains.

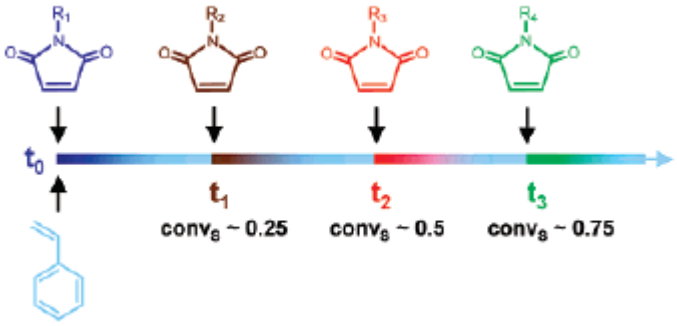

Figure 1-11. Concept of the Sequence-Controlled Copolymerization of Styrene and Various *N*-Substituted Maleimides. Reprinted from Lutz et al.[180] with permission. Copyright 2011 WILEY-VCH.

N-substituted maleimides are mostly used as the acceptor monomer in this approach. One major reason is that the functionalization at the *N*-site is relatively easy and does not significantly affect the electron-deficient nature of the maleimide double bond.[9] Therefore, the enormous stockroom of *N*-substituted maleimides provides abundant combinations for encoding information into the polymer chains. The substituents include alkyl, aryl, acyl, benzyl, propargyl, PEG, etc.[166, 168-169] Some substituents may hinder the polymerization by interfering with the radical or interacting with the metal catalyst, therefore substituents such as phenol,[168] terminal alkynes,[168, 170-171] carboxylic acids,[168] and primary amines[170] need to be protected before being used in this sequence-controlled procedure. There are also some substituents that cannot be used in this procedure due to solubility or other problems, such functionalities can be achieved by post-polymerization modification.[166, 168] For example, protected alkyne-containing maleimides could be easily modified by Cu-catalyzed azide-alkyne "click" reaction, Glaser coupling, thio-yne reaction, Sonogashira coupling,[166, 170-173] or self-reacted by Eglinton coupling,[174] and

pentafluorophenyl ester-containing maleimide could attach the amine groups or add on a variety of functional groups using the thiol-*para* fluoro "click" reaction.[174]

The donor monomer provides the main backbone of the polymer, therefore it defines the most of the properties like the chain rigidity, solubility, and crystallinity.[166, 175-177] Styrene is often used as the donor monomer mainly because the controlled radical homopolymerization and copolymerization of styrene has been extensively studied and it is convenient to monitor the kinetics in the sequence-controlled process.[167-168] Some substituted styrene monomers can also be employed as the donor monomer, however, only electron-donating substituents are suitable for this process because they are favorable to the alternating copolymerization and can ensure the precise insertion of the acceptor monomers into the chains.[166] Therefore, *para*-alkyl-substituted styrene, [167, 175] 4-acetoxystyrene,[178] 4-*tert*-butoxystyrene,[178] and vinyl benzyl amine[179] showed better performances in the precise insertion of maleimides compared to the esters of vinyl benzoic acid or vinyl benzyl chloride.[166]

Controlled radical polymerization (CRP) is crucial for this sequence controlled procedure because it ensures all chains grow simultaneously.[167] ATRP is the most commonly used technique in their process,[166-167, 180] while NMP was also reported.[175, 177] The precision in time-controlled addition also affects the precision insertion of the maleimides units, therefore robotic, automated protocols were shown to improve the experimental conditions.[181] Under such conditions, up to 8 nonoverlapping maleimide zones could be inserted within 100 styrene units, which corresponds to n^8 microstructure arrangements within a chain length of 100 when n kinds different maleimides are used. Other than encoding information on the primary structure of the polymer chains, the precisely enchained maleimides units could also be utilized for creating secondary structures, and further affect the properties of the materials. For example, the small amounts of maleimides have

significant influence on the side-chain crystallinity of poly(octadecylstyrene),[175] and the insertion of maleimides which contain reactive functional groups after deprotection could result in intramolecular bridges[170, 182] (Figure 1-12) and achieve different topology such as α-, P-, Q-, and 8- shapes,[182] periodic multi-block polymers,[183] and compartmentalized single-chain objects.[174]

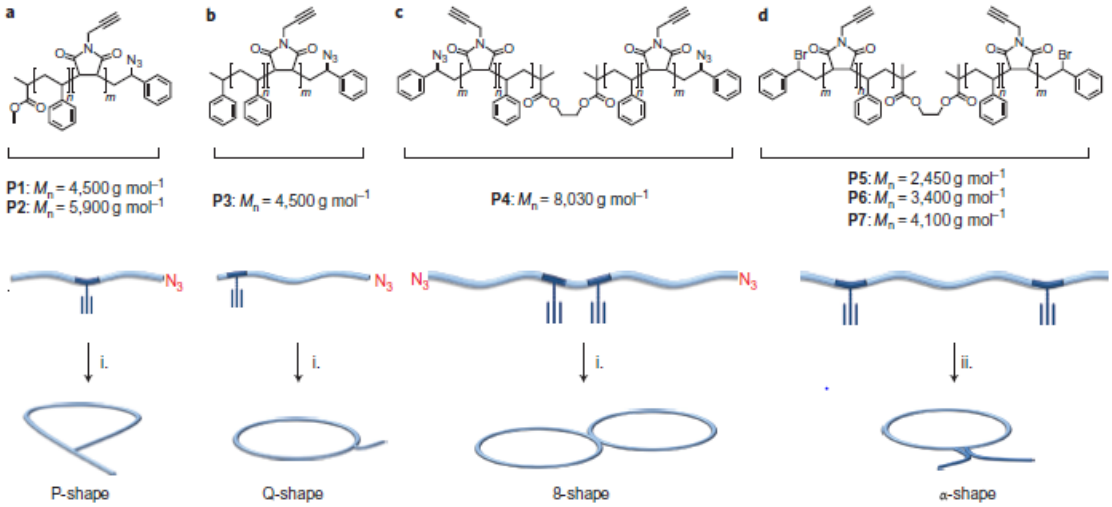

Figure 1-12. Different topology (α-, P-, Q-, and 8- shapes) achieved using sequence-controlled polymers, i represents coppor-catalyzed azide-alkyne 1,3-dipolar cycloaddition, and ii represents Glaser coupling. Reprinted with permission from Schmidt et al.[170] Copyright 2011 Nature Publishing Group.

1.5 Conclusion

Alternating copolymerization has origins dating back, almost 90 years, to the early days of synthetic polymer chemistry,[141] and it has grown to be a vibrant and productive area of current polymer chemistry for producing new creative functional polymer structure with precise placement of functional groups along the polymer backbone. This feature article focuses on one important class of alternating copolymers – electron rich benzylidene monomers such as styrene and stilbene derivatives and their alternating copolymers with electron poor maleic anhydride and *N*-substituted maleimides. The unique nature of the fast cross-propagation step that leads to alternation enables the copolymerization of monomers that do not homopolymerize, such as stilbene and maleic anhydride, to form strictly alternating copolymers. The fast crosspropagation also results in

predominately alternating dyad placements of styrenic monomers with *N*-substituted maleimides at 1:1 comonomer feeds.

The alternating copolymer structures provide a plethora of functional polymer backbones with semi-rigidity, which can be controlled by comonomer selection, that suggest unique optical, mechanical, solution, and biological properties. The fast cross-propagation is now enabling the synthesis of unprecedented sequence regulated structures providing new insights into the power of synthetic polymer chemistry to synthesize precision copolymers. In the future, it is no doubt that benzylidene based monomers will be creatively employed to make new and interesting alternating copolymers that assist polymer scientists in understanding fundamental polymer structure property relationships as well as providing new materials with desired properties for applications in emerging technology areas.

1.6 References

1. Nomenclature, D. o. C.; Pure, S. R. I. U. o.; Chemistry, A.; Nic, M.; Jirat, J.; Kosata, B., *IUPAC goldbook*. IUPAC: 2006.
2. Morris, P. J., *Polymer pioneers: A popular history of the science and technology of large molecules*. Chemical Heritage Foundation: 2005.
3. Yokota, K., Periodic copolymers. *Prog. Polym. Sci.* **1999,** *24* (4), 517-563.
4. Matyjaszewski, K.; Ziegler, M. J.; Arehart, S. V.; Greszta, D.; Pakula, T., Gradient copolymers by atom transfer radical copolymerization. *J. Phys. Org. Chem.* **2000,** *13* (12), 775-786.
5. Lutz, J.-F., Aperiodic copolymers. *ACS Macro Lett.* **2014,** *3* (10), 1020-1023.
6. Lutz, J.-F.; Ouchi, M.; Sawamoto, M.; Meyer, T. Y., *Sequence-controlled polymers: synthesis, self-Assembly, and properties*. American Chemical Society: 2014; Vol. 1170, p 0.

7. Lutz, J.-F., Sequence-controlled polymerizations: the next Holy Grail in polymer science? *Polym. Chem.* **2010,** *1* (1), 55-62.

8. Badi, N.; Chan-Seng, D.; Lutz, J.-F., Microstructure control: An underestimated parameter in recent polymer design. *Macromol. Chem. Phys.* **2013,** *214* (2), 135-142.

9. Odian, G., *Principles of polymerization*. Wiley: 2004.

10. Cowie, J. M. G., *Alternating copolymers*. Springer US: 2013.

11. Mayo, F. R.; Lewis, F. M., Copolymerization. I. A basis for comparing the behavior of monomers in copolymerization; the copolymerization of styrene and methyl methacrylate. *J. Am. Chem. Soc.* **1944,** *66* (9), 1594-1601.

12. Fukuda, T.; Ma, Y. D.; Inagaki, H.; Kubo, K., Penultimate-unit effects in free-radical copolymerization. *Macromolecules* **1991,** *24* (2), 370-375.

13. Barb, W., Effect of nonterminal monomer units on the reactivity of polymeric free radicals. *J. Polym. Sci.* **1953,** *11* (2), 117-126.

14. Jones, S. A.; Prementine, G. S.; Tirrell, D. A., Model copolymerization reactions. Direct observation of a "penultimate effect" in a model styrene-acrylonitrile copolymerization. *J. Am. Chem. Soc.* **1985,** *107* (18), 5275-5276.

15. Klumperman, B., Mechanistic considerations on styrene–maleic anhydride copolymerization reactions. *Polym. Chem.* **2010,** *1* (5), 558-562.

16. Heuts, J. P. A.; Sudarko; Gilbert, R. G., First-principles prediction and interpretation of propagation and transfer rate coefficients. *Macromol. Symp.* **1996,** *111* (1), 147-157.

17. Deb, P.; Meyerhoff, G., Study on kinetics of copolymerization of styrene and maleic anhydride in methyl ethyl ketone. *Polymer* **1985,** *26* (4), 629-635.

18. Dodgson, K.; Ebdon, J., On the role of monomer—monomer donor—acceptor complexes in

the free-radical copolymerisation of styrene and maleic anhydride. *Eur. Polym. J.* **1977,** *13* (10), 791-797.

19. Tsuchida, E.; Tomono, T., Discussion on the mechanism of alternating copolymerization of styrene and maleic anhydride. *Macromol. Chem. Phys.* **1971,** *141* (1), 265-298.
20. Hirai, H., Mechanism of alternating copolymerization of acrylic monomers with donor monomers in the presence of Lewis acid. *J. Polym. Sci. Macromol. Rev.* **1976,** *11* (1), 47-91.
21. Kuntz, I.; Chamberlain, N.; Stehling, F., Poly [2, 2-dimethyl-4-(methoxylcarbonyl) butylene]: Synthesis with an ethylaluminum sesquichloride–peroxide initiator and NMR characterization. *J. Polym. Sci. A Polym. Chem.* **1978,** *16* (7), 1747-1753.
22. Hall, H.; Padias, A. B., "Charge transfer" polymerization—and the absence thereof! *J. Polym. Sci. A Polym. Chem.* **2001,** *39* (13), 2069-2077.
23. Hall, H.; Padias, A. B., Organic and polymer chemistry of electrophilic tri-and tetrasubstituted ethylenes. *J. Polym. Sci. A Polym. Chem.* **2004,** *42* (12), 2845-2858.
24. Saldivar-Guerra, E.; Vivaldo-Lima, E., *Handbook of polymer synthesis, characterization, and processing*. John Wiley & Sons: 2013.
25. Rzaev, Z. M. O., Complex-radical alternating copolymerization. *Prog. Polym. Sci.* **2000,** *25* (2), 163-217.
26. Braun, D.; Hu, F., Polymers from non-homopolymerizable monomers by free radical processes. *Prog. Polym. Sci.* **2006,** *31* (3), 239-276.
27. Dörr, J. M.; Scheidelaar, S.; Koorengevel, M. C.; Dominguez, J. J.; Schäfer, M.; van Walree, C. A.; Killian, J. A., The styrene–maleic acid copolymer: a versatile tool in membrane research. *Eur. Biophys. J.* **2016,** *45* (1), 3-21.
28. Alfrey, T.; Lavin, E., The copolymerization of styrene and maleic anhydride. *J. Am. Chem.*

Soc. **1945,** *67* (11), 2044-2045.

29. Trivedi, B., *Maleic anhydride*. Springer Science & Business Media: 1982.
30. Moore, E. R., Properties of styrene-maleic anhydride copolymers. *Ind. Eng. Chem. Prod. Res. Dev.* **1986,** *25* (2), 315-321.
31. Wang, F. C.-Y., Composition and structure analysis of styrene—maleic anhydride copolymer by pyrolysis-gas chromatography. *J. Chromatogr. A* **1997,** *765* (2), 279-285.
32. Olabisi, O.; Adewale, K., *Handbook of thermoplastics*. CRC press: 2016; Vol. 41.
33. Brydson, J. A., *Plastics materials*. Butterworth-Heinemann: 1999.
34. Polyscope promotes SMA as 'versatile' polymer modifier for amorphous thermoplastics. *Addit. Polymer* **2010,** *2010* (4), 2-3.
35. Walling, C.; Mayo, F. R., The effect of substitution on the reactivity of the styrene double bond towards free-radical attack: the nature of the "alternating effect" in copolymerisation. *Farad. Discuss.* **1947,** *2* (0), 295-303.
36. Walling, C.; Briggs, E. R.; Wolfstirn, K. B.; Mayo, F. R., Copolymerization. X. The effect of meta-and para-substitution on the reactivity of the styrene double bond. *J. Am. Chem. Soc.* **1948,** *70* (4), 1537-1542.
37. Tsuchida, E.; Tomono, T.; Sano, H., Solvent effects on the alternating copolymerization systems. Evaluation on equilibrium constants by NMR spectroscopy. *Macromol. Chem. Phys.* **1972,** *151* (1), 245-264.
38. Bamford, C.; Barb, W., The copolymerization of styrene and maleic anhydride. Free radical reactivities under heterogeneous conditions. *Farad. Discuss.* **1953,** *14*, 208-216.
39. Dodgson, K.; Ebdon, J. R., The terpolymerisation of styrene, methyl methacrylate and maleic anhydride. *Macromol. Chem. Phys.* **1979,** *180* (5), 1251-1256.

40. Matsuda, M.; Abe, K., Polymerization initiated by the charge-transfer complex of styrene and maleic anhydride in the presence of cumene and of cumene and liquid sulfur dioxide. *J. Polym. Sci. A Polym. Chem.* **1968,** *6* (6), 1441-1447.

41. Farmer, R.; Hill, D.; O'donnell, J., Study of the role of charge-transfer complexes in some bulk-phase free-radical polymerizations. *J. Macromol. Sci., Pure Appl. Chem.* **1980,** *14* (1), 51-68.

42. Bonilla-Cruz, J.; Caballero, L.; Albores-Velasco, M.; Saldívar-Guerra, E.; Percino, J.; Chapela, V. *Mechanism and kinetics of the induction period in nitroxide mediated thermal autopolymerizations. Application to the spontaneous copolymerization of styrene and maleic anhydride*, Macromol. Symp., Wiley Online Library: 2007; pp 132-140.

43. Wu, D. C.; Hong, C. Y.; Pan, C. Y.; He, W. D., Study on controlled radical alternating copolymerization of styrene with maleic anhydride under UV irradiation. *Polym. Int.* **2003,** *52* (1), 98-103.

44. Zhao, C.; Dong, J.; Li, S.; Fan, Z., Synthesis and characterization of heat-resistant N-phenylmaleimide–styrene–maleic anhydride copolymers and application in acrylonitrile–butadiene–styrene resin. *J. Appl. Polym. Sci.* **2012,** *126* (1), 169-178.

45. Qiu, G.-M.; Zhu, B.-K.; Xu, Y.-Y.; Geckeler, K. E., Synthesis of ultrahigh molecular weight poly (styrene-alt-maleic anhydride) in supercritical carbon dioxide. *Macromolecules* **2006,** *39* (9), 3231-3237.

46. Buchak, B. E.; Ramey, K. C., Monomer sequence distribution in styrene-maleic anhydride copolymers. *J. Polym. Sci. C Polym. Lett.* **1976,** *14* (7), 401-405.

47. Montaudo, M. S., Determination of the compositional distribution and compositional drift in styrene/maleic anhydride copolymers. *Macromolecules* **2001,** *34* (9), 2792-2797.

48. Schoukens, G.; Martins, J.; Samyn, P., Insights in the molecular structure of low-and high-molecular weight poly (styrene-maleic anhydride) from vibrational and resonance spectroscopy. *Polymer* **2013,** *54* (1), 349-362.

49. Matyjaszewski, K.; Spanswick, J., Controlled/living radical polymerization. *Mater. Today* **2005,** *8* (3), 26-33.

50. Braunecker, W. A.; Matyjaszewski, K., Controlled/living radical polymerization: features, developments, and perspectives. *Prog. Polym. Sci.* **2007,** *32* (1), 93-146.

51. Matyjaszewski, K., *Controlled/living radical polymerization: progress in ATRP, NMP, and RAFT*. ACS Publications: 2000.

52. Chen, G.-Q.; Wu, Z.-Q.; Wu, J.-R.; Li, Z.-C.; Li, F.-M., Synthesis of alternating copolymers of *N*-substituted maleimides with styrene via atom transfer radical polymerization. *Macromolecules* **2000,** *33* (2), 232-234.

53. Jiang, X.; Zhong, Y.; Yan, D.; Yu, H.; Zhang, D., Hyperbranched copolymers of p-(chloromethyl) styrene and N-cyclohexylmaleimide synthesized by atom transfer radical polymerization. *J. Appl. Polym. Sci.* **2000,** *78* (11), 1992-1997.

54. Zhao, Y. L.; Zhang, J. M.; Jiang, J.; Chen, C. F.; Xi, F., Atom transfer radical copolymerization of *N*-hexylmaleimide and styrene in an ionic liquid. *J. Polym. Sci. A Polym. Chem.* **2002,** *40* (20), 3360-3366.

55. Qiang, R.; Fanghong, G.; Bibiao, J.; Dongliang, Z.; Jianbo, F.; Fudi, G., Preparation of hyperbranched copolymers of maleimide inimer and styrene by ATRP. *Polymer* **2006,** *47* (10), 3382-3389.

56. Lessard, B. t.; Maric, M., One-step poly (styrene-*alt*-maleic anhydride)-*block*-poly (styrene) copolymers with highly alternating styrene/maleic anhydride sequences are possible by

nitroxide-mediated polymerization. *Macromolecules* **2009,** *43* (2), 879-885.

57. Harrisson, S.; Wooley, K. L., Shell-crosslinked nanostructures from amphiphilic AB and ABA block copolymers of styrene-*alt*-(maleic anhydride) and styrene: polymerization, assembly and stabilization in one pot. *Chem. Commun.* **2005,** (26), 3259-3261.

58. Park, E. S.; Kim, M. N.; Lee, I. M.; Lee, H. S.; Yoon, J. S., Living radical copolymerization of styrene/maleic anhydride. *J. Polym. Sci. A Polym. Chem.* **2000,** *38* (12), 2239-2244.

59. Benoit, D.; Hawker, C. J.; Huang, E. E.; Lin, Z.; Russell, T. P., One-step formation of functionalized block copolymers. *Macromolecules* **2000,** *33* (5), 1505-1507.

60. Zhu, M.-Q.; Wei, L.-H.; Li, M.; Jiang, L.; Du, F.-S.; Li, Z.-C.; Li, F.-M., A unique synthesis of a well-defined block copolymer having alternating segments constituted by maleic anhydride and styrene and the self-assembly aggregating behavior thereof. *Chem. Commun.* **2001,** (4), 365-366.

61. Bapat, A. P.; Ray, J. G.; Savin, D. A.; Hoff, E. A.; Patton, D. L.; Sumerlin, B. S., Dynamic-covalent nanostructures prepared by Diels–Alder reactions of styrene-maleic anhydride-derived copolymers obtained by one-step cascade block copolymerization. *Polym. Chem.* **2012,** *3* (11), 3112-3120.

62. McLeary, J.; Calitz, F.; McKenzie, J.; Tonge, M.; Sanderson, R.; Klumperman, B., Beyond inhibition: a ^{1}H NMR investigation of the early kinetics of RAFT-mediated polymerization with the same initiating and leaving groups. *Macromolecules* **2004,** *37* (7), 2383-2394.

63. van den Dungen, E. T.; Rinquest, J.; Pretorius, N. O.; McKenzie, J. M.; McLeary, J. B.; Sanderson, R. D.; Klumperman, B., Investigation into the Initialization Behaviour of RAFT-Mediated Styrene–Maleic Anhydride Copolymerizations. *Aust. J. Chem.* **2006,** *59* (10), 742-748.

64. Du, F.-S.; Zhu, M.-Q.; Guo, H.-Q.; Li, Z.-C.; Li, F.-M.; Kamachi, M.; Kajiwara, A., An ESR study of reversible addition-fragmentation chain transfer copolymerization of styrene and maleic anhydride. *Macromolecules* **2002,** *35* (17), 6739-6741.

65. Chernikova, E.; Terpugova, P.; Bui, C.; Charleux, B., Effect of comonomer composition on the controlled free-radical copolymerization of styrene and maleic anhydride by reversible addition–fragmentation chain transfer (RAFT). *Polymer* **2003,** *44* (15), 4101-4107.

66. Wang, Y.; Shen, Y.; Pei, X.; Zhang, S.; Liu, H.; Ren, J., In situ synthesis of poly (styrene-*co*-maleic anhydride)/SiO_2 hybrid composites via "grafting onto" strategy based on nitroxide-mediated radical polymerization. *React. Funct. Polym.* **2008,** *68* (8), 1225-1230.

67. Blomberg, S.; Ostberg, S.; Harth, E.; Bosman, A. W.; Van Horn, B.; Hawker, C. J., Production of crosslinked, hollow nanoparticles by surface-initiated living free-radical polymerization. *J. Polym. Sci. A Polym. Chem.* **2002,** *40* (9), 1309-1320.

68. Boyer, C.; Whittaker, M. R.; Nouvel, C.; Davis, T. P., Synthesis of hollow polymer nanocapsules exploiting gold nanoparticles as sacrificial templates. *Macromolecules* **2010,** *43* (4), 1792-1799.

69. Tang, D.; Jiang, X.; Liu, H.; Li, C.; Zhao, Y., Synthesis and properties of heterografted toothbrush-like copolymers with alternating PEG and PCL grafts and tunable RAFT-generated segments. *Polym. Chem.* **2014,** *5* (16), 4679-4692.

70. Wang, S.; Wu, B.; Liu, F.; Gao, Y.; Zhang, W., A well-defined alternating copolymer based on a salicylaldimine Schiff base for highly sensitive zinc(II) detection and pH sensing in aqueous solution. *Polym. Chem.* **2015,** *6* (7), 1127-1136.

71. De Brouwer, H.; Schellekens, M. A.; Klumperman, B.; Monteiro, M. J.; German, A. L., Controlled radical copolymerization of styrene and maleic anhydride and the synthesis of

novel polyolefin-based block copolymers by reversible addition–fragmentation chain-transfer (RAFT) polymerization. *J. Polym. Sci. A Polym. Chem.* **2000,** *38* (19), 3596-3603.

72. Bapat, A. P.; Ray, J. G.; Savin, D. A.; Sumerlin, B. S., Redox-responsive dynamic-covalent assemblies: stars and miktoarm stars. *Macromolecules* **2013,** *46* (6), 2188-2198.

73. Ishizu, K.; Takashimizu, C.; Shibuya, T.; Uchida, S., Synthesis and solution properties of alternating maleimide/styrene hyperbranched copolymers via controlled radical mechanism. *Polym. Int.* **2003,** *52* (6), 1010-1015.

74. Sauvage, E.; Amos, D.; Antalek, B.; Schroeder, K.; Tan, J.; Plucktaveesak, N.; Colby, R., Amphiphilic maleic acid-containing alternating copolymers—1. Dissociation behavior and compositions. *J. Polym. Sci. Part B Polym. Phys.* **2004,** *42* (19), 3571-3583.

75. Sauvage, E.; Plucktaveesak, N.; Colby, R.; Amos, D.; Antalek, B.; Schroeder, K.; Tan, J., Amphiphilic maleic acid-containing alternating copolymers—2. Dilute solution characterization by light scattering, intrinsic viscosity, and PGSE NMR spectroscopy. *J. Polym. Sci. Part B Polym. Phys.* **2004,** *42* (19), 3584-3597.

76. Banerjee, S.; Pal, T. K.; Guha, S. K., Probing molecular interactions of poly (styrene-*co*-maleic acid) with lipid matrix models to interpret the therapeutic potential of the copolymer. *Biochim. Biophys. Acta* **2012,** *1818* (3), 537-550.

77. Tonge, S.; Tighe, B., Responsive hydrophobically associating polymers: a review of structure and properties. *Adv. Drug Deliv. Rev.* **2001,** *53* (1), 109-122.

78. Shao-Hai, F.; Kuan-Jun, F., Preparation of styrene-maleic acid copolymers and its application in encapsulated pigment red 122 dispersion. *J. Appl. Polym. Sci.* **2007,** *105* (2), 317-321.

79. Maeda, H.; Sawa, T.; Konno, T., Mechanism of tumor-targeted delivery of macromolecular

drugs, including the EPR effect in solid tumor and clinical overview of the prototype polymeric drug SMANCS. *J. Control. Release* **2001,** *74* (1–3), 47-61.

80. Vargas, C.; Arenas, R. C.; Frotscher, E.; Keller, S., Nanoparticle self-assembly in mixtures of phospholipids with styrene/maleic acid copolymers or fluorinated surfactants. *Nanoscale* **2015,** *7* (48), 20685-20696.

81. Greish, K.; Sawa, T.; Fang, J.; Akaike, T.; Maeda, H., SMA–doxorubicin, a new polymeric micellar drug for effective targeting to solid tumours. *J. Control. Release* **2004,** *97* (2), 219-230.

82. Greish, K.; Nagamitsu, A.; Fang, J.; Maeda, H., Copoly(styrene-maleic acid)−Pirarubicin Micelles: High Tumor-Targeting Efficiency with Little Toxicity1. *Bioconjugate Chem.* **2005,** *16* (1), 230-236.

83. Iyer, A. K.; Greish, K.; Fang, J.; Murakami, R.; Maeda, H., High-loading nanosized micelles of copoly(styrene–maleic acid)–zinc protoporphyrin for targeted delivery of a potent heme oxygenase inhibitor. *Biomaterials* **2007,** *28* (10), 1871-1881.

84. Fang, J.; Nakamura, H.; Maeda, H., The EPR effect: Unique features of tumor blood vessels for drug delivery, factors involved, and limitations and augmentation of the effect. *Adv. Drug Deliv. Rev.* **2011,** *63* (3), 136-151.

85. Greish, K., Enhanced Permeability and Retention (EPR) Effect for Anticancer Nanomedicine Drug Targeting. In *Cancer Nanotechnology: Methods and Protocols*, Grobmyer, R. S.; Moudgil, M. B., Eds. Humana Press: Totowa, NJ, 2010; pp 25-37.

86. Maeda, H.; Bharate, G. Y.; Daruwalla, J., Polymeric drugs for efficient tumor-targeted drug delivery based on EPR-effect. *Eur. J. Pharm. Biopharm.* **2009,** *71* (3), 409-419.

87. Knowles, T. J.; Finka, R.; Smith, C.; Lin, Y.-P.; Dafforn, T.; Overduin, M., Membrane

proteins solubilized intact in lipid containing nanoparticles bounded by styrene maleic acid copolymer. *J. Am. Chem. Soc.* **2009,** *131* (22), 7484-7485.

88. Scheidelaar, S.; Koorengevel, Martijn C.; Pardo, Juan D.; Meeldijk, Johannes D.; Breukink, E.; Killian, J. A., Molecular Model for the Solubilization of Membranes into Nanodisks by Styrene Maleic Acid Copolymers. *Biophys. J.* **2015,** *108* (2), 279-290.

89. Jamshad, M.; Lin, Y.-P.; Knowles, T. J.; Parslow, R. A.; Harris, C.; Wheatley, M.; Poyner, D. R.; Bill, R. M.; Thomas, O. R.; Overduin, M., Surfactant-free purification of membrane proteins with intact native membrane environment. *Biochem. Soc. Trans.* **2011,** *39* (3), 813-818.

90. Gulati, S.; Jamshad, M.; Knowles, T. J.; Morrison, K. A.; Downing, R.; Cant, N.; Collins, R.; Koenderink, J. B.; Ford, R. C.; Overduin, M., Detergent-free purification of ABC (ATP-binding-cassette) transporters. *Biochem. J.* **2014,** *461* (2), 269-278.

91. Long, A. R.; O'Brien, C. C.; Malhotra, K.; Schwall, C. T.; Albert, A. D.; Watts, A.; Alder, N. N., A detergent-free strategy for the reconstitution of active enzyme complexes from native biological membranes into nanoscale discs. *BMC Biotechnol.* **2013,** *13* (1), 1.

92. Wang, D.; Li, Z.-C.; Chen, L., Templated synthesis of single-walled carbon nanotube and metal nanoparticle assemblies in solution. *J. Am. Chem. Soc.* **2006,** *128* (47), 15078-15079.

93. Malardier-Jugroot, C.; van de Ven, T. G. M.; Whitehead, M. A., Characterization of a novel self-association of an alternating copolymer into nanotubes in solution. *Mol. Simul.* **2005,** *31* (2-1), 173-178.

94. Malardier-Jugroot, C.; van de Ven, T. G. M.; Whitehead, M. A., Linear conformation of poly(styrene-*alt*-maleic anhydride) capable of self-assembly: A result of chain stiffening by internal hydrogen bonds. *J. Phys. Chem. B* **2005,** *109* (15), 7022-7032.

95. Wang, M.; Braun, H.-G.; Meyer, E., Patterning of polymeric/inorganic nanocomposite and nanoparticle layers. *Chem. Mater.* **2002,** *14* (11), 4812-4818.

96. Henry, S. M.; El-Sayed, M. E. H.; Pirie, C. M.; Hoffman, A. S.; Stayton, P. S., pH-Responsive poly(styrene-*alt*-maleic anhydride) alkylamide copolymers for intracellular drug delivery. *Biomacromolecules* **2006,** *7* (8), 2407-2414.

97. Zovko, M.; BARBARIC, M.; Zorc, B.; Hafner, A.; FILIPOVIC-GRCIC, J., Synthesis of fenoprofen and gemfibrozil styrene-maleic acid copolymer conjugates. *Acta Pharm.* **2005,** *55* (2), 169-176.

98. Maeda, H., SMANCS and polymer-conjugated macromolecular drugs: advantages in cancer chemotherapy. *Adv. Drug Deliv. Rev.* **2001,** *46* (1–3), 169-185.

99. Maeda, H., The link between infection and cancer: Tumor vasculature, free radicals, and drug delivery to tumors via the EPR effect. *Cancer Sci.* **2013,** *104* (7), 779-789.

100. Elvira, C.; Gallardo, A.; Roman, J.; Cifuentes, A., Covalent polymer-drug conjugates. *Molecules* **2005,** *10* (1), 114-125.

101. Tsukigawa, K.; Liao, L.; Nakamura, H.; Fang, J.; Greish, K.; Otagiri, M.; Maeda, H., Synthesis and therapeutic effect of styrene–maleic acid copolymer-conjugated pirarubicin. *Cancer Sci.* **2015,** *106* (3), 270-278.

102. Mu, Y.; Kamada, H.; Kaneda, Y.; Yamamoto, Y.; Kodaira, H.; Tsunoda, S.-i.; Tsutsumi, Y.; Maeda, M.; Kawasaki, K.; Nomizu, M., Bioconjugation of laminin peptide YIGSR with poly (styrene-*co*-maleic acid) increases its antimetastatic effect on lung metastasis of B16-BL6 melanoma cells. *Biochem. Biophys. Res. Commun.* **1999,** *255* (1), 75-79.

103. Khazaei, A.; Saednia, S.; Saien, J.; Kazem-Rostami, M.; Sadeghpour, M.; Borazjani, M. K.; Abbasi, F., Grafting amino drugs to poly(styrene-*alt*-maleic anhydride) as a potential method

for drug release. *J. Braz. Chem. Soc.* **2013,** *24*, 1109-1115.

104. Li, Z.; Song, Y.; Yang, Y.; Yang, L.; Huang, X.; Han, J.; Han, S., Rhodamine-deoxylactam functionalized poly[styrene-*alter*-(maleic acid)]s as lysosome activatable probes for intraoperative detection of tumors. *Chem. Sci.* **2012,** *3* (10), 2941-2948.
105. Ignatova, M.; Stoilova, O.; Manolova, N.; Markova, N.; Rashkov, I., Electrospun mats from styrene/maleic anhydride copolymers: modification with amines and assessment of antimicrobial activity. *Macromol. Biosci.* **2010,** *10* (8), 944-954.
106. Jeong, J.-H.; Byoun, Y.-S.; Lee, Y.-S., Poly (styrene-*alt*-maleic anhydride)-4-aminophenol conjugate: synthesis and antibacterial activity. *React. Funct. Polym.* **2002,** *50* (3), 257-263.
107. Stoilova, O.; Ignatova, M.; Manolova, N.; Godjevargova, T.; Mita, D.; Rashkov, I., Functionalized electrospun mats from styrene–maleic anhydride copolymers for immobilization of acetylcholinesterase. *Eur. Polym. J.* **2010,** *46* (10), 1966-1974.
108. Heravi, M. M.; Hashemi, E.; Beheshtiha, Y. S.; Kamjou, K.; Toolabi, M.; Hosseintash, N., Solvent-free multicomponent reactions using the novel *N*-sulfonic acid modified poly(styrene-maleic anhydride) as a solid acid catalyst. *J. Mol. Catal. A Chem.* **2014,** *392*, 173-180.
109. Abo-Baker, E.; Elkholy, S. S.; Elsabee, M. Z., Modified poly (styrene maleic anhydride) copolymer for the removal of toxic metal cations from aqueous solutions. *Am. J. Polym. Sci.* **2015,** *5* (3), 55-64.
110. Hasanzadeh, R.; Najafi Moghadam, P.; Samadi, N., Synthesis and application of modified poly (styrene-*alt*-maleic anhydride) networks as a nano chelating resin for uptake of heavy metal ions. *Polymer. Adv. Tech.* **2013,** *24* (1), 34-41.
111. Ali, E. A.; Elkholy, S. S.; Morsi, R. E.; Elsabee, M. Z., Studies on adsorption behavior of Cu

(II) and Cd (II) onto aminothiophene derivatives of Styrene Maleic anhydride copolymer. *J. Taiwan Inst. Chem. Eng.* **2016,** *64*, 325-335.

112. Soer, W. J.; Ming, W.; Klumperman, B.; Koning, C.; van Benthem, R., Surfactant-free artificial latexes from modified styrene–maleic anhydride (SMA) copolymers. *Polymer* **2006,** *47* (22), 7621-7627.

113. Chenglin, Y.; Yiqun, Y.; Ye, Z.; Na, L.; Xiaoya, L.; Jing, L.; Ming, J., Self-assembly and emulsification of poly {[styrene-*alt*-maleic acid]-co-[styrene-alt-(*N*-3, 4-dihydroxyphenyl ethyl-maleamic acid)]}. *Langmuir* **2012,** *28* (25), 9211-9222.

114. Lindhoud, S.; Carvalho, V.; Pronk, J. W.; Aubin-Tam, M.-E., SMA-SH: Modified styrene–maleic acid copolymer for functionalization of lipid nanodiscs. *Biomacromolecules* **2016,** *17* (4), 1516-1522.

115. Alex, M. A.; Nagpal, N.; Kulshreshtha, R.; Koul, V., Synthesis and evaluation of cationically modified poly (styrene-*alt*-maleic anhydride) nanocarriers for intracellular gene delivery. *RSC Adv.* **2015,** *5* (28), 21931-21944.

116. Wang, D.; Ji, W.-X.; Li, Z.-C.; Chen, L., A biomimetic "polysoap" for single-walled carbon nanotube dispersion. *J. Am. Chem. Soc.* **2006,** *128* (20), 6556-6557.

117. Öztürk, C.; Küsefoğlu, S. H., New polymers from plant oil derivatives and styrene-maleic anhydride copolymers. *J. Appl. Polym. Sci.* **2010,** *116* (1), 355-365.

118. Monticelli, O.; Fina, A.; Ullah, A.; Waghmare, P., Preparation, characterization, and properties of novel PSMA− POSS systems by reactive blending. *Macromolecules* **2009,** *42* (17), 6614-6623.

119. Zhu, L.-P.; Yi, Z.; Liu, F.; Wei, X.-Z.; Zhu, B.-K.; Xu, Y.-Y., Amphiphilic graft copolymers based on ultrahigh molecular weight poly (styrene-*alt*-maleic anhydride) with poly (ethylene

glycol) side chains for surface modification of polyethersulfone membranes. *Eur. Polym. J.* **2008,** *44* (6), 1907-1914.

120. Duan, H.; Qiu, T.; Guo, L.; Ye, J.; Yuan, Y.; Li, X., The aminolysis of styrene–maleic anhydride copolymers for a new modifier used in urea-formaldehyde resins. *Int. J. Adhes. Adhes.* **2016,** *66*, 138-146.
121. Lu, J.; Kim, S. G.; Lee, S.; Oh, I. K., A biomimetic actuator based on an ionic networking membrane of poly (styrene-*alt*-maleimide)-incorporated poly (vinylidene fluoride). *Adv. Funct. Mater.* **2008,** *18* (8), 1290-1298.
122. Lazzara, T. D.; van de Ven, T. G.; Whitehead, M., Nanotube self-assembly of a styrene and maleimide alternating copolymer. *Macromolecules* **2008,** *41* (18), 6747-6751.
123. Lazzara, T. D.; Whitehead, M. A.; van de Ven, T. G., Effect of chirality on π-stacking in styrene and maleimide alternating copolymers. *J. Phys. Chem. B* **2008,** *112* (16), 4892-4899.
124. Tian, Y.; He, Q.; Tao, C.; Cui, Y.; Ai, S.; Li, J., Fabrication of polyethyleneimine and poly (styrene-*alt*-maleic anhydride) nanotubes through covalent bond. *J. Nanosci. Nanotechnol.* **2006,** *6* (7), 2072-2076.
125. Gao, M.; Jia, X.; Kuang, G.; Li, Y.; Liang, D.; Wei, Y., Thermo-and pH-responsive dendronized copolymers of styrene and maleic anhydride pendant with poly (amidoamine) dendrons as side groups. *Macromolecules* **2009,** *42* (12), 4273-4281.
126. Wang, Z.; Gao, M.; Sun, J.; Liang, D.; Jia, X., Photoresponsive dendronized copolymers of styrene and maleic anhydride pendant with poly (amidoamine) dendrons as side groups. *Macromolecules* **2013,** *46* (5), 1723-1731.
127. Dérand, H.; Wesslén, B., Synthesis and characterization of anionic graft copolymers containing poly (ethylene oxide) grafts. *J. Polym. Sci. A Polym. Chem.* **1995,** *33* (3), 571-

579.

128. Dérand, H.; Wesslén, B.; Wittgren, B.; Wahlund, K.-G., Poly (ethylene glycol) graft copolymers containing carboxylic acid groups: aggregation and viscometric properties in aqueous solution. *Macromolecules* **1996,** *29* (27), 8770-8775.

129. Yin, X.; Stöver, H. D., Thermosensitive and pH-sensitive polymers based on maleic anhydride copolymers. *Macromolecules* **2002,** *35* (27), 10178-10181.

130. Yin, X.; Stöver, H. D., Hydrogel microspheres formed by complex coacervation of partially MPEG-grafted poly (styrene-*alt*-maleic anhydride) with PDADMAC and cross-linking with polyamines. *Macromolecules* **2003,** *36* (23), 8773-8779.

131. Florjanczyk, Z.; Bzducha, W.; Wieczorek, W.; Zygadlo-Monikowska, E.; Krawiec, W.; Chung, S. H., Highly conducting lithium polyelectrolytes based on maleic anhydride-styrene copolymers. *J. Phys. Chem. B* **1998,** *102* (43), 8409-8416.

132. Duan, X.; Xiao, J.; Yin, Q.; Zhang, Z.; Mao, S.; Li, Y., Amphiphilic graft copolymer based on poly (styrene-*co*-maleic anhydride) with low molecular weight polyethylenimine for efficient gene delivery. *Int. J. Nanomed* **2012,** *7*, 4961-4972.

133. Zhu, H.; Deng, G.; Chen, Y., Amphiphilic polymer brushes with alternating PCL and PEO grafts through radical copolymerization of styrenic and maleimidic macromonomers. *Polymer* **2008,** *49* (2), 405-411.

134. Weiss, J.; Li, A.; Wischerhoff, E.; Laschewsky, A., Water-soluble random and alternating copolymers of styrene monomers with adjustable lower critical solution temperature. *Polym. Chem.* **2012,** *3* (2), 352-361.

135. Soejima, T.; Satoh, K.; Kamigaito, M., Main-chain and side-chain sequence-regulated vinyl copolymers by iterative atom transfer radical additions and 1: 1 or 2: 1 alternating radical

copolymerization. *J. Am. Chem. Soc.* **2016,** *138* (3), 944-954.

136. Soejima, T.; Satoh, K.; Kamigaito, M., Monomer sequence regulation in main and side chains of vinyl copolymers: Synthesis of vinyl oligomonomers via sequential atom transfer radical addition and their alternating radical copolymerization. *ACS Macro Lett.* **2015,** *4* (7), 745-749.
137. Turner, S. R., Copolymers of sodium styrene sulfonate and sodium-*N*-(4-sulfophenyl)-maleimide. U.S. Patent: 4540762 (1985).
138. Turner, S. R.; Anderson, C. C.; Kolterman, K. M., Alternating copolymerization as a route for synthesis of novel reactive copolymers. *J. Polym. Sci. Part C Polym. Lett.* **1989,** *27* (8), 253-258.
139. Jia, Y.-g.; Liu, L.-y.; Lei, B.; Li, J.; Zhu, X., Crown ether cavity-containing copolymers via controlled alternating cyclocopolymerization. *Macromolecules* **2011,** *44* (16), 6311-6317.
140. Savage, A. M.; Zhou, X.; Huang, J.; Turner, S. R., A review of semi-rigid, stilbene-containing alternating copolymers. *App. Pet. Res.* **2015,** *5* (1), 27-33.
141. Wagner-Jauregg, T., Über addierende Hetero-polymerisation. *Ber. Dtsch. Chem. Ges.* **1930,** *63* (11), 3213-3224.
142. Hallensleben, M. L., Electron donor-acceptor complexes and polymerization—V copolymerization of maleic anhydride and trans-stilbene under ultra-violet irradiation. *Eur. Polym. J.* **1973,** *9* (3), 227-231.
143. Tanaka, T.; Vogl, O., Preparation and characterization of head-to-head polymer. I. Head-to-head poly (methyl cinnamate). *Polym. J.* **1974,** *6* (6), 522-531.
144. Li, Y.; Turner, S. R., Free radical copolymerization of methyl substituted stilbenes with maleic anhydride. *Eur. Polym. J.* **2010,** *46* (4), 821-828.

145. Mao, M.; Turner, S. R., Aggregation of rod−coil block copolymers containing rigid polyampholyte blocks in aqueous solution. *J. Am. Chem. Soc.* **2007,** *129* (13), 3832-3833.

146. Savage, A. M.; Li, Y.; Matolyak, L. E.; Doncel, G. F.; Turner, S. R.; Gandour, R. D., Anti-HIV activities of precisely defined, semirigid, carboxylated alternating copolymers. *J. Med. Chem.* **2014,** *57* (15), 6354-6363.

147. Li, Y.; Zhang, M.; Mao, M.; Turner, S. R.; Moore, R. B.; Mourey, T. H.; Slater, L. A.; Hauenstein, J. R., Chain stiffness of stilbene containing alternating copolymers by SAXS and SEC. *Macromolecules* **2012,** *45* (3), 1595-1601.

148. Mao, M.; Kim, C.; Wi, S.; Turner, S. R., Chain structure of substituted stilbene−maleic anhydride alternating copolymer probed by solid-state NMR. *Macromolecules* **2008,** *41* (2), 387-389.

149. Zhou, X.; Huang, J.; Barr, K. W.; Lin, Z.; Maya, F.; Abbott, L. J.; Colina, C. M.; Svec, F.; Turner, S. R., Nanoporous hypercrosslinked polymers containing T_g enhancing comonomers. *Polymer* **2015,** *59*, 42-48.

150. Huang, J.; Zhou, X.; Lamprou, A.; Maya, F.; Svec, F.; Turner, S. R., Nanoporous polymers from cross-linked polymer precursors via *tert*-butyl groupdeprotection and their carbon dioxide capture properties. *Chem. Mater.* **2015,** *27* (21), 7388-7394.

151. Zhou, X.; Li, Y.; Hart, K. E.; Abbott, L. J.; Lin, Z.; Svec, F.; Colina, C. M.; Turner, S. R., Nanoporous structure of semirigid alternating copolymers via nitrogen sorption and molecular simulation. *Macromolecules* **2013,** *46* (15), 5968-5973.

152. Li, Y.; Savage, A. M.; Zhou, X.; Turner, S. R.; Davis, R. M., Solution properties of stilbene-containing sterically crowded alternating polyanions. *J. Polym. Sci., Part B: Polym. Phys.* **2013,** *51* (21), 1565-1570.

153. Li, Y.; Mao, M.; Matolyak, L. E.; Turner, S. R., Sterically crowded anionic polyelectrolytes with tunable charge densities based on stilbene-containing copolymers. *ACS Macro Lett.* **2012,** *1* (2), 257-260.

154. Savage, A. M.; Ullrich, E.; Chin, S. M.; Kiernan, Z.; Kost, C.; Turner, S. R., Synthesis and characterization of double hydrophilic block copolymers containing semi-rigid and flexible segments. *J. Polym. Sci., Part A: Polym. Chem.* **2015,** *53* (2), 219-227.

155. Mao, M.; Turner, S. R., Synthesis and characterization of highly functionalized polymers based on *N,N,N′,N′*-tetraalkyl-4,4′-diaminostilbene and maleic anhydride. *Polymer* **2006,** *47* (24), 8101-8105.

156. Savage, A. M.; Ullrich, E.; Kost, C.; Turner, S. R., Salt- and pH-Responsive semirigid/flexible double-hydrophilic block copolymers. *Macromol. Chem. Phys.* **2016**, *217* (15), 1737-1744.

157. Mao, M.; England, J.; Turner, S. R., Alternating stilbene copolymers with negative birefringence. *Polymer* **2011,** *52* (20), 4498-4502.

158. Wadsworth, W. S.; Emmons, W. D., The utility of phosphonate carbanions in olefin synthesis. *J. Am. Chem. Soc.* **1961,** *83* (7), 1733-1738.

159. Sahu, U. S.; Bhadani, S. N., Homopolymerization of maleimide. *Macromol. Chem. Phys.* **1982,** *3* (2), 103-107.

160. Weigand, F.; Fülber, C.; Blümich, B.; Spiess, H. W., Proceedings of the second international meeting on recent advances in MR applications to porous media spatially resolved NMR of rigid polymers and elastomers. *Magn. Reson. Imaging* **1994,** *12* (2), 301-304.

161. Mark, J. E., *Physical properties of polymers handbook*. Springer: 2007; Vol. 1076.

162. Zhang, T.; Yang, S.-L.; Hu, D.-Y.; Jin, J.-H.; Li, G.; Jiang, J.-M., Synthesis and

characterization of a rigid-rod dihydroxy poly(p-phenylene benzobisoxazole) fiber with excellent surface and axial compression properties. *Polym. Bull.* **2008,** *62* (2), 247-254.

163. Chu, Q.; Lu, H.; He, T.; Ding, M., Synthesis and thermal polymerization of a novel stilbene-maleimide AB-monomer. *Polym. Bull.* **2000,** *43* (6), 471-475.
164. Lyon, C. K.; Hill, E. O.; Berda, E. B., Zipping polymers into nanoparticles via intrachain alternating radical copolymerization. *Macromol. Chem. Phys.* **2016,** *217* (3), 501-508.
165. Lutz, J.-F.; Ouchi, M.; Liu, D. R.; Sawamoto, M., Sequence-controlled polymers. *Science* **2013,** *341* (6146), 1238149.
166. Lutz, J.-F., Writing on polymer chains. *Acc. Chem. Res.* **2013,** *46* (11), 2696-2705.
167. Pfeifer, S.; Lutz, J.-F., A facile procedure for controlling monomer sequence distribution in radical chain polymerizations. *J. Am. Chem. Soc.* **2007,** *129* (31), 9542-9543.
168. Pfeifer, S.; Lutz, J.-F., Development of a library of *N*-substituted maleimides for the local functionalization of linear polymer chains. *Chem. Eur. J.* **2008,** *14* (35), 10949-10957.
169. Baradel, N.; Gok, O.; Zamfir, M.; Sanyal, A.; Lutz, J.-F., Sequence-controlled polymerization using dendritic macromonomers: precise chain-positioning of bulky functional clusters. *Chem. Commun.* **2013,** *49* (66), 7280-7282.
170. Schmidt, B. V. K. J.; Fechler, N.; Falkenhagen, J.; Lutz, J.-F., Controlled folding of synthetic polymer chains through the formation of positionable covalent bridges. *Nat. Chem.* **2011,** *3* (3), 234-238.
171. Baradel, N.; Fort, S.; Halila, S.; Badi, N.; Lutz, J.-F., Synthesis of single-chain sugar arrays. *Angew. Chem. Int. Ed.* **2013,** *52* (8), 2335-2339.
172. Lutz, J.-F., 1,3-Dipolar cycloadditions of azides and alkynes: A universal ligation tool in polymer and materials science. *Angew. Chem. Int. Ed.* **2007,** *46* (7), 1018-1025.

173. Zamfir, M.; Lutz, J.-F., Ultra-precise insertion of functional monomers in chain-growth polymerizations. *Nat. Commun.* **2012**, 1138.

174. Roy, R. K.; Lutz, J.-F., Compartmentalization of single polymer chains by stepwise intramolecular cross-linking of sequence-controlled macromolecules. *J. Am. Chem. Soc.* **2014,** *136* (37), 12888-12891.

175. Srichan, S.; Kayunkid, N.; Oswald, L.; Lotz, B.; Lutz, J.-F., Synthesis and characterization of sequence-controlled semicrystalline comb copolymers: influence of primary structure on materials properties. *Macromolecules* **2014,** *47* (5), 1570-1577.

176. Srichan, S.; Oswald, L.; Zamfir, M.; Lutz, J.-F., Precision polyelectrolytes. *Chem. Commun.* **2012,** *48* (10), 1517-1519.

177. Srichan, S.; Mutlu, H.; Badi, N.; Lutz, J.-F., Precision PEGylated polymers obtained by sequence-controlled copolymerization and postpolymerization modification. *Angew. Chem. Int. Ed.* **2014,** *53* (35), 9231-9235.

178. Srichan, S.; Chan-Seng, D.; Lutz, J.-F., Influence of strong electron-donor monomers in sequence-controlled polymerizations. *ACS Macro Lett.* **2012,** *1* (5), 589-592.

179. Srichan, S.; Mutlu, H.; Lutz, J.-F., On the synthesis of sequence-controlled poly(vinyl benzyl amine-co-*N*-substituted maleimides) copolymers. *Eur. Polym. J.* **2015,** *62*, 338-346.

180. Lutz, J.-F.; Schmidt, B. V. K. J.; Pfeifer, S., Tailored polymer microstructures prepared by atom transfer radical copolymerization of styrene and *N*-substituted maleimides. *Macromol. Rapid Commun.* **2011,** *32* (2), 127-135.

181. Chan-Seng, D.; Zamfir, M.; Lutz, J.-F., Polymer-chain encoding: Synthesis of highly complex monomer sequence patterns by using automated protocols. *Angew. Chem. Int. Ed.* **2012,** *51* (49), 12254-12257.

182. Zamfir, M.; Theato, P.; Lutz, J.-F., Controlled folding of polystyrene single chains: design of asymmetric covalent bridges. *Polym. Chem.* **2012,** *3* (7), 1796-1802.

183. Berthet, M.-A.; Zarafshani, Z.; Pfeifer, S.; Lutz, J.-F., Facile synthesis of functional periodic copolymers: A step toward polymer-based molecular arrays. *Macromolecules* **2010,** *43* (1), 44-50.

Chapter 2. Hypercrosslinked Polymers – A Review

(Adapted with permission from Huang, J.; Turner, S. R. *Polymer Reviews* **2017**, 1-41. Copyright 2017 Taylor & Francis.)

2.1 Authors

Jing Huang,[†,‡] and S. Richard Turner*[,†,‡]

[†]Department of Chemistry, Virginia Tech, Blacksburg, VA 24061, United States

[‡]Macromolecules Innovation Institute, Virginia Tech, Blacksburg, VA 24061, United States

2.2 Abstract

Hypercrosslinked polymers (HCPs) represent a class of nanoporous materials with a wide range of practical and potential applications such as gas sorption and separation, heterogeneous catalysis, drug delivery and chromatographic separation. First introduced by Davankov and Tsyurupa in the early 1970s, HCPs have developed rapidly over the past few decades. Mostly based on Friedel-Crafts chemistry, HCP materials can be prepared from the post-crosslinking of polystyrene-type precursors in their swollen state, or from the condensation of small building blocks. HCP materials manifest numerous important advantages, including moderate synthetic conditions, an enormous stockroom of inexpensive monomers, robust structures, and good thermal and chemical stabilities. This review article aims to provide an overview of recent publications on HCPs, and the emphasis is positioned on the synthetic approaches, theoretical studies, characterizations, structure-property relationships, and applications of these HCP materials.

2.3 Introduction

Microporous (pore width < 2 nm) and mesoporous (2 nm < pore width < 50 nm) organic polymers have been intensively investigated in past few decades owing to their numerous active or potential applications, such as gas storage and separation,[1-4] catalyst and sensor substrates,[5-8]

drug delivery,[9] and chromatographic separation.[10] Sometimes the term "nanoporous" is used to include both microporous and mesoporous polymers.[11] Based on different synthetic approaches and final structures, nanoporous organic polymers were divided into different subclasses, including polymers of covalent organic frameworks (COFs),[12,13] conjugated microporous polymers (CMPs),[14-16] hypercrosslinked polymers (HCPs),[10,17,18] covalent triazine frameworks (CTFs),[19,20] and porous aromatic frameworks (PAFs),[21,22] etc. Among them, HCPs were some of the earliest organic porous materials.[10] The history of crosslinked polystyrene networks can be traced back to the 1930s,[23] and after many years of research and development, they are still widely used in adsorption and separation. In the 1970s, Davankov and Tsyurupa first introduced HCPs, which possess more extensive crosslinks than conventional crosslinked polystyrene.[24] The formation of a high level of crosslinks leads to nanoporous structures, and the rigid networks prevent the nanoporous structure from collapse. Compared to traditional divinylbenzene crosslinked polystyrene, HCPs exhibit permanent small pores, high surface areas and large micropore volumes. Ever since the original work, HCPs have been extensively investigated, and several new approaches have been utilized to synthesize HCPs. There have been a number of reviews and books on nanoporous organic polymers and HCPs,[10,17,18,25-27] but the research about HCPs is proliferating and herein we aim to provide a comprehensive up-to-date overview of the HCP materials from a synthetic point of view. At the end of each section, there is a table summarizes the synthesis, porosity and potential applications of the HCPs that are discussed in the section. A list of abbreviations is included before the references.

2.4 Synthesis of different types of hypercrosslinked polymers (HCPs)

2.4.1 Crosslinked and hypercrosslinked polystyrene

2.4.1.1 Gel-type and macroporous polystyrene (first and second generations of polystyrene networks)

Crosslinked polystyrene has been one of the most commonly used polymeric adsorbents because of its simple synthesis and diversified modification. The earliest crosslinked polystyrene was the divinylbenzene (DVB)-styrene network, which was reported by Staudinger in the 1930s.[23] In 1945 the application of DVB-styrene as matrices for the synthesis of ion-exchange resins was patented by D'Alelio.[28] These networks, which was later referred to as gel-type polystyrene are considered the first-generation of crosslinked copolymers. These are homogeneous gels that are copolymerized from bulk styrene with 5-8% of DVB.[25,29] The unmodified gel-type polystyrene network swells in organic non-polar solvents such as toluene or dichloroethane. These gels were functionalized with sulfonic or ammonium groups and the resulting ion-exchange resins could swell in water or strongly polar alcohols.[25] However, the crosslinked polymer beads have very poor permeability even for gases when they are dry, therefore they were also called materials with hidden porosity. Also, no reliable measurements were made for their pore dimensions. The applications of these beads for adsorption of larger molecules was limited due to this poor permeability. The second-generation polystyrene networks, also known as macroporous polymers, were first patented by McBurney in 1952.[30] Different from the first-generation polystyrene, the second-generation copolymers possess permanent porosity. The porosity was generated from polymerization-induced phase separation during the copolymerization of styrene and DVB (6–12%) in presence of a monomer-miscible porogen; a higher percentage of DVB (compared with the first-generation) is employed in the synthesis in order to preserve the structure.[10] The resulting heterogeneous networks show a total pore volume of about 1 ml/g and surface area of 20-300 m^2/g. They possess channels between the gel domains, therefore they are good sorbents for larger

molecules.[25] They have an average pore diameter of about 20 nm, although they were named "macroporous" (pore size>50 nm) gels.[25] Rohm and Haas (now a part of Dow Chemical, Philadelphia, PA, USA) commercialized the second-generation networks as Amberlite™ with different pore sizes.[31]

Crosslinked polystyrene networks are widely used as the stationary phase in chromatography. Although porous silica supports are also useful materials for chromatography, their application range is limited due to degradation by acidic or alkaline aqueous solutions. In contrast, crosslinked polystyrene showed a better chemical stability over a wide pH range. The first generation gel-type copolymers of styrene and divinylbenzene became well-known based on their use as the ion-exchange resin for the separation of rare earths during the Manhattan nuclear weapon project.[10] However, the gel-type copolymers are not ideal to meet all the requirements as column packing materials[10] because the ideal material for column packing should satisfy certain requirements, such as high sorption capacity and permeability; high osmotic resistance, as in the ability to preserve their volume towards the change of the external environment like pH, polarity and concentrations of the eluent; and high mechanical strength to carry the column bed weight and mobile phase pressure.[25] The low osmotic resistance of gel-type copolymers results in rapid swelling/deswelling cycles when the external environment changes, which further shortens the lifetime of the material. Macroporous networks show better swelling properties, but the accessible functional sorption sites are mostly on the surface of the pores, therefore the sorption ability of the macroporous materials is usually insufficient for industrial applications.[10] However, highly crosslinked macroporous polystyrene has shown to be suitable as the packing material for high pressure liquid chromatography (HPLC) and size-exclusion chromatography (SEC).[32] When coated with a hydrophilic layer, the macroporous polystyrenes showed a high protein binding capacity and were

used for protein chromatography at high pressures.[33,34] Other than column chromatography, when the macroporous styrenic monolith was attached to a glass support, it was used as the stationary phase of thin layer chromatography for the separation of proteins and peptides.[35]

2.4.1.2 Hypercrosslinked polystyrene (third generation of polystyrene network)

The third generation of polystyrene networks were first introduced by Davankov and Tsyurupa in the 1970s.[36] These homogeneous networks contain high degrees of crosslinking (> 40% by Friedel-Crafts type crosslinks), therefore they are well-known as *hypercrosslinked* polystyrene, and are also called "Davankov-type resins".[10] To synthesize this type of hypercrosslinked polystyrene, a linear or lightly crosslinked precursor is stirred in a thermodynamically compatible solvent (usually 1,2-dichloroethane) until swollen. This introduces free volume between polymer chains. Then catalysts (Lewis acids, such as $SnCl_4$, $FeCl_3$) and/or external crosslinkers are added to generate crosslinks, and lock the polymer chains in the swollen state. After the solvent is removed in vacuum, the space left by the solvent results in micropores and a microporous hypercrosslinked polystyrene network is generated. Figure 2-1 shows a graphic scheme of the synthesis described above. These networks are highly rigid and expanded, and usually show high specific surface areas (600-2000 m^2/g).[37]

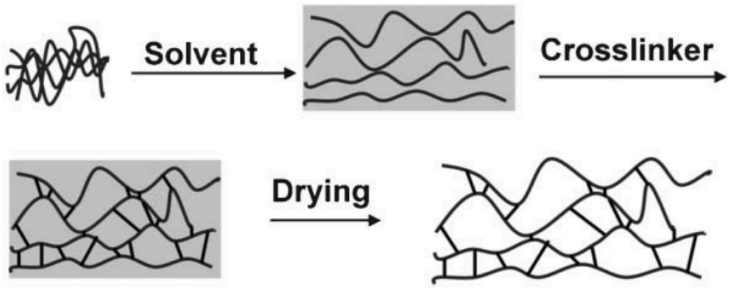

Figure 2-1. Schematic of post-crosslinking route to hypercrosslinked polystyrene network. Reprinted from Germain et al.[38] with permission. Copyright 2007 Royal Society of Chemistry.

Friedel–Crafts alkylation is a fast crosslinking reaction used to synthesize high aromatic density-containing hypercrosslinked polystyrene systems. Initially, Davankov and coworkers employed external bifunctional Friedel–Crafts crosslinking agents, such as 1,4-bis-(chloromethyl)-diphenyl (CMDP),[24] p-xylylene dichloride (XDC),[39-41] 1,4-bis-(p-chloromethylphenyl)-butane (DPB),[42] and tris-chloromethyl compound 1,3,5-tris-(chloromethyl)-mesitylene (CMM),[42] to crosslink polystyrene chains (Figure 2-2). Monochlorodimethyl ether (MCDE) was another efficient crosslinker.[10,24,43-45] It introduces chloromethyl groups to the phenyl rings, which can further react with other phenyl rings forming methylene bridges, the obtained networks have BET surface areas of 680–1000 m^2/g.[46] However, MCDE is highly carcinogenic. Some less toxic alternatives, such as formaldehyde dimethyl acetal (FDA),[47] carbon tetrachloride (CCl_4),[48-50] and dichloroethylene (DCE),[39,51,52] were developed as replacements for crosslinking polystyrene by the alkylation of two phenyl rings. FDA is one of the most used crosslinking agents, and it has been extensively used to crosslink polymer chains and small aromatic building blocks, which will be elaborate in part 2.2 and part 2.4, respectively.

Linear polystyrene and lightly crosslinked polystyrenes (0.3-2% DVB) were most commonly used as precursors to HCPs.[18,53] Highly crosslinked macroporous polystyrenes (up to 30% DVB) were also used as precursors for hypercrosslinking, and in addition to the macropores, micropores from postcrosslinking were observed.[36,53,54] The achievable crosslinking density was lower compared to the HCPs from lightly crosslinked precursors due to steric constraints.[18]

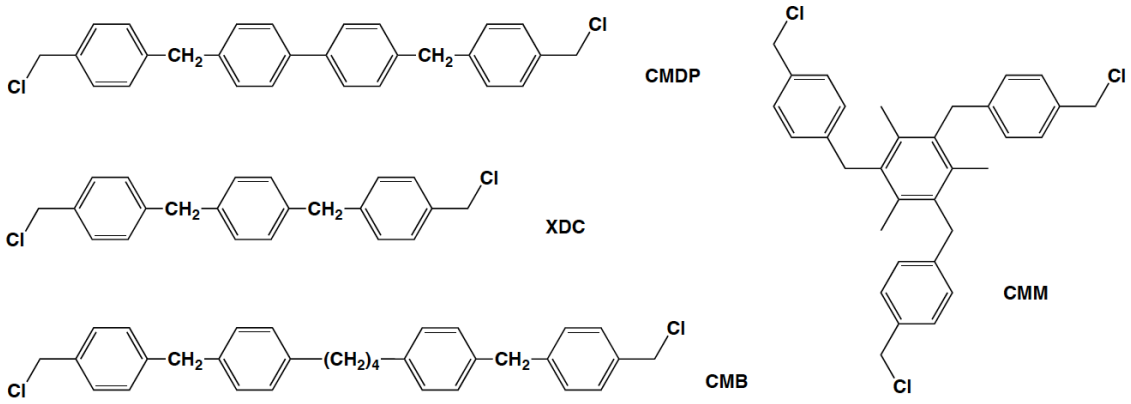

Figure 2-2. Crosslinkers that were used to prepare HCPs. Redrawn from Davankov et al.[10] with permission. Copyright 2011 Elsevier.

While external electrophiles were used as crosslinkers in Davankov's procedures, internal electrophiles were first introduced by pre-chloromethylation before the crosslinking.[55,56] Chloromethylated gel-type styrene-divinylbenzene resins (5% DVB) were used as precursors and were post-crosslinked via Friedel-Crafts reactions. The resulting network showed surface area up to about 1000 m^2/g.[51] The rate of the conversion of the chloromethyl groups into methylene bridges decreased as the rigidity of the networks increased, because of the unavailability of the neighboring phenyl rings to the chloromethyl groups.[57,58]

To completely avoid the inconvenience of chloromethylation, the copolymer of vinyl benzyl chloride (*p*-, and *m*-VBC) and styrene was synthesized as a precursor for post-crosslinking.[59] The BET surface area of the hypercrosslinked polymer increased as the content of VBC increased (up to 691 m^2/g at 90% of VBC). However, the distribution of the chloromethyl groups was not even due to the different reactivity ratios of VBC and styrene (1.41 and 0.71 respectively).

In 2006, Sherrington and coworkers designed a modified route to synthesize hypercrosslinked polystyrene networks with high surface area (Figure 2-3).[54] They directly copolymerized styrene and VBC with small amounts (2% or 20%) of divinyl benzene (DVB) via suspension polymerization, and the resulting lightly crosslinked precursor poly(S-*co*-VBC-*co*-

DVB) was swollen in 1,2-dichloroethane before post-crosslinking by the Lewis acid catalysis. The resulting HCP beads have high BET surface area up to 2090 m^2/g. The higher DVB content precursor (20%) generates HCPs with relatively lower surface area, due to the steric constraints and the limited accessibilities of solvent and catalyst. Also, increased styrene content in the precursor resulted in significantly lower surface area, because of the decrease of the crosslinkable functionalities (chloromethyl group). This work also compared the activities of $FeCl_3$, $AlCl_3$, and $SnCl_4$ as catalysts, and $FeCl_3$ was found to be the most effective catalyst for the post-crosslinking Friedel-Craft reaction. Tan and coworkers studied the pore size distribution and gas uptake of the hypercrosslinked poly(VBC-*co*-DVB) (HCP-VBC-DVB) systems with varying amounts of DVB and VBC.[60] In this study, HCPs with 2% of DVB showed the highest BET surface area of 2060 m^2/g, and a high DVB content led to a high level of micropores. HCPs with DVB content higher than 7% contain solely micropores. It was also suggested by ^{13}C magic angle spinning NMR that the formation of the second bridge on two rings is favorable since the rings are already doubly alkylated and electron rich, and the second bridge would result in a highly favorable six-membered ring.[61]

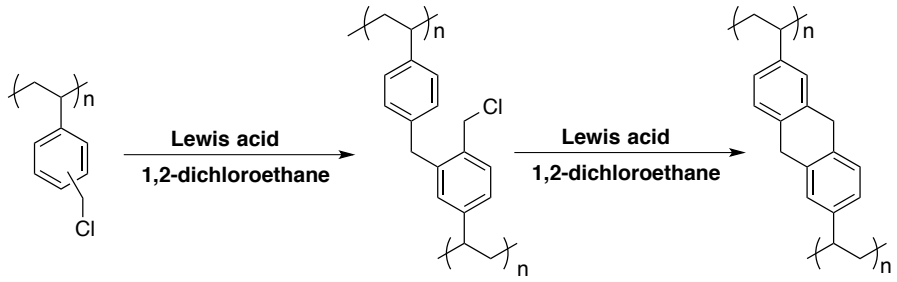

Figure 2-3. Friedel–Crafts catalyzed hypercrosslinked reaction of poly (VBC-co-DVB) precursor. Redrawn from Ahn et al.[54] Copyright 2006 American Chemical Society.

The sorption properties from unfunctionalized hypercrosslinked polystyrene are mostly based on hydrophobic and π-π interactions,[62] but functional groups could no doubt boost sorption properties and bring special applications to hypercrosslinked polystyrene materials. The

functionalization could be achieved by either post-polymerization chemical modifications or introducing functional group-containing monomers to produce functionalized precursors. Sherrington and coworkers found that the conversion of chloromethyl groups to hydroxyl groups via an S_N1 type mechanism was much faster with *para*-VBC because the stabilization of the cationic intermediate.[63] The hydroxyl groups benefited the sorption of polar sorbates and also affected the surface area after the hypercrosslinking step: the hypercrosslinked polymer from pure *para*-VBC has a lower surface area compared to the polymer from the mixed-VBC.

Hypercrosslinked polystyrene beads are considered "ideal" materials for HPLC column packing.[10] These high surface area materials were demonstrated to be chemically and mechanically stable, and compatible with both polar and nonpolar solvents. The micropores restrict the access of large molecules by size exclusion mechanism, while allow the interaction of small molecules with the whole hydrophobic inner surface of the material.[64] This property is useful when analyzing drugs and drug metabolites in biological matrices like blood and plasma. When chelating dyes are absorbed on the hydrophobic hypercrosslinked polystyrene surface, an HPLC column can be used to analyze trace metal ions in aqueous samples.[65] The hypercrosslinked polystyrene networks can be easily sulfonated by concentrated sulfuric acid even under mild conditions, and the resulting resins exhibit high ion exchange capacities.[10]

The *in situ* hyprocrosslinking reactions provide an efficient way to prepare the stationary phase for monolithic columns. This work was pioneered by Fréchet, Svec, and coworkers.[35,66-70] The hypercrosslinking of styrene, vinylbenzyl chloride and divinylbenzene in presence of a porogen and a solvent afforded monolithic capillary columns with high surface area and an array of small pores (Figure 2-4).[66] The composition of the monomers and the reaction conditions were optimized by mathematical design to achieve high column efficiencies for the isocratic separations

of small molecules.[67] Functional groups such as hydroxyl,[70] methyl,[68] and thiol,[69] can be introduced to the column to increase efficiency[68] or for future modifications.[69] The resulting monolithic columns showed extraordinary efficiencies both as liquid chromatographic and size-exclusion chromatographic columns.

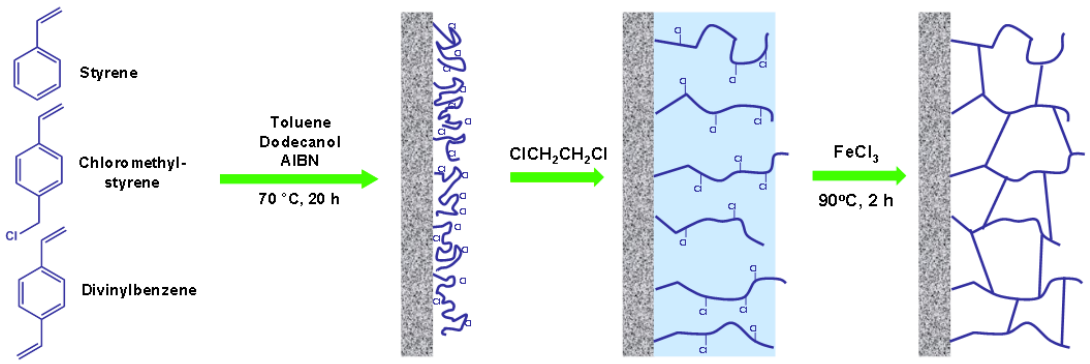

Figure 2-4. The synthesis of hypercrosslinked monolith column. Reprint from Urban et al.[66] with permission. Copyright 2010 American Chemical Society.

Hypercrosslinked microporous polystyrene networks have been commercialized by several companies. Examples include Purolite (Hypersol-Macronet, MN-series), Dow Chemical (Optipore), Lanxess (Lewatit VP OC 1163 and S 7768), Jiangsu N&G Environmental Technology (NG-99 and NG-100) as sorbents in chemical, food and water treatment industries, and International Sorbent Technology (Isolute), and Merk (Lichrolut EN) as analytical-scale sorbents for organic compounds in water and air.[71] Table 2-1 summarized the polymers in Section 2.4.1.1 and 2.4.1.2.

Table 2-1. Summary of typical crosslinked polymers and HCPs in Section 2.4.1.1 and 2.4.1.2

Polymers	Monomers or precursors	Synthetic strategy	BET surface area (m^2/g)	Pore type	(Potential) Applications	Ref.
Gel-type polystyrene	Styrene, DVB (5-8 wt.%)	Free radical (bulk or suspension)	-	-	Ion-exchange	23,28,29
Macroporous polystyrene	Styrene, DVB (6-12 wt.%)	Suspension free radical	20-300	Meso-	Sorbents, chromatography	30,32,34
Macroporous hypercrosslinked styrene-divinylbenzene copolymers	Styrene, DVB (37 wt.%)	Free radical	650	-	-	43
Hypercrosslinked networks	Linear PS with MCDE, XDC, CMDP, CMM	Friedel-Crafts	240-1200	Micro-	-	39,42,44,45,53
Hypercrosslinked networks	PS-DVB (0.3-2%) with MCDE	Friedel-Crafts	60-1500	Micro-	-	53
MN-200	PS-DVB with MCDE	Friedel-Crafts	1500	Micro-, Macro-	HPLC	62
Hypercrosslinked resins	Chloromethylated gel-type PS-DVB (5%)	Friedel-Crafts	Up to 1000	Micro-	-	51
Autocrosslinked Resins	Styrene-VBC copolymers	Friedel-Crafts	145-691	Small meso- (2.5 nm)	-	59
Hyper-cross-linked resins	VBC-DVB (2 mol%)	Friedel-Crafts	Up to 2090	Micro-	-	54
Hyper-cross-linked resins	VBC-DVB (20 mol%)	Friedel-Crafts	Up to 1160	Micro-, meso-	-	54
HCP-DVB-VBC	VBC-DVB (0-10 mol%)	Friedel-Crafts	1260-2060	Micro-, meso-	H_2 and CO_2 adsorption	60
HXLGp	p-VBC-DVB (2 wt%)	Friedel-Crafts	908	-	Solid-phase extraction	63
HXLGmix	p-(30%), m-(70%)VBC-DVB (2 wt%)	Friedel-Crafts	1889	-	Solid-phase extraction	63
Hypercrosslinked monoliths	Styrene (30 wt %), VBC (30 wt %), DVB (40 wt %)	In-situ free radical and Friedel-Crafts	663	Meso-	Chromatographic column	66
Hypercrosslinked monoliths	Styrene, VBC, DVB	In-situ free radical and Friedel-Crafts	Up to 631	Micro-, meso-	Chromatographic column	67
Hypercrosslinked monolithic polymers	4-Acetoxystyrene, styrene, VBC, DBV	In-situ free radical and Friedel-Crafts	Up to 292	Micro-, meso-	Chromatographic column	70

2.4.1.3 Other DVB highly crosslinked polymer networks

Divinylbenzene provides rigid and short crosslinks, and a styrenic polymer becomes insoluble when copolymerized even with as little as 0.5% of divinylbenzene.[72] In the synthesis of macroporous DVB-styrene copolymerization, the void space after the diluents are removed become permanent porosity only if a sufficiently large amount of crosslinking agents are used to hold the pore structure.[10]

Technical grade (80%) DVB was often seen in publications as the crosslinking agent, especially in industrial scale of copolymer synthesis.[10] The commercially available DVB contains 80% of a mixture of *para*- and *meta*- isomers of DVB, while the amount of *ortho*- isomer is negligible since *ortho*-DVB could rapidly cyclize into naphthalene.[10] The other impurities are mostly *para*- and *meta*- isomers of ethylstyrene and diethyl benzene. The contents of the mixture in DVB may cause inhomogeneity of the crosslinked copolymer. For example, while the reactivity of *meta*-DVB is close to that of styrene, the *para*-DVB showed higher reactivity than styrene (*p*-DVB was found to polymerize 2.5 times faster than styrene at 70 ˚C and 3.5 times at 90 ˚C).[73,74] Therefore during the copolymerization, *p*-DVB is consumed first and the distribution of crosslinks can be extremely imhomogeous.[10] Such inhomogeneity of the copolymers may result in poor swelling properties and affect potential applications in adsorption/ion exchange resins. Other than the *p*- and *m*- DVB isomers, the minor amount of diethylbenzene in the mixture (less than 2%) serves as an active chain transfer agent (telogen), and affects the length of the radical chains and can also lead to inhomogeneity of the final polymer.[10]

The electron-deficient maleic anhydride or maleimides are readily copolymerized with electron-rich styrenic monomers in an alternating fashion.[75,76] Styrene-DVB-maleic anhydride beads were reported to be synthesized using suspension polymerization, where glycerol was used

as the continuous phase instead of water to reduce the hydrolysis of the anhydride groups.[77,78] The DVB-maleic anhydride network showed moderate BET surface areas around 400 m^2/g.[78] Different sized DVB-maleic anhydride particles were achieved using various polymerization techniques such as suspension polymerization,[78] precipitation polymerization,[79] and dispersion polymerization.[80] The anhydride groups could be hydrolyzed to diacids or could react with amines to form amide ester.[77] These highly crosslinked DVB-maleic anhydride networks were investigated for potential applications such as heavy metal adsorption,[77] magnetite supporting matrix,[80] and gas sorption.[81]

A novel alternating copolymer-based hypercrosslinked network was prepared by the precipitation polymerization of bismaleimide and divinyl benzene.[82] The bismaleimides were rigid with short middle groups like phenyl or diphenylmethane. These networks have high surface areas in the range of 627-841 m^2/g, due to the rigid building blocks and the high crosslinking degree. They showed high adsorption capacities for CO_2, H_2 and organic vapors.

Porosity in polymer particles could also be achieved by selectively etching a minor component from a crosslinked ordered block copolymer with degradable or etchable blocks such as polylactide (PLA) or poly(*tert*-butyl acrylate) (P*t*BA). This approach requires the etchable block to be accessible to the etching agent, and the remaining matrix to be rigid enough to maintain the porous structure from collapsing. *tert*-Butyl carboxylate-containing stilbene and maleimide copolymers were crosslinked with more than 60% of DVB via suspension polymerizations, the resulting polymer precursor particles were deprotected using TFA to remove the *tert*-butyl protection groups (Figure 2-5).[83] These polymers showed BET surface areas up to 817 m^2/g, and their CO_2 capture ability was boosted by the surface carboxylate acid groups.

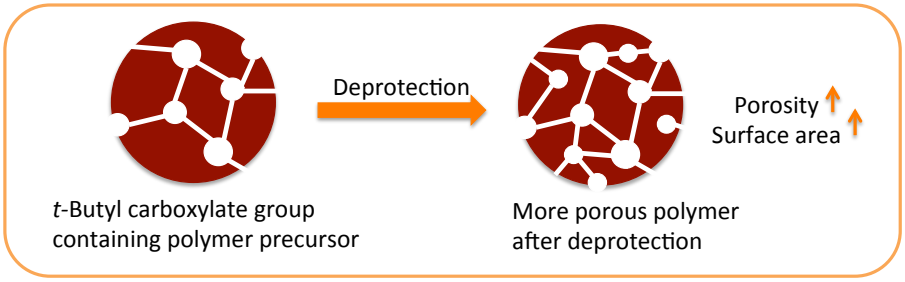

Figure 2-5. Nanoporous polymers from crosslinked polymer precursors via *tert*-butyl group deprotection. Reprint from Huang et al.[83] with permission. Copyright 2015 American Chemical Society.

Hillmyer and coworkers employed the polymerization-induced phase separation by crosslinking DVB and styrene (1:4) in presence of a RAFT agent which contains a chemically etchable PLA segment (Figure 2-6).[84] The resulting copolymer microphase separated into a PLA-rich domain and a styrene-rich domain. When the PLA segments were removed by basic hydrolysis, the remaining matrix maintained the resultant mesopores and formed a reticulated poly(styrene-co-DVB) network with three-dimensional continuous pore structures. The pore diameter (in the range of 4-8 nm) could be tuned by using different lengths of PLA segments-containing RAFT agents. A similar reticulated polymer network with mesopores was prepared by the same approach, in which 4-vinylbenzyl chloride (VBzCl) and DVB (4:1) were copolymerized in presence of the PLA-containing RAFT agent, then the polymer precursor was etched under basic condition to remove the PLA block.[85] Using the same PLA-b-poly(VBzCl-co-DVB) precursor, a hierarchically porous network could be obtained by hypercrosslinking through the Friedel-Crafts reaction and simultaneous etching of PLA by $FeCl_3$. Both mesopores (6-15 nm) from the etching of the PLA block and micropores (<2 nm) from hypercrosslinking of VbzCl were observed in this network. Another example of a hierarchically porous polymers was by adding nonreactive poly(ethylene oxide) (PEO) during the polymerization of styrene and DVB using the PLA-containing RAFT agent.[86] Simultaneous macro- and microphase separation was controlled by the molecular weight

or fraction of PEO. After basic etching, tunable meso- and macropores were achieved. A heterofunctional initiator was designed to simultaneously initiate the ring opening polymerization of D,L-lactide in presence of $Sn(Oct)_2$, and work as a RAFT agent in the copolymerization of styrene and DVB (molar ratio 4:1).[87] This one-pot thermally induced procedure resulted in a phase separated crosslinked block copolymer precursor, and the precursor was further converted to nanoporous polymer by basic hydrolysis of the PLA block.

Solid-state polymer electrolyte membranes were synthesized by the RAFT copolymerization of styrene and DVB using a PEO-containing RAFT agent in presence of an ionic liquid.[88-90] The ionic liquid was partitioning into the PEO domain, which led to a nanostructured membrane with a mechanically robust crosslinked polystyrene phase and an ion conductive PEO/ionic liquid phase. This electrolyte membrane holds potential as an alternative to liquid electrolytes for electrochemical devices. The HCPs that are mentioned in Section 2.4.1.3 are summarized in Table 2-2.

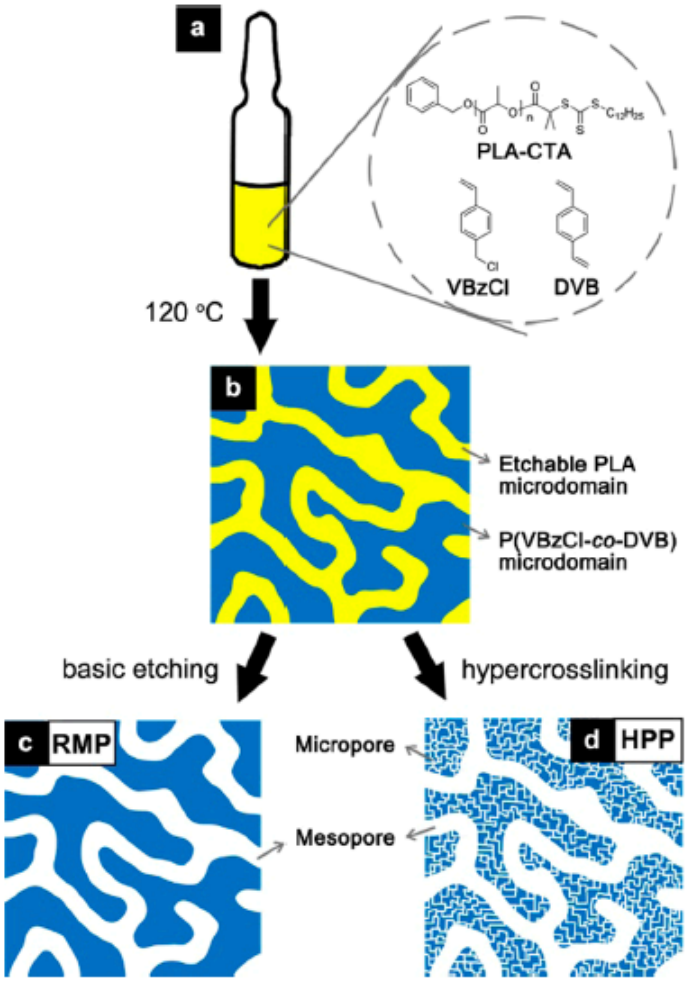

Figure 2-6. The synthesis of hierarchically porous polymers using a PLA-containing RAFT agent, vinylbenzyl chloride and divinyl benzene.[84,85] Reprint from Seo et al.[85] with permission. Copyright 2015 American Chemical Society.

Table 2-2. Summary of HCPs in Section 2.4.1.3

Polymers	Monomer or precursor	Synthetic strategy	BET surface area (m^2/g)	Pore type	(Potential) Applications	Ref.
MA-DVB	Maleic anhydride, DVB (50 mol%)	Free radical suspension	Up to 460	Meso-	-	78
Crosslinked SMA beads	Styrene, Maleic anhydride, DVB	Free radical suspension	-	Meso-	H_2 adsorption	81
DVB series alternating copolymers	Bismaleimides, DVB	Free radical precipitation	627-841	Micro-, meso-	H_2, CO_2, and organic vapor adsorption	82
STB-DVB and Sty-DVB	*tert*-Butyl carboxylate-containing stilbene or styrene, maleimide with DVB	Free radical suspension and deprotection of *tert*-butyl groups	Up to 817	Micro-	CO_2 adsorption	83
Nanoporous monolith	PLA-CTA, styrene, DVB	RAFT copolymerization and PLA degradation	Up to 250	Meso-	-	84
P(VBzCl-co-DVB)	PLA-CTA, VBC, DVB	RAFT copolymerization and Friedel-Crafts with simultaneously PLA degradation	Up to 1180	Micro-, meso-	-	85
(PLA-b-P(S-co-DVB))	Styrene, DVB, D,L-lactide	RAFT copolymerization and PLA degradation	110	Meso-	-	87
PLA-b-P(S-co-DVB)	PLA-CTA, styrene, DVB, PEO	RAFT copolymerization and PLA and PEO degradation	Up to 115	Meso-, macro-	-	86
Polymer electrolyte membranes	PEO-CTA, styrene, DVB, ionic liquids	RAFT copolymerization and PEO degradation	-	Meso-	Polymer electrolyte membranes	88-90

2.4.2 Hypercrosslinked polymers from crosslinking of polymer chains with external crosslinkers

Besides hypercrosslinked polystyrene, several HCP networks have also been synthesized by the post-crosslinking of highly solvated polymer chains through rigid bridges. Hypercrosslinked polysulfones were prepared by crosslinking of bromomethylated polysulfones *via* Friedel-Crafts reaction (Figure 2-7).[43] The bromomethyl group was introduced to every benzene ring of the linear polysulfone by reacting with bromomethylalkyl ether.[91] However, the benzene rings next to the electron-withdrawing sulfone groups were deactivated for Friedel-Crafts reaction. In addition, polysulfones possess more flexible chain structures compared to polystyrene because of the oxygen links. Both the high conformational flexibility and the less efficient crosslinking resulted in relatively low surface areas (up to 72 m^2/g).

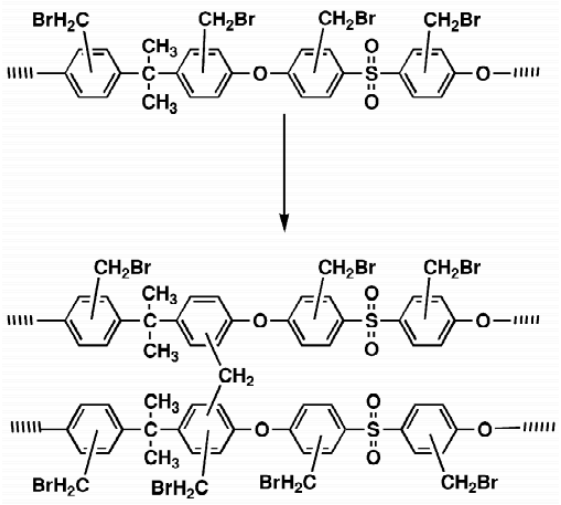

Figure 2-7. Synthesis of hypercrosslinked polysulfone. Reprinted from Tsyrupa et al.[43] with permission. Copyright 2002 Elsevier.

Hypercrosslinked polyaniline was synthesized by crosslinking commercially available polyaniline with diiodomethane or paraformaldehyde to form methylene links between the N atoms (Figure 2-8).[38] Interestingly, no quaternization reaction was observed. The resulting hypercrosslinked polyanilines have BET surface area up to 632 m^2/g. In this study, the authors

varied the lengths of diiodoalkane crosslinkers and found that polyanilines prepared from longer and more flexible crosslinkers have lower surface areas. These long crosslinkers were proposed to be not rigid enough to maintain the pore structure when solvents were removed from the network. Therefore, the rigidity of the crosslinkers is crucial for achieving high surface areas in polymers. Other than diiodoalkanes, dihalogenbenzenes were also used as crosslinkers for hypercrosslinked polyanilines through Ullmann or Buchwald coupling reactions (Figure 2-9).[92] The resulting network exhibited BET surface area up to 316 m^2/g. Buchwald reaction was also utilized to synthesize networks from diaminobenzene and di-, or tribromobenzene. The BET surface area of the network synthesized from tribromobenzene (249 m^2/g) is much higher than the one from dibromobenzene (17 m^2/g) due to the higher crosslinking density. Using a similar strategy, hypercrosslinked polypyrroles were prepared by the reaction of polypyrroles with diiodomethane, triiodomethane, or triiodoborane to form CH_2, CH or B links among the N atoms (Figure 2-10).[93] The short crosslinkers afforded high BET surface area up to 732 m^2/g.

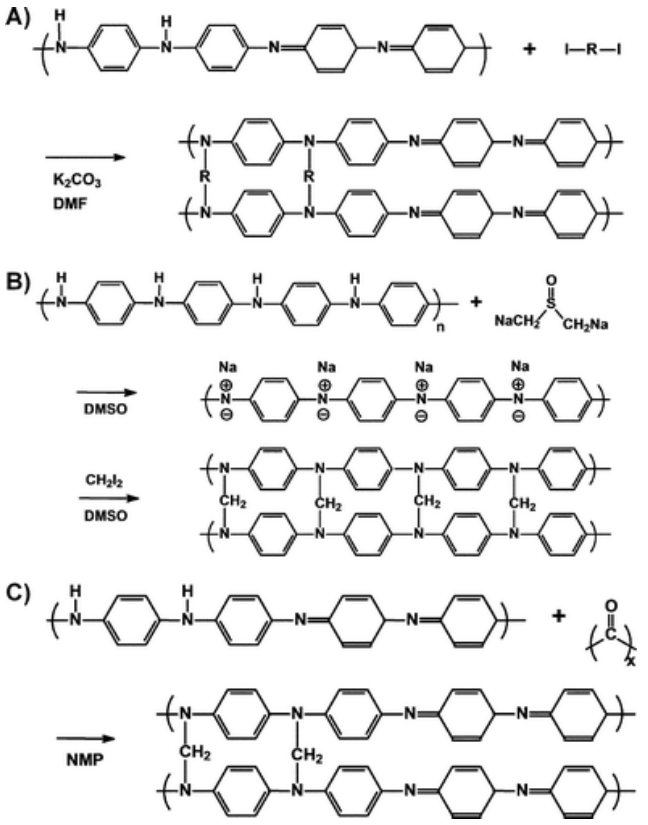

Figure 2-8. Synthesis of hypercrosslinked polyanilines using diiodoalkanes. Reprint from Germain et al.[38] with permission. Copyright 2007 Royal Society of Chemistry.

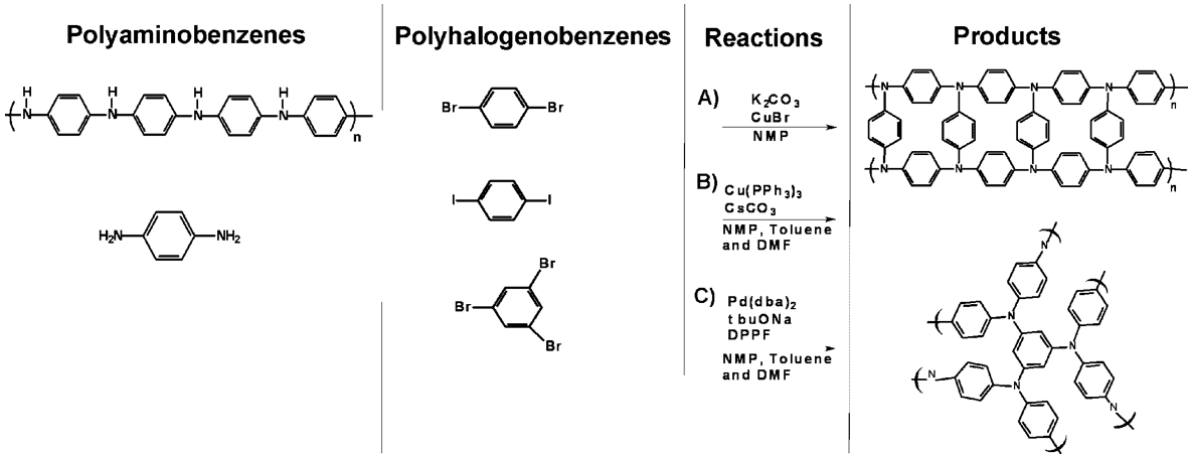

Figure 2-9. Synthesis of hypercrosslinked polyanilines using polyhalogenbenzenes. Reprint from Germain et al.[92] with permission. Copyright 2008 American Chemical Society.

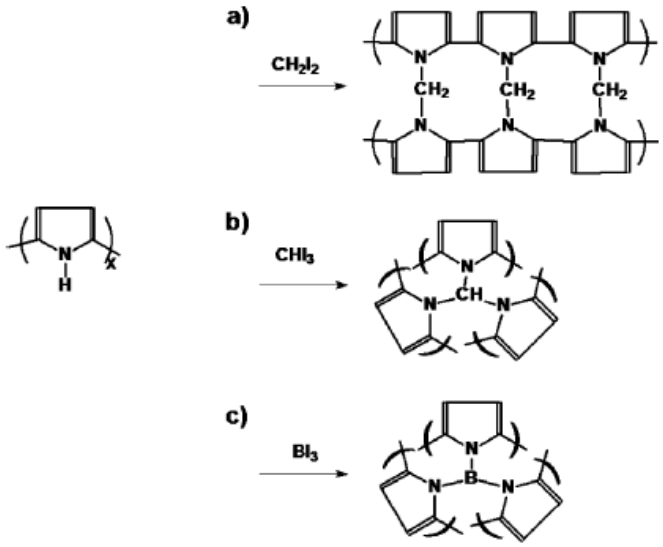

Figure 2-10. Synthesis of hypercrosslinked polypyrroles. Reprint from Germain et al.[93] with permission. Copyright 2009 Royal Society of Chemistry.

Most HCPs are synthesized based on pure organic networks and are fairly hydrophobic. The first hydrophilic HCP was obtained *via* the spontaneous *N*-alkylation and polymerization of the 4-vinylpyridine monomer with *p*-xylylene dichloride (*p*-XDC) crosslinker (Figure 2-11).[94] The reaction proceeded the best in *N*-methyl-*N*-butylimidazolium tetrafluoroborate, an ionic liquid. *p*-XDC yielded a xylene linker between two 4-vinylpyridine molecules, and generated quaternary ammonium salts, thus the final network possessed a high density of positive charges. The surface area of this network is around 100 m^2/g, which is much smaller than hypercrosslinked polystyrene synthesized using the same crosslinker. This is probably due to the extra flexibility at the quaternary nitrogen atom.

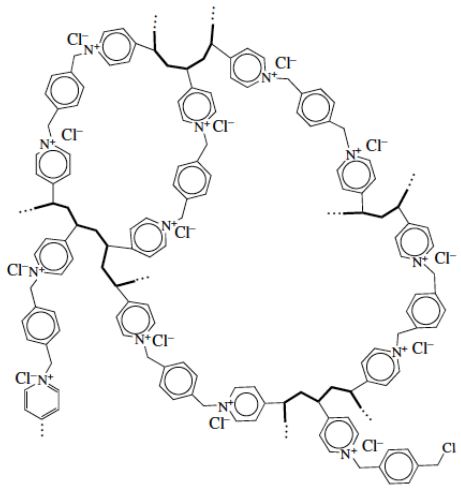

Figure 2- 11. The structure of the hydrophilic HCP based on 4-vinyl pyridine and p-XDC. Reprint from Pavlova et al.[94] with permission. Copyright 2006 Springer.

As previously mentioned, formaldehyde dimethyl acetal (FDA) was used as a less-toxic bifunctional external crosslinker which alkylates two phenyl rings of polystyrene (PS) chains via Friedel-Crafts reaction. This technique is especially convenient to create nanoporous structures using PS precursors. It was found that the BET surface area increases as the degree of polymerization (DP) of PS precursors up until DP=32, and no significant increase of BET surface area was observed beyond this DP.[95] By slowly adding FDA and $FeCl_3$ into highly diluted PS solution, hypercrosslinked PS can form thermodynamically stable homogeneous liquids in various organic solvents.[96] This solution-processable hypercrosslinked PS has BET surface area up to 724 m^2/g and good gas sorption properties. Monodisperse porous nanospheres with diameters as low as 190 nm were synthesized by using FDA to hypercrosslink the emulsion-polymerized PS-DVB precursors.[97] The hypercrosslinking reaction initially occurred rapidly on the periphery of the nanospheres and created an unreactive outer skin for each nanoshpere, which minimized the undesired inter-sphere crosslinking. The resulting nanospheres showed BET surface area up to 527 m^2/g. Polymeric molecular sieve membranes with tailored porosity were synthesized by FDA-hypercrosslinking of non-porous PS membranes.[98] The obtained porous membranes possess

interconnected hierarchical pore networks, and they show high permeability and selectivity in CO_2 separation. Three-dimensional polymeric and carbonaceous nanoscale networks were prepared by FDA-hypercrosslinking of self-assembled poly(methyl methacrylate) (PMMA)@PS core-shell nanospheres (Figure 2-12).[99] The resulting polymeric nanoscale networks were carbonized, and the thermal decomposition of the PMMA core generates larger hierarchical porosity in addition to the micropores from hypercrosslinking, and the BET surface area increased from 288 m^2/g to 839 m^2/g.

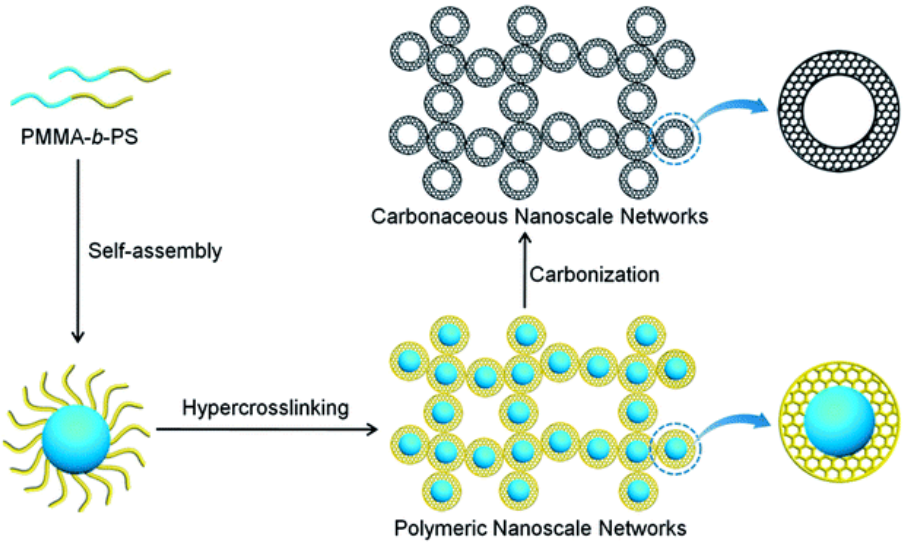

Figure 2-12. The preparation of polymeric and carbonaceous nanoscale networks by FDA-hypercrosslinking of self-assembled PMMA@PS core-shell nanospheres. Reprinted from Li et al.[99] with permission. Copyright 2014 Royal Society of Chemistry.

Lignin is the most abundant phenolic natural polymer. Bio-based renewable polymer organosolv lignin was crosslinked using an external crosslinker FDA to produce a hypercrosslinked network (Figure 2-13).[100] The network showed low surface area (< 5 m^2/g) and moderate CO_2 uptake but good CO_2/N_2 selectivity. The high char yield (> 50%) in thermogravimetric analysis inspired the authors to study the pyrolysis of this network. After treating the network under N_2 at 550 ˚C for 6 h, the surface area of the sample increased to ca. 100

m^2/g, and the CO_2 uptake increased while the selectivity was maintained.

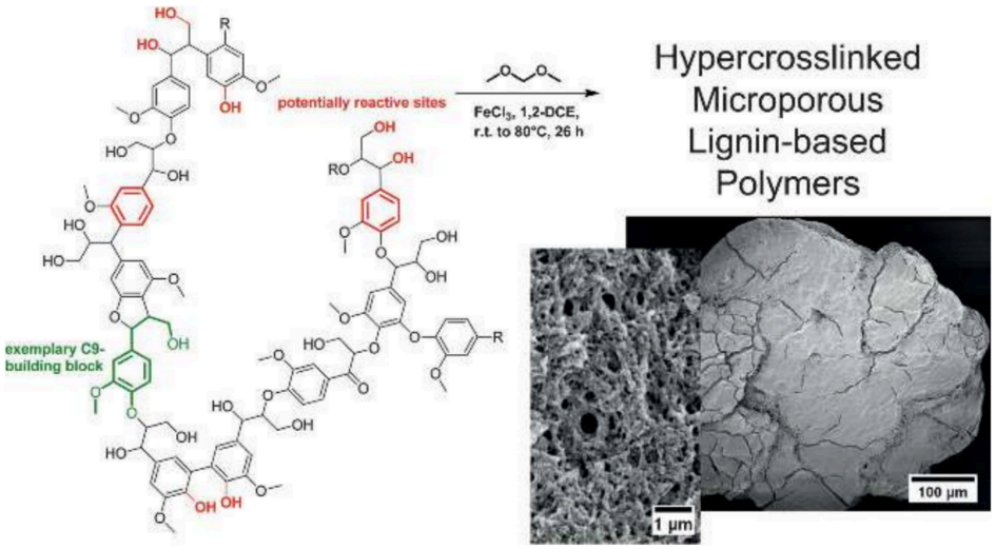

Figure 2-13. Synthesis of hypercrosslinked lignin-based polymers. Reprinted from Meng et al.[100] with permission. Copyright 2014 Wiley-VCH.

The external crosslinker FDA was also used to crosslink with the phenyl groups on phenylmethylsilicone. The silicon-oxygen backbone was then etched by hydrofluoric acid. After etching, the BET surface area of the polymers significantly increased by a factor of two (up to 1201 m^2/g), and the resulting networks shows good adsorption capacity and selectivity towards CO_2 (Figure 2-14).[101] The HCPs that are mentioned in Section 2.4.2 are summarized in Table 2-3.

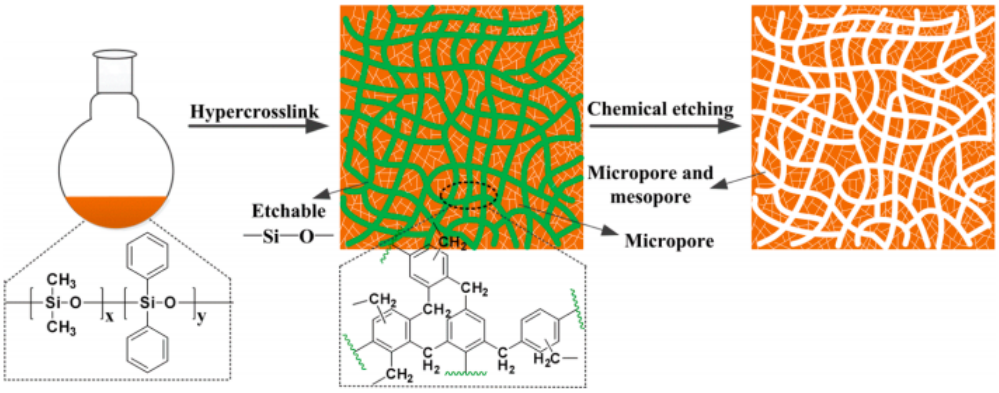

Figure 2-14. Network from crosslinking of phenylmethylsilicone with FDA and etching the silicone backbone. Reprint from Ding et al.[101] with permission. Copyright 2017 American Chemical Society.

Table 2-3. Summary of HCPs in Section 2.4.2

Polymers	Monomer or precursor	Synthetic strategy	BET surface area (m^2/g)	Pore type	(Potential) Applications	Ref.
Hypercrosslinked polysulfone	Bromomethylated polysulfone	Friedel-Crafts	Up to 72	-	-	78
Hypercrosslinked polyaniline	Polyaniline with diiodomethane or paraformaldehyde	*N*-alkylation reactions	Up to 632	Micro-, meso-	H_2 adsorption	38
Nitrogen-linked nanoporous networks of aromatic rings	Polyaminobenzenes or aniline with polyhalogenobenzenes	Ullman reaction or Buchwald Reaction	Up to 316	Micro-, meso-	H_2 adsorption	92
Hypercrosslinked polypyrroles	Polypyrroles with diiodomethane, triiodomethane or triiodoborane	*N*-alkylation reactions	Up to 720	Micro-	H_2 adsorption	93
Hypercrosslinked hydrophillic networks	4-Vinyl pyridine, p-xylylene dichloride	Menshutkin *N*-alkylation reactions	100	-	Ion exchange, catalysis	94
CLPS	Linear polystyrene, FDA	Friedel-Crafts	Up to 974	Micro-	CO_2 adsorption	95
SHCP	Linear polystyrene, FDA	Friedel-Crafts	Up to 724	Micro-, meso-	Solution-processable HCP, H_2, CH_4, CO_2 adsorption	96
MMPNS-CT1	Styrene, DVB, FDA	Free radical emulsion and Friedel-Crafts	527	Micro-	-	97
Hypercrosslinked polymeric membranes	PS membranes, FDA	Friedel-Crafts	Up to 792	Micro-	CO_2/N_2 and O_2/N_2 separation	98
PMMA@PS	PMMA-b-PS, FDA	Self-assembly, Friedel-Crafts and carbonization	Up to 839	Micro-, meso-, macro-	CO_2 adsorption, supercapacitor electrodes	99
OL-HC	Lignin, FDA	Friedel-Crafts and carbonization	100	Micro-	CO_2 adsorption	100
HCP/F-HCP	Phenylmethylsilicone, FDA	Friedel-Crafts and etching of the Si-O bond	Up to 1201		CO_2 and organic vapor adsorption	101

2.4.3 Hypercrosslinked polymers from polycondensation

Polycondensation of multifunctional small organic molecules provides another pathway for obtaining rigid, open-framework structures which share similar properties with the hypercrosslinked polystyrene networks. Numerous organic reactions were utilized to crosslink the building blocks, however, some networks were named as different systems and were exhaustively reviewed, such as the covalent organic frameworks (COFs) via boron-based reversible reactions,[102,103] conjugated microporous polymers (CMPs) by palladium-catalyzed Sonogashira-Hagihara cross coupling,[14,16] porous aromatic frameworks (PAFs) from nickel-catalyzed Yamamoto coupling,[21,22] covalent triazine frameworks (CTFs) through trimerization of aromatic nitrile compounds,[20,104] etc. This chapter mainly focuses on the networks which were synthesized by Friedel-Crafts mechanism and those do not fit in the networks mentioned above.

Some previously mentioned crosslinkers which contain chloromethyl groups could form HCPs by direct condensation *via* Friedel-Crafts mechanism. In 2002, Tsyurupa and Danvankov first reported the polycondensation of *p*-dichloroxylene (*p*-DCX) in the presence of $SnCl_4$.[43] In 2007, Cooper and coworkers synthesized a series of high surface area HCPs by the homo-polycondensation or copolymerization of bis(chloromethyl) aromatic monomers such as *m*-, or *p*-dichloroxylene (DCX), 4,4'-bis(chloromethyl)-1,1'-biphenyl (BCMBP), and 9,10-bis(chloromethyl)anthracene (BCMA) (Figure 2-15).[105] These HCPs have BET surface areas of up to 1904 m^2/g, and the monomer ratio in the copolymerization affects surface area. The HCPs synthesized from DCX and BCMBP showed high CO_2 capture capacity and CO_2/H_2 selectivity under high pressure. These HCPs are proposed to be excellent candidates for the pre-combustion CO_2 capture of syngas, which contains a high percentage of CO_2 at high pressure.[106] BCMBP was also copolymerized with a series of non-functionalized fluorene-based monomers. The rigid and

strongly twisted fluorene monomers afford hypercrosslinked networks with high surface areas up to 1800 m^2/g.[107] Tan and coworkers prepared an HCP via Friedel–Crafts catalyzed self-condensation of 1,4-benzenedimethanol (BDM).[108] The resulting polymer HCP-BDM yielded a BET surface area of 847 m^2/g. They also demonstrated two HCPs synthesized by monofunctional monomers such as benzyl alcohol (BA) and benzyl chloride (BC), and both networks possessed BET surface areas around 740 m^2/g. After the self-condensation of the chloromethyl group-containing monomers, the unreacted chloromethyl groups were further reacted with *N*-methylimidazole to generate a series of imidazolium salt-modified HCPs.[109] These modified HCPs exhibited lower BET surface areas than their unmodified analogues but the CO_2 uptake level remained basically the same. They also showed much higher catalytic activities for the reaction of CO_2 and epoxides to cyclic carbonates compared to both homogeneous and polystyrene supported imidazolium salts.

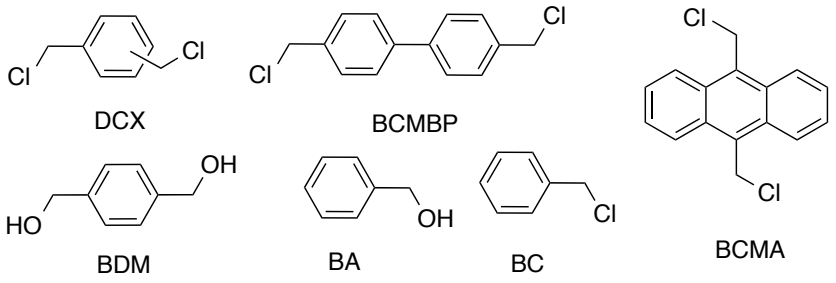

Figure 2-15. Difunctional and monofunctional monomers used for synthesis HCPs by polycondensation.[43,105,106,108]

A similar strategy was also used on the polycondensation of benzyl chloride group-terminated monomers. A monomer of *m*-carborane with two benzyl chloride end groups was self-condensed and copolymerized with BCMBP to yield two HCPs (Figure 2-16a).[110] The hydrogen adsorption properties of this material were studied and the heat of adsorption for hydrogen was related to the concentration of the carborane groups in the network, which could presumably be attributed to the strong electrophilicity of the carborane units. A hierarchically porous siloxane-

organic hybrid HCP was synthesized by the hypercrosslinking of polyhedral oligomeric silsesquioxanes (POSS) containing monomer with benzyl chloride end groups *via* Friedel-Crafts reaction (Figure 2-16b).[111] The ^{29}Si MAS NMR revealed that the double-four-ring (D4R) cage structure in POSS was destroyed, which may due to the structural distortion and the acidic condition during the synthesis. However, the resulting networks showed ultrahigh surface areas (ca. 2500 m^2/g). This work suggested a strategic concept to the synthesis highly porous siloxane-organic hybrids by the simultaneous hypercrosslinking of organic groups and the destruction of the siloxane cages.

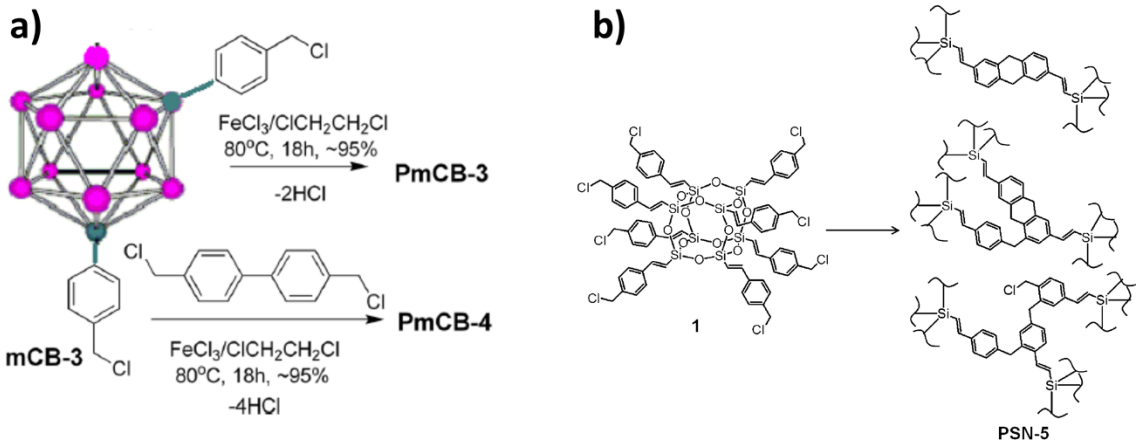

Figure 2-16. The synthesis of a) m-carborane- and b) POSS-containing HCPs by the polycondensation of benzyl chloride end groups. Reprint from Yuan et al.[110] and Chaikittisilp et al.[111] with permission. Copyright 2011 Wiley-VCH and 2011 American Chemical Society.

While most polycondensations require monomers to have specific functional groups to couple with each other, the Scholl reaction provides an alternative to prepare hypercrosslinked polymer networks without designing and synthesizing the monomers. Phenyl group-containing monomers were cross-linked with each other with the aid of a Lewis acid and a protic acid, the resulting networks possess porous and highly conjugated structures (Figure 2-17a).[112] Pd nanoparticles could be immobilized in this microporous network by the reduction of the Pd ion in the presence of the network, the resulting ligand-free catalyst was able to catalyze the fast

conversion of Suzuki-Miyaura coupling even at 0.05 mmol% of Pd loading, and the catalyst showed excellent stability and reusability.[113] A POSS-based HCP network that was prepared by Scholl reactions could resist relatively strong acidic conditions (Figure 2-17b).[114] The steric effect during the Scholl reaction reduced the degree of hypercrosslinking and thus may release the structural stress to maintain the integrity of the D4R structure, the final HCP had a BET surface are of 472 m^2/g.

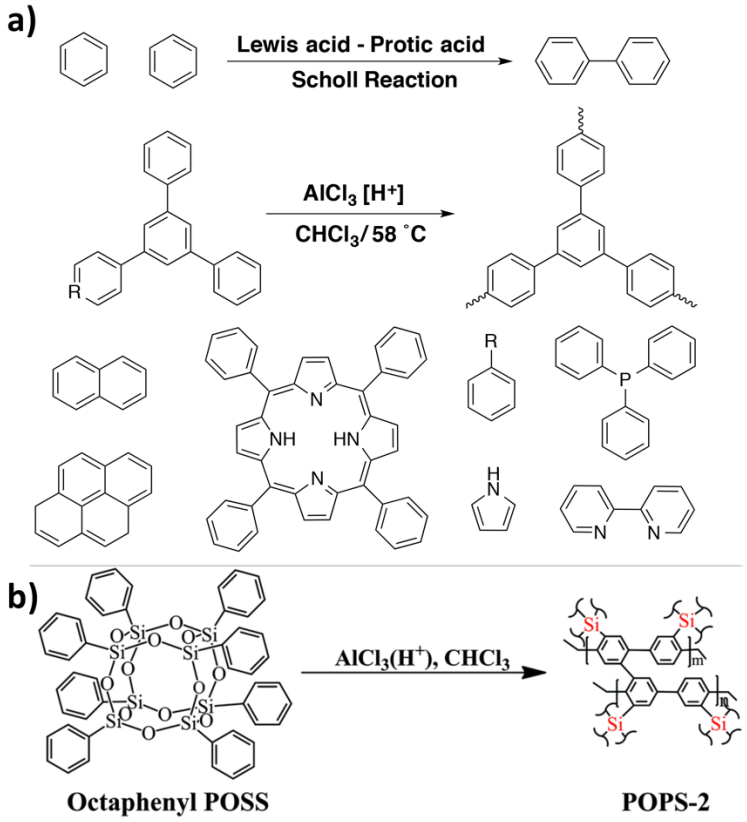

Figure 2-17. The synthesis of HCPs using the Scholl Reaction. Reprint from Li et al.[112] and Wang et al.[114] with permission. Copyright 2014 and 2015 Royal Society of Chemistry.

The oxidative coupling polycondensation of carbazole-containing monomers offers another efficient route towards hypercrosslinked polymer without the requirement of specific end groups for coupling (Figure 2-18).[115-117] Typically, the carbazole-containing monomer was mixed with the suspension of $FeCl_3$ in chloroform, and the mixture was stirred at room temperature for 18 hours

under N_2. The resulting nitrogen-containing, conjugated, and electron-rich network may enhance the interaction between the sorbent and the network. Such networks have BET surface areas up to 2440 m^2/g,[118] and they were investigated on their capture ability on gases such as CO_2,[115,118-120] H_2,[118-120] and CH_4,[119,120] and solvents like toluene,[118] methanol,[120] and water.[120] The porosity of the networks could be tuned by changing the center group,[118] and when the center group was Fe(II)-porphyrin, the network could serve as a heterogeneous catalyst for the oxidation of thioglycosides to glycosyl sulfoxides.[118]

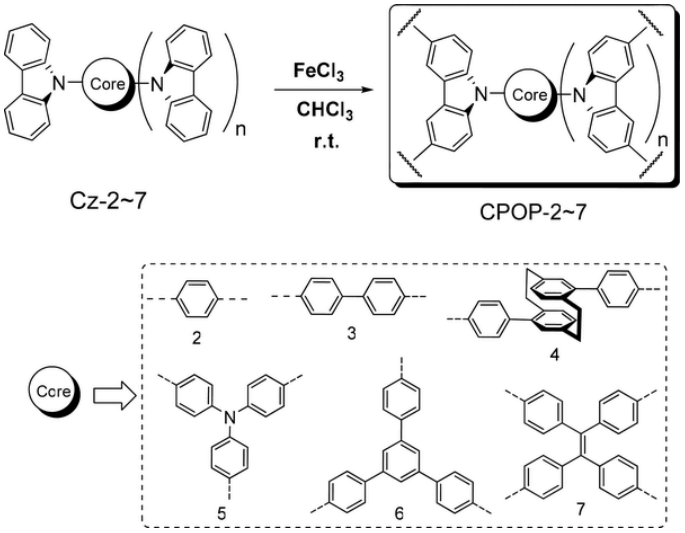

Figure 2-18. Synthesis of carbazole-containing HCPs. Reprint from Chen et al.[119] with permission. Copyright 2013 Wiley-VCH.

The use of sulfur-based chemistry was first reported for the preparation of HCPs by Stefan Bräse and coworkers.[121] They tried several sulfur-related reactions on the tetrakis(thiylphenyl)-methane monomer, but some of the reactions did not result in porous structures, and the formation of the porous structure highly relied on the reaction conditions. The nucleophilic substitutions with diiodomethane in 1,4-dioxane under acidic conditions yielded a network with 177 m^2/g BET surface area, and the thiol-Michael addition with *N*-arylbismaleimide in DMAc and in DMF resulted in HCPs with BET surface area of 1675 and 760 m^2/g, respectively, while no porous structure was observed for the product of the same reaction in NMP (Figure 2-19). These reactions

may contribute to the building of heteroatom-containing HCPs. The HCPs that are mentioned in Section 2.4.3 are summarized in Table 2-4.

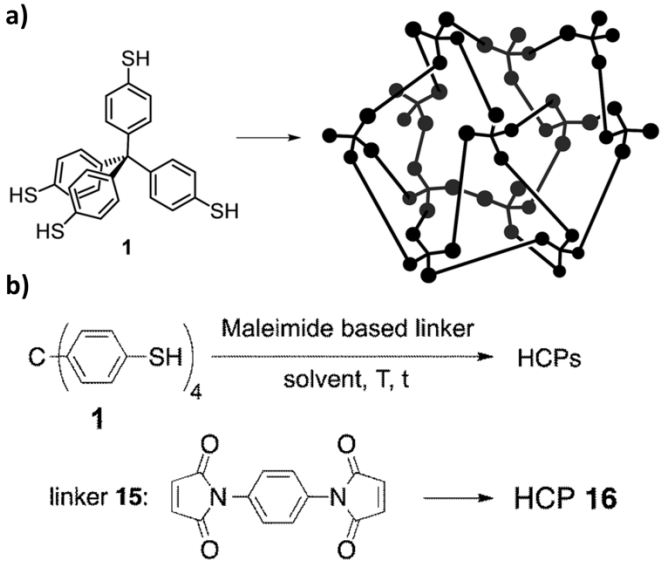

Figure 2-19. The generation of HCPs based on tetrakis(thiylphenyl)-methane 1 and the bismaleimide linker 15, the resulting HCP showed BET surface area of 1675 and 760 m^2/g when the reaction was carried out in DMAc and DMF, respectively. Reprint from Monnereau et al.[121] with permission. Copyright 2015 Royal Society of Chemistry.

Table 2-4. Summary of HCPs in Section 2.4.3

Polymers	Monomer or precursor	Synthetic strategy	BET surface area (m^2/g)	Pore type	(potential) Applications	Ref.
Hypercrosslinked polyxylylene	p-XDC	Friedel-Crafts	Up to 1000	-	-	78
Hypercrosslinked networks	XDC (ortho-, meta-, and para-isomers)	Friedel-Crafts	Up to 1431	Micro-, meso-	H_2 adsorption	105
Hypercrosslinked networks	p-XDC and/or BCMBP	Friedel-Crafts	Up to 1904	Micro-, meso-	H_2 and CO_2 adsorption	105,106
Hypercrosslinked networks	p-XDC and/or BCMA	Friedel-Crafts	Up to 1262	Micro-, meso-	H_2 adsorption	105
FLUO, s-FLUO, DBF, DBT	BCMBP and fluorine-based monomers	Friedel-Crafts	Up to 1800	Micro-, meso-	H_2 and CH_4 adsorption	107
HCP-BDM HCP-BA HCP-BC	BDM, BA, BC	Friedel-Crafts	847, 742, 746	Micro-, meso-, macro-	H_2 and CO_2 adsorption	108
POM	Bis-halomethylated benzenes	Friedel-Crafts	Up to 1089	Micro-, meso-, macro-	CO_2 adsorption	109
POM-IM	Bis-halomethylated benzenes, *N*-methylimidazole	Friedel-Crafts and *N*-alkylation	Up to 926	Micro-, meso-, macro-	CO_2 adsorption and conversion	109
PmCB-3 and PmCB-4	Benzyl chloride-ended m-carborane, BCMBP	Friedel-Crafts	864, 1037	Micro-	H_2 adsorption	110
PSN-5	Benzyl chloride-terminated POSS	Friedel-Crafts	2500	Micro-, meso-	H_2 adsorption	111
SMPs	Naphthalene, pyrene, PPh_3, meso-Tetra phenylporphyrin, benzyl amine, benzoic acid, pyrrole	Scholl reaction	Up to 1421	Micro-	H_2 and CO_2 adsorption, catalyst substrates, fluorescent and semiconducting material	112
Pd/SMP-$PhPh_3$	PPh_3, H_2PdCl_4	Scholl reaction and reduction of Pd ion	1068	Micro-	Heterogeneous catalyst for Suzuk-Miyaura cross-coupling	113
POPS-2	Octaphenyl POSS	Scholl reaction	472	Micro-, meso-	H_2 and CO_2 adsorption	114
CPOPs	Carbazole-based monomers	Oxidative coupling polymerization	Up to 2440	Micro-, meso-	H_2, CH_4, CO_2 and organic vapor adsorption	115-120
CPOPs	Carbazole-based monomers with hydroxylmethyl groups	Friedel-Crafts	Up to 780	Micro-, meso-	H_2, CO_2 and organic vapor adsorption	116
Sulfur-based HCPs	Tetrakis(thiylphenyl)-methane, *N*-arylbismaleimide	Thiol-Michael addition	Up to 1675	Micro-, meso-	-	121

2.4.4 Hypercrosslinked polymers from the crosslinking of small building blocks with external crosslinkers

In 2011, Tan and coworkers introduced a novel approach to synthesize hypercrosslinked polymers, and they called it the "knitting" strategy.[122] Aromatic ring-containing small organic molecules were crosslinked through methylene bonds by FDA as an external crosslinker via the Friedel-Crafts mechanism by the catalysis of a Lewis acid $FeCl_3$ (Figure 2-20). The resulting network showed high thermal stability (T_{dec} > 400 ˚C) and microporous structure. Furthermore, the specific surface area, porous properties and gas sorption properties could be controlled by changing the ratio of the aromatic molecules and the crosslinkers. The highest BET surface area of the networks from benzene and FDA was 1391 m^2/g, when using a 1:3 ratio of benzene and FDA (assuming that each benzene ring has three reactive sites). This network showed a chemoselective swelling phenomenon in CO_2, which resulted in an unusual isotherm shape and high CO_2/H_2 selectivity. These materials are robust enough to tolerate water and concentrated acid.[123]

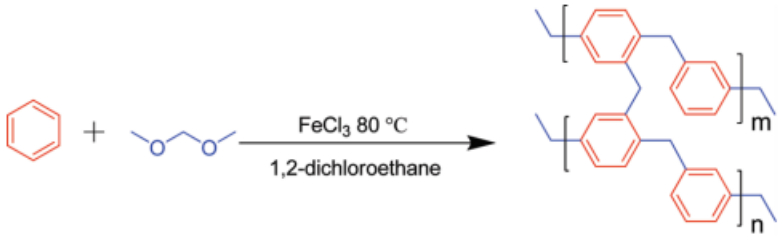

Figure 2-20. The knitting strategy using FDA to prepare hypercrosslinked polymers. Reprint from Li et al.[122] with permission. Copyright 2011 American Chemical Society.

Monomers of different structures that contain phenyl groups were also reported to yield hypercrosslinked networks by the "knitting" strategy, such as naphthalene,[124] anthracene,[124] phenanthrene,[124] biphenyl,[122] 1,3,5-triphenylbenzene,[122,124] tetraphenylmethane,[125,126] triptycene,[127] and inorganic group polyhedral oligomeric silesquioxane (POSS).[114] It is worth

noticing that the network prepared by the three-dimensional (3D) monomers tetraphenylmethane and triptycene showed the highest BET surface areas (1470 m^2/g and 1426 m^2/g, respectively) among all the hypercrosslinked networks using the "knitting" strategy, and the theoretical model on the tetraphenylmethane network showed that the most regular and ordered structure was achieved by connecting each tetraphenylmethane at the para position in a diamond arrangement.[126] All these polymer networks showed an intense brown color, and UV-Vis and FT-IR have confirmed the formation of quinonoid chromophores from the dehydrogenation of the para or ortho methylene groups (-CH_2-) among the aromatic rings.[124] The low bonding and anti-bonding energy gaps in these polymers caused the strong absorbance of light from 1000 to 200 nm, and these materials are proposed to have potential in research on semiconductors, solar cells and optical applications.

Other than FDA, 1,4-dimethoxybenzene,[128] formaldehyde, glyoxylic acid,[129] and dibromo-p-xylene[130] could all be used as the external crosslinker in the "knitting" strategy with $FeCl_3$ as the Friedel-Craft catalyst.

Aromatic heterocyclic monomers, like thiophene, pyrrole, and furan,[131] and fused-heterocyclic rings, such as carbazole,[132-134] benzothiophene,[132] tricarbazolyltriptycene,[135] benzofuran,[132] dibenzofuran[132] or triazine,[134] are also compatible with this approach to form hypercrosslinked networks. The resulting heteroatoms-rich, microporous networks showed high adsorption capacity and selectivity (over N_2) of CO_2. In particular, the network based on pyrrole showed an extraordinary high selectivity of 117 of CO_2/N_2 at 273 K.

Functional groups can be introduced by using specific functional monomers such as chlorobenzene and phenol. The network based on phenol exhibited a BET surface area of 400 m^2/g, but a rather high CO_2 adsorption capacity of 9.4 wt%.[122] This may result from the polar phenolic hydroxyl groups, which can affect the porous structure and also interact with CO_2 molecules.

Cooper and coworkers reported a series of hydroxyl-containing hypercrosslinked networks using polycyclic aromatic monomers. The monomers include naphthols, dihydroxynaphthalene, chiral and racemic bi-2-naphthol (BINOL), biphenol and bisphenol A.[136] Under idealized, dry conditions, the BINOL networks showed higher CO_2 adsorption capacities than their analogues, while under wet conditions the BINOL networks showed lower CO_2 adsorption capacities than their hydrophobic analogues, which suggested that the idealized laboratory experiments on measuring CO_2 capture capacities do not necessarily indicate the CO_2 capture potential of the material under realistic conditions. Because aryl amines can complex with Lewis acid and thus hinder Friedel-Crafts reactions, it is difficult to incorporate amine groups into hypercrosslinked networks, although amine groups are well-known to enhance the selectivity and capacity of CO_2 capture. Dawson et al. reported the synthesis of amine-containing hypercrosslinked networks from the reaction of aniline and benzene.[137] The network synthesized of only aniline was non-porous, while the copolymer of aniline and benzene showed BET surface area up to 1100 m^2/g. As the aniline content was increased, the surface area decreased but the CO_2/N_2 selectivity was improved.

Other than gas sorption, microporous hypercrosslinked networks with high surface areas also showed potential in water purification and treatment.[127] The network from triptycene crosslinked with FDA showed promising absorption capability for organic dyes, such as Congo Red, Methyl Blue, and Methylene Blue, and organic solvents such as chloroform, dimethyl sulfoxide (DMSO), toluene, *N,N*-dimethylformamide (DMF), methanol, acetonitrile, ethyl acetate, and hexanes. Remarkably, this material adsorbs 1100-3100 wt% of organic solvents, which is higher than the value of commercial activated carbon and common adsorbents. The high adsorption capacity was attributed to the high surface area and the hierarchical porosity which facilitated the organic compounds uptake by both adsorption and hierarchical pore filling.

The network synthesized from benzene and triphenylphosphine with FDA by the "knitting" method could be used to immobilize organometallic catalysts.[112,138,139] Triphenylphosphine serves as a ligand to chelate the metal. The heterogeneous microporous structure of the network enhanced the dispersion of the active metal sites and also improved the diffusion of the organic starting materials. Palladium (II) ion was immobilized in the hypercrosslinked network, and the network showed a protective and facilitative effect on the Pd catalyst in promoting aqueous Suzuki-Miyaura cross-coupling under mild conditions.[138,139] The catalyst complex could be recovered by filtration and reused for 3-9 cycles with no more than 5% of Pd leaching in each run. *N*-heterocyclic carbenes (NHCs) were found to work as dual ligands to coordinate with Pd, and compared to triphenylphosphine, NHCs are stronger electron-donors, and have shorter metal–ligand bond lengths, stronger metal–ligand bond energies, and greater bond dissociation energies (Figure 2-21).[140] When triphenylphosphine was replaced with NHC-containing units, the resulting networks showed excellent stability, and the catalyst Poly-NHC-2–Pd^{2+} could be reused to promote Suzuki-Miyaura reaction for at least 5 cycles without significant activity decrease.[140] The same Poly-NHC network could also be utilized to support copper (I, II and III) catalysts.[141] The obtained catalyst complexes HCP-NHC-Cu series were used to catalyze the oxidative condensation reaction of indole, 1,3-dicarbonyl compounds and phenylglyoxal monohydrate, the three-component click reactions of NaN_3, phenylacetylenes and alkyl halides, the Ullmann C–N coupling and Glaser coupling reactions in high yields.

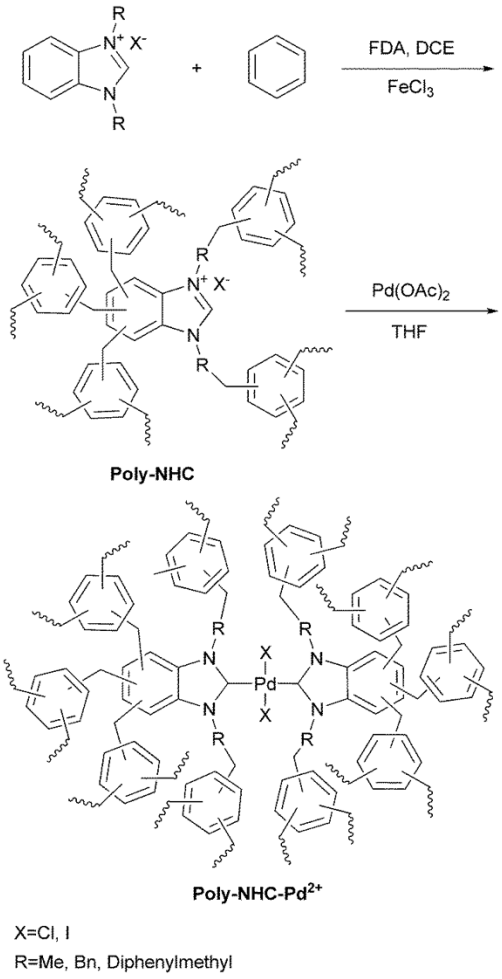

Figure 2-21. The synthesis of hypercrosslinked NHC-Pd^{2+}. Reprint from Xu et al.[140] with permission. Copyright 2014 Royal Society of Chemistry.

The carbonization at above 500 ˚C of the microporous hypercrosslinked networks prepared via a knitting strategy resulted in porous carbon materials with improved surface areas and controlled pore structures. They were studied as substrates for supporting metal nanoparticles.[142,143] The porous carbon-supported Pd nanoparticle catalysts were synthesized from the carbonization network of triphenylbenzene, benzene or chloromethyl polystyrene.[143] The heterogeneous catalysts showed not only high activity in promoting Heck coupling, but also high thermal stability, reusability, and low oxygen sensitivity. The similar porous carbon-supported Pd catalysts were also employed to catalyze oxygen reduction reactions.[142] The NHC-containing

porous carbon showed the best catalytic performance since the NHCs helped to anchor the Pd nanoparticles and inhibit aggregation.

The "knitting" strategy and the simple condensation of properly functionalized small molecules provide an efficient way to synthesize hypercrosslinked networks. The scope of a wide variety of monomers introduces various kinds of functional groups for different potential applications such as selective gas adsorption and catalyst immobilization. The relatively inexpensive monomers and reagents, as well as the high yields and mild conditions of the reaction offer the possibility of large-scale production. The HCPs that are mentioned in Section 2.4.4 are summarized in Table 2-5.

Table 2-5. Summary of HCPs in Section 2.4.4

Polymers	Monomer or precursor	Synthetic strategy	BET surface area (m^2/g)	Pore type	(potential) Applications	Ref.
MOPs	FDA with benzene	Friedel-Crafts	Up to 1391	Micro-	H_2 and CO_2 adsorption	[122,123]
MOPs	FDA with biphenyl, or 1,3,5-triphenylbenzene, or methylbenzene, or chlorobenzene, or phenol	Friedel-Crafts	Up to 1059	Micro-	H_2 and CO_2 adsorption	122
HCPs	FDA with benzene, or other fused aromatic monomers	Friedel-Crafts	Up to 924	Micro-	CO_2 adsorption	124
MOP-E or mPAF	FDA with tetraphenylmethane	Friedel-Crafts	1470	Micro-	CO_2 and CH_4 adsorption	[125,126]
THPS	FDA with triptycene	Friedel-Crafts	1426	Micro-, meso-	H_2, CO_2, organic solvents and dyes adsorption	127
HCCMPs	1,4-Dimethoxybenzene with benzene and other phenyl- containing monomers	Friedel-Crafts	Up to 800	Micro-	H_2 and CO_2 adsorption, fluorescent material	128
TOPF	Paraformaldehyde or glyoxylic acid with triptycene-based monomers	Friedel-Crafts	Up to 1444	Micro-, meso,	Organic vapor adsorption	129
HMP-1	Carbazole and dibromo-*p*-xylene	Friedel-Crafts	913	Micro-,	Solid acid catalyst substrate	130
Hypercrosslinked polycarbazoles	FDA with carbazole-based monomers	Friedel-Crafts	Up to 1845	Micro-, meso-	CO_2, H_2, and CH_4 adsorption	132-135
Hypercrosslinked heterocyclic porous polymers	FDA with fused heterocyclic monomers	Friedel-Crafts	Up to 1022	Micro-	CO_2 and CH_4 adsorption	132
Aromatic heterocyclic microporous polymers	FDA with thiophene, or pyrrole, or furan	Friedel-Crafts	Up to 966	Micro-, meso-	CO_2 adsorption	131
Hydroxyl-containing MOPs	FDA with hydroxyl-containing monomers	Friedel-Crafts	Up to 1015	Micro-	CO_2 adsorption	136
Aniline/benzene co-polymer networks	FDA with aniline and benzene	Friedel-Crafts	Up to 1097	Micro-	CO_2 adsorption	137
KAPs(Ph-PPh_3)	FDA with triphenylphosphine	Friedel-Crafts	1036	Micro-, meso-	Pd catalyst substrate	[138,139]
Poly-NHC	FDA with benzene and *N*-heterocyclic carbenes	Friedel-Crafts	Up to 1229	Micro-, meso-	Pd, and Cu catalyst substrate	[140,141]
Carbonized KAPs	FDA with benzene or $PhPh_3$, or NHC, and $PdCl_2$	Friedel-Crafts, carbonization and gas phase reduction	Up to 933	Meso-	Pd catalyst for oxygen reduction reaction	142
Carbon supported Pd NP	FDA with benzene, or $PhPh_3$, or PS-CH_2Cl and $PdCl_2$	Friedel-Crafts, Pd impregnation, carbonization, and H_2 reduction	Up to 924	Meso-	Pd catalyst for Heck reaction	143

2.5 Simulations of hypercrosslinked polymers

As a complement to instrumental characterization techniques, atomistic and molecular simulations provide valuable information about the structure and properties of hypercrosslinked polymers.[144] However, due to the complexity of the amorphous network structure, the accurate simulations of hypercrosslinked polymers are quite challenging.[105,144,145] Computational modeling of the crosslinked networks usually probes representative clusters which are "synthesized" by mimicking the experimental synthesis routes.[144,145] The simulated polymerization starts with a simulated box with monomers, which are then crosslinked according to pre-determined rules until forming a network.

HCPs based on the self-condensation of *p*-DCX were simulated to investigate their porous properties and gas sorption abilities.[105,146,147] A simplified *p*-DCX dimer was used to create the poly(*p*-DCX) cluster (Figure 2-22). The simulation slightly underestimated the absolute and bulk densities and overestimated the surface area, micropore volume and both H_2 and methane uptakes. Inaccessible pores that are not interconnected or are too small for sorbate gases are likely to be the reason. The simulated gas sorption isotherms fit with the experimental data better when an arbitrary scaling factor Φ was introduced.[105,146] The construction of the simulated structure was further adjusted using a Monte Carlo approach. A nonarbitrary method, which considered the solvent-accessible surface area, was shown to be more representative of the real physical system in estimation of the gas sorption isotherms.[146] Poly(*p*-DCX) was also simulated using an algorithm that the crosslinking and chain formation occur in cycles with equilibrations (Figure 2-23).[145,148] This virtual polymerization algorithm was generalized and released as an open-source software called *Polymatic*, and was shown to be a useful tool in the study of network polymers.[144,145,148-151] The gas sorption properties of hydrogen and methane were obtained using grand canocial Monte

Carlo (GCMC) simulations. The simulated and experimental hydrogen adsorption isotherms were quantitatively consistent, while the simulated methane adsorption was underestimated due to the larger methane molecule diameter. Two factors were found to be crucial to achieve microporous networks: a low concentration of the system during crosslinking that ensures the formation of the pores; and the high degree of crosslinking that locks the network in the expanded state.

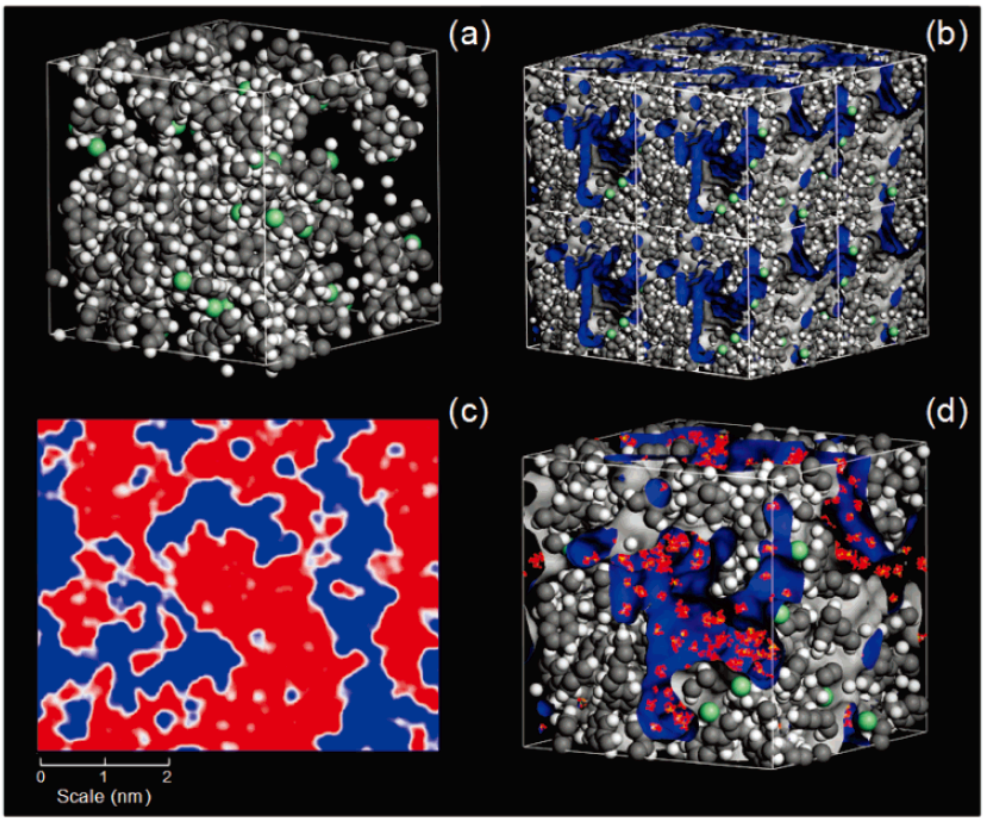

Figure 2-22. Molecular simulation of *p*-DCX (a) a simulation box; (b) three-dimensional array of eight amorphous cells, the Connolly surface (molecular surface) is blue/gray; (c) two dimensional "slice" through an array of amorphous cells, occupied and unoccupied volumes are in red and blue, respectively; and (d) H_2 sorption properties, H_2 molecules are in red/orange. Reprint from Wood et al.[105] with permission. Copyright 2007 American Chemical Society.

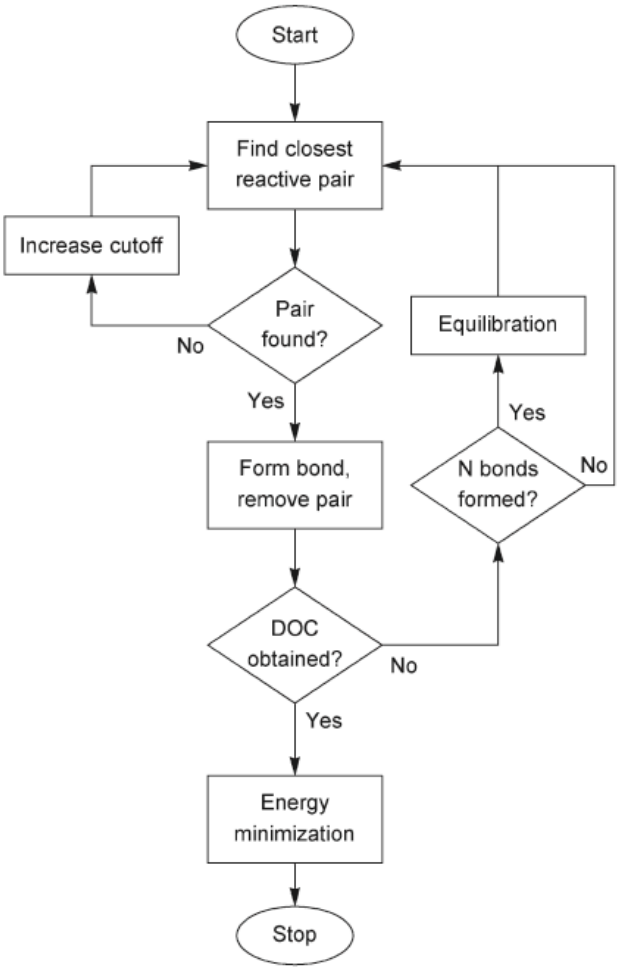

Figure 2-23. Crosslinking procedure flowchart. In which DOC represents the degree of crosslinking. Reprint from Abbott et al.[145] with permission. Copyright 2011 American Chemical Society.

Atomistic simulation was also employed to study the FDA-knitted HCPs. The benzene-based, biphenyl-based, and 1,3,5-triphenylbenzene-based networks were simulated, and the calculated surface areas were found to have the same trend as the experimental Langmuir surface area.[122] The simulated pore size (3-20 Å) was smaller than the experimental value, because the model simulated only micropores. The tetraphenylmethane (TPM)-based network was simulated and an ideal crystal structure was optimized (Figure 2-24).[126] The simulation predicted closely the narrow micropores with pore sizes around 5.82 Å, but underestimated the mesoporous region (between 20 and 60 Å). The argon, carbon dioxide, and methane sorption properties were simulated by Monte

Carlo techniques. The model showed higher gas uptake values than experimental values, but the simulated and experimental isotherms were in good agreement with low pressure experiments, indicating that the model has a good description of the microporous region of the network.

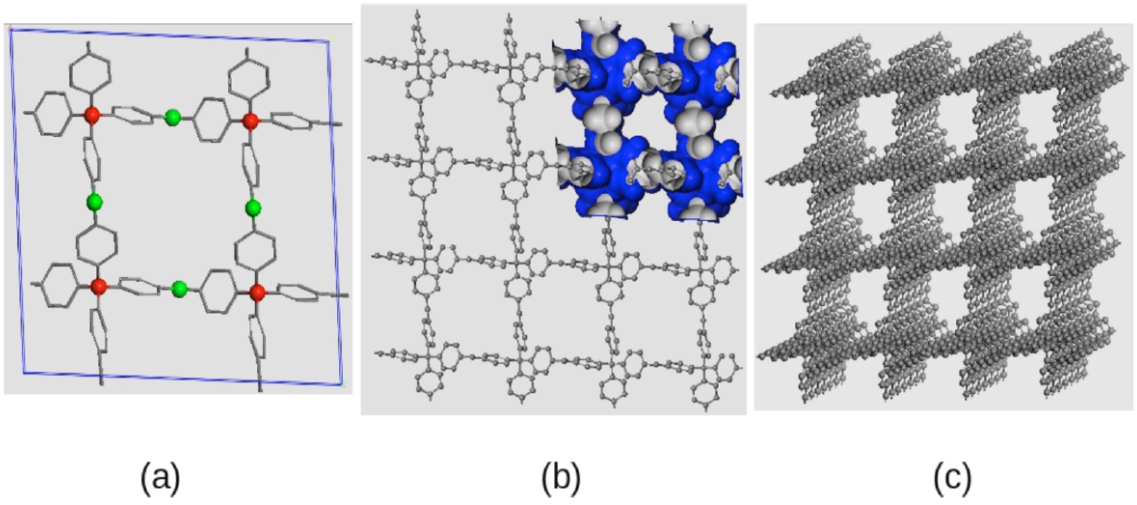

Figure 2-24. Ideal simulated structure of FDA-knitted TPM network. (a) Unit cell; (b), 2x2x1 supercell; (c) 2x2x6 supercell with 3D channel structure. Reprint from Errahali et al.[126] with permission. Copyright 2014 American Chemical Society.

During the synthesis of hypercrosslinked polystyrene networks, different amounts of monomers and crosslinkers in the precursor and final networks, as well as other synthesis conditions, could result in networks with significantly different properties.[60] Molecular simulation of hypercrosslinked polystyrene can provide guidance in the optimization of the systems. Molecular dynamics (MD) simulation was performed on a polystyrene network by three steps: the creation of linear polystyrene bearing different amount of crosslinkable chloromethyl groups; the crosslinking stage; and the relaxation of the network.[152] It was found that the steric hindrance of the substitution, as well as the velocity of the crosslinking, affected the final network structure. The hypercrosslinked styrene-VBC networks were simulated using the previously mentioned software *Polymetic*.[144] The degree of crosslinking was adjusted by using difference amounts of VBC, and the polymer swelling during crosslinking was controlled by setting the density of the

simulations. This process allows the observation of each stage during the virtual synthesis, which is not currently plausible experimentally. They found that the networks have greater porosity when the crosslinking occured at lower density and with higher degrees of crosslinking, and this trend was consistent with available experimental data. When sterically crowded monomers, 4-methyl stilbene (4MSTB) and *N*-(3-methylphenyl) maleimide (3MPMI), were added to the system, the simulated surface areas using *Polymetic* , as well as the experimental results, decreased due to both the dilution of crosslinking functionality (VBC) and the loss of chain mobility.[151] To resemble the actual synthesis of hypercrosslinked polystyrene, DVB was incorporated into the simulated system.[150] The simulated BET surface areas and pore volumes are consistent with the experimental values. The simulation also demonstrated that the structural properties of the network can be tuned by varying the DVB content, but no obvious improvement on H_2/CO_2 gas separation applications was observed from the simulated isotherms. The sulfonated poly(styrene-*co*-divinylbenzene) ion exchange resins were simulated using a generation-relaxation strategy.[153] Two different approaches, which are based on the generation of homogeneous polymeric matrices and the heterogeneous growth of the network, were used for the generation of the initial microstructure. It was found that the homogeneous topology leads to an overestimation of the density and an underestimation of the porosity. However, the density and the porosity from heterogeneous generation are in good agreement with the experimental results. During the heterogeneous approach, "super-crosslinks", which refer to the topological loops consist of two or more crosslinks, were shown to be essential to accurately describe the microstructure of the resins. (Figure 2-25) The "super-crosslinks" also affect the distribution of the sulfonic group, and the frequency of co-facial π-π stacking interactions. Monochlorodimethyl ether (MCDE) post-crosslinked polystyrene networks were studied by atomistic molecular simulations.[154-156] The consecutive stages of the

algorithm include the atomistic molecular dynamics simulation of a polystyrene solution, the mapping of the structure onto coarse-grained model, the crosslinking, the reverse-mapping, the relaxation of the structure in dichloroethane and in dry state, and calculations of the properties. (Figure 2-26) It was found that the elastic modulus and specific surface area increased with the increase of the concentration of MCDE in the system.[154] The rate of the crosslinking also affects the nework properties, and the more slowly formed networks showed smaller surface area, lower density and larger pores.[155]

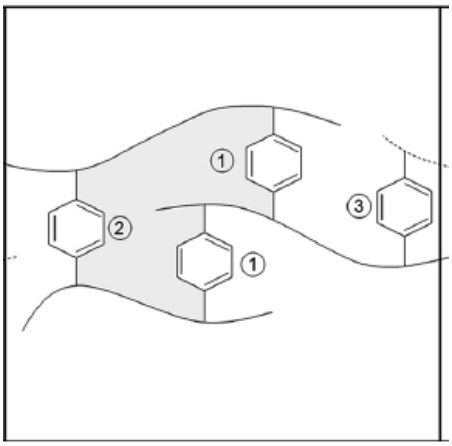

Figure 2-25. The demonstration of a super-crosslink loop. Reprint from Perez-Macia et al.[153] with permission. Copyright 2015 Royal Society of Chemistry.

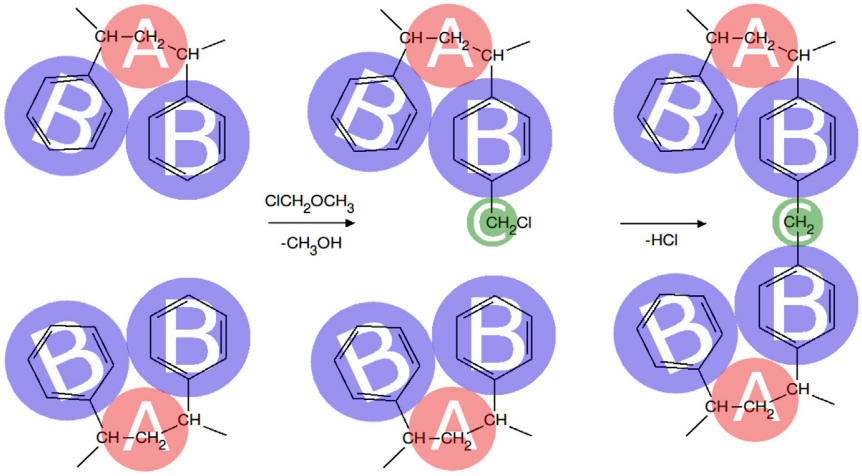

Figure 2-26. The MCDE crosslinked polystyrene in the framework of coarse-grained model. Reprint from Glagolev et al.[155] with permission. Copyright 2016 Elsevier.

2.6 Conclusions

Since their discovery in the early 1970s, HCP materials have continuously received attention from researchers. HCPs evolved from the original styrene-divinylbenzene crosslinked gels, and have grown to be a versatile platform for chemists in developing nanoporous materials with desired properties. In recent years, besides the improvement in traditional applications such as chromatographic packing materials, gas capture and storage matrices, and aqueous pollutant sorbents, HCP materials are now investigated extensively as heterogeneous catalyst substrates, drug delivery carriers and sensors. The inexpensive starting monomers and precursors, diverse synthetic approaches, and moderate reaction conditions enable HCPs to have enormous possibilities in producing new and creative polymer structures, which may lead to other potential important applications.

However, several different challenges remain to be resolved in the future. For example, although techniques such as porosity measurements and solid state NMR have been employed to characterize HCPs, the nanostructures of HCP materials are not completely studied and understood. Also, due to the insoluble nature of most HCPs, the processing of these materials into functional devices can be troublesome. Moreover, the incorporation of specific functionalities, especially amine groups for improved CO_2 sorption properties is still a significant challenge, due to the unfavorable side-reactions of these functional groups in Friedel-Crafts reactions. Furthermore, obstacles remain in the industrialized large-scale production of HCP materials due to the massive amount of heat and corrosive hydrogen chloride generated in the hypercrosslinking process.

These scientific challenges, as well as the development of novel applications for HCP materials will certainly motivate chemists and material scientists to continue to conduct inspiring and exciting research on new functional HCPs.

2.7 References

1. Budd, P. M.; Butler, A.; Selbie, J.; Mahmood, K.; McKeown, N. B.; Ghanem, B.; Msayib, K.; Book, D.; Walton, A., The potential of organic polymer-based hydrogen storage materials. *Phys. Chem. Chem. Phys.* **2007,** *9* (15), 1802-1808.
2. McKeown, N. B.; Budd, P. M.; Book, D., Microporous polymers as potential hydrogen storage materials. *Macromol. Rapid Commun.* **2007,** *28* (9), 995-1002.
3. Germain, J.; Fréchet, J. M.; Svec, F., Nanoporous polymers for hydrogen storage. *small* **2009,** *5* (10), 1098-1111.
4. McKeown, N. B.; Budd, P. M., Polymers of intrinsic microporosity (PIMs): organic materials for membrane separations, heterogeneous catalysis and hydrogen storage. *Chem. Soc. Rev.* **2006,** *35* (8), 675-683.
5. Rose, M., Nanoporous polymers: bridging the gap between molecular and solid catalysts? *ChemCatChem* **2014,** *6* (5), 1166-1182.
6. Du, X.; Sun, Y.; Tan, B.; Teng, Q.; Yao, X.; Su, C.; Wang, W., Tröger's base-functionalised organic nanoporous polymer for heterogeneous catalysis. *Chem. Commun.* **2010,** *46* (6), 970-972.
7. Jiang, K.; Fei, T.; Zhang, T., Humidity sensing properties of LiCl-loaded porous polymers with good stability and rapid response and recovery. *Sens. Actuator B-Chem.* **2014,** *199*, 1-6.
8. Jiang, K.; Kuang, D.; Fei, T.; Zhang, T., Preparation of lithium-modified porous polymer for enhanced humidity sensitive properties. *Sens. Actuator B-Chem.* **2014,** *203*, 752-758.
9. Li, B.; Yang, X.; Xia, L.; Majeed, M. I.; Tan, B., Hollow Microporous Organic Capsules. *Sci. Rep.* **2013,** *3*, 2128.
10. Davankov, V.; Tsyurupa, M. P., *Hypercrosslinked polymeric networks and adsorbing*

materials: synthesis, properties, structure, and applications. Elsevier: 2010; Vol. 56.

11. Dawson, R.; Cooper, A. I.; Adams, D. J., Nanoporous organic polymer networks. *Prog. Polym. Sci.* **2012,** *37* (4), 530-563.
12. Ding, S.-Y.; Wang, W., Covalent organic frameworks (COFs): from design to applications. *Chem. Soc. Rev.* **2013,** *42* (2), 548-568.
13. Huang, N.; Wang, P.; Jiang, D., Covalent organic frameworks: a materials platform for structural and functional designs. *Nat. Rev. Mater.* **2016,** *1*, 16068.
14. Xu, Y.; Jin, S.; Xu, H.; Nagai, A.; Jiang, D., Conjugated microporous polymers: design, synthesis and application. *Chem. Soc. Rev.* **2013,** *42* (20), 8012-8031.
15. Jiang, J.-X.; Su, F.; Trewin, A.; Wood, C. D.; Campbell, N. L.; Niu, H.; Dickinson, C.; Ganin, A. Y.; Rosseinsky, M. J.; Khimyak, Y. Z.; Cooper, A. I., Conjugated microporous poly(aryleneethynylene) networks. *Angew. Chem. Int. Ed.* **2007,** *46* (45), 8574-8578.
16. Cooper, A. I., Conjugated microporous polymers. *Adv. Mater.* **2009,** *21* (12), 1291-1295.
17. Tan, L.; Tan, B., Hypercrosslinked porous polymer materials: design, synthesis, and applications. *Chem. Soc. Rev.* **2017**.
18. Fontanals, N.; Marce, R. M.; Borrull, F.; Cormack, P. A. G., Hypercrosslinked materials: preparation, characterisation and applications. *Polym. Chem.* **2015,** *6* (41), 7231-7244.
19. Ren, S.; Bojdys, M. J.; Dawson, R.; Laybourn, A.; Khimyak, Y. Z.; Adams, D. J.; Cooper, A. I., Porous, fluorescent, covalent triazine-based frameworks via room-temperature and microwave-assisted synthesis. *Adv. Mater.* **2012,** *24* (17), 2357-2361.
20. Kuhn, P.; Antonietti, M.; Thomas, A., Porous, covalent triazine-based frameworks prepared by ionothermal synthesis. *Angew. Chem. Int. Ed.* **2008,** *47* (18), 3450-3453.
21. Ben, T.; Qiu, S., Porous aromatic frameworks: Synthesis, structure and functions.

CrystEngComm **2013,** *15* (1), 17-26.

22. Ben, T.; Ren, H.; Ma, S.; Cao, D.; Lan, J.; Jing, X.; Wang, W.; Xu, J.; Deng, F.; Simmons, J. M.; Qiu, S.; Zhu, G., Targeted synthesis of a porous aromatic framework with high stability and exceptionally high surface area. *Angew. Chem. Int. Ed.* **2009,** *48* (50), 9457-9460.
23. Staudinger, H.; Heuer, W., Über hochpolymere Verbindungen, 93. Mitteil.: Über das zerreißen der faden-moleküle des poly-styrols. *Berichte der deutschen chemischen Gesellschaft (A and B Series)* **1934,** *67* (7), 1159-1164.
24. Davankov, V.; Rogozhin, S.; Tsyurupa, M., New approach to preparation of pniformly crosslinked macroreticular polystyrene structures. *Mezhdunarodnaya Kniga* **1973**, *15*, 463–465.
25. Davankov, V.; Tsyurupa, M.; Ilyin, M.; Pavlova, L., Hypercross-linked polystyrene and its potentials for liquid chromatography: a mini-review. *J. Chromatogr. A* **2002,** *965* (1), 65-73.
26. Zhang, X.; Shen, S.; Fan, L., Studies progress of preparation, properties and applications of hyper-cross-linked polystyrene networks. *J. Mater. Sci.* **2007,** *42* (18), 7621-7629.
27. Tan, L.; Tan, B., Recent developments of hypercrosslinked microporous organic polymers. In *Porous Polymers: Design, Synthesis and Applications*, The Royal Society of Chemistry: 2016; pp 66-94.
28. D'Alelio, G. F. Production of synthetic polymeric compositions comprising sulphonated polymerizates of poly-vinyl aryl compounds and treatment of liquid media therewith. U.S. Patent 2366007 (1944).
29. Abrams, I. M.; Millar, J. R., A history of the origin and development of macroporous ion-exchange resins. *React. Funct. Polym.* **1997,** *35* (1), 7-22.
30. McBurney, C. H. Resinous insoluble reaction products of tertiary amines with haloalkylated

vinyl aromatic hydrocarbon copolymers. U.S. Patent 2591573 (1952).

31. http://www.dow.com/en-us/markets-and-solutions/products/AMBERLITEIonExchangeResinsandPolymericAdsorbents/AMBERLITEFPA98Cl.

32. Galia, M.; Svec, F.; Frechet, J. M. J., Monodisperse polymer beads as packing material for high-performance liquid chromotography: Effect of divinylbenzene content on the porous and chromatographic properties of poly(styrene-*co*-divinylbenzene) beads prepared in presence of linear polystyrene as a porogen. *J. Polym. Sci. A Polym. Chem.* **1994,** *32* (11), 2169-2175.

33. Janson, J. C., *Protein Purification: Principles, High Resolution Methods, and Applications*. Wiley: 2012.

34. Leonard, M.; Fournier, C.; Dellacherie, E., Polyvinyl alcohol-coated macroporous polystyrene particles as stationary phases for the chromatography of proteins. *J. Chromatogr. B* **1995,** *664* (1), 39-46.

35. Lv, Y.; Lin, Z.; Tan, T.; Svec, F., Preparation of porous styrenics-based monolithic layers for thin layer chromatography coupled with matrix-assisted laser-desorption/ionization time-of-flight mass spectrometric detection. *J. Chromatogr. A* **2013,** *1316*, 154-159.

36. Davankov, V.; Rogozhin, V.; Tsjurupa, M., Macronet polystyrene structures for ionites and method of producing same. U.S. Patent 3729457 (1973).

37. Germain, J.; Fréchet, J. M. J.; Svec, F., Nanoporous polymers for hydrogen storage. *Small* **2009,** *5* (10), 1098-1111.

38. Germain, J.; Frechet, J. M. J.; Svec, F., Hypercrosslinked polyanilines with nanoporous structure and high surface area: potential adsorbents for hydrogen storage. *J. Mater. Chem.* **2007,** *17* (47), 4989-4997.

39. Davankov, V.; Rogoshin, S.; Tsyurupa, M. In *Macronet isoporous gels through crosslinking of dissolved polystyrene*, Journal of Polymer Science: Polymer Symposia, Wiley Online Library: 1974; pp 95-101.

40. Grassie, N.; Gilks, J., Friedel-Crafts crosslinking of polystyrene. *J. Polym. Sci. A Polym. Chem.* **1973,** *11* (7), 1531-1552.

41. Grassie, N.; Gilks, J., Thermal analysis of polystyrenes crosslinked by *p*-di (chloromethyl) benzene. *J. Polym. Sci. A Polym. Chem.* **1973,** *11* (8), 1985-1994.

42. Tsyrupa, M.; Lalaev, V.; Davankov, V., On reasons determining unusual properties of hypercrosslinked styrene polymers, Dokl. *AN SSSR* **1984,** *279*, 156-160.

43. Tsyurupa, M. P.; Davankov, V. A., Hypercrosslinked polymers: basic principle of preparing the new class of polymeric materials. *React. Funct. Polym.* **2002,** *53* (2–3), 193-203.

44. Tsyurupa, M. P.; Andreeva, A. I.; Davankov, V. A., On factors determining the swelling ability of crosslinked polymers. *Angew Makromol. Chem.* **1978,** *70* (1), 179-187.

45. Davankov, V. A.; Tsyurupa, M. P.; Rogozhin, S. V., On factors determining the swelling ability of cross-linked polymers, II. *Angew Makromol. Chem.* **1976,** *53* (1), 19-27.

46. Davankov, V.; Ilyin, M.; Tsyurupa, M.; Timofeeva, G.; Dubrovina, L., From a dissolved polystyrene coil to an intramolecularly-hyper-cross-linked Nanosponge". *Macromolecules* **1996,** *29* (26), 8398-8403.

47. Cjurupa, M.; Lalaev, V.; Davankov, V., Synthesis and some physicochemical properties of macronet isoporous styrene polymers having crosslinking bridges of the diphenylmethane type. *Acta Polymerica* **1984,** *35* (6), 451-455.

48. Wu, D.; Hui, C. M.; Dong, H.; Pietrasik, J.; Ryu, H. J.; Li, Z.; Zhong, M.; He, H.; Kim, E. K.; Jaroniec, M., Nanoporous polystyrene and carbon materials with core–shell nanosphere-

interconnected network structure. *Macromolecules* **2011,** *44* (15), 5846-5849.

49. Gadwdzik, B.; Osypiuk, J., Modification of porous poly (styrene-divinylbenzene) beads by friedel-crafts reaction. *Chromatographia* **2001,** *54* (5-6), 323-328.

50. Azanova, V.; Hradil, J., Sorption properties of macroporous and hypercrosslinked copolymers. *React. Funct. Polym.* **1999,** *41* (1), 163-175.

51. Veverka, P.; Jeřábek, K., Mechanism of hypercrosslinking of chloromethylated styrene–divinylbenzene copolymers. *React. Funct. Polym.* **1999,** *41* (1), 21-25.

52. Lee, J.-Y.; Wood, C. D.; Bradshaw, D.; Rosseinsky, M. J.; Cooper, A. I., Hydrogen adsorption in microporous hypercrosslinked polymers. *Chem. Commun.* **2006,** (25), 2670-2672.

53. Davankov, V. A.; Tsyurupa, M. P., Structure and properties of hypercrosslinked polystyrene—the first representative of a new class of polymer networks. *Reactive Polymers* **1990,** *13* (1), 27-42.

54. Ahn, J.-H.; Jang, J.-E.; Oh, C.-G.; Ihm, S.-K.; Cortez, J.; Sherrington, D. C., Rapid generation and control of microporosity, bimodal pore size distribution, and surface area in Davankov-type hyper-cross-linked resins. *Macromolecules* **2006,** *39* (2), 627-632.

55. Hauptmann, R., Chloromethylation of styrene-divinylbenzene copolymers. *Plaste und Kautschuk* **1971,** *18* (5), 330-331.

56. Dima, Chloromethylation of styrene-divinylbenzene copolymers. *Revista de Materiale Plastici* **1971,** *8* (1), 15-19.

57. Pascault, J.-P.; Sautereau, H.; Verdu, J.; Williams, R. J., *Thermosetting polymers*. CRC Press: 2002; Vol. 64.

58. Turi, E., *Thermal characterization of polymeric materials*. Elsevier: 2012.

59. Negre, M.; Bartholin, M.; Guyot, A., Autocrosslinked isoporous polystyrene resins. *Angew*

Makromol. Chem. **1979,** *80* (1), 19-30.

60. Li, B.; Gong, R.; Luo, Y.; Tan, B., Tailoring the pore size of hypercrosslinked polymers. *Soft Matter* **2011,** *7* (22), 10910-10916.

61. Law, R. V.; Sherrington, D. C.; Snape, C. E.; Ando, I.; Kurosu, H., Solid-state ^{13}C MAS NMR studies of hyper-cross-linked polystyrene resins. *Macromolecules* **1996,** *29* (19), 6284-6293.

62. Penner, N. A.; Nesterenko, P. N.; Ilyin, M. M.; Tsyurupa, M. P.; Davankov, V. A., Investigation of the properties of hypercrosslinked polystyrene as a stationary phase for high-performance liquid chromatography. *Chromatographia* **1999,** *50* (9), 611-620.

63. Fontanals, N.; Cortés, J.; Galia, M.; Maria Marcé, R.; Cormack, P. A.; Borrull, F.; Sherrington, D. C., Synthesis of Davankov-type hypercrosslinked resins using different isomer compositions of vinylbenzyl chloride monomer, and application in the solid-phase extraction of polar compounds. *J. Polym. Sci. A Polym. Chem.* **2005,** *43* (8), 1718-1728.

64. Beth, M.; Unger, K. K.; Tsyurupa, M. P.; Davankov, V. A., Microporous hypercrosslinked polystyrene Styrosorb as a restricted access packing in sample clean-up for high performance liquid chromatography. Part I: Evaluation of restricted access properties. *Chromatographia* **1993,** *36* (1), 351-355.

65. Sutton, R. M. C.; Hill, S. J.; Jones, P., Comparison of the chelating ion exchange properties of dye coated cellulose and polystyrene substrates for the separation and determination of trace metals from aqueous media. *J. Chromatogr. A* **1996,** *739* (1), 81-86.

66. Urban, J.; Svec, F.; Fréchet, J. M. J., Efficient separation of small molecules using a large surface area hypercrosslinked monolithic polymer capillary column. *Anal. Chem.* **2010,** *82* (5), 1621-1623.

67. Urban, J.; Svec, F.; Fréchet, J. M. J., Hypercrosslinking: New approach to porous polymer

monolithic capillary columns with large surface area for the highly efficient separation of small molecules. *J. Chromatogr. A* **2010,** *1217* (52), 8212-8221.

68. Chen, X.-J.; Dinh, N. P.; Zhao, J.; Wang, Y.-T.; Li, S.-P.; Svec, F., Effect of ion adsorption on CEC separation of small molecules using hypercrosslinked porous polymer monolithic capillary columns. *J. Sep. Sci.* **2012,** *35* (12), 1502-1506.

69. Lv, Y.; Lin, Z.; Svec, F., Hypercrosslinked large surface area porous polymer monoliths for hydrophilic interaction liquid chromatography of small molecules featuring zwitterionic functionalities attached to gold nanoparticles held in layered structure. *Anal. Chem.* **2012,** *84* (20), 8457-8460.

70. Maya, F.; Svec, F., Porous polymer monoliths with large surface area and functional groups prepared via copolymerization of protected functional monomers and hypercrosslinking. *J. Chromatogr. A* **2013,** *1317*, 32-38.

71. Tsyurupa, M.; Davankov, V., Porous structure of hypercrosslinked polystyrene: state-of-the-art mini-review. *React. Funct. Polym.* **2006,** *66* (7), 768-779.

72. Borsig, E.; Fiedlerová, A.; Haüsler, K.; Sambatra, R.; Michler, G., Structure and properties of an interpenetrating polymer network-like system consisting of polystyrene-polyethylene: 1. Synthesis, elastomeric and thermoanalytical characterization. *Polymer* **1993,** *34* (22), 4787-4792.

73. Wiley, R. H., Crosslinked styrene/divinylbenzene network systems. *Pure Appl. Chem.* **1975,** *43* (1-2), 57-75.

74. Storey, B. T., Copolymerization of styrene and p-divinylbenzene. Initial rates and gel points. *J. Polym. Sci. A Polym. Chem.* **1965,** *3* (1), 265-282.

75. Odian, G., *Principles of polymerization*. John Wiley & Sons: 2004.

76. Huang, J.; Turner, S. R., Recent advances in alternating copolymers: The synthesis, modification, and applications of precision polymers. *Polymer* **2017,** *116*, 572-586.

77. Ogawa, N.; Honmyo, K.; Harada, K.; Sugii, A., Preparation of spherical polymer beads of maleic anhydride–styrene–divinylbenzene and metal sorption of its derivatives. *J. Appl. Polym. Sci.* **1984,** *29* (9), 2851-2856.

78. Maciejewska, M.; Szajnecki, Ł.; Gawdzik, B., Investigation of the surface area and polarity of porous copolymers of maleic anhydride and divinylbezene. *J. Appl. Polym. Sci.* **2012,** *125* (1), 300-307.

79. Frank, R. S.; Downey, J. S.; Stöver, H., Synthesis of divinylbenzene–maleic anhydride microspheres using precipitation polymerization. *J. Polym. Sci. A Polym. Chem.* **1998,** *36* (13), 2223-2227.

80. Donescu, D.; Raditoiu, V.; Spataru, C. I.; Somoghi, R.; Ghiurea, M.; Radovici, C.; Fierascu, R. C.; Schinteie, G.; Leca, A.; Kuncser, V., Superparamagnetic magnetite–divinylbenzene–maleic anhydride copolymer nanocomposites obtained by dispersion polymerization. *Eur. Polym. J.* **2012,** *48* (10), 1709-1716.

81. Gonte, R.; Balasubramanian, K.; Deb, P. C.; Singh, P., Synthesis and characterization of mesoporous hypercrosslinked poly (styrene-*co*-maleic anhydride) microspheres. *Int. J. Polymer. Mater.* **2012,** *61* (12), 919-930.

82. Gao, H.; Ding, L.; Li, W.; Ma, G.; Bai, H.; Li, L., "Hyper-cross-linked organic microporous polymers based on alternating copolymerization of bismaleimide. *ACS Macro Lett.* **2016,** *5* (3), 377-381.

83. Huang, J.; Zhou, X.; Lamprou, A.; Maya, F.; Svec, F.; Turner, S. R., Nanoporous polymers from cross-Linked polymer precursors via *tert*-butyl group deprotection and their carbon

dioxide capture properties. *Chem. Mater.* **2015,** *27* (21), 7388-7394.

84. Seo, M.; Hillmyer, M. A., Reticulated nanoporous polymers by controlled polymerization-induced microphase separation. *Science* **2012,** *336* (6087), 1422-1425.

85. Seo, M.; Kim, S.; Oh, J.; Kim, S.-J.; Hillmyer, M. A., Hierarchically porous polymers from hyper-cross-linked block polymer precursors. *J. Am. Chem. Soc.* **2015,** *137* (2), 600-603.

86. Saba, S. A.; Mousavi, M. P.; Bühlmann, P.; Hillmyer, M. A., Hierarchically porous polymer monoliths by combining controlled macro-and microphase separation. *J. Am. Chem. Soc.* **2015,** *137* (28), 8896-8899.

87. Seo, M.; Murphy, C. J.; Hillmyer, M. A., One-step synthesis of cross-linked block polymer precursor to a nanoporous thermoset. *ACS Macro Lett.* **2013,** *2* (7), 617-620.

88. Schulze, M. W.; McIntosh, L. D.; Hillmyer, M. A.; Lodge, T. P., High-modulus, high-conductivity nanostructured polymer electrolyte membranes via polymerization-induced phase separation. *Nano Lett.* **2013,** *14* (1), 122-126.

89. McIntosh, L. D.; Schulze, M. W.; Irwin, M. T.; Hillmyer, M. A.; Lodge, T. P., Evolution of morphology, modulus, and conductivity in polymer electrolytes prepared via polymerization-induced phase separation. *Macromolecules* **2015,** *48* (5), 1418-1428.

90. Chopade, S. A.; So, S.; Hillmyer, M. A.; Lodge, T. P., Anhydrous proton conducting polymer electrolyte membranes via polymerization-induced microphase separation. *ACS Appl. Mater. Interfaces* **2016,** *8* (9), 6200-6210.

91. Warshawsky, A.; Deshe, A.; Gutman, R., Safe halomethylation of aromatic polymers via BCME-free long chain haloalkylethers. *Polym. Int.* **1984,** *16* (4), 234-238.

92. Germain, J.; Svec, F.; Fréchet, J. M. J., Preparation of Size-Selective Nanoporous Polymer Networks of Aromatic Rings: Potential Adsorbents for Hydrogen Storage. *Chem. Mater.* **2008,**

20 (22), 7069-7076.

93. Germain, J.; Frechet, J. M. J.; Svec, F., Nanoporous, hypercrosslinked polypyrroles: effect of crosslinking moiety on pore size and selective gas adsorption. *Chem. Commun.* **2009,** (12), 1526-1528.

94. Pavlova, L. A.; Pavlov, M. V.; Davankov, V. A., The first representatives of hypercrosslinked hydrophilic networks: Alkylation and polymerization of 4-vinylpyridine in an ionic liquid. *Dokl. Chem.* **2006,** *406* (1), 6-8.

95. Ratvijitvech, T.; Barrow, M.; Cooper, A. I.; Adams, D. J., The effect of molecular weight on the porosity of hypercrosslinked polystyrene. *Polym. Chem.* **2015,** *6* (41), 7280-7285.

96. Yang, Y.; Tan, B.; Wood, C. D., Solution-processable hypercrosslinked polymers by low cost strategies: a promising platform for gas storage and separation. *J. Mater. Chem. A* **2016,** *4* (39), 15072-15080.

97. Ouyang, Y.; Shi, H.; Fu, R.; Wu, D., Highly monodisperse microporous polymeric and carbonaceous nanospheres with multifunctional properties. *Sci. Rep.* **2013,** *3*, 1430.

98. Qiao, Z.-A.; Chai, S.-H.; Nelson, K.; Bi, Z.; Chen, J.; Mahurin, S. M.; Zhu, X.; Dai, S., Polymeric molecular sieve membranes via in situ cross-linking of non-porous polymer membrane templates. *Nat. Commun.* **2014,** *5*, 3705.

99. Li, Z.; Wu, D.; Huang, X.; Ma, J.; Liu, H.; Liang, Y.; Fu, R.; Matyjaszewski, K., Fabrication of novel polymeric and carbonaceous nanoscale networks by the union of self-assembly and hypercrosslinking. *Energy Environ. Sci.* **2014,** *7* (9), 3006-3012.

100. Meng, Q. B.; Weber, J., Lignin-based microporous materials as selective adsorbents for carbon dioxide separation. *ChemSusChem* **2014,** *7* (12), 3312-3318.

101. Ding, L.; Gao, H.; Xie, F.; Li, W.; Bai, H.; Li, L., Porosity-enhanced polymers from hyper-

cross-linked polymer precursors. *Macromolecules* **2017,** *50* (3), 956-962.

102. Côté, A. P.; Benin, A. I.; Ockwig, N. W.; O'Keeffe, M.; Matzger, A. J.; Yaghi, O. M., Porous, crystalline, covalent organic frameworks. *Science* **2005,** *310* (5751), 1166-1170.

103. Waller, P. J.; Gándara, F.; Yaghi, O. M., Chemistry of covalent organic frameworks. *Acc. Chem. Res.* **2015,** *48* (12), 3053-3063.

104. Bojdys, M. J.; Jeromenok, J.; Thomas, A.; Antonietti, M., Rational extension of the family of layered, covalent, triazine-based frameworks with regular porosity. *Adv. Mater.* **2010,** *22* (19), 2202-2205.

105. Wood, C. D.; Tan, B.; Trewin, A.; Niu, H.; Bradshaw, D.; Rosseinsky, M. J.; Khimyak, Y. Z.; Campbell, N. L.; Kirk, R.; Stöckel, E.; Cooper, A. I., Hydrogen storage in microporous hypercrosslinked organic polymer networks. *Chem. Mater.* **2007,** *19* (8), 2034-2048.

106. Martin, C. F.; Stockel, E.; Clowes, R.; Adams, D. J.; Cooper, A. I.; Pis, J. J.; Rubiera, F.; Pevida, C., Hypercrosslinked organic polymer networks as potential adsorbents for pre-combustion CO_2 capture. *J. Mater. Chem.* **2011,** *21* (14), 5475-5483.

107. Schwab, M. G.; Lennert, A.; Pahnke, J.; Jonschker, G.; Koch, M.; Senkovska, I.; Rehahn, M.; Kaskel, S., Nanoporous copolymer networks through multiple Friedel-Crafts-alkylation-studies on hydrogen and methane storage. *J. Mater. Chem.* **2011,** *21* (7), 2131-2135.

108. Luo, Y.; Zhang, S.; Ma, Y.; Wang, W.; Tan, B., Microporous organic polymers synthesized by self-condensation of aromatic hydroxymethyl monomers. *Polym. Chem.* **2013,** *4* (4), 1126-1131.

109. Wang, J.; Sng, W.; Yi, G.; Zhang, Y., Imidazolium salt-modified porous hypercrosslinked polymers for synergistic CO_2 capture and conversion. *Chem. Commun.* **2015,** *51* (60), 12076-12079.

110. Yuan, S.; White, D.; Mason, A.; Liu, D.-J., Porous organic polymers containing carborane for hydrogen storage. *Int. J. Energy Res.* **2013,** *37* (7), 732-740.

111. Chaikittisilp, W.; Kubo, M.; Moteki, T.; Sugawara-Narutaki, A.; Shimojima, A.; Okubo, T., Porous siloxane–organic hybrid with ultrahigh surface area through simultaneous polymerization–destruction of functionalized cubic siloxane cages. *J. Am. Chem. Soc.* **2011,** *133* (35), 13832-13835.

112. Li, B.; Guan, Z.; Yang, X.; Wang, W. D.; Wang, W.; Hussain, I.; Song, K.; Tan, B.; Li, T., Multifunctional microporous organic polymers. *J. Mater. Chem. A* **2014,** *2* (30), 11930-11939.

113. Song, K.; Liu, P.; Wang, J.; Tan, B.; Li, T., Highly active palladium nanoparticles immobilized on knitting microporous organic polymers as efficient catalysts for Suzuki–Miyaura cross-coupling reaction. *J. Porous Mater.* **2016,** *23* (3), 725-731.

114. Wang, S.; Tan, L.; Zhang, C.; Hussain, I.; Tan, B., Novel POSS-based organic-inorganic hybrid porous materials by low cost strategies. *J. Mater. Chem. A* **2015,** *3* (12), 6542-6548.

115. Chen, Q.; Luo, M.; Hammershøj, P.; Zhou, D.; Han, Y.; Laursen, B. W.; Yan, C.-G.; Han, B.-H., Microporous polycarbazole with high specific surface area for gas storage and separation. *J. Am. Chem. Soc.* **2012,** *134* (14), 6084-6087.

116. Pan, L.; Chen, Q.; Zhu, J.-H.; Yu, J.-G.; He, Y.-J.; Han, B.-H., Hypercrosslinked porous polycarbazoles via one-step oxidative coupling reaction and Friedel-Crafts alkylation. *Polym. Chem.* **2015,** *6* (13), 2478-2487.

117. Saleh, M.; Baek, S. B.; Lee, H. M.; Kim, K. S., Triazine-based microporous polymers for selective adsorption of CO_2. *J. Phys. Chem. C* **2015,** *119* (10), 5395-5402.

118. Chen, Q.; Liu, D.-P.; Zhu, J.-H.; Han, B.-H., Mesoporous conjugated polycarbazole with high porosity via structure tuning. *Macromolecules* **2014,** *47* (17), 5926-5931.

119. Chen, Q.; Liu, D.-P.; Luo, M.; Feng, L.-J.; Zhao, Y.-C.; Han, B.-H., Nitrogen-containing microporous conjugated polymers via carbazole-based oxidative coupling polymerization: Preparation, porosity, and gas uptake. *Small* **2014,** *10* (2), 308-315.

120. Feng, L.-J.; Chen, Q.; Zhu, J.-H.; Liu, D.-P.; Zhao, Y.-C.; Han, B.-H., Adsorption performance and catalytic activity of porous conjugated polyporphyrins via carbazole-based oxidative coupling polymerization. *Polym. Chem.* **2014,** *5* (8), 3081-3088.

121. Monnereau, L.; Grandclaudon, C.; Muller, T.; Brase, S., Sulfur-based hyper cross-linked polymers. *RSC Adv.* **2015,** *5* (30), 23152-23159.

122. Li, B.; Gong, R.; Wang, W.; Huang, X.; Zhang, W.; Li, H.; Hu, C.; Tan, B., A new strategy to microporous polymers: Knitting rigid aromatic building blocks by external cross-linker. *Macromolecules* **2011,** *44* (8), 2410-2414.

123. Woodward, R. T.; Stevens, L. A.; Dawson, R.; Vijayaraghavan, M.; Hasell, T.; Silverwood, I. P.; Ewing, A. V.; Ratvijitvech, T.; Exley, J. D.; Chong, S. Y.; Blanc, F.; Adams, D. J.; Kazarian, S. G.; Snape, C. E.; Drage, T. C.; Cooper, A. I., Swellable, Swellable, water- and acid-tolerant polymer sponges for chemoselective carbon dioxide capture. *J. Am. Chem. Soc.* **2014,** *136* (25), 9028-9035.

124. Vinodh, R.; Hemalatha, P.; Ganesh, M.; Peng, M. M.; Abidov, A.; Palanichamy, M.; Cha, W. S.; Jang, H.-T., Novel microporous hypercross-linked conjugated quinonoid chromophores with broad light absorption and CO_2 sorption characteristics. *RSC Adv.* **2014,** *4* (8), 3668-3674.

125. Dawson, R.; Stöckel, E.; Holst, J. R.; Adams, D. J.; Cooper, A. I., Microporous organic polymers for carbon dioxide capture. *Energy Environ. Sci.* **2011,** *4* (10), 4239-4245.

126. Errahali, M.; Gatti, G.; Tei, L.; Paul, G.; Rolla, G.; Canti, L.; Fraccarollo, A.; Cossi, M.; Comotti, A.; Sozzani, P., Microporous hyper-cross-linked aromatic polymers designed for

methane and carbon dioxide adsorption. *J. Phys. Chem. C* **2014,** *118* (49), 28699-28710.

127. Zhang, C.; Zhu, P.-C.; Tan, L.; Liu, J.-M.; Tan, B.; Yang, X.-L.; Xu, H.-B., Triptycene-based hyper-cross-linked polymer sponge for gas storage and water treatment. *Macromolecules* **2015,** *48* (23), 8509-8514.

128. Tan, L.; Li, B.; Yang, X.; Wang, W.; Tan, B., Knitting hypercrosslinked conjugated microporous polymers with external crosslinker. *Polymer* **2015,** *70*, 336-342.

129. Wang, H.; Pan, L.; Deng, W.; Yang, G.; Liu, X., One-pot synthesis of triptycene-based porous organic frameworks with tailored micropore environments for highly efficient and selective amine adsorption. *Polym. J.* **2016**.

130. Bhunia, S.; Banerjee, B.; Bhaumik, A., A new hypercrosslinked supermicroporous polymer, with scope for sulfonation, and its catalytic potential for the efficient synthesis of biodiesel at room temperature. *Chem. Commun.* **2015,** *51* (24), 5020-5023.

131. Luo, Y.; Li, B.; Wang, W.; Wu, K.; Tan, B., Hypercrosslinked aromatic heterocyclic microporous polymers: a new class of highly selective CO_2 capturing materials. *Adv. Mater.* **2012,** *24* (42), 5703-5707.

132. Saleh, M.; Lee, H. M.; Kemp, K. C.; Kim, K. S., Highly stable CO_2/N_2 and CO_2/CH_4 selectivity in hyper-cross-linked heterocyclic porous polymers. *ACS Appl. Mater. Interfaces* **2014,** *6* (10), 7325-7333.

133. Yang, X.; Yu, M.; Zhao, Y.; Zhang, C.; Wang, X.; Jiang, J.-X., Hypercrosslinked microporous polymers based on carbazole for gas storage and separation. *RSC Adv.* **2014,** *4* (105), 61051-61055.

134. Zhu, X.; Mahurin, S. M.; An, S.-H.; Do-Thanh, C.-L.; Tian, C.; Li, Y.; Gill, L. W.; Hagaman, E. W.; Bian, Z.; Zhou, J.-H., Efficient CO_2 capture by a task-specific porous organic polymer

bifunctionalized with carbazole and triazine groups. *Chem. Commun.* **2014,** *50* (59), 7933-7936.

135. Zhai, T. L.; Tan, L.; Luo, Y.; Liu, J. M.; Tan, B.; Yang, X. L.; Xu, H. B.; Zhang, C., Microporous polymers from a carbazole-based triptycene monomer: Synthesis and their applications for gas uptake. *Chem. Asian J.* **2016,** *11* (2), 294-298.

136. Dawson, R.; Stevens, L. A.; Drage, T. C.; Snape, C. E.; Smith, M. W.; Adams, D. J.; Cooper, A. I., Impact of water coadsorption for carbon dioxide capture in microporous polymer sorbents. *J. Am. Chem. Soc.* **2012,** *134* (26), 10741-10744.

137. Dawson, R.; Ratvijitvech, T.; Corker, M.; Laybourn, A.; Khimyak, Y. Z.; Cooper, A. I.; Adams, D. J., Microporous copolymers for increased gas selectivity. *Polym. Chem.* **2012,** *3* (8), 2034-2038.

138. Guan, Z.; Li, B.; Hai, G.; Yang, X.; Li, T.; Tan, B., A highly efficient catalyst for Suzuki–Miyaura coupling reaction of benzyl chloride under mild conditions. *RSC Adv.* **2014,** *4* (69), 36437-36443.

139. Li, B.; Guan, Z.; Wang, W.; Yang, X.; Hu, J.; Tan, B.; Li, T., Highly dispersed Pd catalyst locked in knitting aryl network polymers for Suzuki–Miyaura coupling reactions of aryl chlorides in aqueous media. *Adv. Mater.* **2012,** *24* (25), 3390-3395.

140. Xu, S.; Song, K.; Li, T.; Tan, B., Palladium catalyst coordinated in knitting *N*-heterocyclic carbene porous polymers for efficient Suzuki-Miyaura coupling reactions. *J. Mater. Chem. A* **2015,** *3* (3), 1272-1278.

141. Jia, Z.; Wang, K.; Li, T.; Tan, B.; Gu, Y., Functionalized hypercrosslinked polymers with knitted *N*-heterocyclic carbene–copper complexes as efficient and recyclable catalysts for organic transformations. *Catal. Sci. Tech.* **2016**.

142. Song, K.; Zou, Z.; Wang, D.; Tan, B.; Wang, J.; Chen, J.; Li, T., Microporous organic polymers derived microporous carbon supported Pd catalysts for oxygen reduction reaction: Impact of framework and heteroatom. *J. Phys. Chem. C* **2016,** *120* (4), 2187-2197.

143. Song, K.; Liu, P.; Wang, J.; Pang, L.; Chen, J.; Hussain, I.; Tan, B.; Li, T., Controlled synthesis of uniform palladium nanoparticles on novel micro-porous carbon as a recyclable heterogeneous catalyst for the Heck reaction. *Dalton Trans.* **2015,** *44* (31), 13906-13913.

144. Abbott, L. J.; Colina, C. M., Formation of microporosity in hyper-cross-linked polymers. *Macromolecules* **2014,** *47* (15), 5409-5415.

145. Abbott, L. J.; Colina, C. M., Atomistic structure generation and gas adsorption simulations of microporous polymer networks. *Macromolecules* **2011,** *44* (11), 4511-4519.

146. Trewin, A.; Willock, D. J.; Cooper, A. I., Atomistic simulation of micropore structure, surface area, and gas sorption properties for amorphous microporous polymer networks. *J. Phys. Chem. C* **2008,** *112* (51), 20549-20559.

147. Wood, C. D.; Tan, B.; Trewin, A.; Su, F.; Rosseinsky, M. J.; Bradshaw, D.; Sun, Y.; Zhou, L.; Cooper, A. I., Microporous organic polymers for methane storage. *Adv. Mater.* **2008,** *20* (10), 1916-1921.

148. Abbott, L. J.; Hart, K. E.; Colina, C. M., Polymatic: a generalized simulated polymerization algorithm for amorphous polymers. *Theor. Chem. Acc.* **2013,** *132* (3), 1334.

149. Abbott, L. J.; Hughes, J. E.; Colina, C. M., Virtual synthesis of thermally cross-linked copolymers from a novel implementation of polymatic. *J. Phys. Chem. B* **2014,** *118* (7), 1916-1924.

150. Kupgan, G.; Liyana-Arachchi, T. P.; Colina, C. M., Pore size tuning of poly(styrene-co-vinylbenzyl chloride-*co*-divinylbenzene) hypercrosslinked polymers: Insights from molecular

simulations. *Polymer* **2016,** *99*, 173-184.

151. Zhou, X.; Huang, J.; Barr, K. W.; Lin, Z.; Maya, F.; Abbott, L. J.; Colina, C. M.; Svec, F.; Turner, S. R., Nanoporous hypercrosslinked polymers containing T_g enhancing comonomers. *Polymer* **2015,** *59*, 42-48.

152. Ferrante, F.; Lo Celso, F.; Duca, D., Construction and characterization of models of hypercrosslinked polystyrene. *Colloid Polym. Sci.* **2012,** *290* (14), 1443-1450.

153. Perez-Macia, M. A.; Curco, D.; Bringue, R.; Iborra, M.; Aleman, C., Atomistic simulations of the structure of highly crosslinked sulfonated poly(styrene-co-divinylbenzene) ion exchange resins. *Soft Matter* **2015,** *11* (11), 2251-2267.

154. Glagolev, M. K.; Lazutin, A. A.; Vasilevskaya, V. V., Macroscopic properties of hypercrosslinked polystyrene networks: An atomistic and coarse-grained molecular dynamics simulation. *Macromol. Symp.* **2015,** *348* (1), 14-24.

155. Glagolev, M. K.; Lazutin, A. A.; Vasilevskaya, V. V.; Khokhlov, A. R., Influence of cross-linking rate on the structure of hypercrosslinked networks: Multiscale computer simulation. *Polymer* **2016,** *86*, 168-175.

156. Lazutin, A.; Glagolev, M.; Vasilevskaya, V.; Khokhlov, A., Hypercrosslinked polystyrene networks: An atomistic molecular dynamics simulation combined with a mapping/reverse mapping procedure. *J. Chem. Phys* **2014,** *140* (13), 134903.

Chapter 3. Extraordinarily High Intensity Fluorescence Properties of Stilbene-Containing Alternating Copolymers

(Manuscript accepted by *Macromolecular Rapid Communications*)

3.1 Authors

Jing Huang,[†,‡] Xi Geng,[†,‡]Chong Peng,[†] Tijana Z. Grove,[†,‡] and S. Richard Turner[*,†,‡]

[†]Department of Chemistry, Virginia Tech, Blacksburg, VA 24061, United States

[‡]Macromolecules Innovation Institute, Virginia Tech, Blacksburg, VA 24061, United States

3.2 Abstract

In recent years, non-conjugated, fluorophore-free organic polymers have emerged as potentially useful light-emitting materials. The fluorescence properties of a novel class of non-conjugated, *tert*-butyl carboxylate functionalized stilbene-containing alternating copolymers were investigated in this work. These sterically crowded, semi-rigid copolymers exhibit very strong blue fluorescence in organic solvents upon irradiation. The origin of the fluorescent band with high quantum yield was attributed to the "through space" $\pi - \pi$ interactions between the phenyl rings from the stilbene and C=O groups from the anhydride groups. To the best of our knowledge, the di-*tert*-butyl group-containing stilbene and maleic anhydride alternating copolymer showed one of the highest fluorescent intensities among all fluorophore-free polymers. The excellent linearity of the luminescence property of this copolymer is an important attribute for future potential quantitative applications. The fluorescence is maintained when the *tert*-butyl groups are removed and the resulting carboxylic acid-functionalized copolymer is dissolved in water at neutral pH, which can render these copolymers as attractive candidates for diagnostic and therapeutic applications.

3.3 Introduction

Fluorescent materials have attracted enormous attention from both academia and industry, owing to their remarkable potential in a wide range of applications such as drug delivery,[1-3] chemical sensing,[4, 5] cellular bio-imaging,[2, 6, 7] protein labeling,[8-10] bacterial detection,[11, 12] organic light-emitting diodes (OLEDs),[13, 14] etc. There is a broad variety of materials that exhibit fluorescence upon excitation, including small organic dyes such as pyrene[15] and fluorescein;[16] fluorescent biomacromolecules such as phycobiliproteins;[17] organometallic molecules such as lanthanide complexes[20] and $[Ru(bpy)_3]^{2+}$;[18, 19] inorganic nanoparticles (NPs)[21] such as quantum dots (QDs)[8, 22] and dye-doped silica NPs;[23] and fluorescent polymers.[24] Traditional fluorescent polymers usually feature fluorescent moieties such as rare earth metals or conjugated π-aromatic units.[25] These polymers typically either consist of conjugated polymer backbones, or have fluorophores attached to non-fluorescent backbones.[4] However, the incorporation of the fluorophores can change the physicochemical properties of the polymers, especially their polarities and solubilities.[25-27]

In recent years, conventional fluorophore-free organic polymers have emerged as alternative light-emitting materials.[26] A variety of fluorophore-free organic polymers have been reported, including non-conjugated polymer dots (NCPDs);[27, 28] tertiary amine-containing dendritic and hyperbranched polymers;[29-32] and alternating copolymers which contain maleic anhydride or maleimide units or homopolymers of substituted maleimides.[26, 33-36] For fluorescent polymers, by and large, more rigid chromophore structures lead to stronger light emissions.[37] This is mainly attributed to the restricted freedom of chain movement preventing the excitons from relaxation through non-radiative routes. Nevertheless, most of these materials only exhibit relatively weak emission.[38]

It is well-known that electron deficient maleic anhydride and maleimide monomers can readily form alternating copolymers with electron rich monomers such as styrene, α-methyl styrene, stilbene, vinyl acetate, etc.[39] Of particular interest in our group are the stilbene-maleic anhydride/maleimide alternating copolymers.[39-54] First prepared by Wagner-Jauregg in 1930,[55] the stilbene-maleic anhydride copolymer was regarded to be the earliest reported chain-growth synthetic copolymer in literature.[56] Our previous studies on stilbene-containing alternating copolymers show that they possess semi-rigid backbones due to steric hindrance from the pendant phenyl rings.[49] This backbone steric crowding results in unique optical[42] and surface area properties.[40, 41, 57] Recent publications on photoluminescent properties of maleic anhydride or maleimide-containing alternating copolymers[26, 33, 34, 36, 38] inspired us to investigate the fluorescence behavior of stilbene-containing alternating copolymers. Morawetz reported fluorescence of stilbene-containing alternating copolymer when poly(stilbene-*alt*-maleic anhydride) was used as a control in the excimer effect study of polystyrene analogues.[58] In this communication, we report for the first time the extraordinarily strong blue fluorescence of the *tert*-butyl carboxylate-functionalized stilbene and maleic anhydride copolymer (III in Scheme 3-1a). We also aim to investigate the fluorescence properties of a series of alternating copolymers with different chain stiffness, as well as the influence of different solvents and varied concentrations on the fluorescence properties, which may pave the way for the better understanding and harnessing of the luminescence properties of alternating polymers analogs.

3.4 Results and discussion

It is documented that unsubstituted stilbene and maleic anhydride copolymers have poor solubility in common solvents due to strong aggregation,[52, 59] therefore we selected a series of *tert*-butyl carboxylate substituted stilbene and styrene alternating copolymers for this study. These

copolymers are soluble in common organic solvents such as THF, chloroform, DMF, and NMP, which offers convenience in solution based characterization such as SEC, UV-Vis and fluorescence. These copolymers possess semi-rigid polymer backbones with persistence lengths between 2 and 6 nm,[49] and they exhibit microporosity due to inefficient chain packing.[40] Moreover, these copolymers were easily converted into a series of polyelectrolytes by hydrolysis of the *tert*-butyl carboxylate groups and the anhydride rings, and subsequent neutralization of the pendant carboxylic acids to their corresponding salts.[46] All four *tert*-butyl carboxylate-containing alternating copolymers in this study were synthesized via free radical polymerization based on previously published procedures.[49] Their structures are shown in Scheme 3-1a, detailed synthetic procedure and characterization results are presented in Section 3.8 the supporting information.

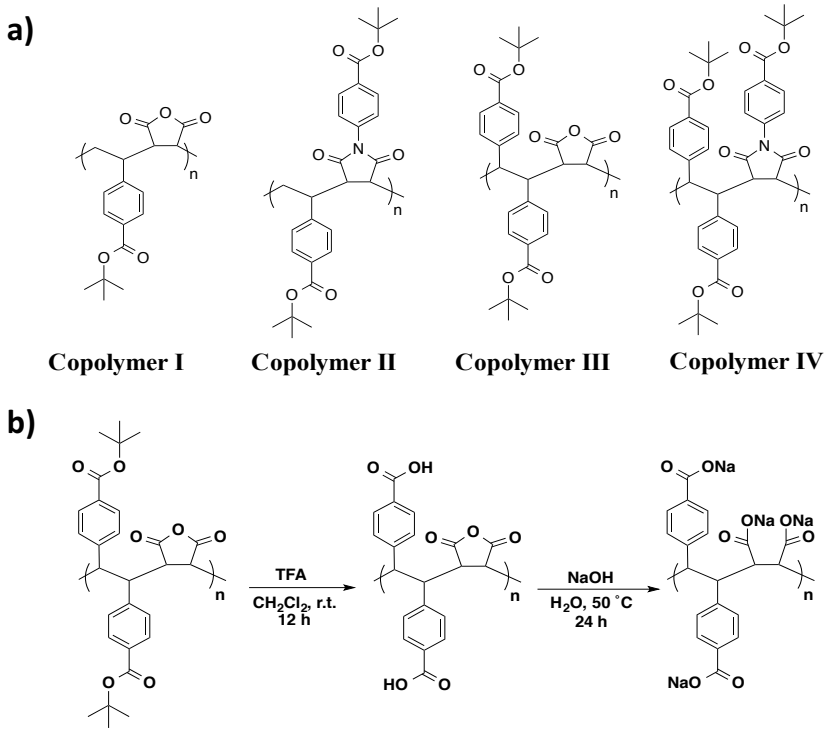

Scheme 3-1. a) Chemical structures of the alternating copolymers in this study; b) conversion of copolymer III into a polyelectrolyte

The UV-Vis absorption spectra of the copolymers in THF are shown in Figure 3-S2 and 3-S3. All four samples showed adsorption peaks at ca. 240 nm, which are assigned to the π–π*

transitions of the phenyl rings (Figure 3-S2). This assignment is consistent with the massic absorbance coefficient (MAC) values (Table 3-S2), in which the MAC values increase as the number of phenyl rings per repeat unit increases. The stilbene copolymers III and IV exhibited appreciable UV adsorption peaks at about 330 nm, while above 300 nm the adsorption of styrene copolymers I and II were very weak (Figure 3-S3). The adsorption at around 330 nm was attributed to the π–π* transitions from the conjugated π orbital of the phenyl rings and C=O groups of the *tert*-butyl ester to the π* orbital from the interactions of the phenyl rings and C=O groups from both the ester carbonyl and the carbonyl in maleic anhydride or maleimide units. Such π–π* transition requires certain juxtaposition and distance between orbitals. The position and distance in III and IV are regulated by the more semi-rigid chain structure, however the position distance in I and II are not favorable for the π–π* transition therefore the absorption is weak.

Despite the absence of conventional fluorophores, these copolymers typically exhibited fluorescence of different intensities when they were irradiated by UV light of the wavelength in the range of 260-350 nm (Figure 3-1). No obvious fluorescence was observed at 230-240 nm, which are the maximum UV absorption wavelengths for the copolymers. III exhibited two distinctive fluorescence bands when irradiated at 250-270 nm and 290-350 nm, and the corresponding fluorescence peaks are at 290 nm and 380 nm, respectively. The fluorescence peak at ca. 380 nm has a much higher intensity even with lower concentration, and the highest intensity is achieved by irradiation at 330 nm. IV only exhibited fluorescence peaks at around 380 nm, and similar to III, the irradiation using 330 nm light affords the highest emission intensity. Both styrene-containing copolymers I and II showed weak fluorescence when irradiated by UV light in the range of 290-350 nm, and the emission redshifted as the excitation wavelength increased. I

exhibited stronger fluorescence than II at most excitation wavelengths, while the highest emission intensity of both copolymers occurred for excitation at 300 nm.

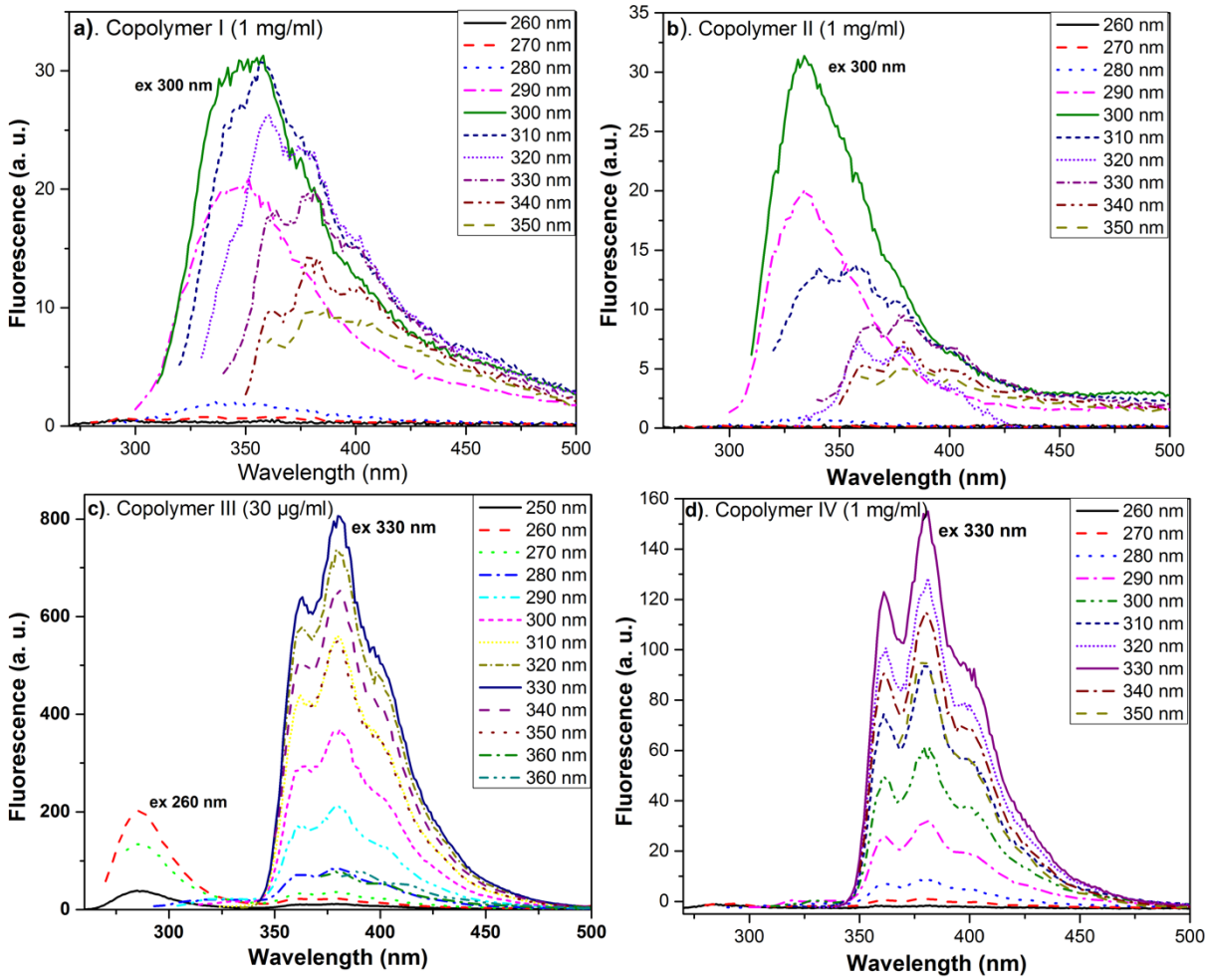

Figure 3-1. Fluorescence spectra of alternating copolymer solutions in THF excited by UV light of different wavelengths. a)-d) represent Copolymers I-IV, respectively. The excitation wavelengths of the highest emission peaks are labeled in each graph.

Figure 3-2a displays fluorescence spectra of the copolymers in THF at their highest emission intensities. The two stilbene-containing copolymers III and IV exhibited high fluorescence at ca. 380 nm, while the styrene-containing copolymers I and II exhibited weak fluorescence at ca. 330 nm. The quantum yields of the copolymers in THF are shown in Table 3-S3. Remarkably, III exhibited an extraordinarily high-intensity fluorescence at even very low concentration (30-40 μg/mL) with high quantum yield (71.2%) when excited at 330 nm. IV showed lower intensity, but

it also absorbs less light in the UV-Vis spectrum, thus it also showed a high quantum yield (65.9%). Both of the styrene copolymers I and II showed low quantum yields (2.6% and 3.1%, respectively). Table 3-1 summarized the excitation and emission wavelengths and quantum yields of each polymer.

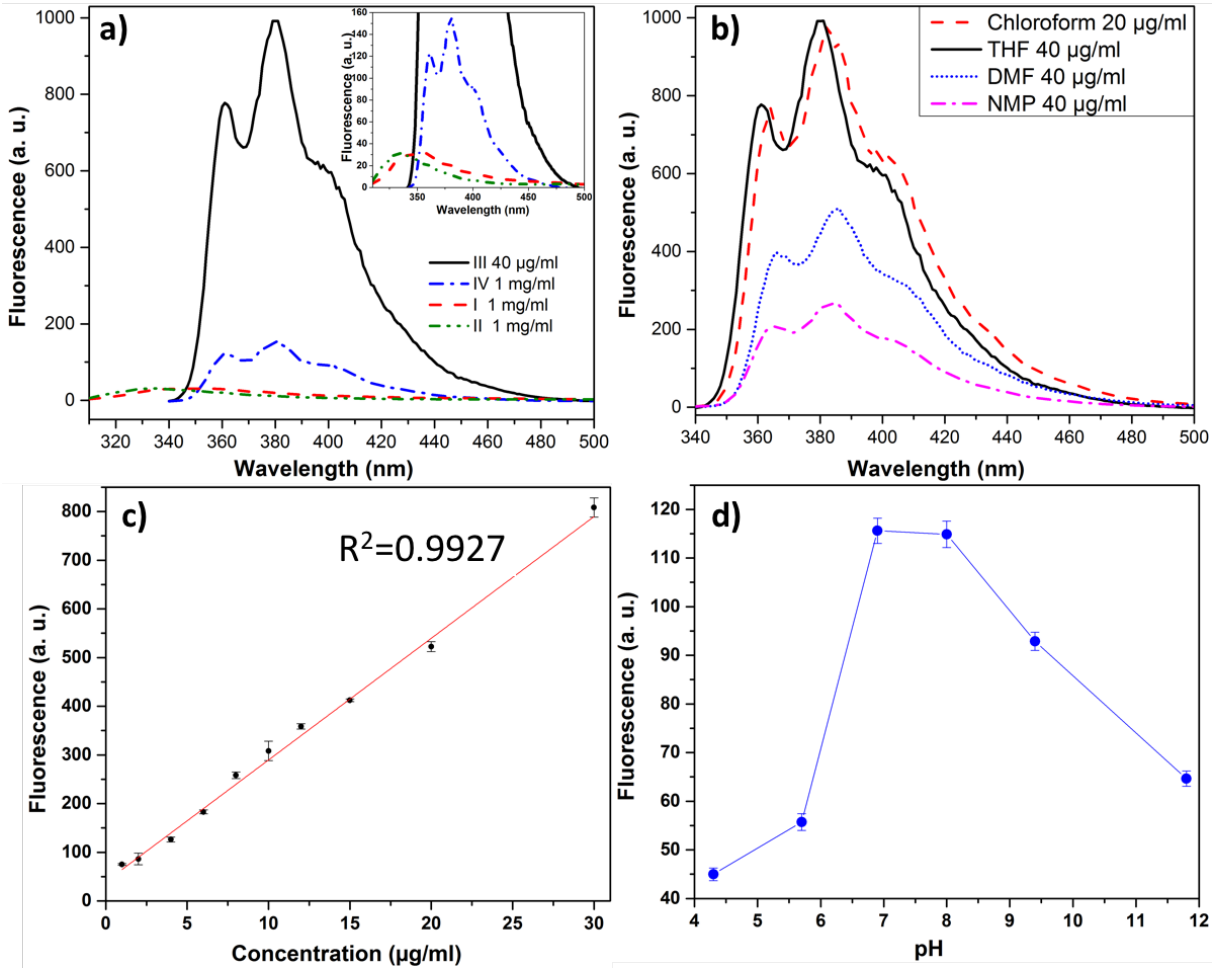

Figure 3-2. a) Fluorescence spectra of alternating copolymers in THF at their maximum emissions (excitation wavelength: 330 nm for III and IV, 300 nm for I and II); b) Fluorescence spectra of the copolymer III in different solvents; c) Linear fit of the fluorescence intensity at 380 nm versus concentration; d) effect of pH on fluorescence intensity of deprotected Copolymer III in water (concentrations: 1 mg/ml).

Table 3- 1. The fluorescence excitation (Ex) and emission (Em) wavelengths, and quantum yields (QY) of the copolymers in THF, "-" means weak or no peak.

Sample	Ex 1 (nm)	Em 1 (nm)	QY (%)	Ex 2 (nm)	Em 2 (nm)	QY (%)
I	260	-	-	300	350	2.6
II	260	-	-	300	340	3.1
III	260	290	1.0	330	380	71.2
IV	260	-	-	330	380	65.9

Trans-stilbene exhibits weak fluorescence in aqueous or common organic solvents.[60, 61] The fluorescence comes from the excitation of π-electrons of the conjugated ethenediyl group into the π* orbitals, and the weak intensity is because of the facile isomerization into the cis-configration.[61, 62] In the alternating copolymerization of *trans*-stilbene with maleic anhydride or maleimide, this conjugated structure is interrupted since the ethenediyl groups are converted into ethylene groups. The fluorescent spectrum of *tert*-butyl carboxylate-containing trans-stilbene solution in THF was measured (Figure 3-S4), and no obvious emission was observed with 330 nm irradiation, which confirmed that the strong fluorescence of the stilbene-containing alternating copolymers was not from residual trans-stilbene monomer.

As previously mentioned, the fluorescence of stilbene-maleic anhydride alternating copolymer was reported in 1975.[58] In that study, the copolymer solution in dioxane was irradiated at 260 nm, and fluorescence emission peaks at 285 nm, and 320-360 nm were observed, which corresponds to the phenyl ring emission and excimer emission, respectively. Studies on the fluorescent properties of α, ω-diphenylalkanes showed that it is necessary to have at least three atoms between two phenyl rings in order to form excimers.[63] Therefore the excimer should be formed between the phenyl rings from two neighboring stilbene units separated by one maleic anhydride unit. The same excimer effect was also observed on the alternating copolymer of

acenaphthylene and maleic anhydride when irradiated at 293 nm.[64] Similarly, when irradiated by 260 nm light, III exhibited two fluorescence bands at 285 nm and 360 nm (Figure 3-S5), which corresponds to phenyl ring emission and excimer emission, respectively. The lack of fluorescence emission at 260 nm excitation of IV is likely because the bulky substituents on the maleimide units hindered the intramolecular excimer formation between two neighboring stilbenes.

Previous studies on the fluorescence of maleic anhydride or maleimide-containing polymers attributed the fluorescence to clustering of the locked carbonyl groups or the "space conjugate" of the carbonyl and the neighboring phenyl groups.[26, 34, 36, 58] For our alternating copolymers, it is likely that the fluorescence of 330 nm irradiation also comes from the π-π interactions between the phenyl rings and C=O groups from the anhydride groups through space. We used density functional theory (DFT) to calculate the molecular orbitals in order to find out if the fluorescence of the alternating copolymers can also result from the "space conjugate". Molecular simulation was conducted on III using the B3LYP/6-311+g** theory in Gaussian (Figure 3-S6). It was found that the conjugated π orbital of one phenyl ring in stilbene and C=O group of the *tert*-butyl ester acts as the HOMO, and the π-π interactions between the other phenyl ring in stilbene and C=O group from both the anhydride groups and the ester group act as the LUMO. Previous studies found that non-fluorescent units generate fluorescence properties when the distance between the "space conjugate" units is within 3.25 Å.[65] The optimized structures showed that the space between the carbonyl in maleic anhydride and to the nearest phenyl ring is 3.18 Å, which is consistent with the "space conjugate" π-π interactions through space as the source of the fluorescence.

The fluorescence properties of styrene-containing alternating copolymers were reported to exhibit low to medium intensities.[26, 33, 36] Compared to styrene-containing alternating copolymers, stilbene-containing alternating copolymers in this study showed much higher fluorescence

intensities when irradiated at 330 nm. The extra phenyl groups on stilbene units not only form more "through space" conjugates with the carbonyl groups of the neighboring maleic anhydride or maleimide units, but also add rigidity into the polymer backbone due to the steric congestion effect.[49] The stiffened chain may also bolster the fluorescence of the stilbene-containing alternating copolymers since a rigid structure can restrict the chain freedom and avert non-radiative relaxation. Figure 3-2b depicts the fluorescence spectra of III in different solvents. The relative fluorescence intensity decreases as the solvent polarity increases while the emission wavelengths remain the same. The environment polarity is known to affect the fluorescence intensity, and similar solvent effects were also observed in other fluorescent systems.[26, 66]

For practical applications of fluorescent materials, especially for quantitative measurements, it is important that the fluorescent intensities have a linear relationship with the concentration of the solution. Figure 3-S7 displays the spectra of III in THF at different concentrations. The peak fluorescence intensity at 380 nm exhibited a linear relationship in the concentration range of 1 μg/ml to 30 μg/ml (Figure 3-2c). We also investigated the aggregation effects on III in THF (good solvent) and deionized water (poor solvent) at different ratios (Figure 3-S8). The fluorescence intensity decreases as the water content increases, which is consistent with the aggregation-caused quenching (ACQ) effect of the fluorescence.[67]

As one of the most commonly used protecting groups for carboxylic acids, *tert*-butyl groups are facilely removed under acidic conditions, and the *tert*-butyl carboxylate groups are converted to corresponding carboxylic acids. The four alternating copolymers I-IV are hydrolyzed to their deprotected forms using trifluoroacetic acid (TFA) (Scheme 3-1b). Figure 3-S9 depicts the fluorescence spectra of the aqueous deprotected copolymer solutions. The deprotected III continues to show strong fluorescence at ca. 380 nm while other deprotected samples exhibited

very weak fluorescence. We investigated the fluorescence properties of the deprotected III in response to pH change since carboxylic acids are known to have pH-responsiveness (Figure 3-2d and 3-S10). The fluorescence intensity increased with the increased pH values until neutral, and then the fluorescence intensity slightly decreased and remained constant till pH 10.0. At lower pH, the carboxylates in the polymers are protonated and the chains are aggregated more due to the lack of the ionic repulsions, which may result in the aggregation-caused quenching (ACQ) effect. The decrease of the fluorescence intensity at higher pH is probably because the deprotonated carboxylate groups become weaker electron acceptors and affect the interaction with the phenyl rings.[54] Previously, the deprotected III was shown to have activities against HIV strains;[50] the newly discovered fluorescence properties provide the possibility of diagnostic and therapeutic applications.

3.5 Conclusions

In summary, we synthesized four alternating copolymers with semi-rigid backbones and studied their fluorescence properties. Indeed we have discovered that steric crowded *tert*-butyl carboxylate substituted stilbene-maleic anhydride alternating copolymer exhibited extraordinarily high fluorescent emission in organic solvents, and the luminescence property is proportional to the concentration of the solution. The fluorescence is maintained when the *tert*-butyl groups are removed and the resulting polymer is dissolved in water. The enhanced fluorescence property likely results from the extra phenyl groups and the "through-space" conjugation of the phenyl groups and the carbonyl groups. A further study of the fluorescence properties of the functionalized stilbene-containing alternating copolymers may lead to the design of novel inherently fluorescent polymeric materials with the potential for technological applications. Further investigation on the effects of molecular weight and different substitution groups is the subject of our on-going research.

3.6 Acknowledgements

This work was supported by the National Science Foundation (NSF) under grant number DMR-0905231, DMR-1206409, and DMR-1310258. We thank the Macromolecules Innovation Institute and the Department of Chemistry at Virginia Tech for support.

3.7 References

1. White, N. S.; Errington, R. J., Fluorescence techniques for drug delivery research: theory and practice. *Adv. Drug Deliv. Rev.* **2005,** *57* (1), 17-42.
2. Kim, J.; Kim, H. S.; Lee, N.; Kim, T.; Kim, H.; Yu, T.; Song, I. C.; Moon, W. K.; Hyeon, T., Multifunctional uniform nanoparticles composed of a magnetite nanocrystal core and a mesoporous silica shell for magnetic resonance and fluorescence imaging and for drug delivery. *Angew. Chem. Int. Ed.* **2008,** *47* (44), 8438-8441.
3. Bae, Y.; Fukushima, S.; Harada, A.; Kataoka, K., Design of environment-sensitive supramolecular assemblies for intracellular drug delivery: Polymeric micelles that are responsive to intracellular pH change. *Angew. Chem. Int. Ed.* **2003,** *115* (38), 4788-4791.
4. Basabe-Desmonts, L.; Reinhoudt, D. N.; Crego-Calama, M., Design of fluorescent materials for chemical sensing. *Chem. Soc. Rev.* **2007,** *36* (6), 993-1017.
5. Thomas, S. W.; Joly, G. D.; Swager, T. M., Chemical sensors based on amplifying fluorescent conjugated polymers. *Chem. Rev.* **2007,** *107* (4), 1339-1386.
6. Guo, Z.; Park, S.; Yoon, J.; Shin, I., Recent progress in the development of near-infrared fluorescent probes for bioimaging applications. *Chem. Soc. Rev.* **2014,** *43* (1), 16-29.
7. Wolfbeis, O. S., An overview of nanoparticles commonly used in fluorescent bioimaging. *Chem. Soc. Rev.* **2015,** *44* (14), 4743-4768.

8. Resch-Genger, U.; Grabolle, M.; Cavaliere-Jaricot, S.; Nitschke, R.; Nann, T., Quantum dots versus organic dyes as fluorescent labels. *Nat. Methods* **2008,** *5* (9), 763-775.

9. Lippincott-Schwartz, J.; Patterson, G. H., Development and use of fluorescent protein markers in living cells. *Science* **2003,** *300* (5616), 87-91.

10. Gonçalves, M. S. T., Fluorescent labeling of biomolecules with organic probes. *Chem. Rev.* **2008,** *109* (1), 190-212.

11. Disney, M. D.; Zheng, J.; Swager, T. M.; Seeberger, P. H., Detection of bacteria with carbohydrate-functionalized fluorescent polymers. *J. Am. Chem. Soc.* **2004,** *126* (41), 13343-13346.

12. Edgar, R.; McKinstry, M.; Hwang, J.; Oppenheim, A. B.; Fekete, R. A.; Giulian, G.; Merril, C.; Nagashima, K.; Adhya, S., High-sensitivity bacterial detection using biotin-tagged phage and quantum-dot nanocomplexes. *Proc. Natl. Acad. Sci. U.S.A.* **2006,** *103* (13), 4841-4845.

13. Wen, S.-W.; Lee, M.-T.; Chen, C. H., Recent development of blue fluorescent OLED materials and devices. *J. Disp. Technol.* **2005,** *1* (1), 90-99.

14. Young, R. H.; Tang, C. W.; Marchetti, A. P., Current-induced fluorescence quenching in organic light-emitting diodes. *Appl. Phys. Lett.* **2002,** *80* (5), 874-876.

15. Piñeiro, L.; Novo, M.; Al-Soufi, W., Fluorescence emission of pyrene in surfactant solutions. *Adv. Colloid Interface Sci.* **2015,** *215*, 1-12.

16. Sjöback, R.; Nygren, J.; Kubista, M., Absorption and fluorescence properties of fluorescein. *Spectrochim. Acta, Part A* **1995,** *51* (6), L7-L21.

17. Glazer, A. N., Phycobiliproteins — a family of valuable, widely used fluorophores. *J. Appl. Phycol.* **1994,** *6* (2), 105-112.

18. Zhou, M.; Robertson, G. P.; Roovers, J., Comparative study of ruthenium(II) tris(bipyridine)

derivatives for electrochemiluminescence application. *Inorg. Chem.* **2005,** *44* (23), 8317-8325.

19. Lee, K. W.; Slinker, J. D.; Gorodetsky, A. A.; Flores-Torres, S.; Abruna, H. D.; Houston, P. L.; Malliaras, G. G., Photophysical properties of tris(bipyridyl)ruthenium(ii) thin films and devices. *Phys. Chem. Chem. Phys.* **2003,** *5* (12), 2706-2709.
20. Elbanowski, M.; Lis, S.; Mąkowska, B., Fluorescence of lanthanide (III) complexes in aqueous solutions the influence ofpH and solution composition. *Monatsh. Chem.* **1985,** *116* (8-9), 901-911.
21. Ng, S. M.; Koneswaran, M.; Narayanaswamy, R., A review on fluorescent inorganic nanoparticles for optical sensing applications. *RSC Adv.* **2016,** *6* (26), 21624-21661.
22. Pietryga, J. M.; Park, Y.-S.; Lim, J.; Fidler, A. F.; Bae, W. K.; Brovelli, S.; Klimov, V. I., Spectroscopic and device aspects of nanocrystal quantum dots. *Chem. Rev.* **2016,** *116* (18), 10513-10622.
23. Bae, S. W.; Tan, W.; Hong, J.-I., Fluorescent dye-doped silica nanoparticles: new tools for bioapplications. *Chem. Commun.* **2012,** *48* (17), 2270-2282.
24. Kim, H. N.; Guo, Z.; Zhu, W.; Yoon, J.; Tian, H., Recent progress on polymer-based fluorescent and colorimetric chemosensors. *Chem. Soc. Rev.* **2011,** *40* (1), 79-93.
25. Hao, W.; Ding, S.; Zhang, L.; Liu, W.; Yang, W., Nacrelike nanocomposite films from fluorescent hyperbranched poly (amido amine)s and clay nanosheets. *ChemPlusChem* **2014,** *79* (2), 211-216.
26. Saha, B.; Bauri, K.; Bag, A.; Ghorai, P. K.; De, P., Conventional fluorophore-free dual pH- and thermo-responsive luminescent alternating copolymer. *Polym. Chem.* **2016,** *7* (45), 6895-6900.

27. Zhu, S.; Song, Y.; Shao, J.; Zhao, X.; Yang, B., Non-conjugated polymer dots with crosslink-enhanced emission in the absence of fluorophore units. *Angew. Chem. Int. Ed.* **2015,** *54* (49), 14626-14637.

28. Zhu, S.; Zhang, J.; Wang, L.; Song, Y.; Zhang, G.; Wang, H.; Yang, B., A general route to make non-conjugated linear polymers luminescent. *Chem. Commun.* **2012,** *48* (88), 10889-10891.

29. Restani, R. B.; Morgado, P. I.; Ribeiro, M. P.; Correia, I. J.; Aguiar-Ricardo, A.; Bonifácio, V. D. B., Biocompatible polyurea dendrimers with pH-dependent fluorescence. *Angew. Chem. Int. Ed.* **2012,** *51* (21), 5162-5165.

30. Wang, D.; Yu, Z.-Q.; Hong, C.-Y.; You, Y.-Z., Strong fluorescence emission from PEGylated hyperbranched poly(amido amine). *Eur. Polym. J.* **2013,** *49* (12), 4189-4194.

31. You, Y.-Z.; Yu, Z.-Q.; Cui, M.-M.; Hong, C.-Y., Preparation of photoluminescent nanorings with controllable bioreducibility and stimuli-responsiveness. *Angew. Chem. Int. Ed.* **2010,** *49* (6), 1099-1102.

32. Sun, M.; Hong, C.-Y.; Pan, C.-Y., A unique aliphatic tertiary amine chromophore: fluorescence, polymer structure, and application in cell imaging. *J. Am. Chem. Soc.* **2012,** *134* (51), 20581-20584.

33. Mohamed, M. G.; Hsu, K.-C.; Hong, J.-L.; Kuo, S.-W., Unexpected fluorescence from maleimide-containing polyhedral oligomeric silsesquioxanes: nanoparticle and sequence distribution analyses of polystyrene-based alternating copolymers. *Polym. Chem.* **2016,** *7* (1), 135-145.

34. Zhao, E.; Lam, J. W. Y.; Meng, L.; Hong, Y.; Deng, H.; Bai, G.; Huang, X.; Hao, J.; Tang, B. Z., Poly[(maleic anhydride)-*alt*-(vinyl acetate)]: A pure oxygenic nonconjugated

macromolecule with strong light emission and solvatochromic effect. *Macromolecules* **2015,** *48* (1), 64-71.

35. Pucci, A.; Rausa, R.; Ciardelli, F., Aggregation-induced luminescence of polyisobutene succinic anhydrides and imides. *Macromol. Chem. Phys.* **2008,** *209* (9), 900-906.

36. Ru, Y.; Zhang, X.; Song, W.; Liu, Z.; Feng, H.; Wang, B.; Guo, M.; Wang, X.; Luo, C.; Yang, W.; Li, Y.; Qiao, J., A new family of thermoplastic photoluminescence polymers. *Polym. Chem.* **2016,** *7* (40), 6250-6256.

37. Müller, J. G.; Anni, M.; Scherf, U.; Lupton, J. M.; Feldmann, J., Vibrational fluorescence spectroscopy of single conjugated polymer molecules. *Phys. Rev. B: Condens. Matter* **2004,** *70* (3), 035205.

38. Guo, Z.; Ru, Y.; Song, W.; Liu, Z.; Zhang, X.; Qiao, J., Water-soluble polymers with strong photoluminescence through an eco-friendly and low-cost route. *Macromol. Rapid Commun.* **2017,** *38* (14), 1700099.

39. Huang, J.; Turner, S. R., Recent advances in alternating copolymers: The synthesis, modification, and applications of precision polymers. *Polymer* **2017,** *116*, 572-586.

40. Zhou, X.; Li, Y.; Hart, K. E.; Abbott, L. J.; Lin, Z.; Svec, F.; Colina, C. M.; Turner, S. R., Nanoporous structure of semirigid alternating copolymers via nitrogen sorption and molecular simulation. *Macromolecules* **2013,** *46* (15), 5968-5973.

41. Zhou, X.; Huang, J.; Barr, K. W.; Lin, Z.; Maya, F.; Abbott, L. J.; Colina, C. M.; Svec, F.; Turner, S. R., Nanoporous hypercrosslinked polymers containing T_g enhancing comonomers. *Polymer* **2015,** *59*, 42-48.

42. Mao, M.; England, J.; Turner, S. R., Alternating stilbene copolymers with negative birefringence. *Polymer* **2011,** *52* (20), 4498-4502.

43. Mao, M.; Kim, C.; Wi, S.; Turner, S. R., Chain structure of substituted stilbene−maleic anhydride alternating copolymer probed by solid-state NMR. *Macromolecules* **2008,** *41* (2), 387-389.

44. Mao, M.; Turner, S. R., Synthesis and characterization of highly functionalized polymers based on *N,N,N′,N′*-tetraalkyl-4,4′-diaminostilbene and maleic anhydride. *Polymer* **2006,** *47* (24), 8101-8105.

45. Mao, M.; Turner, S. R., Aggregation of rod−coil block copolymers containing rigid polyampholyte blocks in aqueous solution. *J. Am. Chem. Soc.* **2007,** *129* (13), 3832-3833.

46. Li, Y.; Mao, M.; Matolyak, L. E.; Turner, S. R., Sterically crowded anionic polyelectrolytes with tunable charge densities based on stilbene-containing copolymers. *ACS Macro Lett.* **2012,** *1* (2), 257-260.

47. Li, Y.; Savage, A. M.; Zhou, X.; Turner, S. R.; Davis, R. M., Solution properties of stilbene-containing sterically crowded alternating polyanions. *J. Polym. Sci., Part B: Polym. Phys.* **2013,** *51* (21), 1565-1570.

48. Li, Y.; Turner, S. R., Free radical copolymerization of methyl substituted stilbenes with maleic anhydride. *Eur. Polym. J.* **2010,** *46* (4), 821-828.

49. Li, Y.; Zhang, M.; Mao, M.; Turner, S. R.; Moore, R. B.; Mourey, T. H.; Slater, L. A.; Hauenstein, J. R., Chain stiffness of stilbene containing alternating copolymers by SAXS and SEC. *Macromolecules* **2012,** *45* (3), 1595-1601.

50. Savage, A. M.; Li, Y.; Matolyak, L. E.; Doncel, G. F.; Turner, S. R.; Gandour, R. D., Anti-HIV activities of precisely defined, semirigid, carboxylated alternating copolymers. *J. Med. Chem.* **2014,** *57* (15), 6354-6363.

51. Savage, A. M.; Ullrich, E.; Chin, S. M.; Kiernan, Z.; Kost, C.; Turner, S. R., Synthesis and

characterization of double hydrophilic block copolymers containing semi-rigid and flexible segments. *J. Polym. Sci., Part A: Polym. Chem.* **2015,** *53* (2), 219-227.

52. Savage, A. M.; Zhou, X.; Huang, J.; Turner, S. R., A review of semi-rigid, stilbene-containing alternating copolymers. *Appl. Petrochem. Res.* **2015,** *5* (1), 27-33.

53. Huang, J.; Turner, S. R., Hypercrosslinked polymers: A review. *Polym. Rev.* **2017**, latest articles.

54. Savage, A. M.; Ullrich, E.; Kost, C.; Turner, S. R., Salt- and pH-responsive semirigid/flexible double-hydrophilic block copolymers. *Macromol. Chem. Phys.* **2016,** *217* (15), 1737-1744.

55. Wagner-Jauregg, T., Über addierende hetero-polymerisation. *Ber. Dtsch. Chem. Ges.* **1930,** *63* (11), 3213-3224.

56. Hallensleben, M. L., Electron donor-acceptor complexes and polymerization—V copolymerization of maleic anhydride and trans-stilbene under ultra-violet irradiation. *Eur. Polym. J.* **1973,** *9* (3), 227-231.

57. Huang, J.; Zhou, X.; Lamprou, A.; Maya, F.; Svec, F.; Turner, S. R., Nanoporous polymers from cross-linked polymer precursors via *tert*-butyl group deprotection and their carbon dioxide capture properties. *Chem. Mater.* **2015,** *27* (21), 7388-7394.

58. Wang, Y.-C.; Morawetz, H., Excimer fluorescence of polymers with aromatic substituents, 1. Dependence of excimer formation on polymer structure. *Macromol. Chem. Phys.* **1975,** *1* (S19751), 283-295.

59. Tanaka, T.; Vogl, O., Preparation and characterization of head-to-head polymer. I. Head-to-head poly(methyl cinnamate). *Polym. J.* **1974,** *6* (6), 522-531.

60. Ams, M. R.; Ajami, D.; Craig, S. L.; Yang, J.-S.; Rebek, J., Jr., Control of stilbene conformation and fluorescence in self-assembled capsules. *Beilstein J. Org. Chem.* **2009,** *5*,

79.

61. Demchenko, A. P., *Introduction to Fluorescence Sensing*. Springer International Publishing: 2015.

62. Gertz, L., *Stilbenes: applications in chemistry, life sciences and materials science.* WILEY-VCH, Germany: 2010.

63. Hirayama, F., Intramolecular excimer formation. I. Diphenyl and triphenyl alkanes. *J. Chem. Phys* **1965,** *42* (9), 3163-3171.

64. Phillips, D.; Roberts, A. J.; Soutar, I., A time-resolved fluorescence spectroscopic study of excimer formation in polyacenaphthylene and an alternating acenaphthylene/maleic anhydride copolymer. *J. Polym. Sci. Polym. Lett. Ed.* **1980,** *18* (2), 123-129.

65. Yan, J.-J.; Wang, Z.-K.; Lin, X.-S.; Hong, C.-Y.; Liang, H.-J.; Pan, C.-Y.; You, Y.-Z., Polymerizing nonfluorescent monomers without incorporating any fluorescent agent produces strong fluorescent polymers. *Adv. Mater.* **2012,** *24* (41), 5617-5624.

66. Fletcher, K. A.; Storey, I. A.; Hendricks, A. E.; Pandey, S.; Pandey, S., Behavior of the solvatochromic probes Reichardt's dye, pyrene, dansylamide, Nile Red and 1-pyrenecarbaldehyde within the room-temperature ionic liquid bmimPF. *Green Chem.* **2001,** *3* (5), 210-215.

67. Ma, X.; Sun, R.; Cheng, J.; Liu, J.; Gou, F.; Xiang, H.; Zhou, X., Fluorescence Aggregation-Caused Quenching versus Aggregation-Induced Emission: A Visual Teaching Technology for Undergraduate Chemistry Students. *J. Chem. Educ.* **2015,** *93* (2), 345-350.

3.8 Supporting information for chapter 3

3.8.1 Experimental section

3.8.1.1 Materials

The monomers (E)-di-*tert*-butyl-4, 4'-stilbene dicarboxylate (DTBSC), *tert*-butyl 4-maleimidobenzoate (TBMI), and *tert*-butyl 4-vinyl benzoate (TBVB) were synthesized and characterized as previously reported.[1] Trifluoroacetic acid (TFA, Oakwood Chemical, 99%), sodium hydroxide (Fisher, certified ACS grade), tetrahydrofuran (THF, Fisher, certified HPLC grade without stabilizer), chlorobenzene (Sigma-Aldrich, 99%) were used as received without further purification. Maleic anhydride (MAH, Sigma-Aldrich, 99%) was recrystallized from toluene. 2, 2'-azobisisobutyronitrile (AIBN, Aldrich, 98%) and dicumyl peroxide (DCP, Aldrich, 99%) was recrystallized from methanol. Deionized water (house DI water) was provided by Virginia Tech.

3.8.1.2 Instrumental characterization.

The structures of the synthesized monomers were determined by proton nuclear magnetic resonance (^{1}H NMR, Varian Inova 400 MHz). The incorporation of the functionalized stilbene and maleimide comonomers and the deprotection of *tert*-butyl groups were confirmed by infrared analysis (IR, Agilent Cary 630 FT-IR Spectrometer). The thermogravimetric analysis (TGA) of the copolymers was measured with a TA instrument model Q5000), samples were heated from 50 to 550 ºC at a heating rate of 10 ºC/min under nitrogen. The fluorescence spectra were obtained using an Agilent Cary Eclipse fluorimeter in a 1 cm path length quartz cuvette, with the excitation and emission slits fixed at 5 nm. The UV-Vis spectra were obtained using an Agilent Cary 5000 UV-Vis-NIR spectrophotometer. Molecular weights of the polymers were determined using an Agilent size exclusion chromatograph (SEC) equipped with a Wyatt light scattering detector in

THF at 30 ˚C. Data were analyzed utilizing a universal calibration made with polystyrene standards to obtain absolute molecular weights.

3.8.1.3 Synthesis of the alternating copolymers.

The alternating copolymers were synthesized via solution free radical polymerizations.[1, 2] The two styrene-containing copolymers Copolymer I and II were prepared at 60 ˚C in THF using AIBN as initiator, and the two stilbene-containing copolymers Copolymer III and IV were prepared at 110 ˚C in chlorobenzene using dicumyl peroxide (DCP) as initiator. For example, to synthesize Copolymer III, DTBSC (0.96 g, 2.5 mmol), MAH (0.25g, 2.5 mmol) and DCP (0.012 g, 1.0 wt%) were dissolved in 4.5 mL chlorobenzene in a 50 mL septum-sealed serum bottle with a stir bar. The bottle was purged with argon for 20 min and the solution was stirred at 80 °C for 24 h. A white solid was recovered by precipitating with hexanes (500 mL). The polymer was redissolved in a minimum amound of THF and precipitated with hexanes. The polymer was filtered and dried under vacuum at 60 °C overnight (0.81 g, 66%).

3.8.1.4 Synthesis of the deprotected polymers.

0.5 g polymer was dissolved in 3 mL dichloromethane (DCM), 3 mL TFA was added at room temperature. The mixture was stirred for 24 h, then filtered and washed with DCM. Then the polymer was stirred in 0.1 M NaOH solution for 24 h and dialyzed with DI water. The aqueous contents were then frozen in liquid nitrogen and lyophilized for 24 h to yield a white fluffy solid.

3.8.2 Supplemental tables and figures

Table 3-S1. The yields, molecular weights, PDI of the alternating copolymers

Samples	Yield (%)	M_n g/mol	M_w g/mol	PDI
Copolymer I	86	41,000	64,600	1.5
Copolymer II	71	54,990	97,600	1.8
Copolymer III	66	39,730	42,810	1.1
Copolymer IV	59	19,850	47,700	2.4

Table 3-S2. The UV-Vis absorption peak wavelengths (Abs) in THF and the calculated massic absorbance coefficients (MAC). MAC is calculated using [MAC=absorbance intensity/(concentration*cell width)]. "-" means weak or no peak.

Sample	Abs 1 (nm)	MAC 1 ($g^{-1}Lcm^{-1}$)	Abs 2 (nm)	MAC 2 ($g^{-1}Lcm^{-1}$)	Abs 3 (nm)	MAC 3 ($g^{-1}Lcm^{-1}$)
I	237	4.77	-	-	-	-
II	239	5.09	-	-	-	-
III	237	5.94	260	0.6236	330	1.22
IV	235	8.05	-	-	330	0.05

Quantum yields of the copolymers. Quinine sulfate was chosen as the external standards for fluorescence quantum yield calculations. The quantum yields of the copolymers were measured by comparing the integrated photoluminescence intensities and the absorbance values with the reference quinine sulfate. The quinine sulfate was dissolved in 0.1M H_2SO_4 (refractive index (η) of 1.33) and the copolymers were dissolved in THF (η=1.407).

Usually the solutions with UV-Vis absorption should be controlled between 0.2 and 0.01. However, because of the weak fluorescence emission of Copolymer III at excitation wavelength 260, the UV absorption was controlled at 2.80. The quantum yields of polymers are calculated using:

$$\Phi = \Phi_r \cdot \frac{I}{I_r} \cdot \frac{A_r}{A} \cdot \frac{\eta^2}{\eta_r^2}$$

where Φ is the quantum yield, Φ_r is the quantum yield of the reference Quinine sulfate (Φ_r= 0.54), I is the measured integrated emission intensity, A is the measured absorption intensity, and η is the refractive index.

Table 3-S3. The excitation and emission wavelengths, and quantum yields of the copolymers in THF

Sample	Excitation wavelength (nm)	Emission wavelength (nm)	Emission Intensity (a.u.)	Absorption at excitation wavelength (a.u.)	Quantum Yield Φ
Copolymer III	330	380	319.06	0.062	0.712
	260	290	201.78	2.821	0.010
Copolymer IV	330	380	155.41	0.033	0.659
Copolymer I	300	350	31.28	0.168	0.026
Copolymer II	300	340	31.37	0.141	0.031

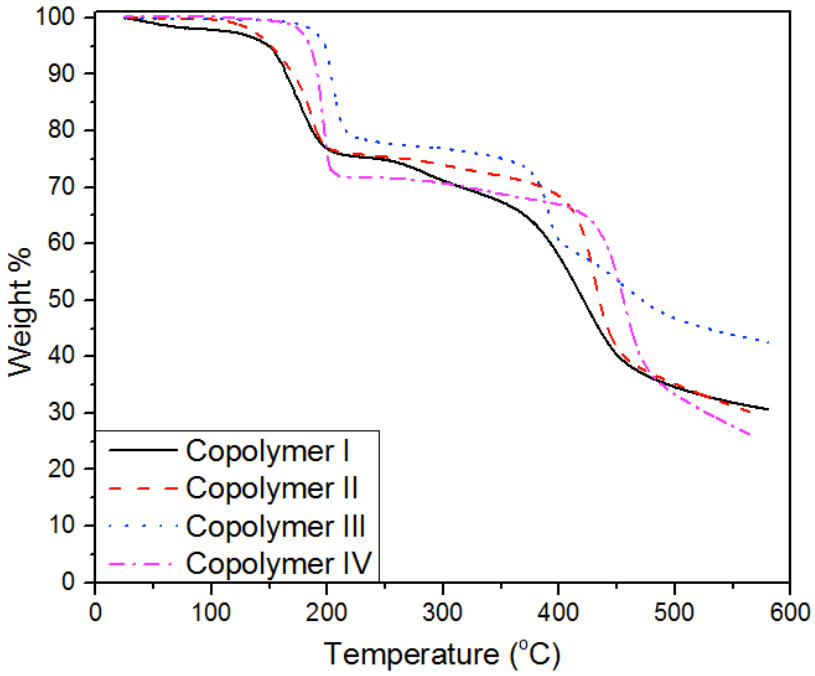

Figure 3-S1. TGA graph of alternating copolymers, the first stage of weight loss represents the loss of *tert*-butyl groups.

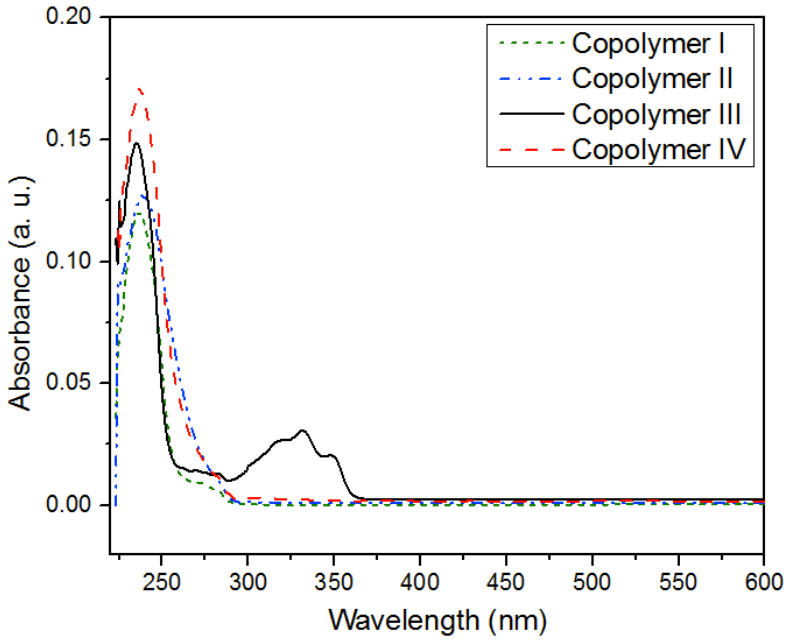

Figure 3-S2. UV/Vis spectra of the alternating copolymers (Concentration 25 µg/mL)

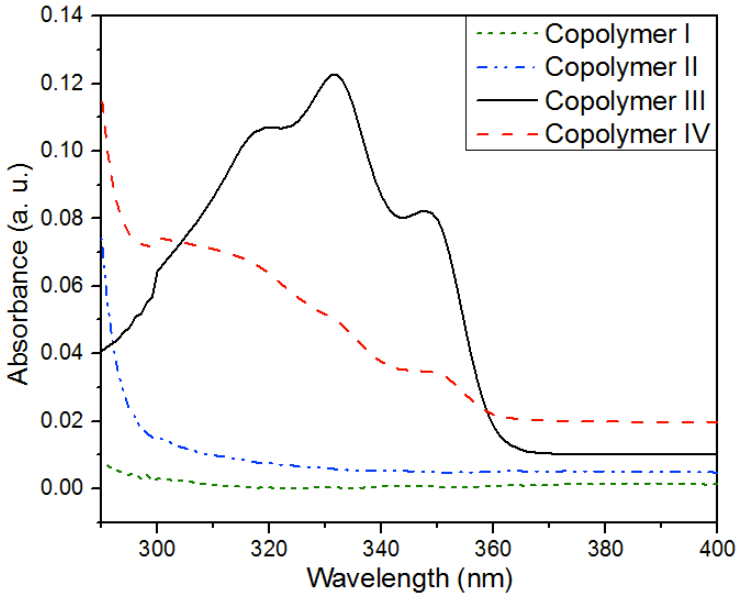

Figure 3-S3. UV/Vis spectra of the alternating copolymers at 290-400 nm region with higher concentration (Concentration of I, II and IV: 1 mg/mL, III: 100 µg/mL)

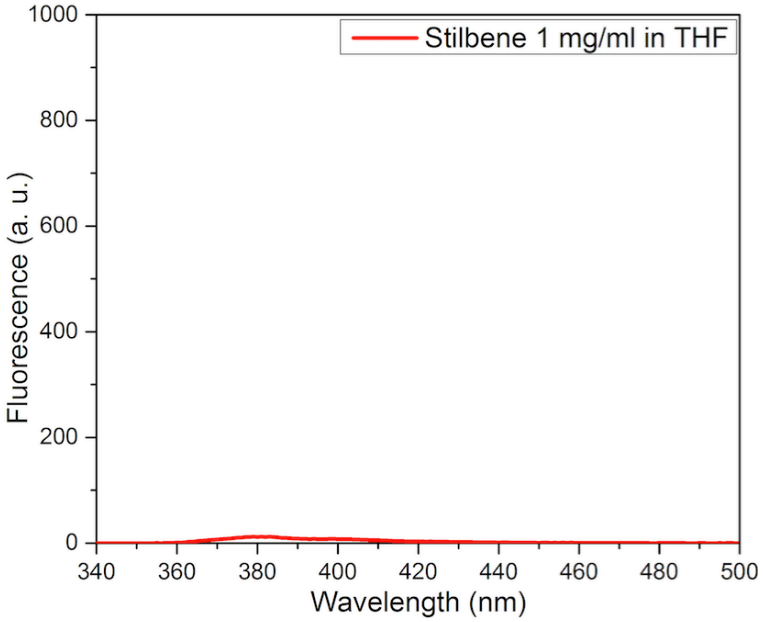

Figure 3-S4. Fluorescence spectrum of *tert*-butyl carboxylate-containing trans-stilbene solution in THF, no obvious fluorescence was observed.

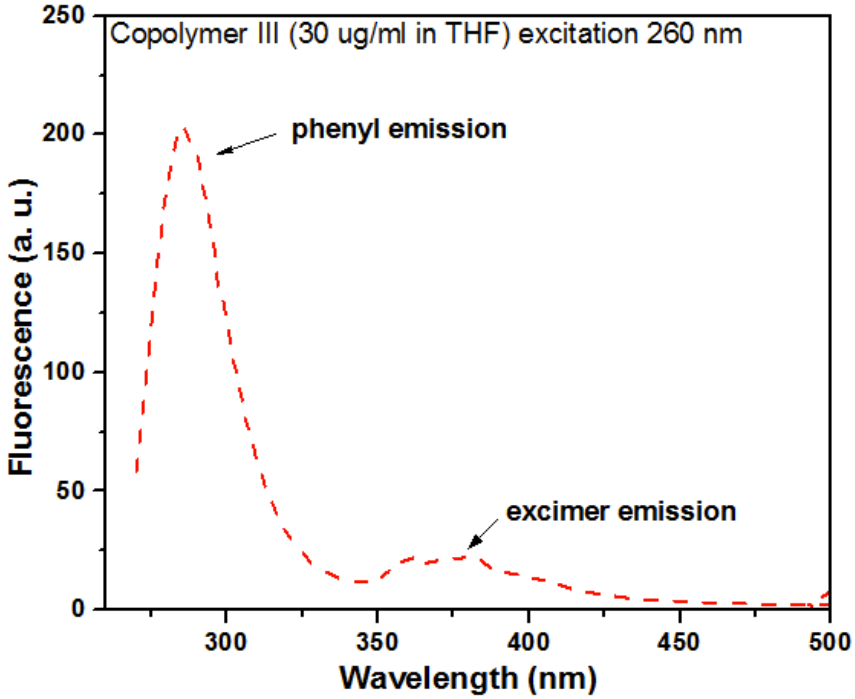

Figure 3-S5. Fluorescence spectrum of Copolymer III in THF when irradiated by 260 nm (concentration 30 µg/mL). The sharp emission corresponds to the phenyl emission and the broad, red-shifted peak corresponds to the excimer emission.

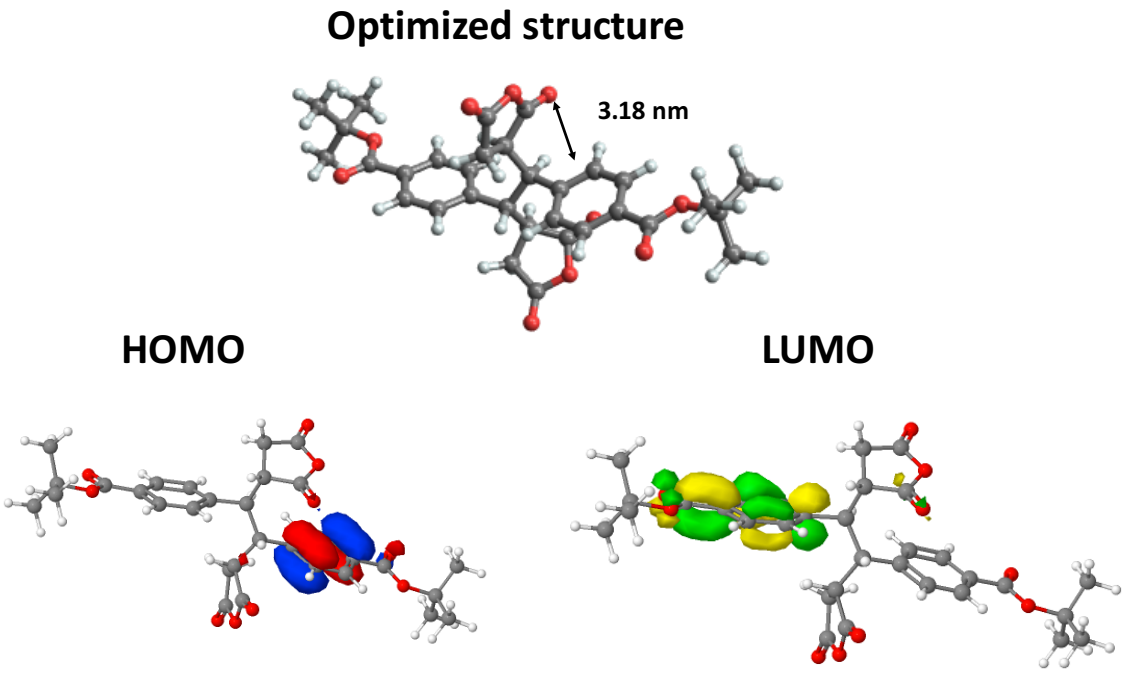

Figure 3-S6. Optimized geometry, HOMO and LUMO of Copolymer III in vacuum using the B3LYP/6-311+g** theory in Gaussian.

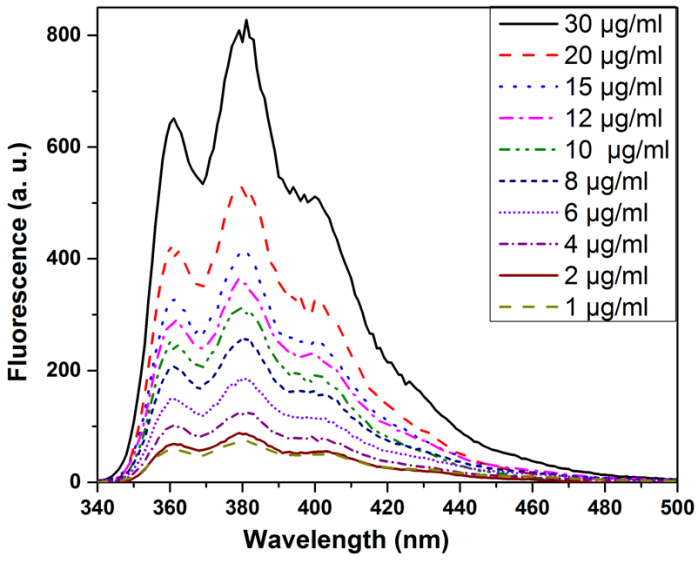

Figure 3-S7. Fluorescence spectra of the copolymer III in THF at different concentration (excitation wavelength: 330 nm).

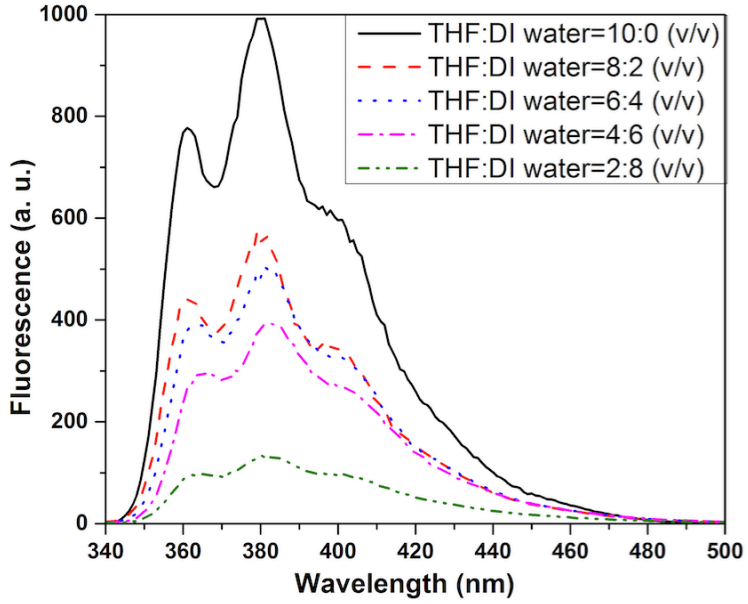

Figure 3-S8. Aggregation effects of Copolymer III in THF and DI water at different ratios.

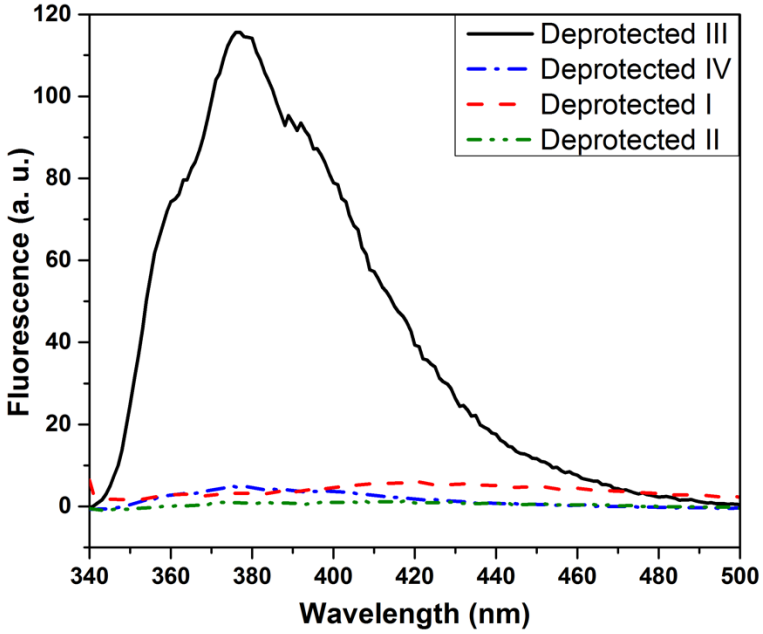

Figure 3-S9. Fluorescence spectra (excitation wavelength: 330 nm) of deprotected copolymers in deionized water (concentrations: 1 mg/mL)

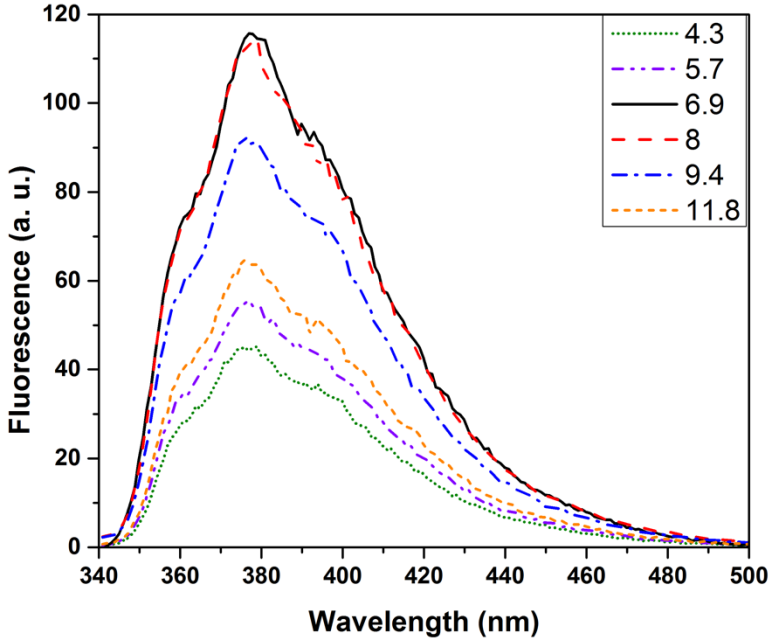

Figure 3-S10. Fluorescence spectra of deprotected III in DI water at different pH values (concentration 1 mg/mL).

Chapter 4. Nanoporous Polymers from Crosslinked Polymer Precursors *via* *tert*-Butyl Group Deprotection and Their Carbon Dioxide Capture Properties

(Adapted with permission from Huang, J.; Zhou, X.; Lamprou, A.; Maya, F.; Svec, F.; Turner, S. R. Chem. Mater. 2015, 27, 7388. Copyright 2015 American Chemical Society.)

4.1 Authors

Jing Huang,[†] Xu Zhou,[†] Alexandros Lamprou,[‡] Fernando Maya,[‡] Frantisek Svec[‡] and S. Richard Turner*[†]

[†]Department of Chemistry, and Macromolecules and Interfaces Institute, Virginia Tech, Blacksburg, VA 24061, United States

[‡]The Molecular Foundry, E.O. Lawrence Berkeley National Laboratory, Mailstop 67R6110, Berkeley, CA 94720-8139, United States

4.2 Abstract

A two-step synthetic strategy has been developed to achieve functionalized nanoporous polymers *via* the deprotection of the crosslinked polymer precursors containing *tert*-butyl carboxylate-functionalized stilbene or styrene and *N*-phenylmaleimide alternating sequences. Three different deprotection methods to generate nanoporosity were examined in this work. The resulting nanoporous polymers showed a significant increase in BET surface area. The effects of crosslinking density and the stiffness of the alternating sequences on the nanoporosity of these polymers were studied. The resulting nanoporous polymers were also investigated as potential CO_2 sorbents.

4.3 Introduction

Since the 1980s, global warming has become a major issue in climate change.[1] Now overwhelming scientific consensus has correlated global warming to the escalating amount of CO_2

in the atmosphere.[2] The combustion of fossil fuels, coal, petroleum, and natural gas provides more than 80% of the worldwide energy supplies[3] and is responsible for more than 86% of global CO_2 emissions.[4] While looking for alternative energy sources—hydrogen, solar and wind—that do not emit CO_2, governments and scientists now consider CO_2 capture and storage (CCS) as a promising technology to control atmospheric CO_2 levels.[5] Currently, amine scrubbing using amine-containing solvents, such as monoethanolamine (MEA) and diethanolamine (DEA), is one of the most well established methods for CO_2 capture in industry.[6] However, due to the solvent emission, degradation, and the high energy demand during the solvent regeneration, researchers are seeking new materials for CCS.[7-8] Solid sorbents, such as zeolites and metal organic frameworks (MOFs), are considered as replacements to solvent absorption for CO_2 capture.[9]

Nanoporous (pore size < 100 nm) organic polymers have attracted substantial interests from both academia and industry, due to their various potential applications such as heterogeneous catalyst substrates,[10-12] chromatography separation materials,[13] drug delivery systems,[14] sensing materials,[15] and gas sorption/separation matrices.[16-17] Recently, the CO_2 capture properties of a number of nanoporous organic polymers were investigated.[18-21] High surface area, good physicochemical stability, low skeleton density and synthetic diversity make these materials good candidates as solid sorbents for CO_2.[16, 20] During the capture, CO_2 physically or chemically adsorbs onto the surface of nanoporous organic polymers, and desorbs *via* a thermal or pressure driven process, which requires less regeneration energy.[22] Most nanoporous organic polymers are non-volatile at the desorption temperature,[16] which avoids pollution through solvent emission.

Various synthetic routes have been employed to achieve nanoporosity in organic polymers. One typical approach involves covalent bonding of small building blocks in highly ordered structures. This strategy is usually utilized in the synthesis of polymers such as covalent organic

frameworks (COFs),[19, 23-24] conjugated microporous polymers (CMPs),[18, 25-26] porous aromatic frameworks (PAFs),[21, 27] etc. Another strategy, as in the synthesis of hypercrosslinked polymers (HCPs), is to crosslink monomers or polymer chains in their swollen state by crosslinking groups/agents. The nanopores are generated from the void space of the leaving solvents.[13, 28] In addition to the two strategies mentioned above, nanoporous polymeric materials can also be prepared by selectively etching a minor component from an ordered block copolymer with degradable or etchable blocks such as polylactide (PLA)[29] or poly(*tert*-butyl acrylate) (PtBA).[30] This approach requires the etchable segments to be physically accessible to the reagents, and the remaining matrix to be able to hold the resultant nanoporous structure from collapsing.[30] The resulting materials are mostly found to have mesopores (2 nm < pore size < 5 nm), and applications such as nanoobject templates[31-32] and separation membranes[33] were developed for these materials. Sterically crowded, functional group-containing, semi-rigid alternating copolymers are under investigation in our group.[34-44] These copolymers can be synthesized *via* conventional or controlled free radical polymerizations. We are able to incorporate various functional groups, such as amine, ether, alkyl, *tert*-butyl carboxylate, into these copolymers by using different substituted monomers. Of special interest are the *tert*-butyl carboxylate-containing copolymers which can be converted to polyelectrolytes, by the deprotection of the *tert*-butyl carboxylates into corresponding carboxylic acids.[37] The *tert*-butyl carboxylate functionalized alternating copolymers showed nanoporosity with modest BET surface areas of 20–40 m^2/g, which increased as the copolymer persistence length increased. The *tert*-butyl carboxylate groups in these copolymers interfere with the efficient chain packing and the semi-rigid backbone prevents chains from relaxing, therefore leading to nanoporosity.[40] Recently, we reported a model system which incorporated the methyl-functionalized alternating copolymer sequences into HCPs *via* suspension polymerization and a

post-crosslinking reaction. The incorporation of these semi-rigid, alternating copolymer sequences showed an enhancement of the T_g of the lightly-crosslinked precursor, which would potentially reduce the possibility of pore collapsing during the post polymerization process.[44]

In this study, we realized a facile and efficient two-step synthetic route that combines the synthesis of crosslinked copolymers and the removal of protection groups from the backbone to prepare nanoporous polymers with high surface area, micropores and carboxylic acid functional groups. The T_g enhancing stilbene and maleimide comonomers with the hydrolysable *tert*-butyl carboxylate functional groups were crosslinked by divinylbenzene (DVB) in the suspension polymerization, and the *tert*-butyl carboxylate groups were then converted to carboxylic acids *via* post-deprotection reactions. We hypothesized that during the deprotection, the space that the *tert*-butyl groups used to occupy became nanopores, and resulting a higher surface area (Figure 4-1). Previously, Gupta *et al.* reported the increase of surface area in a metal-organic framework (MOF) by the deprotection of NH-Boc to NH_2.[45] However, the resulting MOF after deprotection showed no surface area unless it was activated by supercritical CO_2 to obtain a BET surface area of 1381 m^2/g. Our strategy avoided the sample handling and treatment after deprotection and achieved a significant increase of surface area. The chemical and structural compositions of the crosslinked nanoporous polymers were characterized by elemental analysis, thermogravimatric analysis, and infrared spectroscopy. The specific surface areas, nanoporosities, and CO_2 capture abilities of these polymers were also explored and discussed.

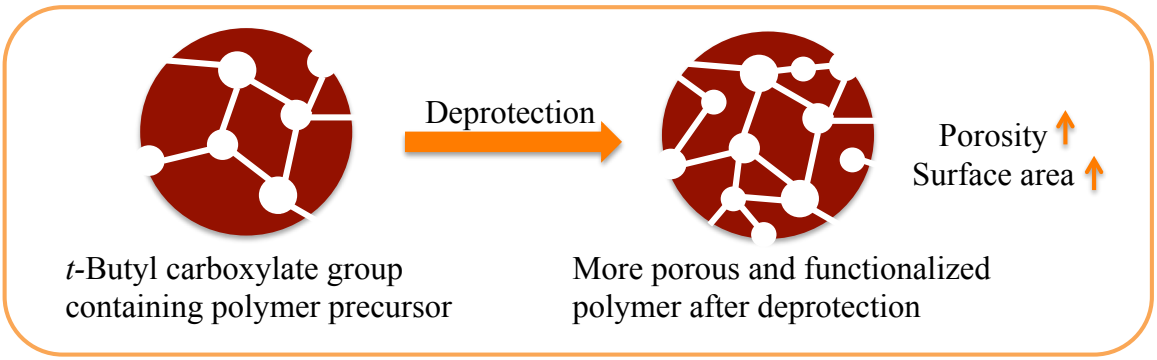

Figure 4-1. Nanoporous polymers from crosslinked polymer precursors via *tert*-butyl group deprotection

4.4 Experimental section

4.4.1 Materials

The *tert*-butyl carboxylate group containing monomers (E)-di-*tert*-butyl-4, 4'-stilbene dicarboxylate (DTBSC), *tert*-butyl 4-maleimidobenzoate (TBMI), and *tert*-butyl 4-vinyl benzoate (TBVB) were synthesized and characterized as previously reported.[37] Divinylbenzene (DVB, Sigma-Aldrich, technical grade, isomer of *p*- and *m*-, 80% purity), trifluoroacetic acid (TFA, Oakwood Chemical, 99%), toluene (Fisher, HPLC grade), poly(vinyl alcohol) (Aldrich, 87-89% hydrolyzed), sodium chloride (Fisher, certified ACS crystalline), zinc bromide (Aldrich, ≥98.0%) dichloromethane (DCM, Fisher, HPLC grade) were used as received without further purification. 2, 2'-azobisisobutyronitrile (AIBN, Aldrich, 98%) was recrystallized from methanol. Deionized water was provided by Virginia Tech.

4.4.2 Instrumental characterization

The structures of the monomers were determined by proton nuclear magnetic resonance (^{1}H NMR, Varian Inova 400 MHz). The incorporation of the functionalized stilbene and maleimide comonomers and the deprotection of *tert*-butyl groups were confirmed by infrared analysis (IR, Agilent Cary 630 FT-IR Spectrometer). Elemental analysis was performed by Atlantic Microlab (Norcross, GA). The thermogravimetric analysis (TGA) of the copolymers was conducted by TA

instrument model Q5000), samples were heated from 50 to 550 ºC at a heating rate of 10 ºC/min under nitrogen. SEM micrographs of the copolymers were obtained using a LEO (Zeiss) 1550 field emission scanning electron microscope. Nitrogen adsorption/desorption isotherms at 77 K were obtained using Micromeritics TriStar II 3020 surface area analyzer, the samples were degassed at 140 °C overnight before measurements. The surface areas were calculated using the Brunauer-Emmett-Teller (BET) equation,[46] the pore sizes determined from nitrogen adsorption isotherm by the two-dimensional non-local density functional theory model with heterogeneous surfaces (2D-NLDFT-HS) using SAIEUS software.[47-49] The CO_2 uptakes were measured at 273 K and 298 K by a Micromeritics ASAP 2020 instrument.

4.4.3 Synthesis of crosslinked polymer precursors

The crosslinked copolymer precursors were synthesized *via* suspension polymerization (Scheme 4-1). For example, DTBSC (1.90 g, 5.0 mmol), TBMI (1.37 g, 5.0 mmol), and DVB (1.95 g, 15 mmol) were dissolved in 40 mL toluene in a 500 mL three-neck round bottom flask equipped with a mechanical stirrer, a condenser and a N_2 gas inlet. Then 250 mL of deionized water was added to the flask, followed by adding poly (vinyl alcohol) (0.52 g, 9.4 wt%) and NaCl (2.60 g, 50 wt%). The mixture was purged with N_2 for 15 min while stirring. AIBN (26 mg, 0.5 wt%) was added to initiate the polymerization. The suspension mixture was stirred under N_2 at 80 ˚C for 24 h. The resulting polymer beads were filtered and purified using Soxhlet extraction with toluene and water for 24 h to further remove the unreacted monomer, poly(vinyl alcohol) and NaCl. The resulting off-white beads were dried in vacuum oven at 50 ˚C for 24 h (65.6%–74.0%). The general nomenclature for these copolymers, STB-#DVB or Sty-#DVB, is employed. STB stands for the stilbene comonomer DTBSC，Sty stands for the styrene comonomer TBVB, and # stands for the mol% of DVB. For simplification, TBMI is not shown in the abbreviations since it is always

charged in a 1:1 molar ratio with DTBSC or TBVB. For example, STB-60DVB represents the copolymer of DTBSC and TBMI with 60 mol% of DVB.

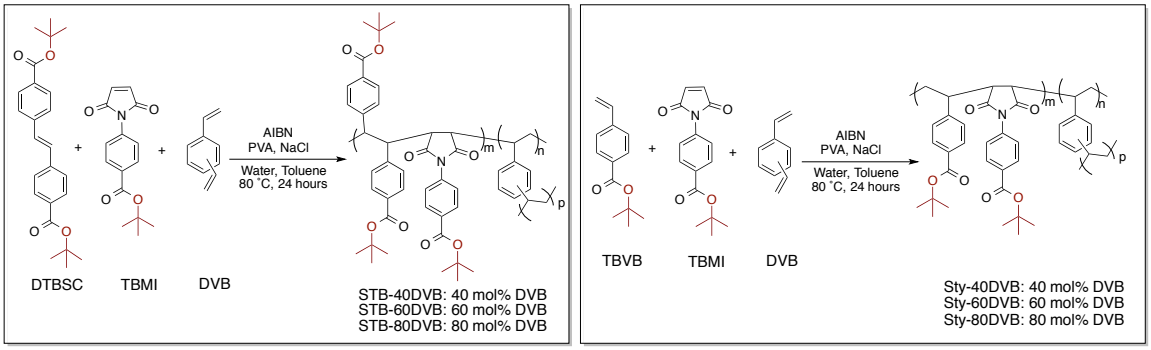

Scheme 4-1. Synthesis of *tert*-butyl group-containing crosslinked polymer precursors

4.4.4 *tert*-butyl group deprotection

Three methods were explored to deprotect the copolymer precursors prepared from suspension polymerization (Scheme 4-2). For thermal deprotection, the polymer was placed in a vacuum oven at 220 ˚C for 30 min. For TFA deprotection, 0.5 g polymer was swollen in 3 mL dichloromethane (DCM), 3 mL TFA was added at room temperature. The mixture was stirred for 24 h, then filtered and washed with DCM. The resulting white powder was further dried in vacuum at room temperature for 24 h. For $ZnBr_2$ deprotection, 0.5 g polymer was swollen in 5 mL dichloromethane, 2 g solid $ZnBr_2$ (500 mol% to *tert*-butyl groups) was added. The mixture was stirred for 24 h at room temperature, then 5 mL water was added and stirred for 2 h. and the polymer was filtered and washed by water. The resulting white powder was dried in vacuum oven at 50 ˚C for 24 h. A general nomenclature for these copolymers, STB-#DVB-d or Sty-#DVB-d, is employed. STB or Sty stands for the stilbene comonomer DTBSC or styrene comonomer TBVB, # stands for the mol% of DVB, and d is short for deprotection.

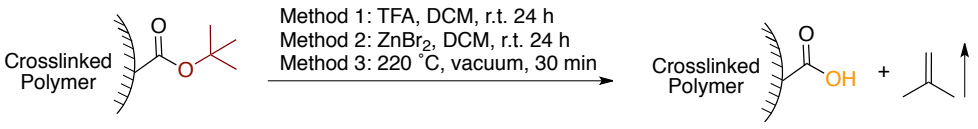

Scheme 4-2. Three methods to deprotect the *tert*-butyl group from polymer precursor

4.5 Results and discussion

The nanoporous polymers were synthesized by a two-step procedure. In the first step, a series of crosslinked polymer precursors were prepared *via* suspension polymerization of *tert*-butyl carboxylate-functionalized stilbene or styrene and *tert*-butyl carboxylate-functionalized *N*-phenylmaleimide in the presence of divinylbenzene as the crosslinker. The polymer precursors were then deprotected to cleave the *tert*-butyl groups. Three different deprotection methods were investigated. Nitrogen isotherms were obtained to study the nanoporous structures of the polymers. CO_2 uptakes of these polymers at two different temperatures were also measured.

4.5.1 Synthesis of *tert*-butyl carboxylate-containing crosslinked polymer precursors

We synthesized the *tert*-butyl group-containing crosslinked polymer precursors *via* a modified suspension polymerization procedure.[50-51] During the polymerization, the *tert*-butyl carboxylate-containing stilbene monomer DTBSC or styrene monomer TBVB, and the *tert*-butyl carboxylate containing maleimide monomer TBMI were copolymerized with the crosslinker DVB. Toluene was added as a porogen and a solvent for dissolving the solid monomers. Spherical beads in the range of 20 – 200 μm were obtained (see Figure 4-S1 for SEM image).

Since the electron rich monomers DTBSC or TBVB preferably polymerize with the electron poor monomer TBMI in an alternating fashion, we assume the ratio of DTBSC: TBMI or TBVB: TBMI in each polymer is 1:1. Elemental analysis data of the crosslinked polymer precursors are shown in Table 4-1. The experimental elemental contents are in general agreement with the theoretical values. The precursors contain 0.85–2.66 wt% of N, indicating that the maleimide

monomers were successfully copolymerized into the precursors. For the DTBSC materials, it is possible that the higher N content arises from the higher amount of TBMI incorporation due to the selective cross propagation of TBMI and DVB.[44] The incorporation of the *tert*-butyl group-containing monomers was also confirmed by thermogravimetric analysis (TGA). The first stage of weight loss at 220 ˚C in TGA curve indicates the thermal cleavage of the *tert*-butyl group (Figure 4-S2 and Figure 4-2).

Table 4-1. Elemental analysis of polymer precursors

Sample	Theoretical (wt%)			Experimental (wt%)		
	C	H	N	C	H	N
STB-40DVB	75.92	6.82	1.70	74.25	6.21	2.66
STB-60DVB	79.36	7.05	1.34	80.71	6.95	1.80
STB-80DVB	84.31	7.31	0.83	84.10	7.49	0.93
Sty-40DVB	76.24	6.86	2.15	76.09	6.76	2.29
Sty-60DVB	80.25	7.08	1.61	80.49	7.32	1.66
Sty-80DVB	85.39	7.37	0.92	84.22	7.78	0.85

4.5.2 Deprotection of *tert*-butyl groups

The next step after successful synthesis of the *tert*-butyl carboxylate-containing crosslinked polymer precursors was to deprotect the *tert*-butyl groups. We hypothesized that after deprotection, the space that was occupied by the bulky *tert*-butyl groups became void space, and the pore volume and surface area of the polymer would increase.

The *tert*-butyl group is one of the most commonly used protecting groups for carboxylic acids.[52] The *tert*-butyl carboxylate can be easily hydrolyzed to the corresponding carboxylic acid under acidic condition through an S_N1 mechanism,[53] and the generated *tert*-butyl cation is then transformed to one molecule of isobutylene and a proton. Both protic acids[52] such as TFA and HCl, and Lewis acids such as $ZnBr_2$[54] and $CeCl_3 \cdot 7H_2O$-NaI[55] can promote the deprotection. The cleavage of the *tert*-butyl group can also be achieved by thermolysis at ca. 220 ˚C.[56]

In our previous work, the alternating copolymers containing *tert*-butyl carboxylates were

deprotected by reacting with TFA in DCM to form the alternating polyanions.[39] In this study, in addition to the protic acid-promoted hydrolysis by TFA, we also examined the deprotection of the *tert*-butyl carboxylates under Lewis acid-promoted hydrolysis and thermolysis.

The 60 mol% DVB crosslinked polymer precursor STB-60DVB, which has a BET surface area of 44 m^2/g, was used for the deprotection. The protic acid-promoted hydrolysis was conducted by mixing STB-60DVB beads with excess TFA in dichloromethane (DCM). FT-IR was used to confirm the deprotection of *tert*-butyl groups (Figure 4-S3), and the O-H stretch of COOH was observed at 3300 cm^{-1} for the deprotected polymer STB-60DVB-d (TFA). The BET surface area of STB-60DVB-d (TFA) increased over 12-fold to 559 m^2/g. STB-60DVB beads were also treated with the suspension of $ZnBr_2$ in DCM. A 11-fold increase of BET surface area to 513 m^2/g. Since both TFA and $ZnBr_2$ deprotection were carried out in DCM, STB-60DVB was swollen in DCM without any acid catalysts as a control experiment. After drying in vacuum oven, the BET surface area of STB-60DVB slightly decreased (Control (DCM) in Figure 4-3), which confirms that the increase of the porosity was not from the swelling of the polymer precursor in DCM. The slightly decreased BET surface area may be caused from the chain relaxing for more efficient packing or chain collapse during drying.

The thermolysis of STB-60DVB was carried out at 220 ˚C under vacuum for 30 minutes. The BET surface area of the deprotected polymer STB-60DVB-d (thermal) only showed a 2-fold increase to 85 m^2/g. The thermolysis temperature is higher than the previously reported T_gs of poly(styrene-alt-*N*-phenylmaleimide)[57] and the divinylbenzene lightly crosslinked poly(4-methylstilbene-3-methyl maleimide-4-vinylbenzyl chloride)[44]. It is highly likely that during thermolysis, with the cleavage of the *tert*-butyl groups, some of the newly generated nanopores collapsed due to the chain motion.[58]

The TGA curves were shown in Figure 4-2, the weight loss at 220 ˚C corresponds to the loss of *tert*-butyl groups. All three deprotection methods exhibited less than 16% of residual *tert*-butyl groups, conforming effective deprotections. The residual *tert*-butyl groups were possibly buried inside the particle and not physically accessible by the acid catalysts,[30] and in thermal deprotection it sometimes requires higher temperature (ca. 290 ˚C) to completely remove all *tert*-butyl groups.[59] The pore sizes distributions of all samples were in the range of 1.1-1.3 nm (Figure 4-S4). Figure 4-3 summarizes the BET surface areas of STB-60DVB and STB-60DVB-d samples. TFA deprotection gives the highest BET surface area, therefore it is used in our following studies.

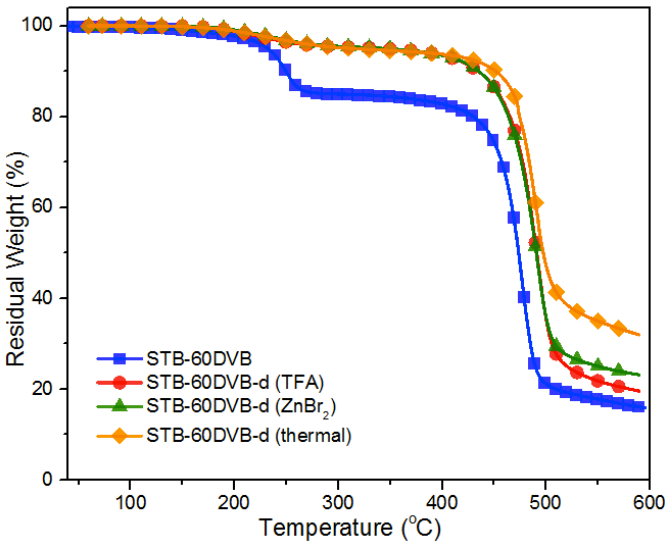

Figure 4-2. The TGA curves of STB-60DVB (blue square) and its corresponding deprotected samples using TFA (red circle), zinc bromide (green triangle), and thermal deprotection (orange diamond).

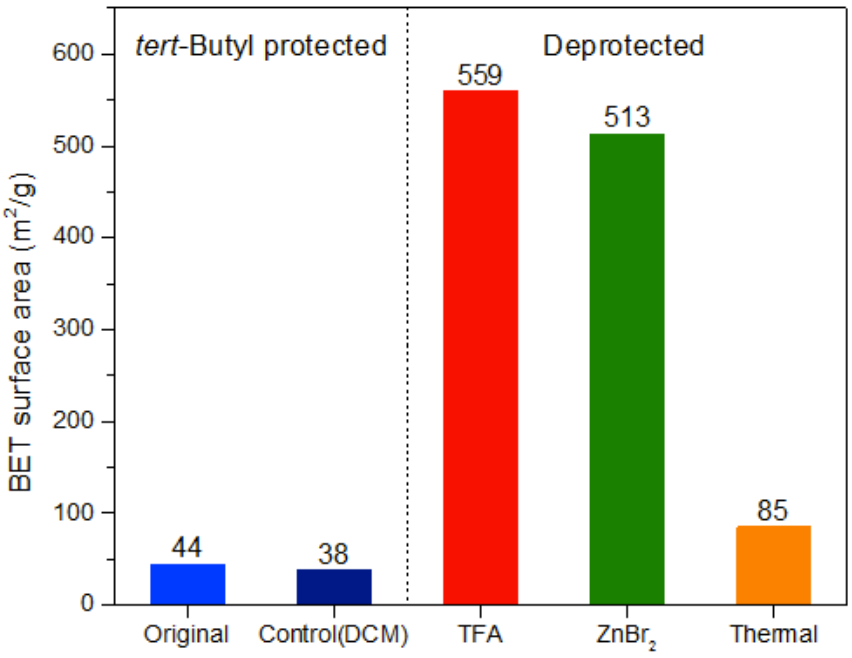

Figure 4-3. BET surface areas of STB-60DVB (before dashed line) and deprotected STB-60DVB-d samples (after dashed line) using different methods.

4.5.3 Porosity and BET surface area

Nitrogen adsorption/desorption isotherms of the polymer precursors and the deprotected polymers are shown in Figure 4-4. The precursors and deprotected polymers exhibited Type I isotherms with high gas uptake at low pressures according to the International Union of Pure and Applied Chemistry (IUPAC) classification, which indicates that these polymers possess micropores (pore width < 2 nm).[60] The pore size distributions are in the range of 1.1-1.3 nm, which further confirm the microporosity of these materials. Figure 4-5 shows the BET surface areas of the polymer precursors and deprotected polymers. The detailed BET surface areas, pore volumes and pore sizes of the polymer precursors and deprotected polymers are listed in Table 4-S2.

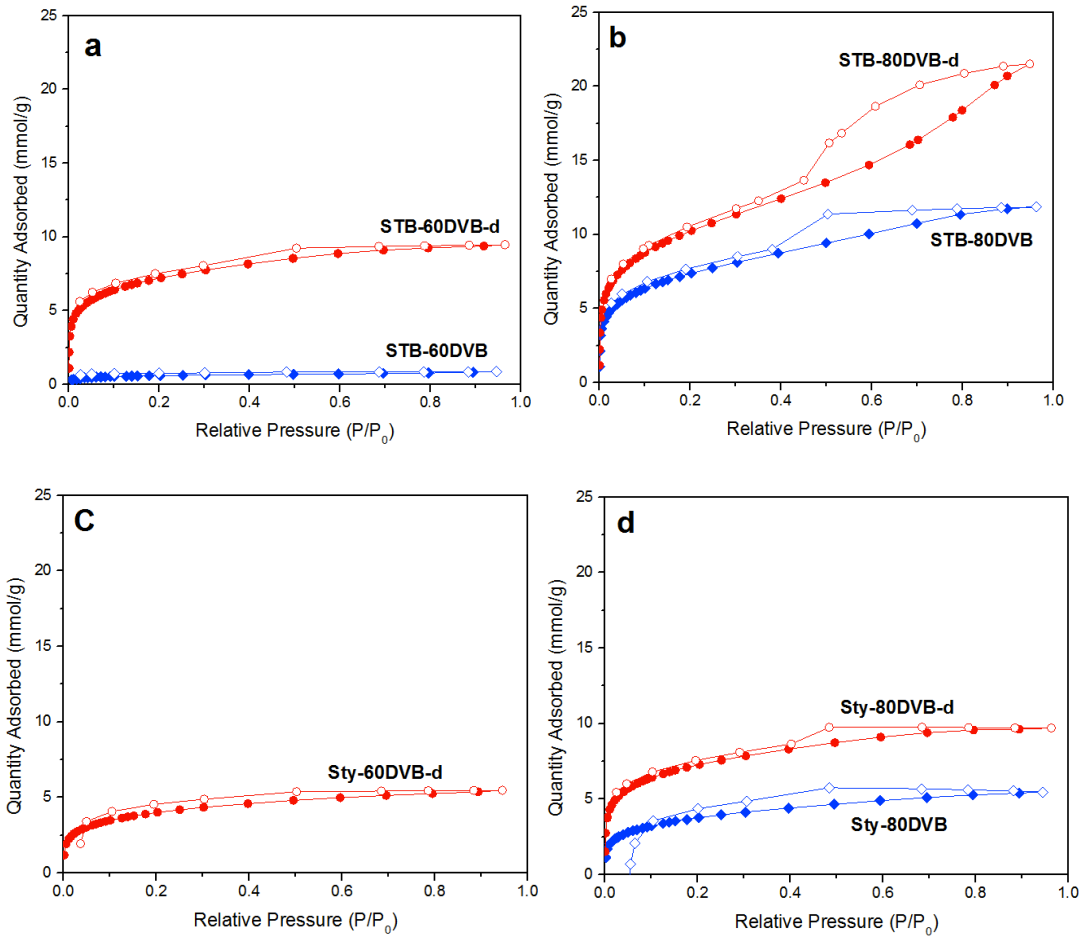

Figure 4-4. Nitrogen adsorption (closed symbol)/desorption (open symbol) isotherms of a) DSTBC-60DVB and DSTBC-60DVB-d, b) DSTBC-80DVB and DSTBC-80DVB-d, c) Sty-60DVB-d, d) Sty-80DVB and Sty-80DVB-d at 77 K.

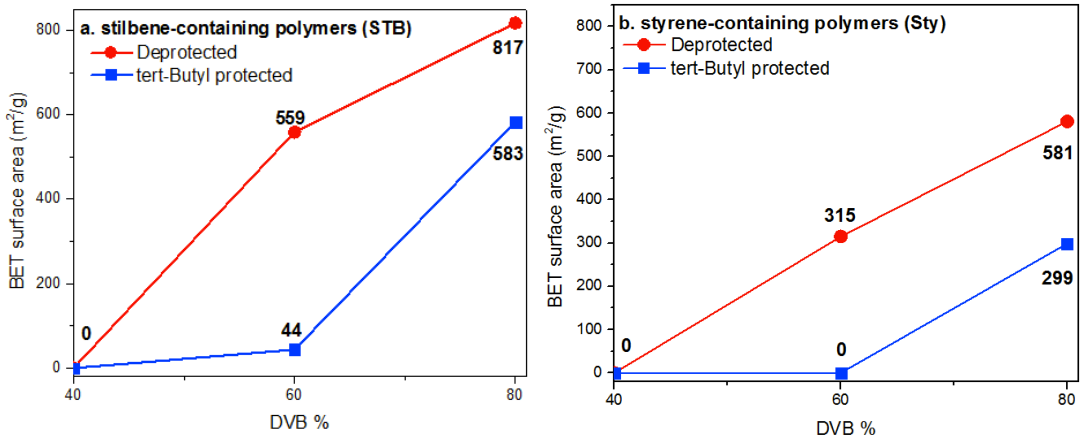

Figure 4- 5. BET surface areas of a) STB-DVB and STB-DVB-d series and b) Sty-DVB and Sty-DVB-d series versus DVB contents, the protected samples are shown in blue square and TFA deprotected samples are shown in red circles

The stilbene-containing polymer precursors STB-40DVB, STB-60DVB and STB-80DVB were synthesized using an increasing amount of DVB. As expected, at low DVB content (40% in feed), no porosity was observed for polymer precursor STB-40DVB and the deprotected polymer STB-40DVB-d. This is probably because the crosslinking density is too low to maintain the porous structures. Similar total loss of porosity was also observed in our previous work,[44] when more than 60 mol% of substituted stilbene and maleimide comonomers were incorporated into the hypercrosslinked polymers. When the DVB content increased to 60%, the crosslinked precursor STB-60DVB exhibited small surface areas of 44 m^2/g. As previously discussed, after TFA deprotection, the BET surface area was a notable 559 m^2/g. Due to the high crosslinking density, STB-80DVB exhibited a BET surface area of 583 m^2/g; and after deprotection, the BET surface area of the polymer STB-80DVB-d increased to 817 m^2/g.

The similar trend in the BET surface areas was also observed in the styrene-containing crosslinked polymers, but with systematically lower values. Previously, we found that the more rigid DTBSC-TBMI is better for preventing pore collapse and therefore exhibited higher surface area.[38] In addition, DTBSC possesses twice the concentration of *tert*-butyl group than TBVB, thus during deprotection, there was more pore volume generated in the stilbene-containing polymers. Therefore a systematically lower surface area of the styrene-containing polymers compared to stilbene-containing polymers was observed.

These results suggested that to achieve high surface areas in these crosslinked polymers, it is important to have a rigid polymer network. Previously, Fréchet, Svec and coworkers also found that the rigidity of the polymer backbone is crucial for maintaining high surface area since decreasing the flexibility in a hypercrosslinked polymer could hinder the collapse of pore structures.[61] In our polymers, the rigidity comes from both the T_g enhancing comonomers and high

crosslinking density. Therefore the surface area increased as the increase of DVB contents, and the stilbene-containing polymers exhibited higher surface area than the styrene-containing polymers.

4.5.4 CO_2 adsorption

Recently, the CO_2 capture properties of a number of nanoporous organic polymers were investigated.[18-21] Previous calculation and experimental results have shown that the CO_2 uptakes in nanoporous materials depend not only on the specific surface area or pore volume, but also on functional groups, pore sizes, and other variability at the molecular level.[18, 62-66]

We investigated the CO_2 sorbent characteristics of our polymers by measuring the CO_2 uptakes up to 0.95 bar at 273 K (Figure 4-6a) and 298 K (Figure 4-6b). The CO_2 uptakes of polymers at 0.95 bar are compared to their BET surface areas in Table 4-2. STB-60DVB-d showed the highest CO_2 uptake at both 273 K and 298 K, absorbing 1.29 mmol/g and 1.05 mmol/g at 0.95 bar, respectively. These CO_2 uptakes values are comparable to some organic polymer networks with similar surface areas, such as the CMP series reported by the Cooper group.[18] Although the BET surface area of STB-80DVB is higher than STB-60DVB-d, it absorbed less CO_2 at 0.95 bar at both temperatures. The similar effect was observed for the styrene-containing polymers Sty-60DVB-d and Sty-80DVB. The computational studies of a series of MIL-53 based MOF showed that polar groups would benefit the CO_2 sorption while bulky nonpolar groups would hinder the CO_2 sorption.[62] This prediction was further validated in the CMP networks, in which COOH showed enhancement in the adsorption to CO_2 compared to other functional groups.[18] Therefore STB-60DVB-d and Sty-60DVB-d with polar carboxylate acid groups exhibited higher CO_2 uptakes than STB-80DVB and Sty-80DVB with bulky nonpolar *tert*-butyl groups.

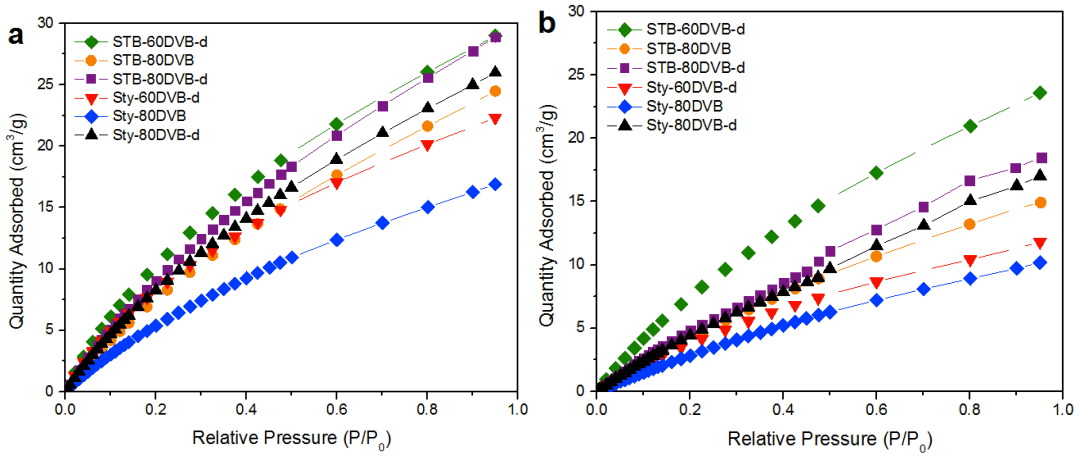

Figure 4-6. CO_2 adsorption isotherms at a) 273 K, and b) 298 K up to 0.95 bar

Table 4-2. CO_2 uptakes of the polymers

Sample	BET surface area (m^2/g)	CO_2 uptake at 273 K, 0.95 bar (mmol/g)	CO_2 uptake at 298 K, 0.95 bar (mmol/g)
STB-60DVB-d	559	1.29	1.03
STB-80DVB	583	1.09	0.67
STB-80DVB-d	817	1.29	0.83
Sty-60DVB-d	315	1.00	0.54
Sty-80DVB	299	0.76	0.46
Sty-80DVB-d	581	1.16	0.76

4.6 Conclusions

A series carboxylate acid-functionalized nanoporous polymers were synthesized *via* a two-step procedure. The *tert*-butyl carboxylate-containing crosslinked polymer precursors synthesized by suspension polymerization were then deprotected to generate the nanoporous polymers. Protic acid-, Lewis acid- and thermal deprotections were conducted on the polymer precursors, and the protic acid-promoted deprotection by TFA was chosen as the most efficient method to generate nanopores. The BET surface area of deprotected polymers increased as the increase of DVB content, and the stilbene-containing polymers showed systematically higher BET surface area than the styrene-containing polymers due to the actual DVB content and the stiffness of the alternating sequences. This work provides a novel deprotection strategy to functionalized, easily synthesized,

nanoporous polymers with tunable porosity, and merits additional studies. The resulting nanoporous polymers hold potential as solid CO_2 sorbents. We continue to investigate other functional group-containing nanoporous polymers, e.g. amine and phosphine, as well as the effect of environmental factors such as humidity on the gas sorption properties of these polymers.

4.7 Acknowledgements

This work was supported by the National Science Foundation (NSF) under grant number DMR-0905231, DMR-1206409, and DMR-1310258, and the Department of Chemistry at Virginia Tech. The BET surface area and CO_2 capture measurements were performed at the Molecular Foundry, Lawrence Berkeley National Laboratory. This work as well as Prof. F. Svec were supported by the Office of Science, Office of Basic Energy Sciences, Scientific User Facilities Division of the U.S. Department of Energy, under Contract No. DE-AC02-05CH11231. We thank Prof. Timothy Long's group for TGA instrument, and Steve McCartney for assistance with SEM.

4.8 References

1. Hughes, L., Biological consequences of global warming: is the signal already apparent? *Trends Ecol. Evol.* **2000,** *15* (2), 56-61.
2. Joos, F.; Plattner, G.-K.; Stocker, T. F.; Marchal, O.; Schmittner, A., Global warming and marine carbon cycle feedbacks on future atmospheric CO_2. *Science* **1999,** *284* (5413), 464-467.
3. Orr Jr, F. M., CO_2 capture and storage: are we ready? *Energy Environ. Sci.* **2009,** *2* (5), 449-458.
4. Metz, B.; Davidson, O.; de Coninck, H.; Loos, M.; Meyer, L. *IPCC special report on carbon dioxide capture and storage*; Intergovernmental Panel on Climate Change, Geneva

(Switzerland). Working Group III: 2005.

5. DOE/NETL *DOE/NETL Carbon Dioxide Capture and Storage RD&D Roadmap*; 2010.
6. Yu, C.-H.; Huang, C.-H.; Tan, C.-S., A review of CO_2 capture by absorption and adsorption. *Aerosol Air Qual. Res.* **2012,** *12* (5), 745-769.
7. MacDowell, N.; Florin, N.; Buchard, A.; Hallett, J.; Galindo, A.; Jackson, G.; Adjiman, C. S.; Williams, C. K.; Shah, N.; Fennell, P., An overview of CO_2 capture technologies. *Energy Environ. Sci.* **2010,** *3* (11), 1645-1669.
8. *Improvements in power generation with post-combustion capture of CO_2*; International Energy Agency: Cheltenham, UK, 2004.
9. D'Alessandro, D. M.; Smit, B.; Long, J. R., Carbon dioxide capture: prospects for new materials. *Angew. Chem., Int. Ed.* **2010,** *49* (35), 6058-6082.
10. Du, X.; Sun, Y.; Tan, B.; Teng, Q.; Yao, X.; Su, C.; Wang, W., Troger's base-functionalised organic nanoporous polymer for heterogeneous catalysis. *Chem. Commun.* **2010,** *46* (6), 970-972.
11. Chen, L.; Yang, Y.; Jiang, D., CMPs as scaffolds for constructing porous catalytic frameworks: A built-in heterogeneous catalyst with high activity and selectivity based on nanoporous metalloporphyrin polymers. *J. Am. Chem. Soc.* **2010,** *132* (26), 9138-9143.
12. Xie, Z.; Wang, C.; deKrafft, K. E.; Lin, W., Highly stable and porous cross-linked polymers for efficient photocatalysis. *J. Am. Chem. Soc.* **2011,** *133* (7), 2056-2059.
13. Tsyurupa, M.; Davankov, V., Porous structure of hypercrosslinked polystyrene: state-of-the-art mini-review. *React. Funct. Polym.* **2006,** *66* (7), 768-779.
14. Zhao, H.; Jin, Z.; Su, H.; Jing, X.; Sun, F.; Zhu, G., Targeted synthesis of a 2D ordered porous organic framework for drug release. *Chem. Commun.* **2011,** *47* (22), 6389-6391.

15. Budd, P. M.; McKeown, N. B., Highly permeable polymers for gas separation membranes. *Polym. Chem.* **2010,** *1* (1), 63-68.

16. Dawson, R.; Cooper, A. I.; Adams, D. J., Nanoporous organic polymer networks. *Prog. Polym. Sci.* **2012,** *37* (4), 530-563.

17. Germain, J.; Fréchet, J. M.; Svec, F., Nanoporous polymers for hydrogen storage. *Small* **2009,** *5* (10), 1098-1111.

18. Dawson, R.; Adams, D. J.; Cooper, A. I., Chemical tuning of CO_2 sorption in robust nanoporous organic polymers. *Chem. Sci.* **2011,** *2* (6), 1173-1177.

19. Furukawa, H.; Yaghi, O. M., Storage of hydrogen, methane, and carbon dioxide in highly porous covalent organic frameworks for clean energy applications. *J. Am. Chem. Soc.* **2009,** *131* (25), 8875-8883.

20. Dawson, R.; Stockel, E.; Holst, J. R.; Adams, D. J.; Cooper, A. I., Microporous organic polymers for carbon dioxide capture. *Energy Environ. Sci.* **2011,** *4* (10), 4239-4245.

21. Lu, W.; Verdegaal, W. M.; Yu, J.; Balbuena, P. B.; Jeong, H.-K.; Zhou, H.-C., Building multiple adsorption sites in porous polymer networks for carbon capture applications. *Energy Environ. Sci.* **2013,** *6* (12), 3559-3564.

22. Stauffer, P. H.; Keating, G. N.; Middleton, R. S.; Viswanathan, H. S.; Berchtold, K. A.; Singh, R. P.; Pawar, R. J.; Mancino, A., Greening coal: breakthroughs and challenges in carbon capture and storage. *Environ. Sci. Technol.* **2011,** *45* (20), 8597-8604.

23. Côté, A. P.; Benin, A. I.; Ockwig, N. W.; O'Keeffe, M.; Matzger, A. J.; Yaghi, O. M., Porous, crystalline, covalent organic frameworks. *Science* **2005,** *310* (5751), 1166-1170.

24. Feng, X.; Ding, X.; Jiang, D., Covalent organic frameworks. *Chem. Soc. Rev.* **2012,** *41* (18), 6010-6022.

25. Dawson, R.; Laybourn, A.; Clowes, R.; Khimyak, Y. Z.; Adams, D. J.; Cooper, A. I., Functionalized conjugated microporous polymers. *Macromolecules* **2009,** *42* (22), 8809-8816.

26. Jiang, J.-X.; Su, F.; Trewin, A.; Wood, C. D.; Campbell, N. L.; Niu, H.; Dickinson, C.; Ganin, A. Y.; Rosseinsky, M. J.; Khimyak, Y. Z.; Cooper, A. I., Conjugated microporous poly(aryleneethynylene) networks. *Angew. Chem.* **2007,** *119* (45), 8728-8732.

27. Ben, T.; Ren, H.; Ma, S.; Cao, D.; Lan, J.; Jing, X.; Wang, W.; Xu, J.; Deng, F.; Simmons, J. M., Targeted synthesis of a porous aromatic framework with high stability and exceptionally high surface area. *Angew. Chem.* **2009,** *121* (50), 9621-9624.

28. Davankov, V.; Tsyurupa, M. P., *Hypercrosslinked polymeric networks and adsorbing materials: synthesis, properties, structure, and applications*. Elsevier: 2010; Vol. 56.

29. Seo, M.; Murphy, C. J.; Hillmyer, M. A., One-step synthesis of cross-linked block polymer precursor to a nanoporous thermoset. *ACS Macro Lett.* **2013,** *2* (7), 617-620.

30. Hillmyer, M., Nanoporous Materials from Block Copolymer Precursors. In *Block Copolymers II*, Abetz, V., Ed. Springer Berlin Heidelberg: 2005; Vol. 190, pp 137-181.

31. Thurn-Albrecht, T.; Schotter, J.; Kästle, G. A.; Emley, N.; Shibauchi, T.; Krusin-Elbaum, L.; Guarini, K.; Black, C. T.; Tuominen, M. T.; Russell, T. P., Ultrahigh-density nanowire arrays grown in self-assembled diblock copolymer templates. *Science* **2000,** *290* (5499), 2126-2129.

32. Hou, S.; Harrell, C. C.; Trofin, L.; Kohli, P.; Martin, C. R., Layer-by-layer nanotube template synthesis. *J. Am. Chem. Soc.* **2004,** *126* (18), 5674-5675.

33. Yang, S. Y.; Ryu, I.; Kim, H. Y.; Kim, J. K.; Jang, S. K.; Russell, T. P., Nanoporous membranes with ultrahigh selectivity and flux for the filtration of viruses. *Adv. Mater.* **2006,** *18* (6), 709-712.

34. Mao, M.; Turner, S. R., Synthesis and characterization of highly functionalized polymers based on *N, N, N′, N′*-tetraalkyl-4, 4′-diaminostilbene and maleic anhydride. *Polymer* **2006,** *47* (24), 8101-8105.

35. Mao, M.; Turner, S. R., Aggregation of rod−coil block copolymers containing rigid polyampholyte blocks in aqueous solution. *J. Am. Chem. Soc.* **2007,** *129* (13), 3832-3833.

36. Mao, M.; Kim, C.; Wi, S.; Turner, S. R., Chain structure of substituted stilbene-maleic anhydride alternating copolymer probed by solid-state NMR. *Macromolecules* **2008,** *41* (2), 387-389.

37. Li, Y.; Mao, M.; Matolyak, L. E.; Turner, S. R., Sterically crowded anionic polyelectrolytes with tunable charge densities based on stilbene-containing copolymers. *ACS Macro Lett.* **2012,** *1* (2), 257-260.

38. Li, Y.; Zhang, M.; Mao, M.; Turner, S. R.; Moore, R. B.; Mourey, T. H.; Slater, L. A.; Hauenstein, J. R., Chain stiffness of stilbene containing alternating copolymers by SAXS and SEC. *Macromolecules* **2012,** *45* (3), 1595-1601.

39. Li, Y.; Savage, A. M.; Zhou, X.; Turner, S. R.; Davis, R. M., Solution properties of stilbene-containing sterically crowded alternating polyanions. *J. Polym. Sci., Part B: Polym. Phys.* **2013,** *51* (21), 1565-1570.

40. Zhou, X.; Li, Y.; Hart, K. E.; Abbott, L. J.; Lin, Z.; Svec, F.; Colina, C. M.; Turner, S. R., Nanoporous structure of semirigid alternating copolymers via nitrogen sorption and molecular simulation. *Macromolecules* **2013,** *46* (15), 5968-5973.

41. Savage, A. M.; Li, Y.; Matolyak, L. E.; Doncel, G. F.; Turner, S. R.; Gandour, R. D., Anti-HIV activities of precisely defined, semirigid, carboxylated alternating copolymers. *J. Med. Chem.* **2014,** *57* (15), 6354-6363.

42. Savage, A.; Zhou, X.; Huang, J.; Turner, S. R., A review of semi-rigid, stilbene-containing alternating copolymers. *Appl. Petrochem. Res.* **2015,** *5* (1), 27-33.

43. Savage, A. M.; Ullrich, E.; Chin, S. M.; Kiernan, Z.; Kost, C.; Turner, S. R., Synthesis and characterization of double hydrophilic block copolymers containing semi-rigid and flexible segments. *J. Polym. Sci., Part A: Polym. Chem.* **2015,** *53* (2), 219-227.

44. Zhou, X.; Huang, J.; Barr, K. W.; Lin, Z.; Maya, F.; Abbott, L. J.; Colina, C. M.; Svec, F.; Turner, S. R., Nanoporous hypercrosslinked polymers containing T_g enhancing comonomers. *Polymer* **2015,** *59* (0), 42-48.

45. Gupta, A. S.; Deshpande, R. K.; Liu, L.; Waterhouse, G. I. N.; Telfer, S. G., Porosity in metal-organic frameworks following thermolytic postsynthetic deprotection: gas sorption, dye uptake and covalent derivatisation. *CrystEngComm* **2012,** *14* (18), 5701-5704.

46. Brunauer, S.; Emmett, P. H.; Teller, E., Adsorption of gases in multimolecular layers. *J. Am. Chem. Soc.* **1938,** *60* (2), 309-319.

47. Jagiello, J., Stable numerical solution of the adsorption integral equation using splines. *Langmuir* **1994,** *10* (8), 2778-2785.

48. Jagiello, J.; Olivier, J. P., 2D-NLDFT adsorption models for carbon slit-shaped pores with surface energetical heterogeneity and geometrical corrugation. *Carbon* **2013,** *55*, 70-80.

49. Jagiello, J.; Ania, C.; Parra, J. B.; Cook, C., Dual gas analysis of microporous carbons using 2D-NLDFT heterogeneous surface model and combined adsorption data of N_2 and CO_2. *Carbon* **2015,** *91*, 330-337.

50. Germain, J.; Hradil, J.; Fréchet, J. M. J.; Svec, F., High surface area nanoporous polymers for reversible hydrogen storage. *Chem. Mater.* **2006,** *18* (18), 4430-4435.

51. Badyal, J. P.; Cameron, A. M.; Cameron, N. R.; Oates, L. J.; Øye, G.; Steel, P. G.; Davis, B.

G.; Coe, D. M.; Cox, R. A., Comparison of the effect of pore architecture and bead size on the extent of plasmachemical amine functionalisation of poly(styrene-*co*-divinylbenzene) permanently porous resins. *Polymer* **2004,** *45* (7), 2185-2192.

52. Wuts, P. G. M.; Greene, T. W., *Greene's protective groups in organic synthesis*. Wiley-Interscience: Hoboken, N.J, 2007.

53. Clayden, J.; Greeves, N.; Warren, S., Organic Chemistry. 2 ed.; Oxford University Press: Oxford, 2012.

54. Wu, Y.-q.; Limburg, D. C.; Wilkinson, D. E.; Vaal, M. J.; Hamilton, G. S., A mild deprotection procedure for *tert*-butyl esters and *tert*-butyl ethers using ZnBr2 in methylene chloride. *Tetrahedron Letters* **2000,** *41* (16), 2847-2849.

55. Marcantoni, E.; Massaccesi, M.; Torregiani, E.; Bartoli, G.; Bosco, M.; Sambri, L., Selective deprotection of *N*-boc-protected *tert*-butyl ester amino acids by the $CeCl_3 \cdot 7H_2O$−NaI system in acetonitrile. *J. Org. Chem.* **2001,** *66* (12), 4430-4432.

56. Theato, P.; Klok, H.-A., *Functional polymers by post-polymerization modification: concepts, guidelines, and applications*. Wiley-VCH: Weinheim, 2013.

57. Yang, P.; Ratcliffe, L. P. D.; Armes, S. P., Efficient synthesis of poly(methacrylic acid)-*block*-poly(styrene-*alt*-*N*-phenylmaleimide) diblock copolymer lamellae using RAFT dispersion polymerization. *Macromolecules* **2013,** *46* (21), 8545-8556.

58. Hiemenz, P. C.; Rajagopalan, R., *Principles of colloid and surface chemistry, revised and expanded*. CRC press: 1997; Vol. 14.

59. Dugas, V.; Chevalier, Y., Chemical reactions in dense monolayers: In situ thermal cleavage of grafted esters for preparation of solid surfaces functionalized with carboxylic acids. *Langmuir* **2011,** *27* (23), 14188-14200.

60. Sing, K. S. W., Reporting physisorption data for gas/solid systems with special reference to the determination of surface area and porosity (Recommendations 1984). *Pure Appl. Chem.* **1985,** *57* (4).

61. Germain, J.; Frechet, J. M. J.; Svec, F., Hypercrosslinked polyanilines with nanoporous structure and high surface area: potential adsorbents for hydrogen storage. *J. Mater. Chem.* **2007,** *17* (47), 4989-4997.

62. Torrisi, A.; Bell, R. G.; Mellot-Draznieks, C., Functionalized MOFs for enhanced CO_2 capture. *Cryst. Growth Des.* **2010,** *10* (7), 2839-2841.

63. Furmaniak, S.; Kowalczyk, P.; Terzyk, A. P.; Gauden, P. A.; Harris, P. J. F., Synergetic effect of carbon nanopore size and surface oxidation on CO_2 capture from CO_2/CH_4 mixtures. *J. Colloid Interface Sci.* **2013,** *397* (0), 144-153.

64. Yao, S.; Yang, X.; Yu, M.; Zhang, Y.; Jiang, J.-X., High surface area hypercrosslinked microporous organic polymer networks based on tetraphenylethylene for CO_2 capture. *J. Mater. Chem. A* **2014,** *2* (21), 8054-8059.

65. Kowalczyk, P.; Furmaniak, S.; Gauden, P. A.; Terzyk, A. P., Carbon dioxide adsorption-induced deformation of microporous carbons. *J. Phys. Chem. C* **2010,** *114* (11), 5126-5133.

66. Palmer, J. C.; Moore, J. D.; Roussel, T. J.; Brennan, J. K.; Gubbins, K. E., Adsorptive behavior of CO_2, CH_4 and their mixtures in carbon nanospace: a molecular simulation study. *Phys. Chem. Chem. Phys.* **2011,** *13* (9), 3985-3996.

4.9 Supporting information for chapter 4

4.9.1 Materials

Potassium *tert*-butoxide (^{t}BuOK, Sigma-Aldrich, ≥98%), *tert*-butanol (HO^{tBu}, Sigma-Aldrich, anhydrous, ≥99.5%), *N*-bromosuccinimide (NBS, Aldrich, 99%), *p*-toluic acid (Aldrich, 98%), formaldehyde (Aldrich, 37 wt. % in H_2O), triphenylphosphine (Alfa Aesar, 99%), thionyl chloride (Alfa Aesar, ≥99.0%), acetic anhydride (Sigma-Aldrich, ≥98.0%), sodium acetate (Sigma-Aldrich, ≥99.0%), 4-aminobenzoic acid (Sigma-Aldrich, ≥99.0%), divinylbenzene (Sigma-Aldrich, technical grade, isomer of *p*- and *m*-, 80%), trifluoroacetic acid (TFA, Oakwood Chemical, 99%), poly(vinyl alcohol) (Aldrich, 87-89% hydrolyzed), sodium chloride (Fisher, certified ACS crystalline) were used as received without purification. Maleic anhydride (Aldrich, ≥99.0%) was recrystallized from toluene, 2, 2'-azobisisobutyronitrile (AIBN, Aldrich, 98%) was recrystallized from methanol. (E)-Dimethyl-4,4'- stilbenedicarboxylate (DMSC) was received as a donation from Eastman Chemical Company. Tetrahydrofuran (Fisher, HPLC grade), hexanes (Fisher, HPLC grade), methylene chloride (CH_2Cl_2, Fisher, HPLC grade), diethyl ether (Fisher, HPLC grade), toluene (Fisher, HPLC grade), benzene (Sigma Aldrich, anhydrous, ≥99.8%), and acetone (Fisher, HPLC grade) were used without further purification. Water was deionized before use.

4.9.2 Monomer synthesis[1]

(E)-di-*tert*-butyl 4,4'-stilbenedicarboxylate (DTBSC). (E)-di-*tert*-butyl 4,4'-stilbenedicarboxylate was synthesized via transesterification of (E)-dimethyl-4,4'-stilbenedicarboxylate and potassium *tert*-butoxide (Scheme 4-S1). A suspension of (E)-dimethyl-4,4'-stilbenedicarboxylate (5.92 g, 20 mmol) in toluene (100 mL) was refluxed at 110 ˚C for 15 min, then the solid potassium *tert*-butoxide (6.73 g, 60 mmol) was added portionwise for 30 min.

The reaction mixture was slowly cooled down to room temperature and stirred overnight. The reaction mixture was then poured into saturated NH_4Cl aqueous solution (50 mL), and the aqueous layer was extracted with toluene. The organic layer was combined and dried over Na_2SO_4. The crude product was obtained by rotary evaporation of toluene and further purified by column chromatography (hexanes/ethyl acetate 98:2 v/v). The white crystalline solid was obtained with a yield of 82%. ^{1}H NMR ($CDCl_3$, 400MHz) δ ppm: 7.99 (d, *J*=8.6 Hz, 4H), 7.56 (d, *J*=8.6 Hz, 4H), 7.21 (s, 2H), 1.61 (s, 18H). ^{13}C NMR (CDCl3, 400MHz) δ ppm: 165.6, 140.9, 131.4, 130.0, 129.9, 126.5, 81.2, 28.3. Melting point: 168.6-169.1 ˚C (Lit.:170 ˚C)[37].

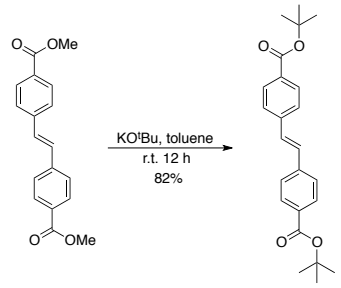

Scheme 4-S1. Synthesis of (E)-di-*tert*-butyl 4,4'-stilbenedicarboxylate

***tert*-Butyl 4-maleimidobenzoate (TBMI).** *tert*-Butyl 4-maleimidobenzoate was synthesized by a multistep procedure (Scheme 4-S2). The mixture of 4-aminobenzoic acid (10.0 g, 73 mmol) and thionyl chloride (43.4 g, 365 mmol) was stirred at 80 ˚C for 4 h. Excess thionyl chloride was passed through a NaOH solution and removed by vacuum. The resulting 4-sulfinylaminobenzoyl chloride A was further purified by azotropic distill with dichloromethane twice (yield: 99%). To the solution of A (4.4 g, 22 mmol) in 30 mL dichloromethane, the solution of HO^{tBu} (6.58 g, 66 mmol) in 10 mL dichloromethane was added dropwise at 0 ˚C. The resulting mixture was stirred for 12 h before the dichloromethane was removed by vacuum. The yellow solid was suspended in ethyl acetate and filter. Then the solid was suspended in sat. $NaHCO_3$ solution (60 mL) and the resulting mixture was extracted by dichloromethane. The crude product

B is achieved after removing solvents in vacuum (yield: 57%). To the solution of B (2.43 g, 12.6 mmol) in 20 mL THF, maleic anhydride was added at room temperature. The resulting mixture was stirred at room temperature for 12 h. Then the precipitate of maleic acid C was filtered and washed with diethyl ether before drying in vacuum for 12 h (yield: 79%). In the solution of C (1.65 g, 5.7 mmol) in acetic anhydride (5.2 g, 51 mmol), sodium acetate (0.23 g, 2.84 mmol) was added. The resulting mixture was stirred at 80 ˚C for 24 h. The solution was neutralized by sat. $NaHCO_3$ solution and extract by dichloromethane. The crude product D was further purified by column chromatography (hexane: ethyl acetate 5:1 v/v) as a light yellow solid (Yield: 80%). ^{1}H NMR ($CDCl_3$, 500 MHz) δ ppm: 8.08 (d, *J*=8.9 Hz, 2H), 7.45 (d, *J*=8.9 Hz, 2H), 6.87 (s, 2H), 1.59 (s, 9H). Elemental Analysis: calculated C, 65.93; H, 5.49; N, 5.13; Found C, 65.88; H, 5.47; N, 5.07. Melting point: 115˚C (Lit.: 114.8-115.4 ˚C)[37].

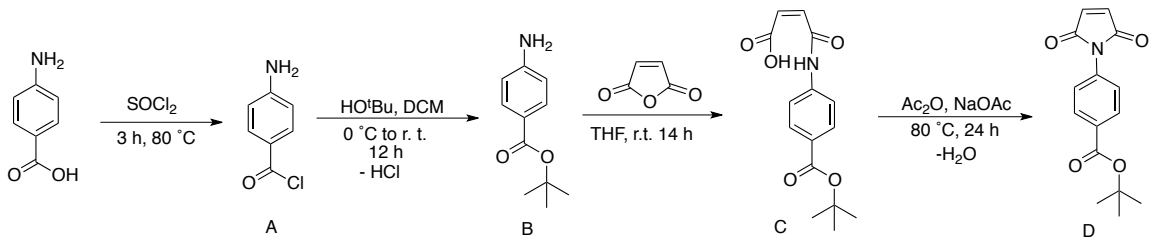

Scheme 4-S2. Synthesis of *tert*-butyl 4-maleimidobenzoate

***tert*-butyl 4-vinyl benzoate (TBVB).** *tert*-butyl 4-vinyl benzoate was synthesized by a previous reported procedure (Scheme 4-S3)[37]. To the refluxing suspension of *p*-toluic acid (20.07g, 147.6 mmol) in 200 mL benzene, *N*-bromosuccinimide (27.60 g, 155.0 mmol) and AIBN (0.48 g, 1 wt%) was added portionwise over 30 min. The reaction mixture was then stirred and refluxed for another 1.5 hour before it was cooled to room temperature. The precipitate was filtered and washed with toluene. The crude product A was recrystallized from methanol (yield: 89%). The mixture of A (8.96 g, 41.67 mmol) and triphenylphosphine (10.92 g, 41.67 mmol) was refluxed in 320 mL acetone for 2 h. The mixture was then cooled to room temperature and filtered, washed

with diethyl ether, and vacuum dried to afford B (yield: 95 %). To the mixture of B (4.77 g, 10 mmol) and formaldehyde (24 mL, 37% solution in water) in 15 mL DI water, the solution of NaOH (3 g, 75 mmol) in 15 mL DI water was added dropwise at room temperature. The mixture was stirred at room temperature for 1 h before filtration. The aqueous filtrate was acidified with 1 N HCl till pH reached 1. The solid C formed was filtered and washed with water, and vacuum dried at 50 ˚C for 24 h (yield: 90%). C (1.0 g, 7.3 mmol) was added protionwise to the flask of well-stirred $SOCl_2$ (4.34 g, 36.5 mmol) at 0 ˚C. The mixture was then warmed to room temperature and stirred for 4 h, and then stirred at 40 ˚C for 1 h. The excess $SOCl_2$ was removed by vacuum. The crude product D was further purified by azotropic distillation with 5 mL dichloromethane twice (yield: 99 %). To a solution of D (2.02 g, 10 mmol) in 15 mL THF, an ice-water bath, HO^{tBu} (7.48 g, 100 mmol) was added slowly. Then KO^{tBu} (1.68 g, 15 mmol) was added portionwise for 15 min. The mixture was stirred at room temperature for 1 h, and at 60 ˚C for 6 h, and 80 ˚C for 1 h. The resulting orange mixture was then cooled to room temperature. 1 M HCl solution was added to quench the reaction, and sat. $NaHCO_3$ solution was added to neutralize excess HCl. The aqueous layer was extracted by diethyl ether, dried by Na_2SO_4. After removing solvents, the crude product E was further purified by column chromatography (pure hexanes) as a colorless liquid (yield: 82 %). ^{1}H NMR ($CDCl_3$, 400 MHz) δ ppm: 7.92 (d, *J*=8.4 Hz, 2H), 7.39 (d, *J*=8.6 Hz, 2H), 6.69 (dd, *J*=17.6 Hz, 1H), 5.80 (d, *J*=17.6, 10.9 Hz, 1H), 5.31 (d, *J*=10.9 Hz, 1H), 1.56 (s, 9H). ^{13}C NMR ($CDCl_3$, 400MHz) δ ppm: 165.6, 141.4, 136.1, 131.2, 129.7, 125.9, 116.1, 80.9, 20.1.

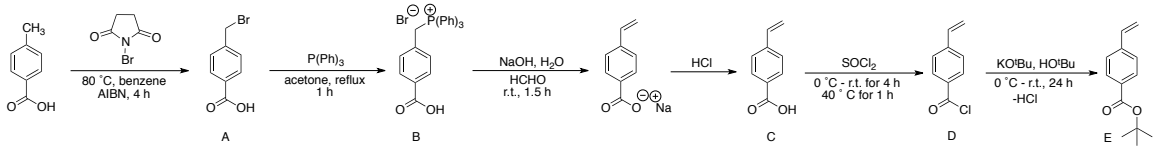

Scheme 4-S3. Synthesis of *tert*-butyl 4-vinyl benzoate

4.9.3 Supplemental figures and tables

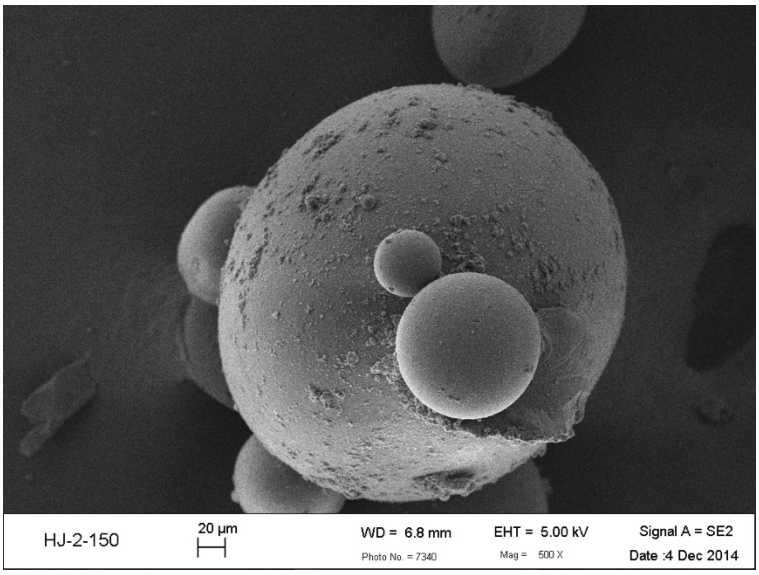

Figure 4-S1. SEM image of STB-60DVB (scale bar: 20 um)

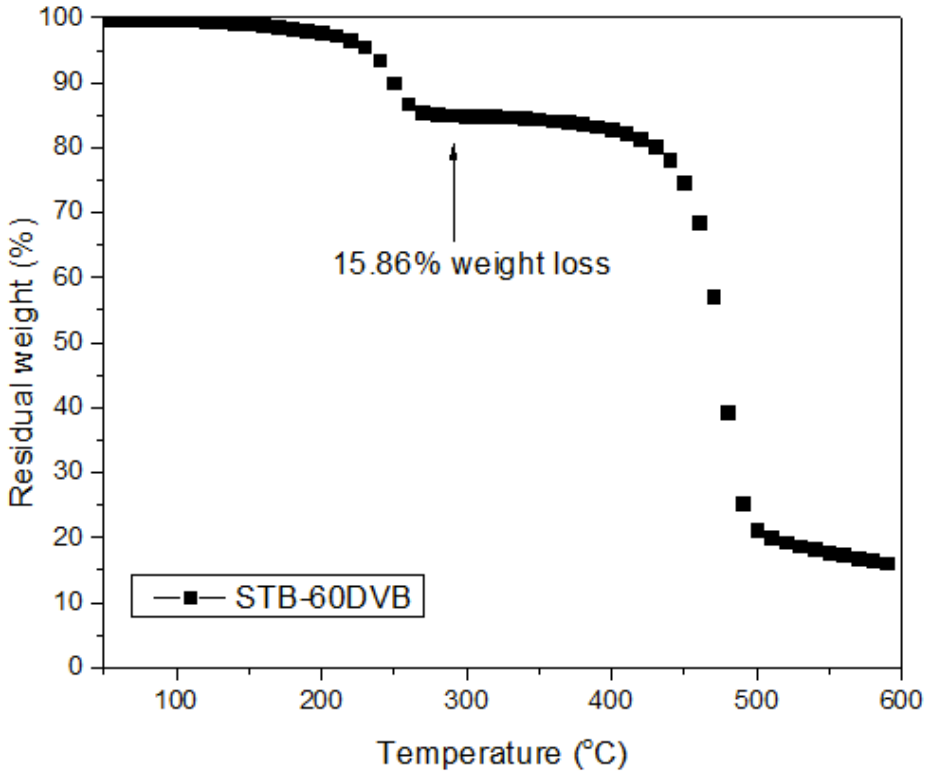

Figure 4-S2. TGA curve of STB-60DVB, weight loss of 15.86% at 220 ˚C is very close to the theoretical weight loss 16.11%.

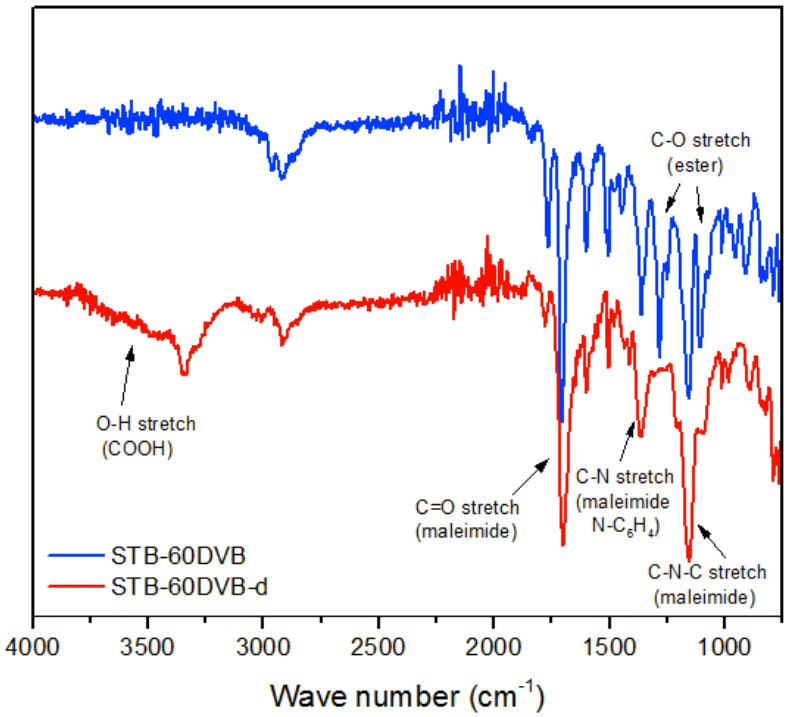

Figure 4-S3. FT-IR spectra of STB-60DVB and STB-60DVB-d

Table 4-S1. BET surface area, pore volumes and pore sizes of STB-60DVB and STB-60DVB-d samples

Polymers	SA_{BET} (m^2/g)	$V_{p,}^{mic}$ (cm^3/g)[a]	$V_{p,}^{tot}$ (cm^3/g)[b]	Pore size (nm)[c]
STB-60DVB	44	0.021	0.030	1.3
STB-60DVB(DCM)	38	0.020	0.027	1.3
STB-60DVB-d (TFA)	559	0.234	0.328	1.1
STB-60DVB-d ($ZnBr_2$)	513	0.217	0.306	1.1
STB-60DVB-d (thermal)	85	0.038	0.042	1.2

[a]Micropore volumes determined from nitrogen adsorption isotherm at $P/P_0 = 0.14$; [b]Total pore volumes determined from nitrogen adsorption isotherm at $P/P_0 = 0.98$; [c]Pore sizes determined from nitrogen adsorption isotherm by 2D-NLDFT.

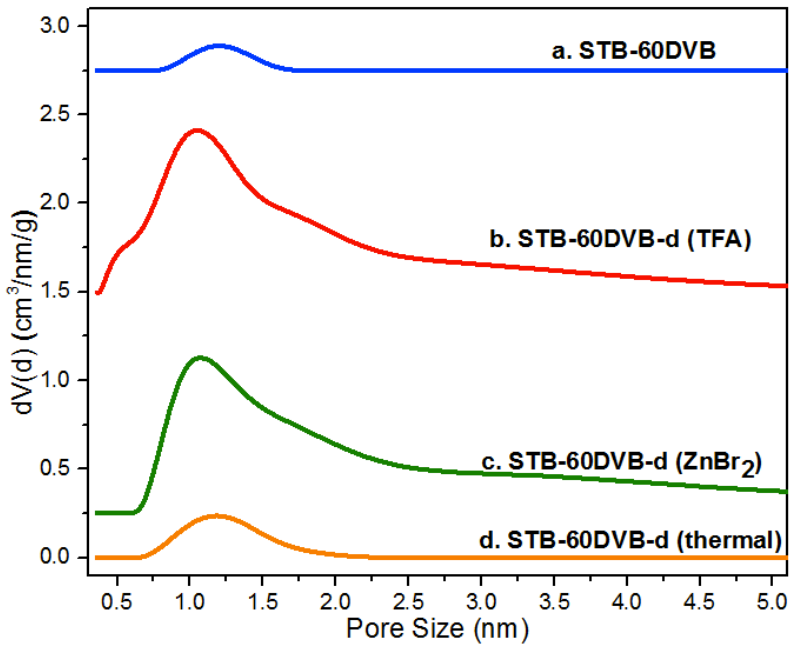

Figure 4-S4. The pore size distributions (PSD) from nitrogen isotherms at 77 K by non-local density functional theory method (NLDFT). The curves for a) STB-60DVB, b) STB-60DVB-d (TFA), c) STB-60DVB-d (ZnBr2), d) STB-60DVB-d (thermal) are shifted vertically by 2.75, 1.50, 0.25, 0.00 cm3 nm g-1, respectively.

Table 4-S2. BET surface area, pore volumes and pore sizes of polymer precursors and deprotected polymers

Sample	SA_{BET} (m^2/g)	$V_{p,}^{micro}$ (cm^3/g)[a]	$V_{p,}^{total}$ (cm^3/g)[b]	Pore size (nm)[c]
STB-DVB40	0	-	-	-
STB-DVB40-d	0	-	-	-
STB-60DVB	44	0.021	0.030	1.3
STB-60DVB-d	559	0.234	0.328	1.1
STB-DVB80	583	0.235	0.411	1.3
STB-DVB80-d	817	0.326	0.745	1.3
Sty-DVB40	0	-	-	-
Sty-DVB40-d	0	-	-	-
Sty-60DVB	0	-	-	-
Sty-60DVB-d	315	0.129	0.190	1.2
Sty-DVB80	299	0.120	0.190	1.3
Sty-DVB80-d	581	0.235	0.336	1.3

[a]Micropore volumes determined from nitrogen adsorption isotherm at $P/P_0 = 0.14$; [b]Total pore volumes determined from nitrogen adsorption isotherm at $P/P_0 = 0.98$; [c]Pore sizes determined from nitrogen adsorption isotherm by NLDFT.

Chapter 5. Highly Functionalized Microgels via Miniemulsion Polymerization for Aqueous Lead and Copper Ion Removal

5.1 Authors

Jing Huang,[†,‡] Xi Geng,[†,‡] Brian M. Tissue,[†] and S. Richard Turner*[,†,‡]

[†]Department of Chemistry, Virginia Tech, Blacksburg, VA 24061, United States

[‡]Macromolecules Innovation Institute, Virginia Tech, Blacksburg, VA 24061, United States

5.2 Abstract

Microgels are gel particles with diameters in the range of 50 nm to 5 μm. They have been investigated for applications such as sensing, drug delivery and adsorption. Compared to macrogels, they showed faster responsive rate to external stimuli such as pH and temperature. Traditional synthetic methods for microgels such as emulsion polymerization and precipitation polymerization usually require liquid or aqueous-soluble monomers; therefore hydrophobic solid monomers are rarely used. In this work, using a miniemulsion polymerization technique, we successfully achieved microgels with 100-200 nm diameters from *tert*-butyl carboxylate-containing hydrophobic solid monomers. The obtained organic microgels were then converted to aqueous hydrogels by removing the *tert*-butyl group using acidic deprotection. The resulting hydrogel particles showed good swelling properties as well as high and reversible lead and copper ion adsorption ability.

5.3 Introduction

Heavy metal contamination in water is a severe environmental and public health problem.[1-4] Heavy metal ions are persistent in the environment, and they tend to accumulate in living organisms.[5-6] Industrial waste water from mining, metal plating, tanning, and manufacturing of fertilizers, batteries, electronics, paper, and pesticides, which are directly or indirectly discharged

into the environment, constitutes the major source of heavy metal pollution in water.[7] Furthermore, lead and copper ions can easily enter drinking water by the corrosion of plumbing materials such as water pipes, plumbing fittings, fixtures, solder, and flux.[8] Exposure to lead and copper ions even at low concentrations can cause various diseases and disorders to humans. Recognizing this problem, in 1991, the U.S. Environmental Protection Agency (EPA) first published the Lead and Copper Rule (LCR) to control the level of lead and copper in drinking water.[9] The rule established an action level of 15 ppb (0.015 mg/L) of lead or 1.3 ppm (1.3 mg/L) of copper. Once the level is exceeded, actions, including water quality parameter monitoring, corrosion control treatment, public education, and lead service line replacement, must be taken. The recent Flint water crisis raised the public awareness of the LCR.[10] The corroded lead pipeline and the resultant polluted toxic water with high levels of lead and copper ions affected over 100,000 households in Flint.[11-12] With these dangers in mind, it is both necessary and urgent to investigate new techniques to remove lead and copper from drinking water.

Adsorption is one of the most studied methods for heavy metal ion removal. Various materials, from biomaterials such as chitosan,[13-15] lignin,[16-17] sawdust,[18-21] nutshells,[22-23] to synthetic materials, such as nanoporous silica,[24-26] carbon nanotubes,[27-30] and chelating resins,[31-33] have been investigated as sorbent for heavy metal ions. Hydrogels are a class of crosslinked hydrophilic polymers. Hydrogels with sulfonic,[34-35] phosphoric,[36-37] and carboxylate groups[38-40] have been used as sorbent to capture heavy metal ions. These groups serve as chelating sites to bind with heavy metal ions. Additionally, these groups can be ionized or deionized based on pH, and the hydrophilicity, along with the swelling property of the hydrogels is changed in response to pH.[40]

Aqueous microgels are a special category of hydrogels; they are hydrogel particles with

diameters in the range of 50 nm to 5 μm.[41] Compared to their analogue macrogels, microgels response faster to external stimuli such as pH and temperature, and their dispersion has lower viscosity.[41] The most common techniques to synthesize microgels are by traditional emulsion polymerization or aqueous precipitation polymerization. However, these techniques all require liquid monomers or monomers that can be soluble in water or minimum amount of organic solvent, which limits the use of solid and less soluble monomers in microgel synthesis. Larger quantities of organic solvent can be used to dissolve monomers in suspension polymerization, but the resulting particle size is in the range of 0.1-10 mm, which is too large for microgels.

Miniemulsion polymerization provides an effective solution. Miniemulsion polymerization takes place in submicron monomer droplets, which are stabilized by surfactants at low concentration (well below critical micelle concentration). A costabilizer, which is a low molecular weight and non-aqueous-soluble compound, is added to prevent Ostwald ripening. Previously, miniemulsion polymerization was employed to polymerize a wide variety of monomers, such as acrylates,[42] methacrylates,[43] styrene,[44] and vinyl acetate.[45] However, to the best of our knowledge, all these monomers are either liquid or have good aqueous solubility. In this research, we report for the first time, the synthesis of microgels using hydrophobic solid monomers by miniemulsion polymerization.

Sterically crowded, functional group-containing, semi-rigid stilbene and *N*-phenylmaleimide alternating copolymers have been investigated in our group.[39, 46-58] The incorporation of these semi-rigid alternating copolymer sequences into crosslinked copolymers can introduce specific functional groups by using different substituted stilbene and *N*-phenylmaleimide monomers.[48-49, 56] Recently, we reported the two-step synthesis of a series of carboxylate acid-containing nanoporous crosslinked polymers by the deprotection of the *tert*-butyl carboxylate-functionalized

polymer precursors. These polymers showed high surface areas and significant CO_2 adsorption ability.[56] These carboxylic acid functionalized crosslinked polymers inspired us to incorporate the same monomers into microgels and investigate the properties of these new materials. Herein, we describe the synthesis of highly functionalized microgels using hydrophobic solid monomers – *tert*-butyl carboxylate substituted trans-stilbene and *N*-phenylmaleimide via miniemulsion technique. These *tert*-butyl carboxylate-containing microgels were also hydrolyzed to their carboxylic acid-containing aqueous microgel analogues. The swelling properties and lead and copper adsorption abilities of the aqueous microgels were also explored and discussed.

5.4 Experimental section.

5.4.1 Materials.

The monomers (E)-di-*tert*-butyl-4, 4'-stilbene dicarboxylate (DTBSC), *tert*-butyl 4-maleimidobenzoate (TBMI), and *tert*-butyl 4-vinyl benzoate (TBVB) were synthesized and characterized as previously reported. Divinylbenzene (DVB, Sigma-Aldrich, technical grade, isomer of p- and m-, 80% purity), trifluoroacetic acid (TFA, Oakwood Chemical, 99%), toluene (Fisher, HPLC grade), sodium dodecyl sulfate (SDS, Sigma-Aldrich, 98%), hexadecane (Sigma-Aldrich, 99%), sodium hydroxide (Fisher, certified ACS grade), sodium chloride (Fisher, certified ACS crystal-line), dichloromethane (DCM, Fisher, HPLC grade), lead(II) nitrite (Sigma-Aldrich, ACS grade, >99.0%), copper(II) nitrite hemi(pentahydrate) (Sigma-Aldrich, ACS grade, 98%) were used as received without further purification. Maleic anhydride (MAH, Sigma-Aldrich, 99%) was recrystallized from toluene. 2, 2'-azobisisobutyronitrile (AIBN, Aldrich, 98%) was recrystallized from methanol. Deionized water was provided by Virginia Tech.

5.4.2 Instrumental characterization.

The structures of the synthesized monomers were determined by proton nuclear magnetic resonance (^{1}H NMR, Varian Inova 400 MHz). The incorporation of the functionalized stilbene and maleimide comonomers and the deprotection of *tert*-butyl groups were confirmed by infrared analysis (IR, Varian 670 FT-IR Spectrometer). Elemental analysis was performed by Atlantic Microlab (Norcross, GA). The thermogravimetric analysis (TGA) of the copolymers was conducted by TA instrument model Q5000, samples were heated from 50 to 600 ºC at a heating rate of 10 ºC/min under nitrogen. The miniemulsification was achieved by ultrasonicating using a Branson CV 33 sonicator. The particle size was measured using a Brookhaven Instruments BI-200SM machine equipped with a TurboCorr Digital Correlator and a HeNe laser diode (35mW, 637 nm). Very dilute samples were used for sample preparation and filtered through 1.0 μm or 5.0 μm (for aggregated samples) PTFE syringe filter. TEM analysis was performed on a Philips EM420 at an accelerating voltage of 120 kV. The concentration of heavy metal ions in solution was determined using an Agilent 200 flame atomic absorption spectrophotometer.

5.4.3 Synthesis of non-aqueous microgels using miniemulsion polymerization.

The precursors were synthesized via miniemulsion polymerization (Scheme 5-1). For example, DTBSC (1.82 g, 4.75 mmol), TBMI (1.30 g, 4.75 mmol), and DVB (0.065 g, 0.5 mmol) were dissolved in 5 mL toluene in a 100 mL round bottom flask, then 25 mL of deionized water was added to the flask, followed by adding SDS (0.25 g, 4 wt% of organic phase), hexadecane (0.34 mL, 6 vol% of organic phase) and AIBN (0.011g, 1 wt%). The mixture was stirred for 30 min under N_2, then ultra-sonicated under 70% intensity for 2 min under an ice bath. The white miniemulsion was then stirred under N_2 at 75 ˚C for 24 h. The resulting mixture was shaken vigorously with 2 g of NaCl to break the emulsion, and then dialyzed against DI water for 48 h to remove salt, unreacted monomer, surfactant and costabilzer. The off-white fluffy microgels were

obtained by freeze drying (yield 59.1%–65.6%). *tert*-Butyl 4-vinyl benzoate (TBVB) was also used in replace of DTBSC to synthesize a microgel as a control. A general nomenclature G_{STB}-tbu and G_{Sty}-tbu were employed, in which G is short for gel, STB or Sty stands for the stilbene comonomer DTBSC or styrene comonomer TBVB, and tbu represents the *tert*-butyl protecting group. For both copolymers, the crosslinking density was held at 5 mol% of DVB.

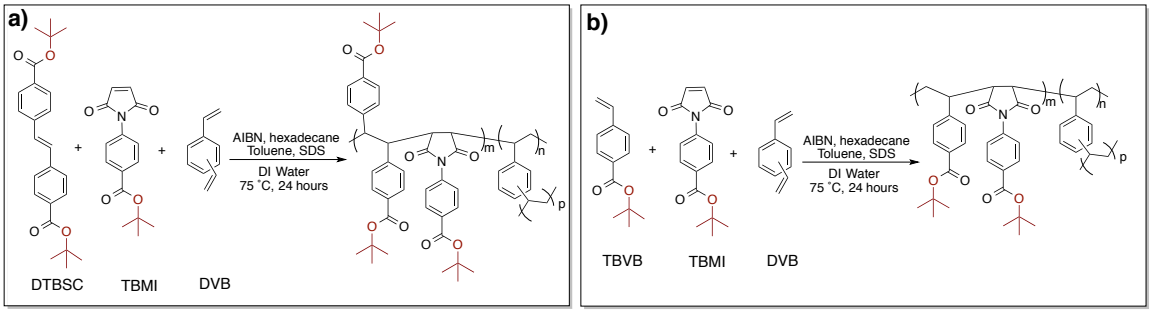

Scheme 5-1. Synthesis of *tert*-butyl group-containing microgels (a) G_{STB}-tbu (b) G_{Sty}-tbu

5.4.4 Synthesis of aqueous microgels.

As shown in scheme 5-2, 0.5 g gel precursor was swollen in 3 mL dichloromethane (DCM), and 3 mL TFA was added at room temperature. The mixture was stirred for 24 h, then filtered and washed with DCM. Next, the gel was stirred in 0.1 M NaOH solution for 24 h before being filtered and washed thoroughly with DI water. The resulting white solid was further dried in vacuum at room temperature for 24 h.

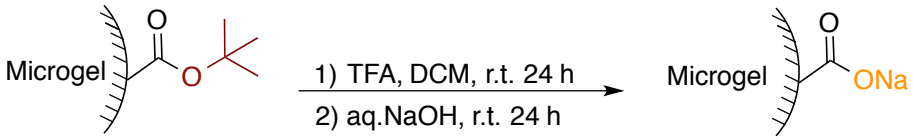

Scheme 5-2. Conversion of organic microgels to aqueous microgels by deprotection of *tert*-butyl groups.

5.4.5 Adsorption/desorption experiments.

A weighted gel sample (~100 mg) was added to a flask containing 50 mL metal ion solution of a certain concentration (500 ppm for Pb^{2+}, and 200 ppm for Cu^{2+}), and the resulting mixture

was stirred on a magnetic stir plate for a specific period of time (3 min – 480 min, see Figure 5-4) at room temperature. The pH of the solution was adjusted with diluted HCl (0.01 M) to pH 5.5, measured using a pH meter. The gel-solution mixture was then filtered and the concentration of the residual metal ion remaining in the solution was then analyzed by an Agilent flame atomic absorption spectrophotometer. The amount of adsorption was calculated using the following equation:

$$\text{Quantity adsorbed (mg/g)} = (c_0 - c_t) \cdot \frac{V}{m}$$

in which c_0 (ppm, mg/L) and c_t (ppm, mg/L) are the initial and final metal ion concentrations of the solution, respectively, V (L) is the volume of the metal ion solution, and m (g) is the mass of the hydrogel.

The regeneration of the hydrogel was achieved using HCl as the desorbing agent. The hydrogel resulting from the adsorption experiment was soaked in 50 mL of 0.2 M HCl aqueous solution. The resulting mixture was stirred for 2 hours before filtering off. The desorption process was then repeated one more time and the hydrogel was washed with DI water and dried at 60 ˚C under vacuum for 24 h before using for another cycle of adsorption. The adsorption time in each cycle is fixed to 8 hours.

5.5 Results and discussion.

5.5.1 Synthesis and characterization

The synthesis of the *tert*-butyl carboxylate-containing organic microgels is depicted in Scheme 5-1, in which the hydrophobic solid momoners (E)-di-*tert*-butyl-4, 4'-stilbene dicarboxylate (DTBSC) and *tert*-butyl 4-maleimidobenzoate (TBMI) were crosslinked with 5 mol% of divinylbenzene in miniemulsion copolymerization. Toluene was added to dissolve the solid monomers, SDS served as the surfactant, hexadecane was used as the hydrophobe to costabilize

the monomer droplets, and AIBN was used as the radical initiator. After emulsification using a high power ultrasonicator in an ice-bath, the resulting miniemulsion remained stable for more than 3 days at room temperature. After stirring the miniemulsion at 75 ˚C for 24 hours, saturated sodium chloride solution was added to break the miniemulsion, and the mixture was dialyzed against DI water for 48 hours to remove unreacted monomers, surfactant, organic solvent, and salt. The detailed synthesis procedure is described in supporting information. Elemental analysis and thermogravimetric analysis (TGA) were used to confirm the composition of the copolymers. The weight loss in TGA curves at 220 ˚C corresponds to the thermal cleavage of the *tert*-butyl group (Figure 5-1c). The electron rich monomers DTBSC or TBVB preferably polymerize with the electron poor monomer TBMI in an alternating fashion, therefore we calculate the theoretical elemental contents based on 1:1 ratio of DTBSC: TBMI or TBVB: TBMI in each polymer. The experimental elemental analysis data is in general agreement with the theoretical value (Table 5-1). The representative TEM micrographs of G_{STB}-tbu and G_{Sty}-tbu deposited from diluted DCM suspensions are shown in Figure 5-1a and 5-1b. Spherical particles with diameters in the range of 80-160 nm were observed. Dynamic light scattering (Figure 5-1d) showed that G_{STB}-tbu and G_{Sty}-tbu have hydrodynamic diameters of 153nm and 137 nm, respectively.

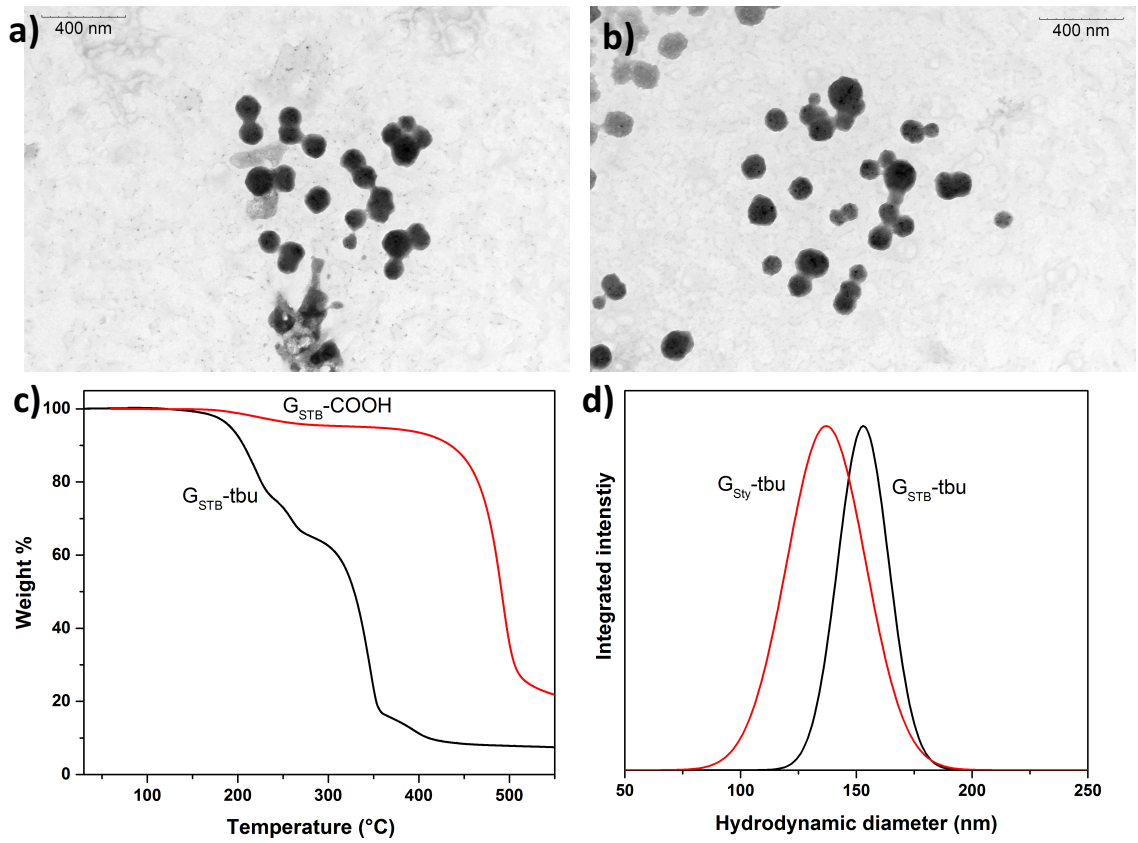

Figure 5-1. a) Typical TEM micrograph of G_{STB}-tbu; b) Typical TEM micrograph of G_{Sty}-tbu; c) TGA curves of G_{STB}-tbu and G_{STB}-COOH; d) DLS CONTIN plots of G_{STB}-tbu and G_{Sty}-tbu.

Table 5-1. Elemental analysis of the organic microgels

Sample	Theoretical (wt%)			Experimental (wt%)		
	C	H	N	C	H	N
G_{STB}-tbu	72.07	6.65	2.10	74.20	8.74	2.02
G_{Sty}-tbu	71.03	6.57	2.85	70.53	7.35	2.83

The TFA-catalyzed deprotection was carried out in DCM at room temperature for 24 hours, and the resultant gel was dried and neutralized using 0.1 M NaOH solution.[56] The corresponding aqueous microgels were named G_{STB}-COOH and G_{Sty}-COOH, respectively, in which COOH stands for the carboxylic acid groups. Fourier Transform Infrared spectroscopy (FT-IR) was used to study the deprotection. The FT-IR spectra of G_{STB}-tbu and G_{STB} microgels are shown in Figure

5-3. After deprotection, the typical ester C=O stretch peak at 1735 cm^{-1} was almost completely gone; while two new bands at 1700 cm^{-1} and 1550 cm^{-1} appeared, corresponding to the C=O stretch of the carboxylic acid and the sodium carboxylate salt, respectively. Additionally, the broad peak from O-H stretch of COOH was observed at 3300 cm^{-1} for G_{STB}-COOH. After deprotection, the TGA curve showed less than 10% of residual *tert*-butyl groups, conforming effective deprotection (Figure 5-1c).

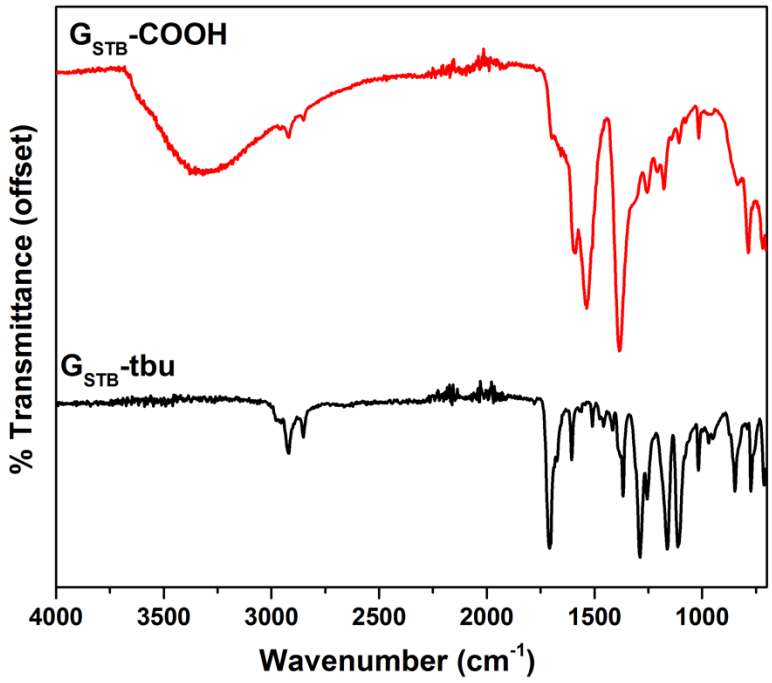

Figure 5-2. FT-IR spectra of G_{STB}-tbu and G_{STB}-COOH.

5.5.2 Swelling properties.

The pH-responsive swelling properties of aqueous microgels G_{STB}-COOH and G_{Sty}-COOH were investigated using dynamic light scattering. Figure 5-3 depicts the intensity-weighted hydrodynamic diameters of G_{STB}-COOH and G_{Sty}-COOH at different pH values. From the plot, both microgels underwent a similar volume change with an increase in pH. In particular, the size of the gels first increased until neutral pH, then decreased when pH was continually increased. This observation is consistent with other carboxylic acid containing microgels[59] and macrogels.[60]

At lower pH, the carboxylates in the polymers are protonated and the swelling ratio is small due to the lack of the ionic repulsions. With increasing pH, the carboxylic acid groups started to disassociate, and the charge density of the gel particles also increased. At the same time, the increasing concentration of the mobile counter ion also caused the increasing internal osmotic pressure, which further enhanced the swelling of the gels until the maximum of ionization. The pKa of the pendent benzoic acid is around 4.5, therefore the carboxylic acid groups are basically fully ionized at pH 7. With continually increasing pH, the high NaOH concentration in the solution decreased the difference between the interior mobile ion concentration and the ion concentration in the solution. Also, due to the screening effect, the carboxylate groups are more highly shielded, which results in a decrease of charge density. Both the decreasing internal osmotic pressure and charge density caused the decrease in the swelling ratio of the microgels at high pH. It is also worth noticing that flocculation occurs for both G_{STB}-COOH and G_{Sty}-COOH at pH 3, as evidenced by the high hydrodynamic diameter of 4.6 μm and 4.2 μm, respectively. The flocculation at low pH is caused by the low electrostatic stabilization and the high Hamaker constants of the particles and the solvent due to deswelling.[59]

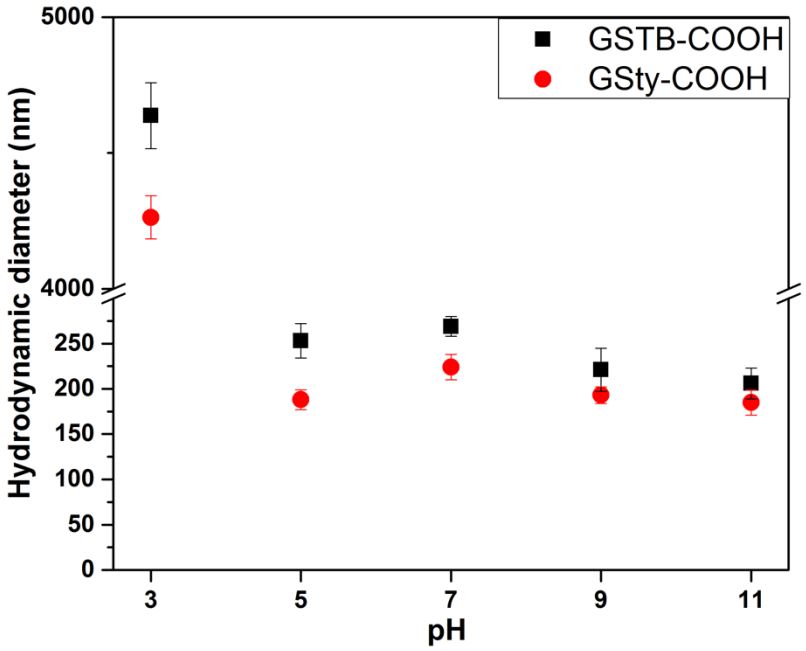

Figure 5-3. Intensity-weighted hydrodynamic diameter of microgels at different pH values

5.5.3 Microgel on lead and copper adsorption

The adsorption properties of the G_{STB}-COOH were evaluated by measuring the Pb^{2+} and Cu^{2+} uptakes at pH 5.5. Figure 5-4 illustrates the adsorption capacities of G_{STB}-COOH microgel over time. For both ions, the same trend was observed. The adsorption quantity increased rapidly over the first 30 minutes, then the increase of adsorption slowed down between 30 minutes and 4 hours, and the adsorption quantity remained basically stable after 4 hours. The fast adsorption rate in the beginning stage is attributed to the rapid interaction of the carboxylate groups with the ions on the gel surface, along with the ions also migrating into the gel particles through osmotic permeation. The divalent ions can work as crosslinking sites that may lead to deswell, thus decreasing the adsorption rate at the later stage. The lead and copper ion adsorption capacities of G_{STB}-COOH microgel are comparatively higher than some of the previously reported materials.[7, 22, 27, 61-62] Such high adsorption capacities are related to the high content of carboxylate groups in the gels.

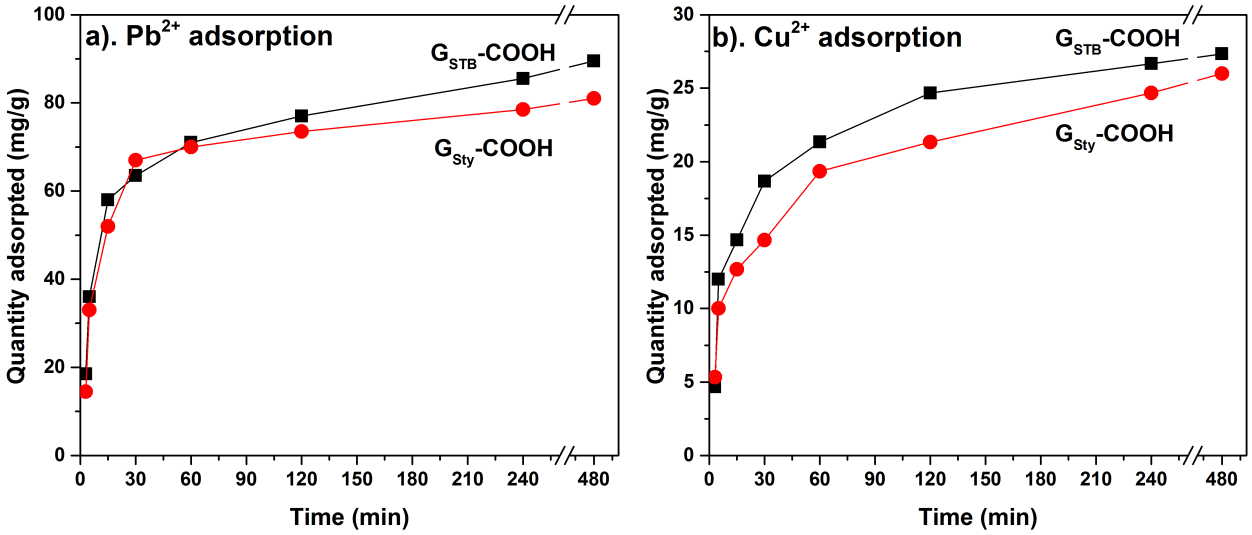

Figure 5-4. a) Lead and b) copper ions adsorption of G_{STB}-COOH microgel as a function of time.

In order to study the regeneration ability of the microgels, five adsorption and desorption cycles of Pb^{2+} (Figure 5-5a) and Cu^{2+} (Figure 5-5b) ions were conducted on the G_{STB}-COOH microgel. Each adsorption capacity was compared with the capacity of the first adsorption (100%). The first time after the desorption using 0.3 M HCl solution, the regenerated microgel showed obvious decrease in adsorption capacity towards both ions, and then the capacity remained basically constant for the rest four cycles. After five cycles, the adsorption capacity only decreased to 13% compared to first Pb^{2+} adsorption and 19% of first Cu^{2+} adsorption, indicating good regeneration ability.

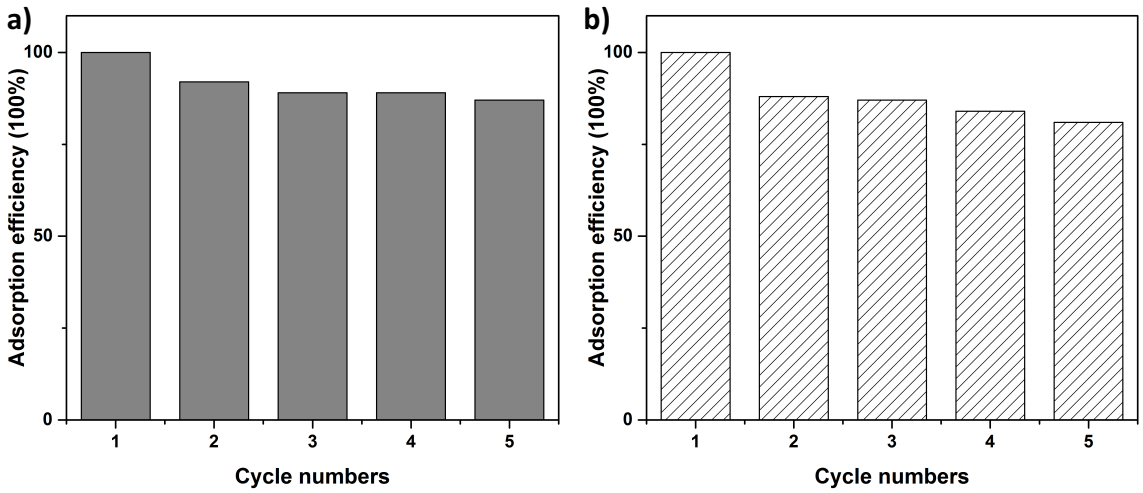

Figure 5-5. The adsorption efficiency of five adsorption and desorption cycles of G_{STB}-COOH microgel towards a) Pb^{2+} and b) Cu^{2+} ions.

5.6 Conclusions

We have broadened the monomer choices for microgels by using miniemulsion polymerization to synthesize microgels from hydrophobic solid monomers. The addition of the costabilizer allowed the use of organic solvents for dissolving the solid monomers. Spherical microgel particles with diameters between 100-200 nm were achieved. The resulting *tert*-butyl carboxylate-containing organic microgels were converted to aqueous gels by acidic hydrolysis. The rich carboxylic acid groups in the aqueous microgels enhanced the adsorption ability of lead and copper ions. Our future study will involve efforts to control particle sizes by varying the ratio of surfactant, costabilizer, and organic solvent.

5.7 Acknowledgements

This work was supported by the National Science Foundation (NSF) under grant number DMR-0905231, DMR-1206409, and DMR-1310258. We thank the Macromolecules Innovation Institute and the Department of Chemistry at Virginia Tech.

5.8 References

1. Coombs, T., Heavy metal pollutants in the aquatic environment. *Anim. Environ. Fitness* **2013**, 283-302.
2. Järup, L., Hazards of heavy metal contamination. *Br. Med. Bull.* **2003,** *68* (1), 167-182.
3. Tchounwou, P. B.; Yedjou, C. G.; Patlolla, A. K.; Sutton, D. J., Heavy metal toxicity and the environment. In *Molecular, clinical and environmental toxicology: Volume 3: Environmental toxicology*, Luch, A., Ed. Springer Basel: Basel, 2012; pp 133-164.
4. Wang, S.-L.; Xu, X.-R.; Sun, Y.-X.; Liu, J.-L.; Li, H.-B., Heavy metal pollution in coastal areas of South China: a review. *Mar. Pollut. Bull.* **2013,** *76* (1), 7-15.
5. Kobya, M.; Demirbas, E.; Senturk, E.; Ince, M., Adsorption of heavy metal ions from aqueous solutions by activated carbon prepared from apricot stone. *Bioresour. Technol.* **2005,** *96* (13), 1518-1521.
6. Bailey, S. E.; Olin, T. J.; Bricka, R. M.; Adrian, D. D., A review of potentially low-cost sorbents for heavy metals. *Water Res.* **1999,** *33* (11), 2469-2479.
7. Hernández-Morales, V.; Nava, R.; Acosta-Silva, Y.; Macías-Sánchez, S.; Pérez-Bueno, J.; Pawelec, B., Adsorption of lead (II) on SBA-15 mesoporous molecular sieve functionalized with–NH_2 groups. *Microporous Mesoporous Mater.* **2012,** *160*, 133-142.
8. Isaac, R.; Gil, L.; Cooperman, A.; Hulme, K.; Eddy, B.; Ruiz, M.; Jacobson, K.; Larson, C.; Pancorbo, O., Corrosion in drinking water distribution systems: a major contributor of copper and lead to wastewaters and effluents. *Environ. Sci. Technol.* **1997,** *31* (11), 3198-3203.
9. Pontius, F. W., LEGISLATION/REGULATION: The new lead and copper rule. *J. Am. Water Works Assoc.* **1991,** *83* (7), 12-109.

10. Edwards, M. A.; Pruden, A., The Flint water crisis: Overturning the research paradigm to advance science and defend public welfare. ACS Publications: 2016.

11. Gostin, L. O., Politics and public health: The Flint drinking water crisis. *Hastings Cent. Rep* **2016,** *46* (4), 5-6.

12. Masten, S. J.; Davies, S. H.; McElmurry, S. P., Flint water crisis: What happened and why? *J. Am. Water Works Assoc.* **2016,** *108* (12), 22-34.

13. Minamisawa, M.; Minamisawa, H.; Yoshida, S.; Takai, N., Adsorption behavior of heavy metals on biomaterials. *J. Agric. Food. Chem.* **2004,** *52* (18), 5606-5611.

14. Ngah, W. W.; Teong, L.; Hanafiah, M., Adsorption of dyes and heavy metal ions by chitosan composites: A review. *Carbohydr. Polym.* **2011,** *83* (4), 1446-1456.

15. Ngah, W. W.; Endud, C.; Mayanar, R., Removal of copper (II) ions from aqueous solution onto chitosan and cross-linked chitosan beads. *React. Funct. Polym.* **2002,** *50* (2), 181-190.

16. Guo, X.; Zhang, S.; Shan, X.-q., Adsorption of metal ions on lignin. *J. Hazard. Mater.* **2008,** *151* (1), 134-142.

17. Celik, A.; Demirbaş, A., Removal of heavy metal ions from aqueous solutions via adsorption onto modified lignin from pulping wastes. *Energ. sources* **2005,** *27* (12), 1167-1177.

18. Yu, B.; Zhang, Y.; Shukla, A.; Shukla, S. S.; Dorris, K. L., The removal of heavy metal from aqueous solutions by sawdust adsorption—removal of copper. *J. Hazard. Mater.* **2000,** *80* (1), 33-42.

19. Argun, M. E.; Dursun, S.; Ozdemir, C.; Karatas, M., Heavy metal adsorption by modified oak sawdust: Thermodynamics and kinetics. *J. Hazard. Mater.* **2007,** *141* (1), 77-85.

20. Bulut, Y., Removal of heavy metals from aqueous solution by sawdust adsorption. *J. Environ. Sci.* **2007,** *19* (2), 160-166.

21. Yu, B.; Zhang, Y.; Shukla, A.; Shukla, S. S.; Dorris, K. L., The removal of heavy metals from aqueous solutions by sawdust adsorption—removal of lead and comparison of its adsorption with copper. *J. Hazard. Mater.* **2001,** *84* (1), 83-94.

22. Vázquez, G.; Calvo, M.; Freire, M. S.; González-Alvarez, J.; Antorrena, G., Chestnut shell as heavy metal adsorbent: optimization study of lead, copper and zinc cations removal. *J. Hazard. Mater.* **2009,** *172* (2), 1402-1414.

23. Vaghetti, J. C.; Lima, E. C.; Royer, B.; da Cunha, B. M.; Cardoso, N. F.; Brasil, J. L.; Dias, S. L., Pecan nutshell as biosorbent to remove Cu (II), Mn (II) and Pb (II) from aqueous solutions. *J. Hazard. Mater.* **2009,** *162* (1), 270-280.

24. Pinnavaia, T., Selective adsorption of Hg^{2+} by thiol-functionalized nanoporous silica. *Chem. Commun.* **1999,** (1), 69-70.

25. Yantasee, W.; Rutledge, R. D.; Chouyyok, W.; Sukwarotwat, V.; Orr, G.; Warner, C. L.; Warner, M. G.; Fryxell, G. E.; Wiacek, R. J.; Timchalk, C., Functionalized nanoporous silica for the removal of heavy metals from biological systems: adsorption and application. *ACS Appl. Mater. Interfaces* **2010,** *2* (10), 2749-2758.

26. Ravikovitch, P. I.; Neimark, A. V., Density functional theory of adsorption in spherical cavities and pore size characterization of templated nanoporous silicas with cubic and three-dimensional hexagonal structures. *Langmuir* **2002,** *18* (5), 1550-1560.

27. Tofighy, M. A.; Mohammadi, T., Adsorption of divalent heavy metal ions from water using carbon nanotube sheets. *J. Hazard. Mater.* **2011,** *185* (1), 140-147.

28. Stafiej, A.; Pyrzynska, K., Adsorption of heavy metal ions with carbon nanotubes. *Sep. Purif. Technol.* **2007,** *58* (1), 49-52.

29. Li, Y.-H.; Ding, J.; Luan, Z.; Di, Z.; Zhu, Y.; Xu, C.; Wu, D.; Wei, B., Competitive adsorption

of Pb^{2+}, Cu^{2+} and Cd^{2+} ions from aqueous solutions by multiwalled carbon nanotubes. *Carbon* **2003,** *41* (14), 2787-2792.

30. Li, Y.-H.; Wang, S.; Wei, J.; Zhang, X.; Xu, C.; Luan, Z.; Wu, D.; Wei, B., Lead adsorption on carbon nanotubes. *Chem. Phys. Lett.* **2002,** *357* (3), 263-266.

31. Liu, R.; Zhang, B.; Tang, H., Adsorption properties of poly (acrylaminophosphonic-carboxyl-hydrazide) type chelating fiber for heavy metal ions. *J. Appl. Polym. Sci.* **1998,** *70* (1), 7-14.

32. Dinu, M. V.; Dragan, E. S., Heavy metals adsorption on some iminodiacetate chelating resins as a function of the adsorption parameters. *React. Funct. Polym.* **2008,** *68* (9), 1346-1354.

33. Baraka, A.; Hall, P.; Heslop, M., Preparation and characterization of melamine–formaldehyde–DTPA chelating resin and its use as an adsorbent for heavy metals removal from wastewater. *React. Funct. Polym.* **2007,** *67* (7), 585-600.

34. Atta, A. M.; Ismail, H. S.; Elsaaed, A. M., Application of anionic acrylamide-based hydrogels in the removal of heavy metals from waste water. *J. Appl. Polym. Sci.* **2012,** *123* (4), 2500-2510.

35. Krishna Rao, K. S. V.; Ha, C.-S., pH Sensitive hydrogels based on acryl amides and their swelling and diffusion characteristics with drug delivery behavior. *Polym. Bull.* **2008,** *62* (2), 167.

36. Popa, A.; Davidescu, C.-M.; Negrea, P.; Ilia, G.; Katsaros, A.; Demadis, K. D., Synthesis and characterization of phosphonate ester/phosphonic acid grafted styrene-divinylbenzene copolymer microbeads and their utility in adsorption of divalent metal ions in aqueous solutions. *Ind. Eng. Chem. Res.* **2008,** *47* (6), 2010-2017.

37. Nowack, B., Environmental chemistry of phosphonates. *Water Res.* **2003,** *37* (11), 2533-

2546.

38. Saraydin, D.; Karadağ, E.; Güven, O., Adsorptions of some heavy metal ions in aqueous solutions by acrylamide/maleic acid hydrogels. *Sep. Sci. Technol.* **1995,** *30* (17), 3287-3298.

39. Chen, J.; Ahmad, A.; Ooi, B., Poly (*N*-isopropylacrylamide-*co*-acrylic acid) hydrogels for copper ion adsorption: equilibrium isotherms, kinetic and thermodynamic studies. *J. Environ. Chem. Eng.* **2013,** *1* (3), 339-348.

40. Ramírez, E.; Burillo, S. G.; Barrera-Díaz, C.; Roa, G.; Bilyeu, B., Use of pH-sensitive polymer hydrogels in lead removal from aqueous solution. *J. Hazard. Mater.* **2011,** *192* (2), 432-439.

41. Fernandez-Nieves, A.; Wyss, H.; Mattsson, J.; Weitz, D. A., *Microgel suspensions: fundamentals and applications*. John Wiley & Sons: 2011.

42. Agirre, A.; Nase, J.; Degrandi, E.; Creton, C.; Asua, J. M., Miniemulsion Polymerization of 2-Ethylhexyl Acrylate. Polymer Architecture Control and Adhesion Properties. *Macromolecules* **2010,** *43* (21), 8924-8932.

43. Bradley, M. A.; Prescott, S. W.; Schoonbrood, H. A. S.; Landfester, K.; Grieser, F., Miniemulsion copolymerization of methyl methacrylate and butyl acrylate by ultrasonic initiation. *Macromolecules* **2005,** *38* (15), 6346-6351.

44. Miller, C.; Sudol, E.; Silebi, C.; El-Aasser, M., Miniemulsion polymerization of styrene: evolution of the particle size distribution. *J. Polym. Sci., Part A: Polym. Chem.* **1995,** *33* (8), 1391-1408.

45. Graillat, C.; Guyot, A., High solids vinyl acetate polymers from miniemulsion polymerization. *Macromolecules* **2003,** *36* (17), 6371-6377.

46. Mao, M.; Turner, S. R., Aggregation of rod-coil block copolymers containing rigid

polyampholyte blocks in aqueous solution. *J. Am. Chem. Soc.* **2007,** *129* (13), 3832-3833.

47. Mao, M.; Kim, C.; Wi, S.; Turner, S. R., Chain structure of substituted stilbene-maleic anhydride alternating copolymer probed by solid-state NMR. *Macromolecules* **2008,** *41* (2), 387-389.

48. Li, Y.; Mao, M.; Matolyak, L. E.; Turner, S. R., Sterically Crowded Anionic Polyelectrolytes with Tunable Charge Densities Based on Stilbene-Containing Copolymers. *ACS Macro Lett.* **2012,** *1* (2), 257-260.

49. Li, Y.; Zhang, M.; Mao, M.; Turner, S. R.; Moore, R. B.; Mourey, T. H.; Slater, L. A.; Hauenstein, J. R., Chain stiffness of stilbene containing alternating copolymers by SAXS and SEC. *Macromolecules* **2012,** *45* (3), 1595-1601.

50. Li, Y.; Savage, A. M.; Zhou, X.; Turner, S. R.; Davis, R. M., Solution properties of stilbene-containing sterically crowded alternating polyanions. *J. Polym. Sci., Part B: Polym. Phys.* **2013,** *51* (21), 1565-1570.

51. Zhou, X.; Li, Y.; Hart, K. E.; Abbott, L. J.; Lin, Z.; Svec, F.; Colina, C. M.; Turner, S. R., Nanoporous structure of semirigid alternating copolymers via nitrogen sorption and molecular simulation. *Macromolecules* **2013,** *46* (15), 5968-5973.

52. Savage, A. M.; Li, Y.; Matolyak, L. E.; Doncel, G. F.; Turner, S. R.; Gandour, R. D., Anti-hiv activities of precisely defined, semirigid, carboxylated alternating copolymers. *J. Med. Chem.* **2014,** *57* (15), 6354-6363.

53. Savage, A. M.; Zhou, X.; Huang, J.; Turner, S. R., A review of semi-rigid, stilbene-containing alternating copolymers. *Appl. Petrochem. Res.* **2015,** *5* (1), 27-33.

54. Savage, A. M.; Ullrich, E.; Chin, S. M.; Kiernan, Z.; Kost, C.; Turner, S. R., Synthesis and characterization of double hydrophilic block copolymers containing semi-rigid and flexible

segments. *J. Polym. Sci., Part A: Polym. Chem.* **2015,** *53* (2), 219-227.

55. Zhou, X.; Huang, J.; Barr, K. W.; Lin, Z.; Maya, F.; Abbott, L. J.; Colina, C. M.; Svec, F.; Turner, S. R., Nanoporous hypercrosslinked polymers containing T g enhancing comonomers. *Polymer* **2015,** *59*, 42-48.

56. Huang, J.; Zhou, X.; Lamprou, A.; Maya, F.; Svec, F.; Turner, S. R., Nanoporous polymers from cross-linked polymer precursors via *tert*-butyl group deprotection and their carbon dioxide capture properties. *Chem. Mater.* **2015,** *27* (21), 7388-7394.

57. Savage, A. M.; Ullrich, E.; Kost, C.; Turner, S. R., Salt- and pH-responsive semirigid/flexible double-hydrophilic block copolymers. *Macromol. Chem. Phys.* **2016,** *217* (15), 1737-1744.

58. Huang, J.; Turner, S. R., Recent advances in alternating copolymers: The synthesis, modification, and applications of precision polymers. *Polymer* **2017,** *116*, 572-586.

59. Saunders, B. R.; Crowther, H. M.; Vincent, B., Poly[(methyl methacrylate)-*co*-(methacrylic acid)] microgel particles: swelling control using pH, cononsolvency, and osmotic deswelling. *Macromolecules* **1997,** *30* (3), 482-487.

60. Ricka, J.; Tanaka, T., Swelling of ionic gels: quantitative performance of the Donnan theory. *Macromolecules* **1984,** *17* (12), 2916-2921.

61. El-Ghaffar, M. A.; Elhalawany, N.; Ahmed, E.; Sabaa, M., Synthesis and characterization of some chelating polymers bearing maleic acid and/or sodium maleate moieties for removal of some toxic heavy metal ions. *Clean Technol. Environ. Policy* **2013,** *15* (6), 1013-1021.

62. Jiang, L.; Liu, P., Novel magnetic fly ash/poly (acrylic acid) composite microgel for selective adsorption of Pb (II) ion: synthesis and evaluation. *Ind. Eng. Chem. Res.* **2014,** *53* (8), 2924-2931.

Chapter 6. Nanoporous Hypercrosslinked Polymer Networks with Covalently-Bonded Amines for CO_2 Capture

6.1 Authors

Jing Huang,[†,‡] Jie Zhu,[†,‡] Xi Geng,[†,‡] Samuel Snyder,[†,‡] Amanda J. Morris,[†,‡] and S. Richard Turner*[,†,‡]

[†]Department of Chemistry, Virginia Tech, Blacksburg, VA 24061, United States

[‡]Macromolecules Innovation Institute, Virginia Tech, Blacksburg, VA 24061, United States

6.2 Abstract

Amine-containing polymers are considered to be promising CO_2 capture materials and considerable research effort has been invested in designing and preparing new high surface area materials containing various amine structures. In this work, a series of nanoporous hypercrosslinked polymers (HCPs) with covalently bonded amines were prepared by post-modification of hypercrosslinked DVB-MAH precursor with various diamines. The successful incorporation of the diamines was confirmed using Fourier transform infrared spectroscopy (FT-IR), thermogravimetric analysis (TGA) and elemental analysis. The resulting amine-containing HCPs possessed both micropores and mesopores, and they exhibited BET surface area of 183-500 m^2/g. The CO_2 capture capacity of these polymers varied in relation to the amine content in the HCP network. The inexpensive starting material, facile synthesis, good thermal stability, and high CO_2 adsorption capacity make them potential candidates as solid sorbents for CO_2.

6.3 Introduction

For the past decades, increasing atmospheric CO_2 concentrations due to the combustion of fossil fuels and other anthropogenic emissions have caused public concerns.[1-3] CO_2 capture and sequestration (CCS) was proposed to be an effective technology option in controlling atmospheric

CO_2 levels.[4] Liquid amine scrubbing is currently the most mature technology for industrial CO_2 capture, the reversible reaction between amine groups and CO_2 ensures effective and selective sorption of CO_2.[5-6] Nonetheless, due to solvent emission and degradation, equipment corrosion, and intensive energy-demand during the regeneration, scientists and governments are shifting their attention toward new, efficient, and cost-effective materials for CO_2 capture.[7-8] In particular, porous solid sorbents, including organic, inorganic, or organic-inorganic hybrid materials, appear to be promising alternatives.[9] Various attempts have been made to incorporate amines onto porous solid sorbents to achieve selective CO_2 sorption. For example, amines were immobilized onto mesoporous silica,[10-15] metal-organic frameworks (MOFs),[16-17] and polymer networks,[18] either physically via wet impregnation,[12] or covalently by grafting[10-11, 13, 15, 17] or cocondensation[14, 18]. The disadvantages of liquid amine scrubbing can be easily overcome by using solid amine sorbents, and these materials exhibit fast adsorption kinetics, low operating temperatures and high selectivity.[15] However, challenges, such as low immobilized amine content, low thermal stability, and high cost, still remain prior to the actual CCS applications.[13, 19-20]

Nanoporous (pore width < 50 nm) hypercrosslinked polymers have generated increasing attention owing to their advantages such as synthetic diversity, high surface area, good physicochemical stability, and low skeleton density.[21-24] Divinylbenzene (DVB) is one of the most commonly used crosslinking agents, since it provides rigid and short crosslinks. As an analogue of the electron-rich styrenic monomer, DVB could quickly cross-propagate and crosslink with electron-deficient maleic anhydride (MAH) or maleimide monomers.[25-26] Previously we reported a two-step synthesis of carboxylic acid functionalized porous polymers via the deprotection of DVB-crosslinked alternating copolymer precursors. The resulting polymer networks showed high BET surface area and moderate CO_2 capture capacity.[27] In this study, we report a facile approach

to covalently immobilize amines onto nanoporous DVB-MAH to prepare solid amine sorbents with high amine contents. Their CO_2 capture abilities are also explored and discussed.

6.4 Experimental section

6.4.1 Materials

Divinylbenzene (DVB, Sigma-Aldrich, technical grade, isomer of p- and m-, 80% purity, toluene (Fisher, HPLC grade), poly(vinyl alcohol) (Aldrich, 87-89% hydrolyzed), sodium chloride (Fisher, certified ACS crystal-line), dichloromethane (DCM, Fisher, HPLC grade), thionyl chloride (Sigma-Aldrich, 97%), *p*-phenylenediamine (Sigma-Aldrich, 99%), ethylenediamine (Sigma-Aldrich, 99%), 1,4-diaminobutane (Sigma-Aldrich, 99%), diethylenetriamine (Sigma-Aldrich, 99%), and pentaethylenehexamine (Sigma-Aldrich, 99%) were used as received without further purification. Maleic anhydride (MAH, Sigma-Aldrich, 99%) was recrystallized from toluene. 2, 2'-azobisisobutyronitrile (AIBN, Aldrich, 98%) was recrystallized from methanol. Deionized water was provided by Virginia Tech.

6.4.2 Instrumental characterization.

The successful incorporation of the amines was confirmed by infrared analysis (FT-IR, Agilent Cary 630 FT-IR Spectrometer). Elemental analysis was performed by Atlantic Microlab (Norcross, GA). The thermogravimetric analysis (TGA) of the copolymers was conducted by TA instrument model Q5000, samples were heated from 50 to 550 ºC at a heating rate of 10 ºC/min under nitrogen. SEM micrographs of the copolymers were obtained using a LEO (Zeiss) 1550 field emission scanning electron microscope. Nitrogen adsorption/desorption isotherms at 77 K were obtained using a Quantachrome Autosorb 1 surface area analyzer, and the samples were degassed at 140 °C overnight before measurements. The surface areas were calculated using the Brunauer-Emmett-Teller (BET) equation. The pore sizes were determined from nitrogen adsorption isotherm

by the two-dimensional non-local density functional theory model with heterogeneous surfaces (2D-NLDFT-HS) using SAIEUS software. The CO_2 uptakes were measured at 273 K and 298 K by a Quantachrome Autosorb 1 instrument.

6.4.3 Synthesis of the DVB-MAH precursor

The DVB-MAH precursor was synthesized via suspension polymerization (Scheme 6-1). DVB (1.95 g, 15.0 mmol), and MAH (1.47 g, 15.0 mmol) were dissolved in 5 mL toluene in a 250 mL three-neck round bottom flask equipped with a mechanical stirrer, a condenser, and an N_2 gas inlet. Then 250 mL of de-ionized water was added to the flask, followed by adding poly (vinyl alcohol) (0.21g) and NaCl (1.13 g). The mixture was purged with N_2 for 15 min while stirring. AIBN (44 mg, 1.3 wt%) was added to initiate the polymerization. The suspension mixture was stirred under N_2 at 80 ˚C for 24 h. The resulting polymer beads were filtered and purified using Soxhlet extraction with toluene and water for 24 h to further remove the unreacted monomer, poly(vinyl alcohol) and NaCl. The resulting off-white beads were dried in vacuum oven at 50 ˚C for 24 h (72.0%-78.5%).

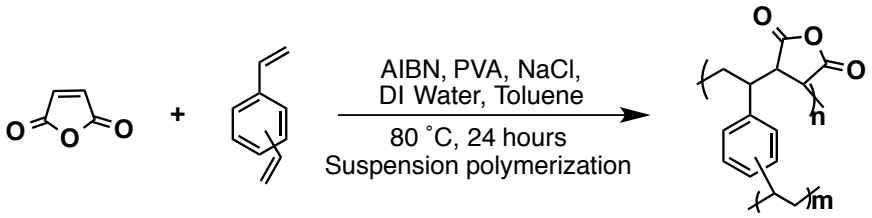

Scheme 6-1. Synthesis of the DVB-MAH precursor by suspension polymerization

6.4.4 Preparation of amine-grafted DVB-MAH networks

The DVB-MAH precursor was hydrolyzed by stirring with 0.5 N NaOH aqueous solution at 60 ˚C for 24 h. After filtration and thorough washing using DI water, the resulting polymer beads were immersed into 0.5 N HCl solution and stirred for 2 h at room temperature. The beads were then filtered and dried in a vacuum oven for 24 h at 80 ˚C. Then the polymers were stirred with

thionyl chloride at 80 ˚C for 2 h, and the excess thionyl chloride was removed by vacuum with an acid trap (0.5 N NaOH solution). The resulting acid-chloride functionalized polymer networks were immediately dispersed in excess diamine (2.0 mole eq. to theoretical acid chloride units) solutions in anhydrous CH_2Cl_2. The resulting mixtures were stirred at room temperature for 24 h and then filtered and washed thoroughly by DCM and 0.5 N NaOH solution. After drying in vacuum for 24 h, light brown or yellow powders were obtained. The general nomenclature for these copolymers, HCP-X, is employed, in which HCP stands for hypercrosslinked polymer, and the letter X represents the functional group on the surface (eg. COOH) and different diamines A-E (Scheme 6-2).

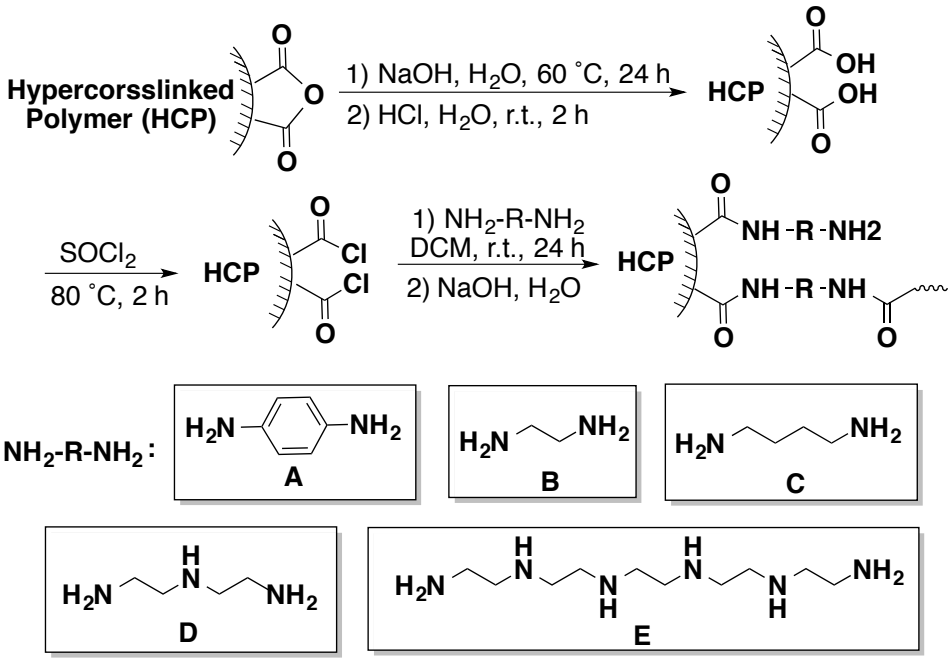

Scheme 6-2. Preparation of amine-grafted HCP networks by post-modification of DVB-MAH.

6.5 Results and discussion

6.5.1 Synthesis and characterization.

DVB-MAH copolymers of different microstructures were synthesized using various polymerization techniques such as suspension polymerization,[28-29] precipitation polymerization[30],

and dispersion polymerization[31]. Nanoporous DVB-MAH copolymers were previously reported using suspension polymerization, in which poly(vinylpyrrolidone) was the suspension stabilizer, and a mixture of 1,4-dioxane and n-dodecane was used as a pore-forming diluent.[29] These copolymers showed BET surface area from 4 to 535 m^2/g, and the average pore diameter was around 4.5 nm. In this work, using poly(vinyl achohol) as the stabilizer and toluene as the organic solvent and porogen, we were able to obtain DVB-MAH beads with a higher BET surface area (667 m^2/g). The SEM micrograph of DVB-MAH under low magnification is shown in Figure 6-1a. Spherical structures with diameters in the range of 10-300 μm were observed, which are typical for the products of suspension polymerization. Rough surfaces were observed under higher magnification, although the narrow nanopores (pore width < 5 nm) are too small to be observed under such magnification (Figure 6-1b).

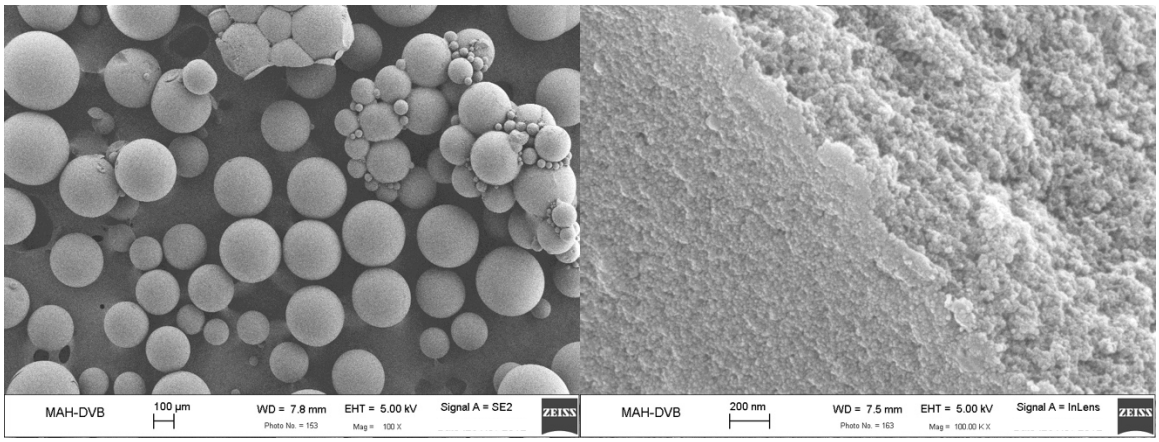

Figure 6-1. SEM micrographs of DVB-MAH particles at a) low magnification (scale bar 100 μm), and b) higher magnification (scale bar 200 nm)

The modification of DVB-MAH consisted of two major steps. First, the anhydride groups were converted to acid chlorides by basic hydrolysis, acidification, and then then chlorination with thionyl chloride. This was followed by the amidation of the acid chloride functionalized crosslinked polymers with excess of diamine.

The HCPs were first investigated using Fourier transform infrared (FT-IR) spectroscopy.

Figure 6-2a illustrates the full FT-IR spectra of DVB-MAH, the hydrolyzed HCP-COOH, and the amine grafted HCP-A to HCP-E. For better observation, Figure 6-2b depicts the spectra of DVB-MAH and HCP-COOH in the wavenumber range of 3500-1600 cm^{-1}. A broad peak at 3367 cm^{-1} was observed for HCP-COOH, which is attributed to the O-H stretch of the carboxylic acid. This broad peak was also observed in the spectrum of DVB-MAH, which indicates the anhydride units are partially ring-opened to the acid form during the suspension polymerization. The characteristic anhydride twin peaks at 1859 and 1781 cm^{-1} were observed for DVB-MAH, which corresponds to the C=O stretch of the anhydride carbonyl groups. The C=O stretch peak of the carboxylic acid at 1716 cm^{-1} was observed for both HCP-COOH and DVB-MAH, which further suggests the partial hydrolysis of the anhydride units in DVB-MAH. Figure 6-2c is the spectra of HCP-A to HCP-E in the range of 1700-1000 cm^{-1}. The characteristic peaks at 1664 cm^{-1} (secondary amide C=O stretch), 1605 cm^{-1} (N-H bend) and 1085 cm^{-1} (C-N stretch) can be seen. Moreover, all five modified polymers showed broad amide and amine peaks at around 3400 cm^{-1} (Figure 6-2a).

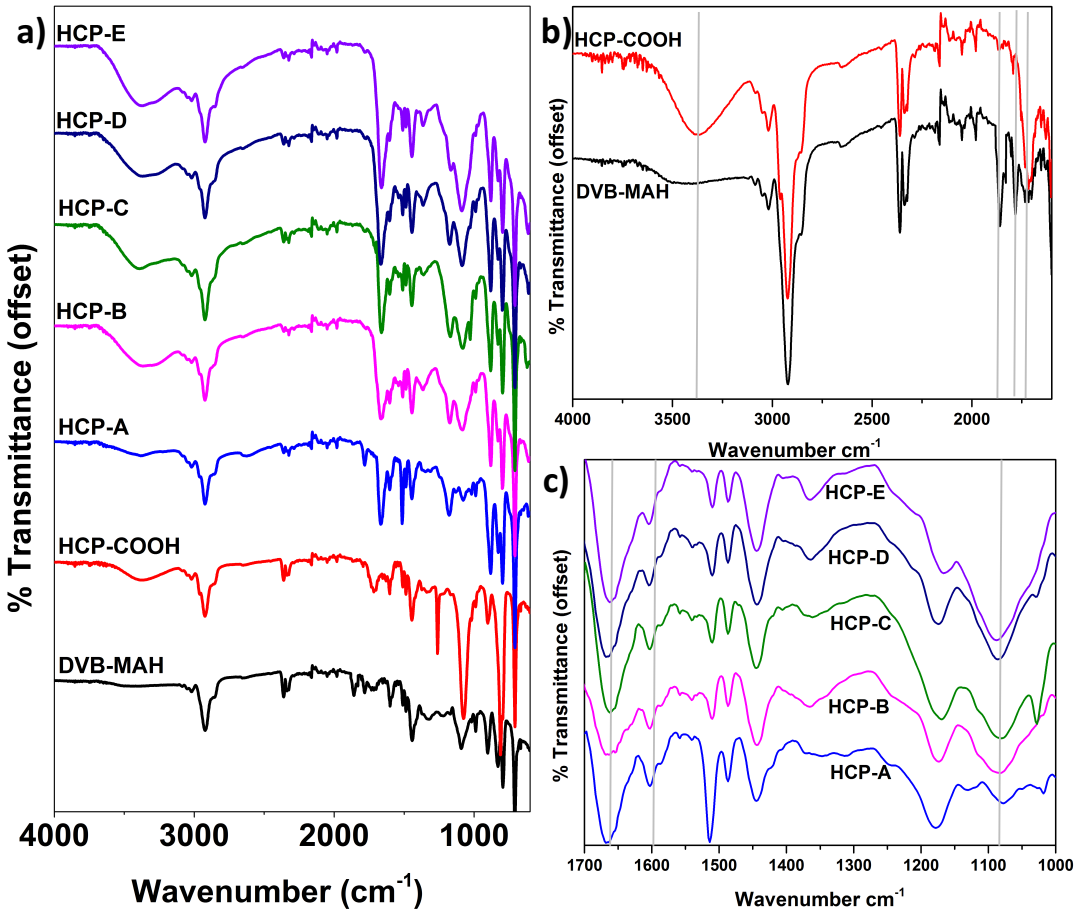

Figure 6-2. a) Full FT-IR spectra of DVB-MAH, HCP-COOH, and HCP-A to HCP-E; b) FT-IR spectra of DVB-MAH and HCP-COOH in the range of 3500-1600 cm^{-1}; c) FT-IR spectra of HCP-A to HCP-E in the range of 1700-1000 cm^{-1}.

The incorporation of diamines was further confirmed by elemental analysis (Table 6-1). HCPs contain 4.39-9.71 wt% of nitrogen, which are lower than the values assuming each anhydride unit is attaching to one diamine unit. It is likely that some acid chloride groups did not react with diamines, or some diamine monomers react with two acid chlorides on both primary amine ends.

The thermal stability of a porous material is important in practical applications; therefore, we examined the thermal stability of the polymers using thermogravimetric analysis (TGA) (Figure 6-3). The DVB-MAH precursor has a 5% degradation temperature of 308 ˚C, while all the

modified HCPs showed two-stage degradation curves. For the modified HCPs, the first weight loss starting at ca. 180 ˚C is attributed to the decomposition of the grafted diamines,[32] and the second stage degradation around 300 ˚C corresponds to the degradation of the hypercrosslinked backbone.

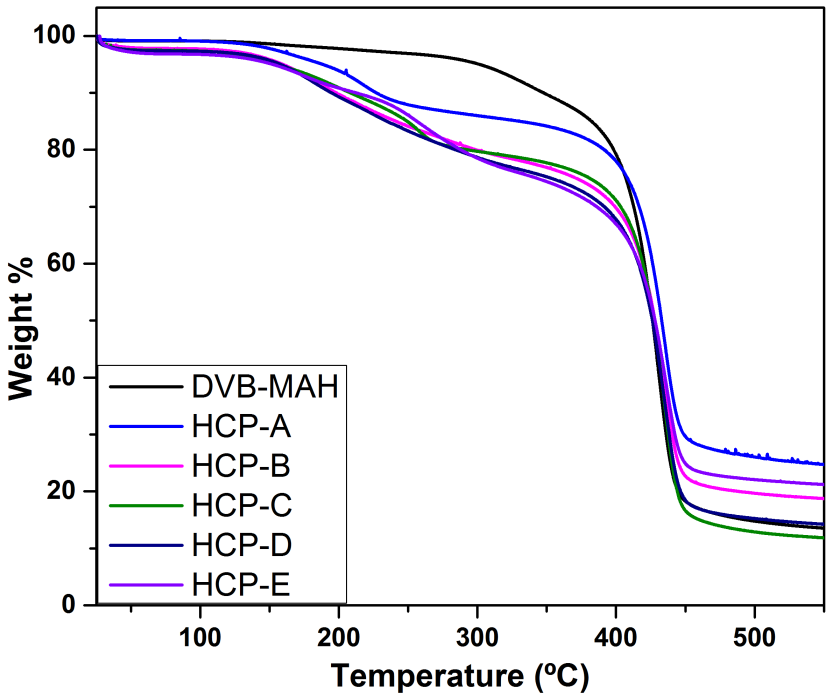

Figure 6- 3. TGA curves of DVB-MAH and modified HCPs.

6.5.2 Porosity and BET surface area.

Nitrogen adsorption/desorption isotherms of the polymers in this study are shown in Figure 6-4. All the polymers in this work exhibited Type I isotherms.[33] The high gas uptakes at low pressure indicate that these polymers possess both micropores (pore width < 2 nm), and the hysteresis loops suggest the presense of mesopores (2 nm < pore width < 50 nm).[33-34] The pore size distributions were assessed by the non-local density functional theory method (NLDFT) on nitrogen adsorption isotherms by using the SAIEUS program.[35] The calculated pore size distribution also reveals the presence of both micropores and mesopores (Figure 6-5). Surface areas were calculated using the Brunauer-Emmett-Teller (BET) equation.[36] The detailed BET surface areas and pore volumes of the polymers are listed in Table 6-1.

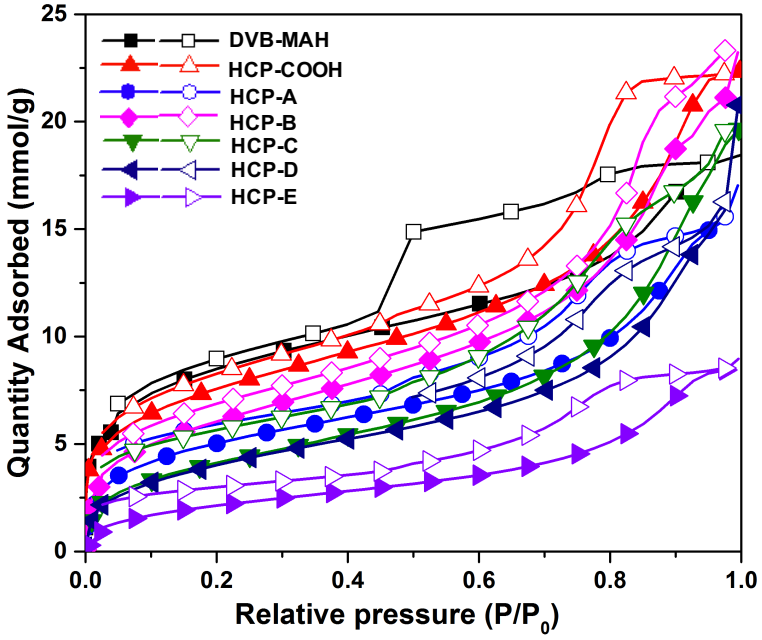

Figure 6-4. Nitrogen adsorption (closed symbol)/desorption (open symbol) isotherms at 77 K for the polymers in this study

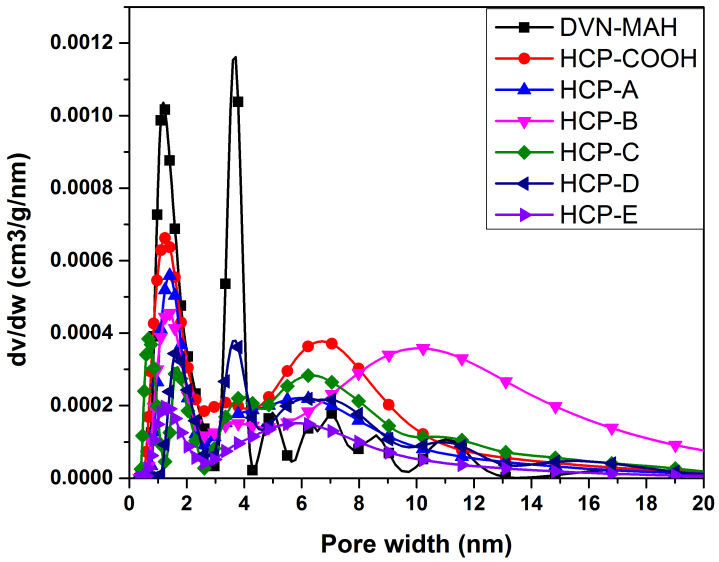

Figure 6-5. The pore size distributions (PSD) from nitrogen isotherms at 77 K by the non-local density functional theory method (NLDFT).

Table 6-1. Porous properties and elemental analysis of polymers

Sample	BET surface area (m^2/g)	Micro pore volume (cm^3/g)[a]	Total pore volume (cm^3/g)[b]	Elemental analysis (wt%)		
				C	H	N
DVB-MAH	667	0.28	0.64			-
HCP-COOH	607	0.24	0.7	-	-	-
HCP-A	412	0.16	0.59	75.83	6.79	4.39
HCP-B	500	0.19	0.61	69.78	6.71	9.71
HCP-C	346	0.13	0.57	73.71	6.34	5.93
HCP-D	343	0.13	0.55	69.42	6.82	9.38
HCP-E	183	0.06	0.29	70.39	6.74	8.45

[a]Micropore volumes determined from nitrogen adsorption isotherm at $P/P_0 = 0.14$; [b]Total pore volumes determined from nitrogen adsorption isotherm at $P/P_0 = 0.98$

As previously mentioned, the DVB-MAH precursor from suspension polymerization exhibited a BET surface area of 667 m^2/g. After hydrolysis, the resulting HCP-COOH showed a slight decrease in surface area to 607 m^2/g. After grafting the diamines onto the precursor, obvious decrease in BET surface areas was shown in all samples. Interestingly, it was observed the larger size of the diamine molecule resulted in relatively lower surface area, and the micropore volume decreased faster than the total pore volume. The most obvious example is HCP-E, which has the pentaethylenehexamine graft. The BET surface area of HCP-E decreased by 73% to 183 m^2/g compared to DVB-MAH, and it only showed 0.06 cm^3/g of micropore volume, which suggests that the grafting of bulky diamines results in blocking of micropores. However, the BET surface area of HCP-A only decreased to 412 m^2/g although p-phenylenediamine is also a large diamine. This is probably because less p-phenylenediamine was incorporated, as evidenced by the elemental analysis. HCP-B is grafted with the smallest ethylenediamine, therefore it has the highest BET surface area among the five modified polymers. 1,4-diaminobutane and diethylenetriamine are similar in their size, which means that HCP-C and HCP-D have close BET surface area, micro- and total pore volume.

6.5.3 CO_2 adsorption.

The CO_2 adsorption properties of the polymers were investigated at 273 K and 298K up to 1 bar (Figure 6-6). The CO_2 uptakes of polymers at 1 bar are compared to their BET surface areas in Table 6-2. The precursor DVB-MAH showed CO_2 uptakes of 0.99 mmol/g at 273 K and 0.87 mmol/g at 298 K, which is close to other polymer networks with similar BET surface area. HCP-D showed the highest CO_2 uptake at both 273 K and 298 K, even with a relatively low BET surface area. This suggests that the extra secondary amine groups provided a favored site for the reaction of CO_2 to reversibly form carbamates.[37-38] With similar BET surface area, HCP-C showed 25% lower CO_2 uptake than HCP-D at 273 K. This is likely due to the lack of secondary amine in 1,4-diaminobutane, and the flexible 1,4-diaminobutane may facilitate the formation of amides with both terminal amine groups, which can further decrease the available sites for specific CO_2 adsorption. The CO_2 uptake of HCP-B was slightly lower than HCP-D, which is a result of both the high surface area and higher amine content. The CO_2 uptake of HCP-E was close to the unmodified DVB-MAH even with such a low BET surface area, thanks to the abundant secondary amine groups in the grafted pentaethylenehexamine. However, the low BET surface area and pore volume limited the CO_2 adsorption ability of HCP-E.

It is also worth noticing that the CO_2 adsorption/desorption isotherms of modified HCP-A to HCP-E all showed hysteresis. This is because the strong interaction between CO_2 and the amine groups makes the desorption process more difficult. The similar hysteresis on CO_2 isotherms was also observed for some other amine-containing materials.

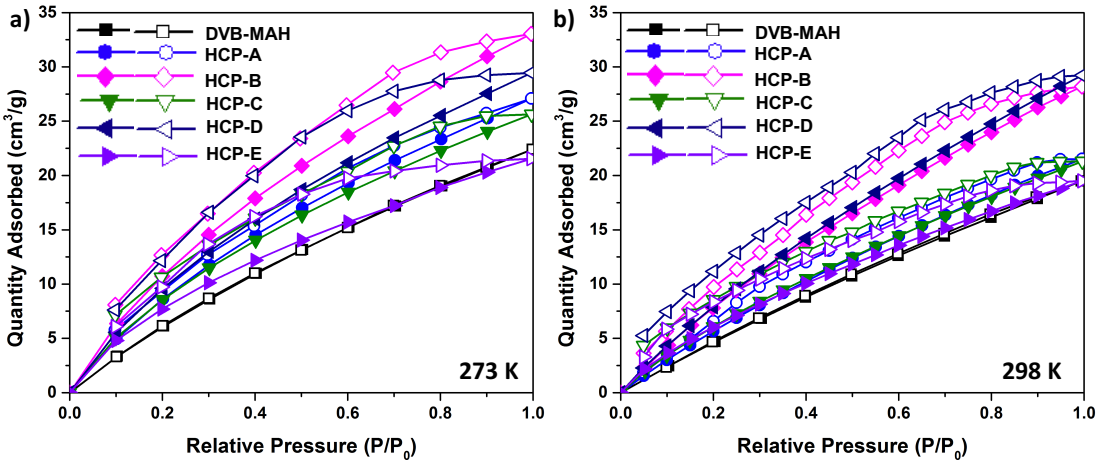

Figure 6-6. CO_2 adsorption isotherms at a) 273 K, and b) 298 K up to 1 bar

Table 6-2. CO_2 uptakes of the polymers

Sample	BET surface area (m^2/g)	CO_2 uptake at 1 bar (mmol/g)	
		273 K	298 K
DVB-MAH	667	0.99	0.87
HCP-A	412	1.21	0.96
HCP-B	500	1.46	1.26
HCP-C	346	1.15	0.95
HCP-D	343	1.53	1.30
HCP-E	183	0.96	0.87

6.6 Conclusion

A series of amine-containing nanoporous polymers were prepared by post-modification of the DVB-MAH precursor with various diamines. High amine-contents were achieved by covalently reacting a series of multiamines with the acid-chloride functionalized polymer surface. With good thermal stability and good CO_2 adsorption capacity, these amine-functionalized polymers hold potential as solid CO_2 sorbents. This work also provides an efficient strategy for grafting amine to anhydride- or carboxylic acid-functionalized polymer surface. Together with our previous work on synthesizing carboxylic acid-containing nanoporous polymers,[27] our future work

will involve developing other amine-rich porous polymer networks for CCS applications.

6.7 Acknowledgement

This work was supported by the National Science Foundation (NSF) under grant number DMR-0905231, DMR-1206409, and DMR-1310258. We thank the Macromolecules Innovation Institute and the Department of Chemistry at Virginia Tech for support.

6.8 References

1. de Coninck, H.; Stephens, J. C.; Metz, B., Global learning on carbon capture and storage: A call for strong international cooperation on CCS demonstration. *Energy Policy* **2009,** *37* (6), 2161-2165.
2. Joos, F.; Plattner, G.-K.; Stocker, T. F.; Marchal, O.; Schmittner, A., Global warming and marine carbon cycle feedbacks on future atmospheric CO_2. *Science* **1999,** *284* (5413), 464-467.
3. Orr, J. F. M., CO_2 capture and storage: are we ready? *Energy Environ. Sci.* **2009,** *2* (5), 449-458.
4. Chu, S., Carbon capture and sequestration. *Science* **2009,** *325* (5948), 1599-1599.
5. Rao, A. B.; Rubin, E. S., A technical, economic, and environmental assessment of amine-based CO_2 capture technology for power plant greenhouse gas control. *Environ. Sci. Technol.* **2002,** *36* (20), 4467-4475.
6. Rochelle, G. T., Amine scrubbing for CO_2 capture. *Science* **2009,** *325* (5948), 1652-1654.
7. MacDowell, N.; Florin, N.; Buchard, A.; Hallett, J.; Galindo, A.; Jackson, G.; Adjiman, C. S.; Williams, C. K.; Shah, N.; Fennell, P., An overview of CO_2 capture technologies. *Energy Environ. Sci.* **2010,** *3* (11), 1645-1669.
8. *Improvements in power generation with post-combustion capture of CO_2*; International

Energy Agency: Cheltenham, UK, 2004.

9. D'Alessandro, D. M.; Smit, B.; Long, J. R., Carbon dioxide capture: prospects for new materials. *Angew. Chem. Int. Ed.* **2010,** *49* (35), 6058-6082.

10. Mello, M. R.; Phanon, D.; Silveira, G. Q.; Llewellyn, P. L.; Ronconi, C. M., Amine-modified MCM-41 mesoporous silica for carbon dioxide capture. *Microporous Mesoporous Mater.* **2011,** *143* (1), 174-179.

11. Harlick, P. J.; Sayari, A., Applications of pore-expanded mesoporous silica. 5. Triamine grafted material with exceptional CO_2 dynamic and equilibrium adsorption performance. *Ind. Eng. Chem. Res.* **2007,** *46* (2), 446-458.

12. Heydari-Gorji, A.; Belmabkhout, Y.; Sayari, A., Polyethylenimine-impregnated mesoporous silica: effect of amine loading and surface alkyl chains on CO_2 adsorption. *Langmuir* **2011,** *27* (20), 12411-12416.

13. Hicks, J. C.; Drese, J. H.; Fauth, D. J.; Gray, M. L.; Qi, G.; Jones, C. W., Designing Adsorbents for CO_2 Capture from Flue Gas-Hyperbranched Aminosilicas Capable of Capturing CO_2 Reversibly. *J. Am. Chem. Soc.* **2008,** *130* (10), 2902-2903.

14. Kim, S.-N.; Son, W.-J.; Choi, J.-S.; Ahn, W.-S., CO_2 adsorption using amine-functionalized mesoporous silica prepared via anionic surfactant-mediated synthesis. *Microporous Mesoporous Mater.* **2008,** *115* (3), 497-503.

15. Qi, G.; Fu, L.; Giannelis, E. P., Sponges with covalently tethered amines for high-efficiency carbon capture. *Nat. Commun.* **2014,** *5*, 5796.

16. Couck, S.; Denayer, J. F.; Baron, G. V.; Rémy, T.; Gascon, J.; Kapteijn, F., An amine-functionalized MIL-53 metal− organic framework with large separation power for CO_2 and CH_4. *J. Am. Chem. Soc.* **2009,** *131* (18), 6326-6327.

17. Choi, S.; Watanabe, T.; Bae, T.-H.; Sholl, D. S.; Jones, C. W., Modification of the Mg/DOBDC MOF with amines to enhance CO_2 adsorption from ultradilute gases. *J. Phys. Chem. Lett.* **2012,** *3* (9), 1136-1141.

18. Dawson, R.; Ratvijitvech, T.; Corker, M.; Laybourn, A.; Khimyak, Y. Z.; Cooper, A. I.; Adams, D. J., Microporous copolymers for increased gas selectivity. *Polym. Chem.* **2012,** *3* (8), 2034-2038.

19. Acosta, E. J.; Carr, C. S.; Simanek, E. E.; Shantz, D. F., Engineering nanospaces: iterative synthesis of melamine-based dendrimers on amine-functionalized SBA-15 leading to complex hybrids with controllable chemistry and porosity. *Adv. Mater.* **2004,** *16* (12), 985-989.

20. Chaikittisilp, W.; Lunn, J. D.; Shantz, D. F.; Jones, C. W., Poly(L-lysine) brush–mesoporous silica hybrid material as a biomolecule-based adsorbent for CO_2 capture from simulated flue gas and air. *Chem. Eur. J* **2011,** *17* (38), 10556-10561.

21. Dawson, R.; Cooper, A. I.; Adams, D. J., Nanoporous organic polymer networks. *Prog. Polym. Sci.* **2012,** *37* (4), 530-563.

22. Dawson, R.; Stockel, E.; Holst, J. R.; Adams, D. J.; Cooper, A. I., Microporous organic polymers for carbon dioxide capture. *Energy Environ. Sci.* **2011,** *4* (10), 4239-4245.

23. Zhou, X.; Huang, J.; Barr, K. W.; Lin, Z.; Maya, F.; Abbott, L. J.; Colina, C. M.; Svec, F.; Turner, S. R., Nanoporous hypercrosslinked polymers containing T_g enhancing comonomers. *Polymer* **2015,** *59*, 42-48.

24. Huang, J.; Turner, S. R., Hypercrosslinked polymers: A review. *Polym. Rev.* **2017,** *Latest articles*.

25. Huang, J.; Turner, S. R., Recent advances in alternating copolymers: The synthesis,

modification, and applications of precision polymers. *Polymer* **2017,** *116*, 572-586.

26. Savage, A. M.; Zhou, X.; Huang, J.; Turner, S. R., A review of semi-rigid, stilbene-containing alternating copolymers. *Appl. Petrochem. Res.* **2015,** *5* (1), 27-33.

27. Huang, J.; Zhou, X.; Lamprou, A.; Maya, F.; Svec, F.; Turner, S. R., Nanoporous polymers from cross-linked polymer precursors via tert-butyl group deprotection and their carbon dioxide capture properties. *Chem. Mater.* **2015,** *27* (21), 7388-7394.

28. Ogawa, N.; Honmyo, K.; Harada, K.; Sugii, A., Preparation of spherical polymer beads of maleic anhydride–styrene–divinylbenzene and metal sorption of its derivatives. *J. Appl. Polym. Sci.* **1984,** *29* (9), 2851-2856.

29. Maciejewska, M.; Szajnecki, Ł.; Gawdzik, B., Investigation of the surface area and polarity of porous copolymers of maleic anhydride and divinylbezene. *J. Appl. Polym. Sci.* **2012,** *125* (1), 300-307.

30. Frank, R. S.; Downey, J. S.; Stöver, H., Synthesis of divinylbenzene–maleic anhydride microspheres using precipitation polymerization. *J. Polym. Sci., Part A: Polym. Chem.* **1998,** *36* (13), 2223-2227.

31. Donescu, D.; Raditoiu, V.; Spataru, C. I.; Somoghi, R.; Ghiurea, M.; Radovici, C.; Fierascu, R. C.; Schinteie, G.; Leca, A.; Kuncser, V., Superparamagnetic magnetite–divinylbenzene–maleic anhydride copolymer nanocomposites obtained by dispersion polymerization. *Eur. Polym. J.* **2012,** *48* (10), 1709-1716.

32. Ngo, C. L.; Le, Q. T.; Ngo, T. T.; Nguyen, D. N.; Vu, M. T., Surface modification and functionalization of carbon nanotube with some organic compounds. *Adv. Nat. Sci.: Nanosci. Nanotechnol.* **2013,** *4* (3), 035017.

33. Sing, K. S. W., Reporting physisorption data for gas/solid systems with special reference to

the determination of surface area and porosity (Recommendations 1984). *Pure Appl. Chem.* **1985,** *57* (4).

34. Aligizaki, K. K., *Pore structure of cement-based materials: testing, interpretation and requirements*. CRC Press: 2005.

35. Jagiello, J., Stable numerical solution of the adsorption integral equation using splines. *Langmuir* **1994,** *10* (8), 2778-2785.

36. Brunauer, S.; Emmett, P. H.; Teller, E., Adsorption of gases in multimolecular layers. *J. Am. Chem. Soc.* **1938,** *60* (2), 309-319.

37. Fernandes, D.; Conway, W.; Burns, R.; Lawrance, G.; Maeder, M.; Puxty, G., Investigations of primary and secondary amine carbamate stability by ^{1}H NMR spectroscopy for post combustion capture of carbon dioxide. *J. Chem. Thermodyn.* **2012,** *54*, 183-191.

38. Ciftja, A. F.; Hartono, A.; Svendsen, H. F., Carbamate formation in aqueous - diamine - CO_2 systems. *Energy Procedia* **2013,** *37*, 1605-1612.

Chapter 7. Overall Summary, Conclusions, and Future Work

This dissertation described the incorporation of functionalized semi-rigid stilbene and maleic anhydride/maleimide alternating copolymer sequences into different polymer systems. The resulting polymeric materials exhibited interesting chemical and physical properties. The dissertation consists of seven chapters, including two literature reviews, four research manuscripts, and the current chapter on the summary, conclusion and future work.

Chapter 1

An overview on the state-of-art progress of alternating copolymers was provided in this chapter, which was published as a feature article in Polymer. Emphasis was placed on alternating copolymers that were formed by benzylidene monomers such as styrene or stilbene with maleic anhydride or *N*-substituted maleimides. Detailed synthetic and modification pathways, structure-property relationship measurements, and various current and potential applications of these copolymers were also discussed in this chapter.

Chapter 2

This chapter, which was published in Polymer Reviews, described the history and recent advances on hypercrosslinked polymers. Synthetic approaches, theoretical studies, characterization, structure-property relationships, and applications of these materials were the focus of this chapter. Our work on the incorporation of alternating copolymer sequences into hypercrosslinked polymers[1-2] was also included in this review.

Chapter 3

The non-conjugated, *tert*-butyl carboxylate functionalized stilbene-containing alternating copolymers described in Chapter 3 exhibited fluorescence of extraordinarily high intensity and excellent linearity versus concentration. The enhanced fluorescence property likely results from the "through-space" conjugation of the phenyl groups and the carbonyl groups. The semi-rigidity backbone of these polymers forced the functional groups to locate at a favorable juxtaposition for the conjugation to take place. The fluorescence is maintained when the *tert*-butyl groups are removed and the resulting polymer is dissolved in water.

For future work, the effects of molecular weight and different substitution groups on the fluorescence properties of these polymers are opportunities to probe this effect in more details. The molecular weight of stilbene-containing alternating copolymers can be controlled using RAFT polymerization.[3] It would be interesting to find the lowest molecular weight that can still generate the fluorescence. Other than *tert*-butyl carboxylate, we have successfully synthesized alternating polymers with other functional groups, such as methyl[4] and diakylamino[5] groups, on the phenyl rings. It is important to investigate how the size, the electron effect, and the substitution position of the functional groups can affect the fluorescence properties of the alternating copolymers.

Chapter 4

In this chapter published on Chemistry of Materials, we reported that a series of carboxylic acid-functionalized nanoporous polymers were achieved using a two-step synthetic strategy. The first step involves the suspension polymerization of *tert*-butyl carboxylate-functionalized stilbene or styrene and *tert*-butyl carboxylate-functionalized *N*-phenylmaleimide in the presence of

divinylbenzene as the crosslinker. In the second step, the polymer precursors were deprotected to cleave the *tert*-butyl groups. The spaces that were occupied by the bulky *tert*-butyl groups became pores. The BET surface area of deprotected polymers increased as the increase of DVB content, and the stilbene-containing polymers showed systematically higher BET surface area because the more rigid polymer backbone may help to maintain the pore structure from collapsing. The resulting nanoporous polymers were also investigated as potential CO_2 sorbents, and the carboxylic acid groups showed enhancement in the CO_2 adsorption.

Possible future work involves incorporating other functional groups into nanoporous polymers. For example, it is proposed that amine functionalized nanoporous polymer materials can be prepared using a similar two-step strategy to that which was described above by using boc-protected amine-containing stilbene and maleimide monomers. The amine-functionalized nanoporous polymers are expected to show improvement in both capacity and selectivity for CO_2 adsorption.

Chapter 5

This chapter described the synthesis of microgels from hydrophobic solid monomers using miniemulsion polymerization. The addition of the costabilizer allowed the use of organic solvents for dissolving the solid monomers. The resulting *tert*-butyl carboxylate-containing organic microgels were then converted to aqueous hydrogels by removing the *tert*-butyl group using acidic deprotection. These hydrogel particles showed good lead and copper ion adsorption ability.

Using the same miniemulsion strategy, we should be able to synthesize other microgels using

various vinyl monomers with different functional groups. One kind of interesting monomer is vinyl functionalized macromonomers. Microgels with grafted on microstructures may be synthesized using miniemulsion polymerization.

Chapter 6.

In this chapter, a series of nanoporous polymers with covalently bonded amines were prepared by post-modification of hypercorsslinked DVB-MAH precursor with various diamines. The modified polymers showed high CO_2 capture capacity because of the high amine content.

We proposed another novel synthetic method to covalently incorporate amines into porous crosslinked polymers. Benzyl chloride can be used as a cationic initiator for the synthesis of poly(2-oxazoline).[6] A short chain poly(2-ethyl-2-oxazoline) with a phenyl chain end can be achieved. The phenyl chain end can then be crosslinked using the "knitting" strategy by reacting with formaldehyde dimethyl acetal (the "knitting" strategy is described in 2.4.4). Then the grafted poly(2-ethyl-2-oxazoline) can be converted to polyethylenimine by acidic or basic hydrolysis.[7] The resulting network would likely possess high crosslinking density and high secondary amine contents. It is also expected to have good thermal stability and CO_2 adsorption property.

References

1. Huang, J.; Zhou, X.; Lamprou, A.; Maya, F.; Svec, F.; Turner, S. R., Nanoporous polymers from cross-Linked polymer precursors via *tert*-butyl group deprotection and their carbon dioxide capture properties. *Chem. Mater.* **2015,** *27* (21), 7388-7394.
2. Zhou, X.; Huang, J.; Barr, K. W.; Lin, Z.; Maya, F.; Abbott, L. J.; Colina, C. M.; Svec, F.;

Turner, S. R., Nanoporous hypercrosslinked polymers containing T_g enhancing comonomers. *Polymer* **2015,** *59*, 42-48.

3. Savage, A. M.; Li, Y.; Matolyak, L. E.; Doncel, G. F.; Turner, S. R.; Gandour, R. D., Anti-HIV activities of precisely defined, semirigid, carboxylated alternating copolymers. *J. Med. Chem.* **2014,** *57* (15), 6354-6363.
4. Li, Y.; Turner, S. R., Free radical copolymerization of methyl substituted stilbenes with maleic anhydride. *Eur. Polym. J.* **2010,** *46* (4), 821-828.
5. Mao, M.; Turner, S. R., Synthesis and characterization of highly functionalized polymers based on *N,N,N′,N′*-tetraalkyl-4,4′-diaminostilbene and maleic anhydride. *Polymer* **2006,** *47* (24), 8101-8105.
6. Fijten, M. W. M.; Hoogenboom, R.; Schubert, U. S., Initiator effect on the cationic ring-opening copolymerization of 2-ethyl-2-oxazoline and 2-phenyl-2-oxazoline. *J. Polym. Sci. A* **2008,** *46* (14), 4804-4816.
7. de la Rosa, V. R.; Bauwens, E.; Monnery, B. D.; De Geest, B. G.; Hoogenboom, R., Fast and accurate partial hydrolysis of poly(2-ethyl-2-oxazoline) into tailored linear polyethylenimine copolymers. *Polym. Chem.* **2014,** *5* (17), 4957-4964.